

PHARMACOLOGICAL  
CHARACTERISATION OF NEURONAL  
NICOTINIC ACETYLCHOLINE  
RECEPTORS

---

Anna Chatzidaki

August 2015

A thesis presented for the degree of Doctor of Philosophy to  
University College London.

Department of Neuroscience, Physiology and Pharmacology

UCL

London

WC1E 6BT



PHARMACOLOGICAL  
CHARACTERISATION OF NEURONAL  
NICOTINIC ACETYLCHOLINE  
RECEPTORS

---

I, Anna Chatzidaki, confirm that the work presented in this thesis is my own.

Where information has been derived from other sources, I confirm that this has been indicated in the thesis.

Signature:

Date:

# ABSTRACT

---

Nicotinic acetylcholine receptors (nAChRs) are the targets for the endogenous neurotransmitter acetylcholine and represent a diverse family of ligand-gated ion channels. They are expressed in the neuromuscular junction, the peripheral nervous system and the central nervous system. In the brain, the most prevalent subtypes are the heteromeric  $\alpha 4\beta 2$  and homomeric  $\alpha 7$  nAChRs. Neuronal nAChRs are implicated in numerous physiological and pathophysiological functions and are therefore important targets for therapeutic drug discovery for conditions such as Alzheimer's disease, schizophrenia and tobacco addiction. This thesis aims to further our understanding of the pharmacological and molecular characteristics of neuronal nAChRs.

Acetylcholine activates nAChRs by binding at an extracellular orthosteric site. Previous studies have described several ligands that potentiate agonist-evoked responses by binding to an allosteric site of the  $\alpha 7$  nAChRs that is distinct from the acetylcholine binding site. These ligands, termed positive allosteric modulators (PAMs) can be described as type I, when they have little or no effect on desensitisation, or type II, when they dramatically slow down the fast desensitisation kinetics of the  $\alpha 7$  nAChR subtype. Here, a novel series of  $\alpha 7$ -selective PAMs with a range of effects on receptor desensitisation is described, using recombinant human receptors. This series consists of PAMs with type I and type II profiles, in addition to PAMs with intermediate properties on desensitisation, therefore increasing the nAChR pharmacological toolbox. Furthermore, the effect of a number of mutations on the pharmacological properties of the receptor is investigated. Three point mutations, two in the transmembrane domain (L247T and M260L) and one in the N-terminal domain (W54A), are shown to have the ability to convert PAMs into agonists. Moreover, the M260L mutation displays this property only with PAMs that have a significant effect on receptor desensitisation. These observations can provide insights into the role of these residues on receptor gating and desensitisation.

In addition to the studies on recombinant receptors, the expression and functional properties of nAChRs in neurons derived from human induced pluripotent stem cells (iPSC) is examined. The iPSC-derived neurons represent a potentially valuable tool for the characterisation of neuronal receptors and ion channels in a native environment.

# ACKNOWLEDGEMENTS

---

This work would have not been possible without the help of many people, to whom I am deeply thankful.

Firstly, I would like to thank Professor Neil Millar for allowing me to carry out this research in his lab. His expertise, understanding, guidance and support made it possible for me to work on a topic that was of great interest to me. It has been a pleasure working with him.

Big thanks go to members of the Millar lab, past and present. Without your support this PhD would have not been possible and these four years not nearly as enjoyable! Jas Gill-Thind, thank you for teaching me pretty much everything in the lab, for giving me great advice on so many things and for all the hilarious moments. Stuart Lansdell and Mirel Puinean, your help and company have been invaluable all these years – I couldn't have made it without you. And to the newest member of the lab, Charlie Smelt, it's been a fun year. Good luck with the rest of your PhD - you're going to do brilliantly.

I am very grateful to Emanuele Sher, Daniel Ursu and Antoine Fouillet for their time and support during my placement at Eli Lilly. It was a very enjoyable and valuable experience, which helped me learn a lot.

Many thanks also go to Tom Sheppard and Jarryl D'Oyley, our collaborators from the UCL Department of Chemistry, who synthesised some of the compounds used in this thesis.

I would like to thank my parents for encouraging me during my PhD and for all their love and support throughout the years. My thanks also go to all of my friends; particularly, Alina Zigkiri, who's been my friend for as long as I can remember and Nat Macabuag and Terri Stephen for their company during this PhD. Finally, I am forever grateful to Daniel Waddington for his understanding, patience and support when it was most needed.

# LIST OF PUBLICATIONS

---

Gill J. K., **Chatzidaki A.**, Ursu D., Sher E., Millar N. S. (2013). Contrasting properties of  $\alpha 7$ -selective orthosteric and allosteric agonists examined on native nicotinic acetylcholine receptors. *PLOS ONE* **8**, e55047.

**Chatzidaki A.**, Fouillet A., Li J., Dage J., Millar N. S., Sher E., Ursu D. (2015). Pharmacological characterisation of nicotinic acetylcholine receptors expressed in human iPSC-derived neurons. *PLOS ONE* **10**, e0125116.

**Chatzidaki A.**, D'Oyley J. M., Gill-Thind J. K., Sheppard T. D., Millar N. S. (2015). The influence of allosteric modulators and transmembrane mutations on desensitisation and activation of  $\alpha 7$  nicotinic acetylcholine receptors. *Neuropharmacol* **97**, 75-85.

**Chatzidaki A.**, Millar N. S. (2015). Allosteric modulation of nicotinic acetylcholine receptors. *Biochem Pharmacol* **97**, 408-417.

# TABLE OF CONTENTS

---

<b>Title page</b> .....	<b>1</b>
<b>Declaration page</b> .....	<b>2</b>
<b>Abstract</b> .....	<b>3</b>
<b>Acknowledgements</b> .....	<b>4</b>
<b>List of Publications</b> .....	<b>5</b>
<b>Table of Contents</b> .....	<b>6</b>
<b>List of Figures</b> .....	<b>10</b>
<b>List of Tables</b> .....	<b>14</b>
<b>List of Abbreviations</b> .....	<b>15</b>
<b>CHAPTER 1 Introduction</b> .....	<b>20</b>
<b>1.1 THE NICOTINIC ACETYLCHOLINE RECEPTOR: A BRIEF HISTORY</b> .....	<b>21</b>
1.1.1 Acetylcholine and chemical neurotransmission .....	21
1.1.2 Purification of the nicotinic acetylcholine receptor.....	22
1.1.3 Cloning of the nicotinic acetylcholine receptor.....	23
<b>1.2 ACETYLCHOLINE AND ITS RECEPTORS</b> .....	<b>25</b>
1.2.1 Acetylcholine and cholinergic transmission.....	25
1.2.2 Acetylcholine receptors .....	27
<b>1.3 NICOTINIC ACETYLCHOLINE RECEPTORS</b> .....	<b>28</b>
1.3.1 The Cys-loop receptor superfamily .....	28
1.3.2 Nicotinic acetylcholine receptors from the fish electric organ.....	29
1.3.3 Muscle nicotinic acetylcholine receptors .....	31
1.3.4 Neuronal nicotinic acetylcholine receptors .....	32
<b>1.4 STRUCTURE OF NICOTINIC ACETYLCHOLINE RECEPTORS</b> .....	<b>34</b>
1.4.1 Subunit structure.....	34
1.4.2 Stoichiometry .....	35
1.4.3 Extracellular agonist binding domain.....	36
1.4.4 Ion channel .....	37
1.4.5 Three-dimensional structure.....	38
1.4.5.1 Electron microscopy of Torpedo nAChRs.....	39
1.4.5.2 Snail acetylcholine binding protein.....	41
1.4.5.3 Mouse $\alpha 1$ subunit bound to $\alpha$ -bungarotoxin .....	42

1.4.5.4	Crystal structures of bacterial homologues .....	44
1.4.5.5	Crystal structures of eukaryotic Cys-loop receptors .....	46
<b>1.5</b>	<b>FUNCTION OF NICOTINIC ACETYLCHOLINE RECEPTORS .....</b>	<b>47</b>
<b>1.5.1</b>	Agonist binding .....	47
<b>1.5.2</b>	Gating .....	48
<b>1.5.3</b>	Desensitisation.....	50
<b>1.6</b>	<b>LIGANDS OF NICOTINIC ACETYLCHOLINE RECEPTORS .....</b>	<b>52</b>
<b>1.6.1</b>	Orthosteric agonists .....	52
<b>1.6.2</b>	Competitive antagonists .....	53
<b>1.6.3</b>	Channel blockers .....	55
<b>1.6.4</b>	Allosteric modulators .....	55
1.6.4.1	Positive allosteric modulators and allosteric agonists.....	55
1.6.4.2	Negative allosteric modulators.....	59
1.6.4.3	Allosteric binding sites.....	60
1.6.4.4	Therapeutic uses.....	63
<b>1.7</b>	<b>PHYSIOLOGICAL ROLE AND DISTRIBUTION .....</b>	<b>65</b>
<b>1.7.1</b>	Central nervous system.....	65
<b>1.7.2</b>	Peripheral nervous system.....	69
<b>1.7.3</b>	Non-neuronal tissues .....	70
<b>1.8</b>	<b>ROLE IN DISEASE .....</b>	<b>71</b>
<b>1.8.1</b>	Myasthenia gravis and congenital myasthenic syndrome .....	71
<b>1.8.2</b>	Alzheimer's disease.....	71
<b>1.8.3</b>	Parkinson's disease.....	72
<b>1.8.4</b>	Schizophrenia .....	73
<b>1.9</b>	<b>THESIS AIMS .....</b>	<b>74</b>
<b>CHAPTER 2</b>	<b>Materials and methods.....</b>	<b>75</b>
<b>2.1</b>	<b>MOLECULAR BIOLOGY TECHNIQUES.....</b>	<b>76</b>
<b>2.1.1</b>	Plasmids.....	76
<b>2.1.2</b>	Restriction digestion of DNA .....	76
<b>2.1.3</b>	DNA ligation .....	76
<b>2.1.4</b>	Site-directed mutagenesis.....	77
<b>2.1.5</b>	XL1-Blue supercompetent cell transformation .....	78
<b>2.1.6</b>	Small-scale plasmid DNA preparation.....	78
<b>2.1.7</b>	Large-scale plasmid DNA preparation.....	79
<b>2.1.8</b>	Agarose gel electrophoresis.....	80
<b>2.1.9</b>	Determination of DNA yield.....	81
<b>2.1.10</b>	DNA nucleotide sequencing.....	81

2.1.11	Linearisation of DNA .....	82
2.1.12	Purification of DNA .....	83
2.1.13	<i>In vitro</i> RNA synthesis .....	83
2.1.14	Determination of RNA yield .....	84
<b>2.2</b>	<b>CELL CULTURE .....</b>	<b>85</b>
2.2.1	Mammalian cell culture and transfection .....	85
2.2.2	Human neuronal cells, derived from induced pluripotent stem cells .....	86
<b>2.3</b>	<b><i>XENOPUS LAEVIS</i> OOCYTE PREPARATION .....</b>	<b>88</b>
<b>2.4</b>	<b>ELECTROPHYSIOLOGICAL TECHNIQUES .....</b>	<b>89</b>
2.4.1	Two-electrode voltage-clamp recording .....	89
2.4.2	Patch-clamp recording .....	89
2.4.3	Drug application .....	90
2.4.4	Data analysis .....	91
<b>2.5</b>	<b>DISPLACEMENT RADIOLIGAND BINDING ASSAY .....</b>	<b>92</b>
<b>2.6</b>	<b>INTRACELLULAR CALCIUM ASSAYS .....</b>	<b>93</b>
2.6.1	Fluorometric imaging plate reader assays .....	93
2.6.2	Single cell intracellular calcium imaging .....	93
<b>2.7</b>	<b>STATISTICAL ANALYSIS .....</b>	<b>95</b>
<b>2.8</b>	<b>CHEMICAL SYNTHESIS .....</b>	<b>96</b>
<b>CHAPTER 3 A novel series of positive allosteric modulators with diverse</b>		
<b>pharmacological properties.....97</b>		
<b>3.1</b>	<b>INTRODUCTION .....</b>	<b>98</b>
<b>3.2</b>	<b>RESULTS.....</b>	<b>101</b>
3.2.1	Characterisation of the effects of TBS compounds on activation of $\alpha 7$ nAChRs by acetylcholine.....	101
3.2.2	Examination of the ability of TBS compounds to facilitate recovery from desensitisation on $\alpha 7$ nAChRs.....	109
3.2.3	Displacement of [ <sup>3</sup> H]- $\alpha$ -bungarotoxin by TBS compounds .....	112
3.2.4	Selectivity of TBS compounds .....	114
<b>3.3</b>	<b>DISCUSSION .....</b>	<b>119</b>
<b>CHAPTER 4 Effect of mutations on modulation of <math>\alpha 7</math> nicotinic acetylcholine</b>		
<b>receptors by allosteric ligands..... 122</b>		
<b>4.1</b>	<b>INTRODUCTION .....</b>	<b>123</b>
<b>4.2</b>	<b>RESULTS.....</b>	<b>126</b>
4.2.1	L247T (9') and M260L (22') transmembrane mutations .....	126

4.2.2	Effects of transmembrane mutations on modulation of $\alpha 7$ nAChRs by type I and type II PAMs .....	128
4.2.3	Effects of transmembrane mutations on modulation of $\alpha 7$ nAChRs by TBS compounds.....	130
4.2.4	Type I PAMs block agonist effects of type II PAMs on M260L in a surmountable manner .....	139
4.2.5	Effects of the W54A mutation on modulation of $\alpha 7$ nAChRs by allosteric ligands .....	141
<b>4.3</b>	<b>DISCUSSION .....</b>	<b>145</b>
<b>CHAPTER 5 Atypical pharmacological properties of A-867744 .....</b>		<b>148</b>
<b>5.1</b>	<b>INTRODUCTION .....</b>	<b>149</b>
<b>5.2</b>	<b>RESULTS.....</b>	<b>151</b>
5.2.1	A-867744 is a type II PAM of $\alpha 7$ nAChRs .....	151
5.2.2	The influence of M260L on the pharmacological properties of A-867744.....	154
5.2.3	The influence of W54A on the pharmacological properties of A-867744.....	154
5.2.4	The influence of L247T on the pharmacological properties of A-867744.....	157
5.2.5	The influence of M253L on the pharmacological properties of A-867744.....	157
<b>5.3</b>	<b>DISCUSSION .....</b>	<b>160</b>
<b>CHAPTER 6 Characterisation of native nicotinic acetylcholine receptors on neurons derived from induced pluripotent stem cells .....</b>		<b>163</b>
<b>6.1</b>	<b>INTRODUCTION .....</b>	<b>164</b>
<b>6.2</b>	<b>RESULTS.....</b>	<b>167</b>
6.2.1	Characterisation of nAChRs with a FLIPR-based assay .....	167
6.2.2	Characterisation of nAChRs by single-cell calcium imaging .....	170
6.2.3	Effect of temperature on agonist-induced nAChR responses.....	172
6.2.4	Characterisation of $\alpha 7$ nAChRs expressed in iPSC-derived neurons.....	174
6.2.5	Potentiated nAChR responses detected by patch-clamp recording .....	180
<b>6.3</b>	<b>DISCUSSION .....</b>	<b>182</b>
<b>CHAPTER 7 Final conclusions and future directions.....</b>		<b>185</b>
<b>CHAPTER 8 References.....</b>		<b>194</b>

# LIST OF FIGURES

---

<b>Figure 1.1:</b> Acetylcholine synthesis and degradation. ....	26
<b>Figure 1.2:</b> Cys-loop receptor architecture and membrane topology. ....	30
<b>Figure 1.3:</b> High-resolution structure of the <i>Torpedo</i> nAChR at 4 Å (figure from (Unwin, 2005)). ....	40
<b>Figure 1.4:</b> High-resolution structure of the <i>Lymnaea</i> ACh-binding protein (figure from (Brejc <i>et al.</i> , 2001)). ....	43
<b>Figure 1.5:</b> High-resolution structure of the nAChR homologues ELIC and GLIC (figure from (Hilf & Dutzler, 2008, 2009)). ....	45
<b>Figure 1.6:</b> Distribution of nAChR subtypes in the rodent brain (figure adapted from (Millar & Gotti, 2009)). ....	67
<b>Figure 3.1:</b> Chemical structures of allosteric ligands examined in this chapter. ....	100
<b>Figure 3.2:</b> Agonist activation of recombinant human $\alpha 7$ nAChRs by ACh, examined by two-electrode voltage-clamp recording in <i>Xenopus</i> oocytes. ....	103
<b>Figure 3.3:</b> Positive allosteric modulation of $\alpha 7$ nAChRs by TBS-346, examined by two-electrode voltage-clamp recording in <i>Xenopus</i> oocytes. ....	104
<b>Figure 3.4:</b> Positive allosteric modulation of $\alpha 7$ nAChRs by TBS-546, examined by two-electrode voltage-clamp recording in <i>Xenopus</i> oocytes. ....	105
<b>Figure 3.5:</b> Positive allosteric modulation of $\alpha 7$ nAChRs by TBS-345, examined by two-electrode voltage-clamp recording in <i>Xenopus</i> oocytes. ....	106
<b>Figure 3.6:</b> Positive allosteric modulation of $\alpha 7$ nAChRs by TBS-556, examined by two-electrode voltage-clamp recording in <i>Xenopus</i> oocytes. ....	107
<b>Figure 3.7:</b> Positive allosteric modulation of $\alpha 7$ nAChRs by TBS-516, examined by two-electrode voltage-clamp recording in <i>Xenopus</i> oocytes. ....	108

<b>Figure 3.8:</b> Influence of TBS compounds on the recovery of $\alpha 7$ nAChRs from desensitisation, examined by two-electrode voltage-clamp recording in <i>Xenopus</i> oocytes. ....	110
<b>Figure 3.9:</b> Displacement of [ $^3\text{H}$ ]- $\alpha$ -bungarotoxin from the orthosteric site of $\alpha 7$ nAChRs by TBS compounds, examined by competition radioligand binding. ....	113
<b>Figure 3.10:</b> Nicotinic subtype selectivity of TBS compounds, examined by two-electrode voltage-clamp recording in <i>Xenopus</i> oocytes.....	115
<b>Figure 3.11:</b> Contrasting effects of TBS compounds between $\alpha 7$ nAChR, 5-HT <sub>3A</sub> R and a subunit chimaera, examined by two-electrode voltage-clamp recording in <i>Xenopus</i> oocytes.....	116
<b>Figure 3.12:</b> Subtype selectivity of TBS compounds, examined by two-electrode voltage-clamp recording in <i>Xenopus</i> oocytes.....	117
<b>Figure 4.1:</b> Chemical structures of allosteric ligands examined in this chapter. ....	125
<b>Figure 4.2:</b> The influence of $\alpha 7$ nAChR mutations (L247T and M260L) on activation by ACh. ....	127
<b>Figure 4.3:</b> The influence of a type I (NS-1738) and a type II PAM (TQS) on wild-type and mutated (L247T or M260L) $\alpha 7$ nAChRs. ....	129
<b>Figure 4.4:</b> Potentiation and agonist effects of TBS compounds on wild-type and mutated $\alpha 7$ nAChRs. ....	131
<b>Figure 4.5:</b> Antagonism of agonist responses on L247T $\alpha 7$ nAChRs by MLA. ....	132
<b>Figure 4.6:</b> Antagonism of agonist responses on M260L $\alpha 7$ nAChRs by MLA. ....	133
<b>Figure 4.7:</b> Concentration-response curves for wild-type and mutated $\alpha 7$ nAChRs. ....	135
<b>Figure 4.8:</b> Potentiation of ACh responses by allosteric modulators on M260L $\alpha 7$ nAChRs..	138
<b>Figure 4.9:</b> Type I PAMs block agonist activity of TQS and TBS-516 on $\alpha 7$ nAChRs containing the M260L mutation. ....	140

<b>Figure 4.10:</b> Agonist activation of recombinant human $\alpha 7$ nAChRs containing the W54A mutation.....	143
<b>Figure 4.11:</b> Antagonism of agonist responses on W54A $\alpha 7$ nAChRs by MLA.....	144
<b>Figure 5.1:</b> Chemical structures of allosteric ligands examined in this chapter. ....	150
<b>Figure 5.2:</b> Positive allosteric modulation of wild-type $\alpha 7$ nAChRs by A-867744, examined by two-electrode voltage-clamp recording in <i>Xenopus</i> oocytes.....	152
<b>Figure 5.3:</b> Displacement of [ <sup>3</sup> H]- $\alpha$ -bungarotoxin from the orthosteric site of $\alpha 7$ nAChRs by A-867744, examined by competition radioligand binding.....	153
<b>Figure 5.4:</b> The effects of A-867744 on $\alpha 7$ nAChRs containing the M260L mutation.....	155
<b>Figure 5.5:</b> The effects of A-867744 on $\alpha 7$ nAChRs containing the W54A mutation. ....	156
<b>Figure 5.6:</b> The effects of A-867744 on $\alpha 7$ nAChRs containing the L247T mutation.....	158
<b>Figure 5.7:</b> The effects of A-867744 on $\alpha 7$ nAChRs containing the M253L mutation.....	159
<b>Figure 6.1:</b> Relative Expression of nAChR subunits in iPSC-derived neurons examined by RT-PCR (from (Chatzidaki <i>et al.</i> , 2015) <sup>a</sup> ).....	166
<b>Figure 6.2:</b> Nicotinic agonist-induced responses in iPSC-derived neurons, examined by FLIPR. ....	169
<b>Figure 6.3:</b> Characterisation of nAChRs in iPSC-derived neurons, examined by single-cell intracellular calcium imaging. ....	171
<b>Figure 6.4:</b> Influence of temperature on potentiation of compound B responses by PNU-120596, examined by FLIPR.....	173
<b>Figure 6.5:</b> Potentiation and antagonism of nAChR agonist responses in iPSC-derived neurons, examined by FLIPR.....	175

<b>Figure 6.6:</b> Characterisation of $\alpha 7$ -selective type I and type II PAMs in iPSC-derived neurons, examined by FLIPR.....	177
<b>Figure 6.7:</b> Agonist activity of 4BP-TQS in iPSC-derived neurons, examined by FLIPR. ....	178
<b>Figure 6.8:</b> Agonist-induced responses in iPSC-derived neurons, examined by patch-clamp electrophysiology. ....	181
<b>Figure 7.1:</b> Homology model of the $\alpha 7$ nAChR subunit highlighting the position of the mutated residues in relation to the orthosteric and allosteric binding sites.....	187

# LIST OF TABLES

---

<b>Table 1:</b> Pharmacological properties of TBS PAMs on $\alpha 7$ nAChRs.....	111
<b>Table 2:</b> Subtype selectivity of TBS compounds.....	118
<b>Table 3:</b> Agonist properties on wild-type and mutated $\alpha 7$ nAChRs.....	136
<b>Table 4:</b> Pharmacological properties of nAChR ligands on iPSC-derived neurons, as examined by FLIPR.....	179
<b>Table 5:</b> Summary of compound effects on wild-type and mutated human $\alpha 7$ nAChRs. ....	188

# LIST OF ABBREVIATIONS

---

4BP-TQS	cis-cis-4-(4-bromophenyl)-3a,4,5,9b-tetrahydro-3H-cyclopenta-[c]quinoline-8-sulfonamide
5-HI	5-Hydroxyindole
5-HT	5-Hydroxytryptamine
5-HT <sub>3</sub> R	5-Hydroxytryptamine receptor type 3
$\alpha$ -BTX	$\alpha$ -Bungarotoxin
A-867744	4-(5-(4-chlorophenyl)-2-methyl-3-propionyl-1H-pyrrol-1-yl)benzenesulfonamide
Acetyl CoA	Acetyl coenzyme A
ACh	Acetylcholine
AChBP	Acetylcholine binding protein
AChE	Acetylcholinesterase
AD	Alzheimer's disease
ANOVA	Analysis of variance
ANS	Autonomic nervous system
A $\beta$	Amyloid $\beta$
BSA	Bovine serum albumin
C-terminus	Carboxyl-terminus
<i>C. elegans</i>	<i>Caenorhabditis elegans</i>

CCD	Charge-coupled device
CDI	Cellular dynamics international
ChAT	Choline acetyltransferase
CNS	Central nervous system
Compound B	(R)-N-(1-azabicyclo[2.2.2]oct-3-yl)(5-(2-pyridyl)thiophene-2-carboxamide
CPZ	Chlorpromazine
dFBr	Desformylflustrabromine
Dh $\beta$ E	Dihydro- $\beta$ -erythroidine
DMEM	Dulbecco's modified Eagle's medium
DMPP	Dimethylphenylpiperazinium
DMSO	Dimethyl sulfoxide
DNA	Deoxyribonucleic acid
dNTP	Deoxyribonucleotide triphosphate
<i>E. coli</i>	<i>Escherichia coli</i>
EC	Effective concentration
EC <sub>50</sub>	Half maximal effective concentration
EDTA	Ethylenediaminetetraacetic acid
ELIC	<i>Erwinia chrysanthemi</i> ligand-gated ion channel
ER	Endoplasmic reticulum

FCS	Foetal calf serum
FLIPR	Fluorometric imaging plate reader
GABA	$\gamma$ -aminobutyric acid
GABA <sub>A</sub>	$\gamma$ -aminobutyric acid type A
GABA <sub>C</sub>	$\gamma$ -aminobutyric acid type C
GLIC	<i>Gloeobacter violaceus</i> ligand-gated ion channel
GluCl	Glutamate-gated chloride channel
GPCR	G protein-coupled receptor
HBTS	HEPES-buffered Tyrode's solution
iPSC	Induced pluripotent stem cells
LGIC	Ligand-gated ion channel
MA	Membrane-associated
mAChR	Muscarinic acetylcholine receptor
MLA	Methyllycaconitine
MOD-1	Invertebrate 5-HT-gated chloride channel
mRNA	Messenger ribonucleic acid
N-terminus	Amino-terminus
nAChR	Nicotinic acetylcholine receptor
NAM	Negative allosteric modulator

NMJ	Neuromuscular junction
PAGE	Polyacrylamide gel electrophoresis
PAM	Positive allosteric modulator
PBS	Phosphate-buffered saline
PCP	Phencyclidine
PDL	Poly-D-lysine
PNS	Peripheral nervous system
RNA	Ribonucleic acid
RT	Reverse transcription
SAM	Silent allosteric modulator
SCAM	Substituted cysteine accessibility method
SD	Standard deviation
SDM	Site-directed mutagenesis
SEM	Standard error of the mean
SLURP-1	Secreted mammalian Ly-6/uPAR-related protein 1
TBS-345	4-(3-(4-bromophenyl)-5-phenyl-1H-1,2,4-triazol-1-yl)-benzenesulfonamide
TBS-346	4-(3-(4-bromophenyl)-5-(4-methoxyphenyl)-1H-1,2,4-triazol-1-yl)benzenesulfonamide
TBS-516	4-(5-benzyl-3-(4-bromophenyl)-1H-1,2,4-triazol-1-yl)-benzenesulfonamide
TBS-546	4-(3-(4-bromophenyl)-5-propyl-1H-1,2,4-triazol-1-yl)-benzenesulfonamide

TBS-556	4-(3-(4-bromophenyl)-5-phenethyl-1H-1,2,4-triazol-1-yl)-benzenesulfonamide
TMD	Transmembrane domain
TPMP <sup>+</sup>	Triphenylmethylphosphonium
TQS	cis-cis-4-(naphthalen-1-yl)-3a,4,5,9b-tetrahydro-3H-cyclopenta[c]quinoline-8-sulfonamide
UV	Ultraviolet
<i>X. laevis</i>	<i>Xenopus laevis</i>

## CHAPTER 1

# INTRODUCTION

---

## 1.1 THE NICOTINIC ACETYLCHOLINE RECEPTOR: A BRIEF HISTORY

### 1.1.1 Acetylcholine and chemical neurotransmission

The nicotinic acetylcholine receptor (nAChR) has been at the centre of receptor pharmacology research for almost a century. It was the first membrane receptor that was characterised and its biochemical isolation in 1970 constitutes a landmark in the history of pharmacology. The concept of a pharmacological receptor dates back to the mid 19<sup>th</sup> century, when Claude Bernard attempted to localise the site of action of the poison ‘curare’, which causes rapid muscle paralysis and death from asphyxiation. South American tribes were using preparations containing curare, isolated from plants such as *Strychnos toxifera*, *Chondrodendron tomentosum* and other related species, as poison for hunting arrows. Bernard studied curare samples and was able to demonstrate that the poison blocked the communication between a nerve and the striated muscle it innervated, while it did not affect smooth and cardiac muscles. He found that while he could not induce contraction of the paralysed frog muscle through stimulation of the associated nerve, the muscle would contract after direct electrical stimulation (Bernard, 1850). Although Bernard thought that the nerve was paralysed by curare, Arthur Vulpian later determined that curare acted on an ‘intermediate zone’ between the nerve terminal and the muscle, the motor endplate region (Vulpian, 1866). John Newport Langley first proposed the idea of the existence of a ‘receptive substance’ on the surface of skeletal muscle, in order to explain his observation that nicotine induced muscular contraction on chicken muscle, despite the absence of innervation. He also demonstrated that curare blocked the ability of nicotine to induce muscle contraction (Langley, 1907). Langley’s studies, taken together with the theory of chemical transmission proposed by Du Bois-Reymond (Du Bois-Reymond, 1877), gave rise to the concept of receptor-mediated transmission in the nervous system.

Acetylcholine was first identified in 1914 as a potential chemical neurotransmitter by Henry Dale, a student of Langley. Dale described how different esters and ethers of choline, such as acetylcholine mimicked the effects of muscarine and nicotine on smooth and striated muscles, respectively (Dale, 1914). However, at that time it was

unclear whether signalling in the nervous system was electrical or chemical in nature. It was not until Otto Loewi's famous experiment in 1921 that the theory of chemical transmission was demonstrated. For his experiment, Loewi used isolated frog hearts. Frog hearts were perfused via a cannula with Ringer's solution and the left vagus nerve was preserved. The vagus nerve of one heart was then electrically stimulated. This action had a well-known negative inotropic and chronotropic effect. Some of the solution that was bathing the first heart, which had been stimulated, was then transferred to the second heart and the same effect was observed, as if the vagus nerve of the second heart had also been stimulated. This effect could be blocked with atropine. Loewi's interpretation was that a heart-inhibiting substance, which he called '*Vagusstoff*', must have been released in the solution during vagus stimulation. He excluded potassium as a candidate substance, because the effects of potassium are not antagonised by atropine (Loewi, 1921). *Vagusstoff* was later identified as acetylcholine (Dale & Feldberg, 1934) and was also identified as an endogenous transmitter released by neurons innervating striated muscles (Dale *et al.*, 1936).

Following the work by Loewi and Dale, the location of Langley's receptive substance was determined by del Castillo and Katz. Using electrophysiological techniques and intracellular microinjection of acetylcholine, they found that at the neuromuscular junction, acetylcholine was acting on muscle cells rather than neurons. In addition, it was demonstrated that the acetylcholine receptors were located on the outer surface of the muscle cells, because acetylcholine did not induce muscle contraction when injected intracellularly (Del Castillo & Katz, 1955).

### 1.1.2 Purification of the nicotinic acetylcholine receptor

Two important steps that contributed to the purification of the nAChR were the discovery of a high affinity snake toxin (Lee *et al.*, 1967) and the use of a rich source of nAChRs from the electric fish. Soon after the identification of acetylcholine as the endogenous transmitter in the neuromuscular junction, the cholinergic nature of transmission in the electric ray, *Torpedo marmorata*, was established (Feldberg & Fessard, 1942). The electric organ (electroplaque tissue), which is common to all electric fish, such as *Torpedo marmorata*, *Torpedo californica* and *Electrophorus*

*electricus*, produces an electrical discharge to stun prey and deter predators. The electroplaques are embryonically derived from myoblasts and form a collection of modified motor endplates. The cholinergic nature of the electric organ was determined when it was shown that the electrical discharge could be blocked with curare (Dale *et al.*, 1936) and that acetylcholine could induce an electrical discharge (Feldberg & Fessard, 1942). The rich cholinergic innervation of postsynaptic membranes found in these electric organs made them an ideal source from which to isolate and purify the acetylcholine receptor.

The isolation of the acetylcholine receptor was greatly facilitated by the discovery of  $\alpha$ -bungarotoxin, a snake toxin from *Bungarus multicinctus*, which binds to the receptor with high affinity. The toxin was first isolated from snake venom in 1963 and was shown to induce muscle paralysis, by binding irreversibly to muscle tissue (Chang & Lee, 1963). This effect could be antagonized by (+)-tubocurarine (the active ingredient of curare) and it was proposed consequently that the toxin was acting on the nAChR (Lee & Chang, 1966).

The nAChR was first biochemically purified in 1970 by Changeux, Kasai and Lee, using the potent and highly selective  $\alpha$ -bungarotoxin and the electric organ of the electric fish, *Electrophorus electricus* (Changeux *et al.*, 1970). This was followed by the purification of the nAChR from *Torpedo marmorata* (Miledi *et al.*, 1971). The purified receptors were later shown to be pentameric, with five homologous subunits arranged around a centrally located transmembrane pore (Brisson & Unwin, 1985). There were four different subunits identified, named  $\alpha$ ,  $\beta$ ,  $\gamma$  and  $\delta$ , in order of their increasing molecular mass (Hucho *et al.*, 1976) and they were shown to adopt the stoichiometry  $(\alpha)_2\beta\gamma\delta$  to form the pentameric nAChR (Unwin, 1993).

### 1.1.3 Cloning of the nicotinic acetylcholine receptor

The purification of the nAChR from *Electrophorus electricus* and *Torpedo marmorata* made the cloning of the receptor possible. In 1983, the nAChR was the first ligand-gated ion channel (LGIC) for which the DNA and protein were defined using molecular genetics. Genes encoding  $\alpha$ ,  $\beta$ ,  $\gamma$  and  $\delta$  nAChR subunits were identified and cloned from *Torpedo californica* (Noda *et al.*, 1982; Noda *et al.*, 1983a; Noda *et al.*, 1983b).

Subsequently, many other nicotinic subunits have been identified. 17 nAChR subunits have been cloned in vertebrate species (Millar & Gotti, 2009) and many have been identified in invertebrates (Millar & Denholm, 2007; Millar & Lansdell, 2010).

## 1.2 ACETYLCHOLINE AND ITS RECEPTORS

### 1.2.1 Acetylcholine and cholinergic transmission

Acetylcholine (ACh) was the first neurotransmitter to be identified (Dale, 1914) and is one of the best characterised neurotransmitters. Acetylcholine is a low molecular weight transmitter (146.2 g/mol) and is an ester of acetic acid and choline. It is synthesised in neurons containing the enzyme choline acetyltransferase (ChAT) from the precursors choline and acetyl-CoA. These cholinergic neurons regulate neural transmission through the release of acetylcholine in the central and peripheral nervous system. Once released, acetylcholine is rapidly broken down into acetic acid and choline by the enzyme acetylcholinesterase (AChE) in the synaptic cleft of cholinergic synapses, thus limiting the duration of acetylcholine activity. Choline is then taken up in the presynaptic terminal by a choline carrier, where it is used in the acetylcholine synthesis again (Figure 1.1).

Acetylcholine is a major excitatory neurotransmitter in the peripheral nervous system (PNS) of numerous organisms, including humans, while its role in the central nervous system (CNS) is less well defined. In the somatic branch of the PNS, acetylcholine is the major neurotransmitter and it is released by motor neurons in the neuromuscular junction (NMJ), where it acts on the nAChRs located on the muscle cells and induces muscle contraction. Acetylcholine also plays a major role in the autonomic nervous system (ANS), with pre-ganglionic neurons being cholinergic in the sympathetic system and both pre- and post-ganglionic neurons being cholinergic in the parasympathetic system. Neuronal acetylcholine receptors are expressed widely in the CNS, although they are often pre-synaptic, suggesting that they play a largely modulatory role by regulating the release of a number of neurotransmitters, including dopamine, acetylcholine, 5-hydroxytryptamine (5-HT), glutamate, noradrenaline and  $\gamma$ -aminobutyric acid (GABA).

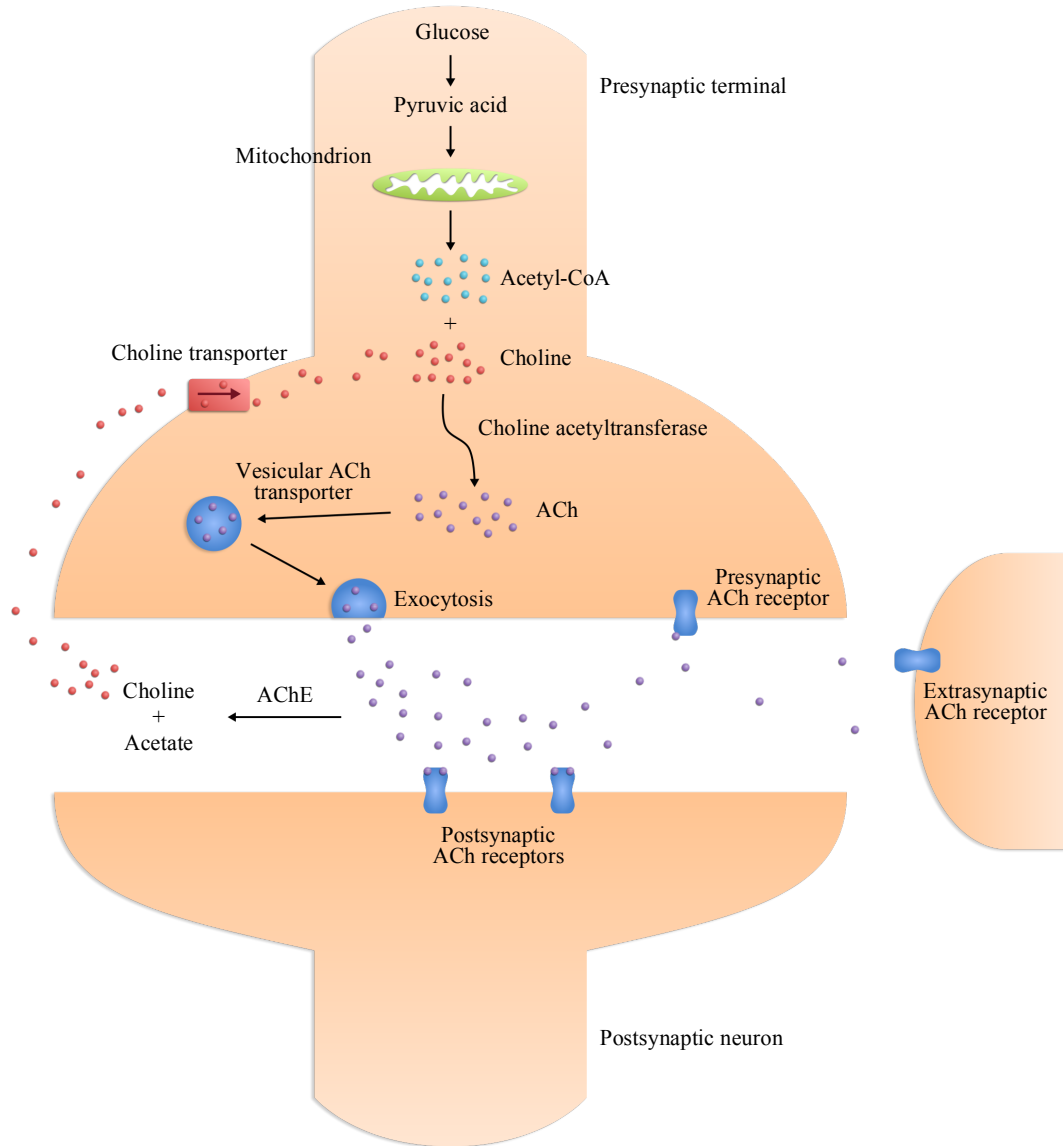


**Figure 1.1: Acetylcholine synthesis and degradation.**

Schematic of events at a cholinergic synapse. Acetylcholine (ACh) is made from acetyl-CoA and choline. In the synaptic cleft acetylcholine is broken down by the enzyme acetylcholinesterase (AChE) to choline and acetate. Choline is transported back to the axon terminal and is used to make more acetylcholine.

### 1.2.2 Acetylcholine receptors

Acetylcholine acts on two classes of receptors, termed nicotinic and muscarinic receptors, with this nomenclature being a consequence of their sensitivity to the alkaloids nicotine (isolated from the Solanaceae plant family) and muscarine (from *Amanita muscaria*), respectively. Both types of receptors are membrane proteins, but are structurally dissimilar, despite being the target for the same ligand. Nicotinic receptors are members of the ‘ionotropic’ family of receptors, or ligand-gated ion channels, which act via an intrinsic cation-permeable ion channel (Sine & Engel, 2006). Muscarinic acetylcholine receptors (mAChRs) are classified as ‘metabotropic’, or G protein-coupled receptors (GPCRs), which mediate their effects via heterotrimeric G proteins (Ishii & Kurachi, 2006).

## 1.3 NICOTINIC ACETYLCHOLINE RECEPTORS

### 1.3.1 The Cys-loop receptor superfamily

The nAChRs belong to a superfamily of structurally related LGICs, often referred to as ‘Cys-loop’ receptors. Cys-loop receptors contain a characteristic 13-residue motif flanked by cysteines forming a disulfide bridge. All members of the Cys-loop family of receptors are assembled from five homologous polypeptide subunits arranged around a centrally located pore, which forms the ion channel. Receptor subunits that belong to this family are typically 300 to 600 amino acids long. They contain a signal peptide, a large extracellular hydrophilic amino-terminal (N-terminal) domain, 4 membrane spanning  $\alpha$ -helical domains and a short extracellular carboxyl-terminal (C-terminal) domain (Figure 1.2).

In vertebrates, more than 40 Cys-loop receptor subunits have been identified and are further classified into distinct families, named according to neurotransmitter pharmacology: nAChRs and 5-HT type 3 receptors (5-HT<sub>3</sub>Rs) are receptors forming a cation channel, while GABA type A (GABA<sub>A</sub>) receptors, GABA type C (GABA<sub>C</sub>) receptors and glycine receptors form an anion-permeable channel (Ortells & Lunt, 1995; Sine & Engel, 2006). In invertebrates, GABA, 5-HT, glutamate, histidine and proton-gated receptors have also been identified, as well as nAChRs with anion conductance (Millar, 2003; van Nierop *et al.*, 2005).

Eukaryotic Cys-loop receptors are found on the extracellular membranes of numerous cell types, including muscle, epithelial and immune cells, but are expressed predominantly in the CNS and PNS, where they mediate and modulate synaptic transmission, neurotransmitter release and cell excitability. In prokaryotic organisms, these receptors are possibly involved in chemotaxis and cell adaptation towards the extracellular environment.

Extensive study of the genomes of different organisms have revealed the existence of prokaryotic homologues of Cys-loop receptors, including one of the cyanobacterium *Gloeobacter violaceus*, which functions as a proton-gated channel, but lacks the two characteristic cysteines (Bocquet *et al.*, 2007). Comparative genetic studies within the

superfamily suggest that the members originate from a common ancestral gene, with a high degree of mobility and losses throughout evolution (Ortells & Lunt, 1995).

### 1.3.2 Nicotinic acetylcholine receptors from the fish electric organ

As discussed in section 1.1.2, the nAChR was originally purified from the electric organs of the electric eel, *Electrophorus electricus* (Changeux *et al.*, 1970), and the electric ray, *Torpedo marmorata* (Miledi *et al.*, 1971) with the use of  $\alpha$ -bungarotoxin, a snake toxin with high affinity for the nAChR (Lee & Chang, 1966). Electroplaques from electric organs are highly innervated with cholinergic projections and densely packed with nAChRs, therefore providing an abundant source of receptors ideal for purification. Purification of the nAChRs was carried out initially from *Electrophorus electricus*, but the *Torpedo* rays contain a greater concentration of receptors and have been studied more extensively.

The nAChR purified from the fish electric organ was initially thought to contain four subunits (Miledi *et al.*, 1971), but was subsequently shown to contain five subunits arranged around a centrally located ion channel (Brisson & Unwin, 1985). *Torpedo* nAChRs can exist as pentameric monomers of ~250 kDa, or as disulfide-linked dimers of ~500 kDa, which migrate on a sucrose gradient with sedimentation coefficients of 9 S and 13 S, respectively (Gibson *et al.*, 1976; Reynolds & Karlin, 1978). Four different subunits were identified, named  $\alpha$ ,  $\beta$ ,  $\gamma$  and  $\delta$  (now more commonly referred to as  $\alpha 1$ ,  $\beta 1$ ,  $\gamma$  and  $\delta$ ), in order of their increasing molecular mass of approximately 40 kDa, 48 kDa, 62 kDa and 66 kDa, respectively (Hucho *et al.*, 1976), which adopt the stoichiometry  $(\alpha)_2\beta\gamma\delta$  to form the pentameric nAChR (Unwin, 1993). The structural information obtained from studies on *Torpedo* nAChRs has been proved very important for our understanding of the Cys-loop receptor structure and will be discussed in more detail in section 1.4.5.

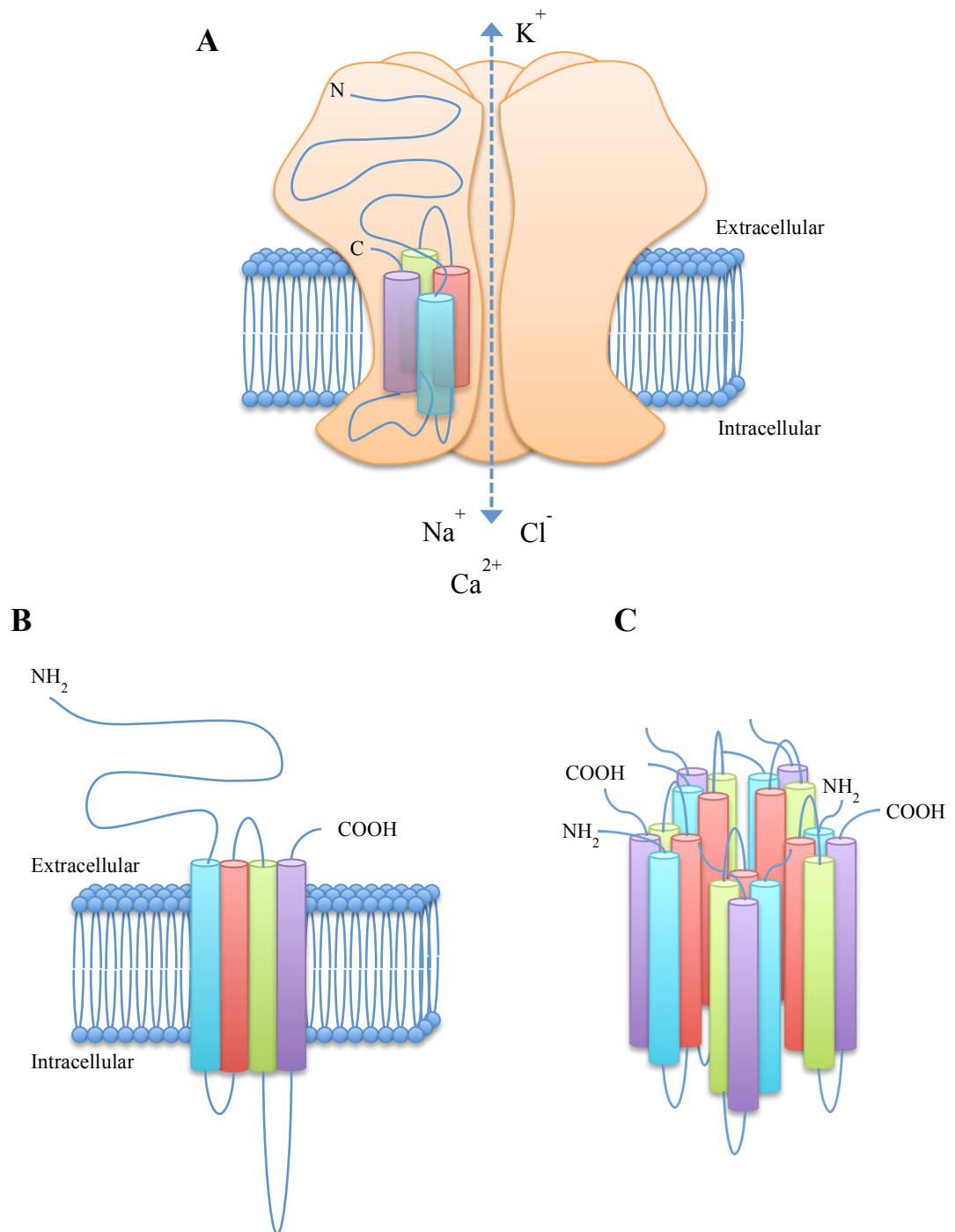


**Figure 1.2: Cys-loop receptor architecture and membrane topology.**

A) Side view of a Cys-loop receptor with two of the five subunits being shown embedded in the lipid bilayer. The arrows represent ion flow through the channel pore. Ion selectivity depends on the receptor family.

B) Schematic of the transmembrane topology of a single Cys-loop receptor subunit.

C) Five identical or homologous subunits co-assemble around a transmembrane pore, surrounded by a total of 20 transmembrane  $\alpha$ -helical domains. The second transmembrane domain of each subunit lines the pore.

### 1.3.3 Muscle nicotinic acetylcholine receptors

The nAChR of the vertebrate neuromuscular junction (NMJ) is one of the best-characterised LGICs, in large part due to the ease of access of this tissue, which allowed early physiologists to study it extensively. Muscle nAChR structure and function, as well as electrophysiological properties such as channel gating, conductance and desensitisation are well established (Peper *et al.*, 1982; Sakmann & Neher, 1984; Colquhoun & Ogden, 1988). These receptors are responsible for converting signals of the somatic PNS into skeletal muscle contractions. Most of the acetylcholine synthesised in the presynaptic nerve terminal is packed into synaptic vesicles at a high concentration (100 mM). Action potentials reaching the motor nerve endings trigger calcium entry, which stimulates acetylcholine release via exocytosis. At the NMJ, a single nerve impulse releases about 300 vesicles (about three million acetylcholine molecules). Acetylcholine then diffuses about 50 nm across the synaptic cleft to the post-synaptic membrane, rapidly reaching concentrations of 0.1-1.0 mM, and binds to the nAChRs (Katz & Miledi, 1972). Two molecules of acetylcholine bind to the receptors, stabilising the open conformational state, which allows primarily sodium, but also potassium and calcium, to flow through the ion channel resulting in depolarisation of the muscle cell. This depolarisation induces release of calcium from the sarcoplasmic reticulum, which results in muscle contraction via the sliding filament mechanism (Huxley, 2008). The acetylcholine molecules remain bound to the receptor for approximately 2 ms and are quickly hydrolysed by AChE after dissociation, making the entire process very rapid and brief (Katz & Miledi, 1972), which is very important for a synapse that has to initiate fast, fine-tuned muscular responses at high frequency.

The nAChR found at the vertebrate NMJ is very similar to the nAChR from the *Torpedo* electric organ. In both systems,  $\alpha$ -bungarotoxin and (+)-tubocurarine block nerve transmission. Both receptors are pentameric and the five subunits of the denervated rat muscle nAChR have apparent molecular weights similar to those of the *Torpedo* (Froehner *et al.*, 1977). The sequence of the mammalian foetal muscle nAChR subunits is similar to the ones from *Torpedo*, however an additional  $\gamma$ -like subunit, named  $\epsilon$ , has been identified in adult vertebrate muscle and is not present in the *Torpedo* (Takai *et al.*, 1985).

Mammalian muscle nAChRs exist as one of two types, with each type expressed according to the developmental stage of the animal. Foetal muscle nAChRs have the stoichiometry  $(\alpha 1)_2\beta 1\gamma\delta$ . However, in a developmental switch, the  $\gamma$  subunit is replaced by the  $\epsilon$  subunit found in adult muscle. This exchange is essential for the maturation of the NMJ and coincides with important developmental transitions (Missias *et al.*, 1996; Missias *et al.*, 1997). Recombinant nAChRs containing the  $\alpha 1$ ,  $\beta 1$ ,  $\gamma$  and  $\delta$  subunits expressed in *Xenopus laevis* oocytes had single-channel conductance of 39 pS, resembling those typical of foetal bovine muscle, while recombinant  $\alpha 1$ ,  $\beta 1$ ,  $\gamma$  and  $\epsilon$  subunits formed receptors with larger conductance of 59 pS and shorter open times, which resemble the channels found in the adult muscle (Mishina *et al.*, 1986). Muscle nAChRs are comparable to those of *Torpedo* and are collectively referred to as ‘muscle-type’ nAChRs.

#### 1.3.4 Neuronal nicotinic acetylcholine receptors

Neuronal nAChRs are expressed throughout the vertebrate central and peripheral nervous system. Although acetylcholine is an excitatory neurotransmitter, glutamate is the major excitatory neurotransmitter within the mammalian brain. However, nAChRs are found in many parts of the brain, suggesting that they have a modulatory role. In the PNS, nAChRs are expressed in both sympathetic and parasympathetic ganglia and control fast synaptic transmission.

In vertebrates, twelve neuronal nAChR subunits have been identified (Millar & Gotti, 2009) and they consist of nine  $\alpha$ -type subunits ( $\alpha 2$ - $\alpha 10$ ) and three  $\beta$ -type subunits ( $\beta 2$ - $\beta 4$ ). Subunits that have a pair of two conserved adjacent cysteines at positions that correspond to 192 and 193 at the *Torpedo*  $\alpha 1$  subunit are classified as  $\alpha$  subunits, while subunits lacking the conserved cysteines are classified as  $\beta$  subunits. The  $\alpha 8$  subunit has only been identified in avian species and appears to have no mammalian counterpart (Schoepfer *et al.*, 1990).

Neuronal nAChRs can exist as heteromeric complexes, consisting of two or more different subunits, with at least two  $\alpha$ - and two  $\beta$ -type subunits, or as homomeric complexes, containing only one type of subunit ( $\alpha 7$ - $\alpha 9$ ). However there is evidence that subunits  $\alpha 7$ - $\alpha 9$  do not exclusively form homomeric receptors and have been identified

in some heteromeric complexes, such as  $\alpha 7\beta 2$  (Khiroug *et al.*, 2002; Liu *et al.*, 2009) and  $\alpha 9\alpha 10$  (Sgard *et al.*, 2002). Homomeric nAChRs are blocked by  $\alpha$ -bungarotoxin, similar to the muscle nAChRs, and exhibit generally lower affinity for acetylcholine. Homomeric  $\alpha 7$  nAChRs account for the majority of  $\alpha$ -bungarotoxin binding sites in the brain, with the distribution of the  $\alpha 7$  gene transcript in rodent brain overlapping with  $\alpha$ -bungarotoxin binding sites (Séguéla *et al.*, 1993). There is considerable subtype diversity amongst neuronal nAChRs, but not all subunits can co-assemble to form functional receptors (Millar & Gotti, 2009). Subunit composition is important in determining receptor function and it will be discussed in more detail later.

## 1.4 STRUCTURE OF NICOTINIC ACETYLCHOLINE RECEPTORS

### 1.4.1 Subunit structure

The subunits within the nAChR superfamily have 40-50% amino acid sequence identity and they share the same membrane topology with other members of the Cys-loop receptor superfamily (Lester *et al.*, 2004). Each subunit is a polypeptide consisting of 450-700 amino acids, which assembles with other subunits to form the pentameric, membrane-spanning receptor, with a central, transmembrane ion pore (Figure 1.2).

Each nAChR contains a signal peptide of about 20 amino acids at its N-terminus, which is cleaved to form the mature protein. The N-terminal domain of the subunit is a large hydrophilic extracellular section of approximately 200 amino acids. It consists mainly of  $\beta$ -sheets that are separated by loop motifs, which form the main components of the agonist binding site (loops A-F) (Unwin, 2005). As mentioned previously, the characteristic 'Cys-loop', formed by the disulfide bridge of the cysteine residues that align to 128 and 142 of the *Torpedo*  $\alpha 1$  subunit, is also located at the N-terminus. This is followed by four hydrophobic transmembrane domains (TM1, TM2, TM3 and TM4), which adopt  $\alpha$ -helical structure (Unwin, 2005). The ion channel is lined primarily by residues of the TM2 domain, as demonstrated by photolabelling experiments with channel blockers such as chlorpromazine (Heidmann & Changeux, 1984; Giraudat *et al.*, 1989; Revah *et al.*, 1990) and substituted cysteine accessibility mutagenesis studies (Akabas *et al.*, 1994). The four transmembrane helices are separated by loops, of which the loop between TM3 and TM4 is much larger than the rest. This loop varies greatly between subunits and is thought to be involved in subunit trafficking to various cellular locations (Williams *et al.*, 1998; Xu *et al.*, 2006), as well as containing several potential sites for phosphorylation (Huganir & Greengard, 1990; Millar, 2002). Subunit sequences terminate with a short extracellular C-terminal domain, which has been implicated in oestradiol binding (Curtis *et al.*, 2002).

## 1.4.2 Stoichiometry

The nAChRs from both the *Torpedo* electric organ and the mammalian muscle are arranged as pentamers with the same stoichiometry  $(\alpha 1)_2\beta 1\gamma\delta$ , except that the  $\gamma$  subunit is replaced by the  $\epsilon$  subunit in adult muscle nAChRs (Sealock, 1982; Unwin, 1993). Studies on the *Torpedo* nAChR reveal that the subunits are arranged around the central channel pore in the anticlockwise order  $\alpha$ - $\delta$ - $\beta$ - $\alpha$ - $\gamma$ , as viewed from the extracellular side of the membrane (Unwin, 2005).

A classification system for the nAChR subunits has been proposed on the basis of amino acid sequence and gene structure (Corringer *et al.*, 2000). According to this system there are four subfamilies: subfamily I consists of subunits  $\alpha 9$  and  $\alpha 10$ ; subfamily II consists of subunits  $\alpha 7$  and  $\alpha 8$ ; subfamily III consist of subunits  $\alpha 2$ - $\alpha 6$  and  $\beta 2$ - $\beta 4$ ; subfamily IV consists of the muscle subunits  $\alpha 1$ ,  $\beta 1$ ,  $\gamma$ ,  $\delta$  and  $\epsilon$ . Subfamilies III and IV can be further divided into ‘tribes’ 1-3, depending on the role that each subunit plays in the receptor complex (Le Novère *et al.*, 2002). Subunits forming the  $\alpha$  and non- $\alpha$  components of the binding site belong to tribes 1 and 2, respectively. Subunits that do not participate in the formation of the agonist binding site belong to tribe 3. The subunits from subfamily III and IV are, therefore, further classified into tribe III-1:  $\alpha 2$ ,  $\alpha 3$ ,  $\alpha 4$  and  $\alpha 6$ ; tribe III-2:  $\beta 2$  and  $\beta 4$ ; tribe III-3:  $\alpha 5$  and  $\beta 3$ ; tribe IV-1:  $\alpha 1$ ; tribe IV-2:  $\gamma$ ,  $\delta$  and  $\epsilon$ ; tribe IV-3:  $\beta 1$ .

Subunit stoichiometry is significantly more diverse in neuronal nAChRs and, in some cases, the exact composition of endogenous receptors is not clear. However, a general rule of assembly from heterologous expression experiments in *Xenopus laevis* oocytes and mammalian cells is that heteromeric receptors consist of at least two subunits from tribe 1 and 2 and may contain one subunit from tribe 3 (Ramirez-Latorre *et al.*, 1996; Groot-Kormelink *et al.*, 1998). Subunits from subfamily I and II usually form homomeric receptors, although heteromeric receptors have been reported (Corringer *et al.*, 2000). The most common nAChR subtypes in the brain are the homomeric  $\alpha 7$  nAChRs and the heteromeric  $\alpha 4\beta 2^*$  nAChRs, while the  $\alpha 3\beta 4^*$  nAChR subtype is abundant in the PNS. The asterisks used in receptor nomenclature indicate the potential presence of additional nAChR subunits in the receptor complex. Even though  $\alpha 4\beta 2$  and  $\alpha 3\beta 4$  heteromeric receptors are thought to consist of two  $\alpha$  and three  $\beta$  subunits,

evidence exists for alternative stoichiometries with three  $\alpha$  and two  $\beta$  subunits, which confer different pharmacological properties to the receptor (Zwart & Vijverberg, 1998; Nelson *et al.*, 2003).

### 1.4.3 Extracellular agonist binding domain

The nAChR binding site for traditional agonists and competitive antagonists, also termed orthosteric binding site, is located at the extracellular N-terminal domain. The  $\beta$ -sheet-rich N-terminal domains of each subunit fold into a  $\beta$ -barrel structure with an inner and outer sheet (Unwin, 2005). The  $\beta$ -strands are connected with short hairpin loops, which are essential for ligand binding (Corringer *et al.*, 2000).

The agonist-binding site is located at the interface between subunits ( $\alpha 1/\gamma$  and  $\alpha 1/\delta$  in muscle-type nAChRs) and this has been determined by several approaches. *Torpedo*  $\alpha$  subunits co-expressed with either  $\gamma$  or  $\delta$  subunits form functional binding sites (Blount & Merlie, 1989). Affinity labelling experiments using competitive antagonists were found to label the  $\alpha$  subunits primarily and the  $\gamma$  and  $\delta$  subunits to a lesser extent (Pedersen & Cohen, 1990; Corringer *et al.*, 2000). These unequal levels of labelling suggested an asymmetric binding site, with the principal binding component found at the  $\alpha$  subunit and the complementary component found at the  $\gamma/\epsilon$  and  $\delta$  subunits in the case of muscle-type nAChRs, or  $\beta$  subunits in the case of heteromeric neuronal nAChRs.  $\alpha$  subunits carry both the principal and complementary binding components in the case of homomeric receptors.

Individual residues important for agonist binding have been identified mostly in the loops connecting the  $\beta$ -sheets. These loops, defined as binding components A-F, exist in the principal subunit (A-C) and the complementary (D-F). However some residues that contribute to the binding site are not located on these loops (Lester *et al.*, 2004). Residues that were labelled by photoaffinity ligands in the principal component of the  $\alpha$  subunit in the *Torpedo* include Trp 86 and Tyr 93 in loop A, Trp 149 and Tyr 151 in loop B and Tyr 190, Cys 192, Cys 193 and Tyr 198 in loop C. The  $\gamma$  and  $\delta$  subunits were labelled in homologous positions  $\gamma$ Trp 55 and  $\delta$ Trp 57 in loop D and  $\gamma$ Tyr 111 and  $\delta$ Arg 113 in loop E (Corringer *et al.*, 2000). These residues have been shown by homology modelling to form an electron-rich 'aromatic box'. Sequence comparisons

also reveal that these residues are highly conserved in the  $\alpha$ 2- $\alpha$ 4 and  $\alpha$ 6- $\alpha$ 8 subunits (loop A-C) in the  $\beta$ 2,  $\beta$ 4,  $\alpha$ 7 and  $\alpha$ 8 subunits (loop D) (Corringer *et al.*, 2000).

#### 1.4.4 Ion channel

The ion channel pore is located within the 20  $\alpha$ -helices bundle (four from each subunit) of the nAChR transmembrane domain. Early affinity labelling experiments with channel blockers, such as chlorpromazine, identified key residues contributing to the ion channel. Those residues are located at positions 2', 6', 9', 13' and 20' of the TM2 domains of the five subunits (Heidmann & Changeux, 1984; Giraudat *et al.*, 1989; Corringer *et al.*, 2000), using the terminology of Christopher Miller (Miller, 1989), which assigns position 1' to the first amino acid (towards the N-terminus) of the TM2 domain. The labelling of all five subunits is consistent with the TM2 domains of each subunit contributing equally to form the ion channel, with the same side of each TM2 domain facing the pore and pentameric rings of homologous amino acids forming the channel. The pattern of labelling is also consistent with the predicted  $\alpha$ -helical structure of the TM2 domain (Corringer *et al.*, 2000). Later studies, using the substituted cysteine accessibility method (SCAM) confirmed the importance of the TM2 domain in lining the channel (Akabas *et al.*, 1992) and located the site in the pore where water could not permeate when the channel is closed closer to the cytoplasmic side of the lumen rather than midway along the TM2 domain (Wilson & Karlin, 1998). The secondary structure of this part of the subunit appears to deviate from the  $\alpha$ -helical structure, which is adopted by the rest of the TM2, to a looser loop structure, with adjacent residues being labelled (Wilson & Karlin, 1998).

As well as allowing the flux of ions, the ion channel pore also contains the ion selectivity filter. The whole channel is thought to act as a cation-selective filter, with side chains located throughout the channel lumen contributing to an overall negative charge (Unwin, 2005). Conserved rings of hydrophilic residues also exist at the cytoplasmic border (Corringer *et al.*, 2000). Mutation of a number of residues in these ring domains results in altered cation selectivity (Cohen *et al.*, 1992), conversion of cationic to anionic selectivity (Galzi *et al.*, 1992) and disruption of calcium permeability (Bertrand *et al.*, 1993). This region containing the conserved rings constitutes the most

restricted part of the channel in its open conformation and is involved in monovalent ion selection, possibly through a specific dehydration mechanism (Wang *et al.*, 2008).

The narrowest region of the pore is located at the intracellular end of TM2, near  $\alpha$ T244 (*Torpedo* numbering), and is proposed to act as the gate of the channel, by determining ion flow (Villarroel *et al.*, 1991). A highly conserved leucine is found in the middle of the TM2 in almost all subunits of the Cys-loop receptor superfamily. This leucine is found at the 9' position (L9') and has a profound effect in channel gating. A number of roles have been proposed for this residue. Initially, a model was proposed where this residue moves into the lumen of the channel during desensitisation to form a non-conducting state (Revah *et al.*, 1991; Bertrand *et al.*, 1992). This conclusion was largely supported by studies on nAChRs with mutations on the 9' position, which dramatically reduce the desensitisation of the macroscopic current and convert antagonists into agonists. A different model was proposed by Nigel Unwin from examination of the early *Torpedo* nAChR structure in both the closed and open channel conformation (Unwin, 1993, 1995). According to this model, the leucine residues from the five subunits serve as the gate of the pore, through leucine-leucine interactions that form a constricted ring in the closed conformation of the channel. Further studies on the muscle receptor, showing that mutating individual L9' residues in a receptor have an additive and independent effect, rendered the desensitisation theory unlikely (Filatov & White, 1995). However, it was suggested that L9' mutations stabilised the open state rather than disrupting the closed state of the receptor, because the main effect that could be observed was prolonged open-times, without an increase in the opening rate (Filatov & White, 1995). In contrast, a different study on the muscle nAChRs demonstrates that mutating the L9' residue appears to increase the opening rate and contribute to an increased presence of monoliganded and unliganded open channels, supporting the notion that L9' mutations could exert their effects by disrupting the closed gate (Labarca *et al.*, 1995).

#### 1.4.5 Three-dimensional structure

Structure-function studies of the Cys-loop receptor superfamily have been initially guided by electron microscopy images of the *Torpedo* nAChR (Unwin, 2005) and by

crystal structures of a family of soluble proteins, the acetylcholine-binding proteins (AChBP), which display high sequence homology with the extracellular domain of the nAChRs (Brejc *et al.*, 2001). This was followed by studies that initially obtained high-resolution X-ray crystals of bacterial homologues of the Cys-loop receptors (Hilf & Dutzler, 2008; Bocquet *et al.*, 2009; Hilf & Dutzler, 2009), followed by crystal structures of eukaryotic Cys-loop receptors (Hibbs & Gouaux, 2011; Hassaine *et al.*, 2014; Miller & Aricescu, 2014). These studies, which revealed the three-dimensional structure of the receptors in different conformational states, have provided insight into the mechanism of channel opening and closing, as well as the changes that occur after agonist binding.

#### *1.4.5.1 Electron microscopy of Torpedo nAChRs*

Cryo-electron microscopy studies of the *Torpedo* nAChR provided three-dimensional structure of the closed receptor at a resolution of 17 Å (Toyoshima & Unwin, 1990), 9 Å (Unwin, 1993) and finally 4 Å (Unwin, 2005). Traditional X-ray crystallography has been proved difficult for intact nAChRs, since they contain hydrophobic transmembrane regions that prevent the generation of a three-dimensional crystal. Therefore, these studies were performed on purified post-synaptic membranes from the *Torpedo* electric organ, which contain helically ordered nAChRs. Numerous two-dimensional images were obtained from the crystals and were subsequently averaged to provide the structural model of the receptor (Figure 1.3).

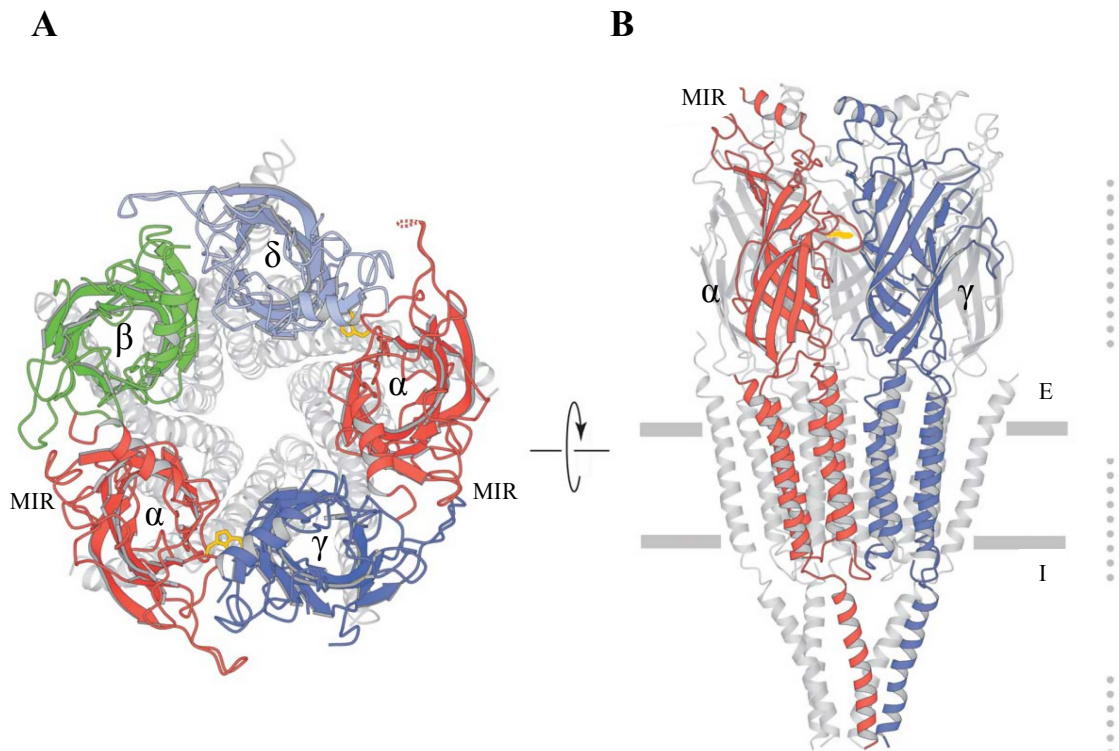


**Figure 1.3: High-resolution structure of the *Torpedo* nAChR at 4 Å (figure from (Unwin, 2005)).**

Ribbon diagrams of the *T. marmorata* nAChR as viewed (A) from the synaptic cleft and (B) parallel with the membrane plane. For clarity, only the ligand-binding domain is highlighted in (A) and only the front two subunits are highlighted in (B). The receptor subunits are highlighted in red ( $\alpha$ ), green ( $\beta$ ), blue ( $\gamma$ ) and light blue ( $\delta$ ). Also shown are locations of the  $\alpha$ Trp149 residue (gold), the main immunogenic regions (MIR) and the lipid bilayer (horizontal bars; E: extracellular; I: intracellular). The dotted lines on the right denote the three main zones of subunit-subunit contacts. The apex of the C-loop of  $\alpha_\delta$  (broken trace in (A)) was not visible in the densities.

A vast amount of structural information about the extracellular agonist binding domain and the pore of the channel has been obtained from structural studies (sections 1.4.3 and 1.4.4). The length of the receptor was calculated to be approximately 160 Å, with the N-terminal domain protruding out of the membrane by ~80 Å and the dimensions of each subunit being approximately 30 Å × 40 Å × 160 Å (Unwin, 2005). The intracellular part of the receptor remains largely unresolved, possibly because of its increased flexibility, resulting in a not well-defined diffraction pattern. However, a part of the intracellular TM3-TM4 loop that adopts a more rigid structure compared to the rest of the loop (the membrane associated (MA)-helix) has been resolved in the refined 4 Å structure (Unwin, 2005). Low-resolution images of the *Torpedo* nAChR have also been obtained at the open state (Unwin, 1995). This was achieved by spraying acetylcholine on the tube preparation, followed by rapid freezing, in order to preserve the conformational state. Comparison of these receptors in the closed and open states can provide some insight into the conformational changes taking place after agonist binding (Unwin, 1995).

#### 1.4.5.2 *Snail acetylcholine binding protein*

The high-resolution crystal structure of the molluscan acetylcholine-binding protein (AChBP) has greatly contributed to our knowledge of the nAChR extracellular ligand binding domain structure. The AChBP is a water-soluble protein that was first identified in the mollusc *Lymnea stagnalis*. It is present in cholinergic synapses and it is believed to regulate synaptic transmission, by binding acetylcholine and limiting its action in the synapse (Smit *et al.*, 2001). It forms a homopentameric structure and has been identified as a homologous protein to the N-terminus of the nAChR, with 20-24% amino acid identity, but lacking the transmembrane and intracellular domains present in the superfamily (Smit *et al.*, 2001). In addition to acetylcholine, the AChBP has also been shown to bind other known nicotinic agonists and competitive antagonists, such as nicotine, tubocurarine, and  $\alpha$ -bungarotoxin (Smit *et al.*, 2001). Because this protein is water-soluble, it is easier to crystallise and, therefore, its structure has been obtained at high resolution using X-ray crystallography. Its structure has been resolved at 2.7 Å (Brejc *et al.*, 2001), 2.2 Å (Ulens *et al.*, 2006) and 1.74 Å (Hansen & Taylor, 2007) (Figure 1.4).

The three-dimensional structure of AChBP is remarkably similar to the N-terminus of the *Torpedo* nAChR. Several crystal structures and the co-crystallisation of the protein with various ligands have assisted in the study and interpretation of nAChR ligand binding and have identified different movements associated with agonist and antagonist binding. The AChBP has been crystallised in the presence of nicotine and carbachol (Celie *et al.*, 2004) and the antagonists  $\alpha$ -conotoxin (Celie *et al.*, 2005) and  $\alpha$ -cobratoxin (Bourne *et al.*, 2005).

#### *1.4.5.3 Mouse $\alpha 1$ subunit bound to $\alpha$ -bungarotoxin*

An additional interesting structure is the 1.94 Å high-resolution crystal structure of the extracellular domain of the mouse  $\alpha 1$  nAChR subunit bound to  $\alpha$ -bungarotoxin (Dellisanti *et al.*, 2007). This structure was shown to be similar to the *Torpedo* nAChR and the AChBP, with some exceptions. Firstly, hydrophilic residues form a water-filled pocket deep in the core of the  $\alpha 1$  subunit, which is absent in the AChBP and not detectable in the *Torpedo* structure. Secondly, the structure contained an N-linked glycosylation site at residue Asn 151, which appears to be important in receptor maturation (Dellisanti *et al.*, 2007).

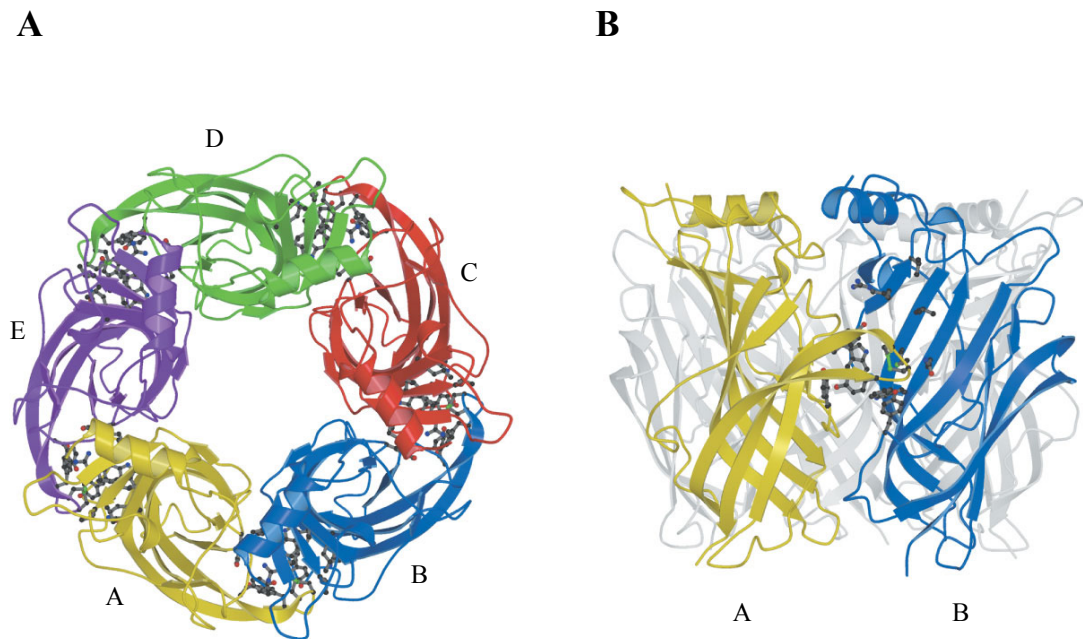


**Figure 1.4: High-resolution structure of the *Lymnaea* ACh-binding protein (figure from (Brejc *et al.*, 2001)).**

A) Ribbon diagram of the pentameric structure of AChBP, with different colours representing each protomer. Subunits are labelled anti-clockwise, with A–B, B–C, C–D, D–E and E–A forming the plus and minus interface side, with the principal and complementary ligand-binding sites, respectively (ball-and-stick representation).

B) View of the AChBP pentamer perpendicular to the five-fold axis. The equatorially located ligand-binding site (ball-and-stick representation) is highlighted only in the A (yellow) – B (blue) interface.

#### 1.4.5.4 Crystal structures of bacterial homologues

High-resolution crystal structures of two bacterial receptors that are homologous to the Cys-loop receptors have been obtained recently (Figure 1.5). The crystal structure of the *Erwinia chrysanthemi* ligand-gated ion channel (ELIC) was obtained at a resolution of 3.3 Å (Hilf & Dutzler, 2008) and the crystal structure of the *Gloeobacter violaceus* ligand-gated ion channel (GLIC) was obtained at 3.1 Å and 2.9 Å (Bocquet *et al.*, 2009; Hilf & Dutzler, 2009).

There is evidence for the Cys-loop superfamily having a prokaryotic origin, with more than 20 homologues having been discovered in bacteria (Tasneem *et al.*, 2005). The crystal structures of ELIC and GLIC revealed that, even though these receptors have only 16-20% sequence identity with the nAChRs and are not gated by acetylcholine, they still adopt a highly similar general architecture to that of the *Torpedo* nAChR and the AChBP (Hilf & Dutzler, 2008; Bocquet *et al.*, 2009; Hilf & Dutzler, 2009). This includes extracellular structures, such as the  $\beta$ -sheets and the connecting loops with semi-conserved 'Cys-loops' that lack the flanking cysteines, as well as the transmembrane domains, which include the  $\alpha$ -helices. Most importantly, the crystal structure of ELIC is thought to represent a receptor in the closed conformation, while GLIC a receptor in the open conformation and, therefore, these structures provide valuable information about the changes that occur after agonist binding. A mechanism of channel opening has been suggested from the study of these structures, which consists of both a quaternary twist and a tertiary deformation (Bocquet *et al.*, 2009; Hilf & Dutzler, 2009), which will be discussed in more detail later. More recently, the structure of GLIC has been established in a locally closed conformation (Prevost *et al.*, 2012) and in a closed conformation at neutral pH (Sauguet *et al.*, 2014).

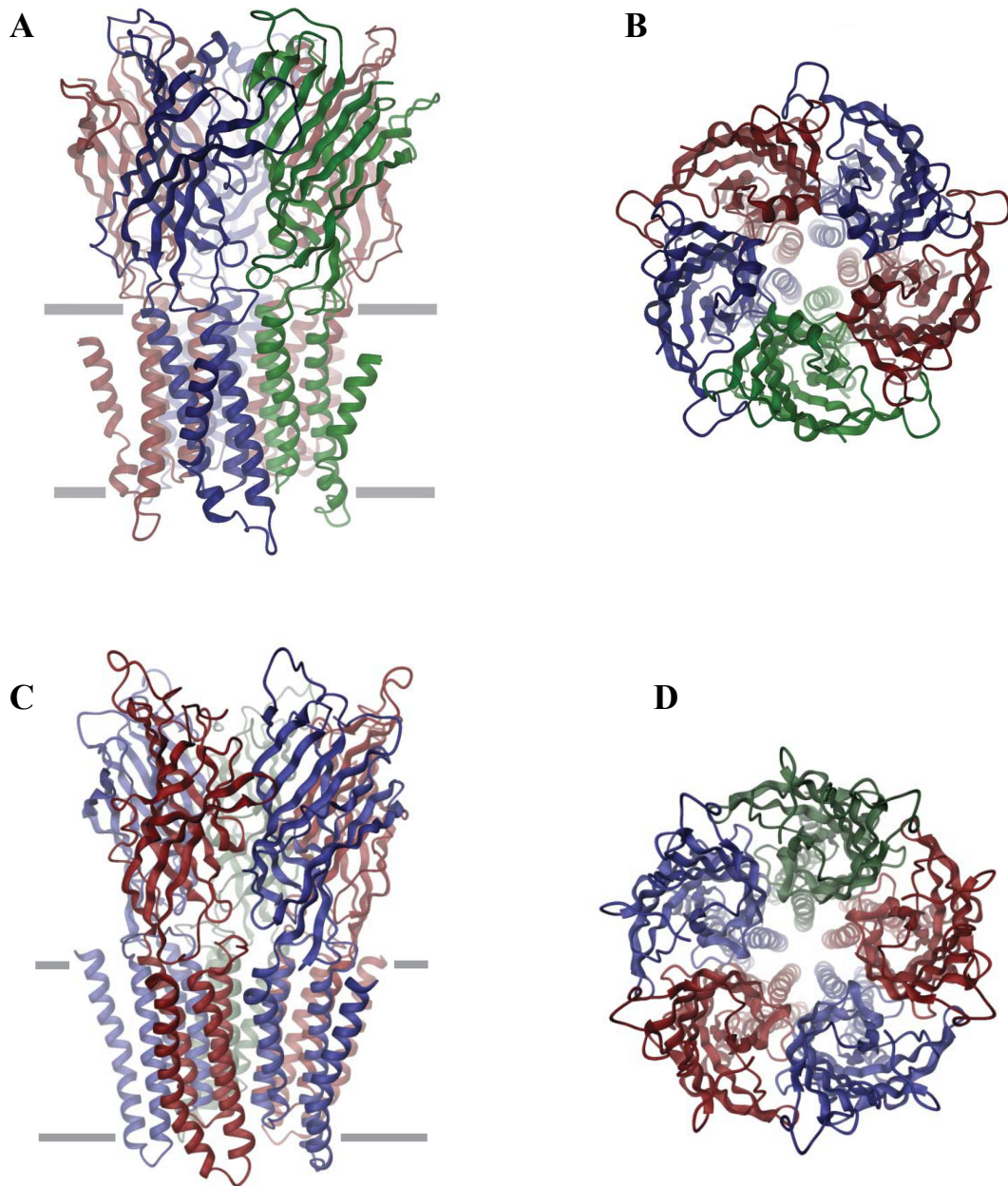


**Figure 1.5: High-resolution structure of the nAChR homologues ELIC and GLIC (figure from (Hilf & Dutzler, 2008, 2009)).**

ELIC structure in an apparently closed conformation at 3.3 Å resolution. A) Ribbon representation of ELIC viewed parallel with the membrane plane, with the extracellular site on top. The approximate membrane boundaries are indicated by the horizontal bars. B) Structure of the pentameric channel as viewed from the extracellular site (Hilf & Dutzler, 2008).

GLIC structure in an apparently open conformation at 3.1 Å resolution. C) Ribbon representation of GLIC viewed parallel with the membrane plane, with the extracellular site on top. The approximate membrane boundaries are indicated by the horizontal bars. D) Structure of the pentameric channel as viewed from the extracellular site (Hilf & Dutzler, 2009).

#### 1.4.5.5 Crystal structures of eukaryotic Cys-loop receptors

Recently, high-resolution crystal structures of three members of the Cys-loop receptor superfamily bound to a number of ligands have been obtained. The X-ray structure of the glutamate-gated chloride channel (GluCl) from *Caenorhabditis elegans* (*C. elegans*) was obtained at 3.3 Å resolution, initially bound to the allosteric agonist ivermectin. Crystal structures of the GluCl-ivermectin complex were also obtained in the presence of the endogenous neurotransmitter glutamate, as well as in the presence of the open channel blocker picrotoxin (Hibbs & Gouaux, 2011). These structures provided some insight into the structure of an open state of a eukaryotic Cys-loop receptor, the basis of ion selectivity and channel block, as well as the mechanism of action of ivermectin. The same group subsequently published crystal structures of the *C. elegans* GluCl without ivermectin, in the ‘*apo*’ (or unbound and presumably closed) state, which provided some information about the shut gate of the channel and the mechanism of receptor opening and closing (Althoff *et al.*, 2014). In addition, the crystal structure of the human GABA<sub>A</sub> receptor (β3 homopentamer) has been resolved at 3 Å (Miller & Aricescu, 2014). The receptor was crystallised in the presence of an agonist, benzamidine, and analysis of the structure suggests that the receptor has been captured in the closed, desensitised state. The study provides insight in the mechanism of numerous human disease mutations on the GABA<sub>A</sub> receptor and also suggests that an N-linked glycan in a conserved site in the extracellular domain may facilitate signal transduction between the extracellular agonist-binding domain and the transmembrane domain. Furthermore, the crystal structure of the mouse 5-HT<sub>3A</sub>R was obtained at 3.5 Å resolution, in complex with an antibody termed VHH15, which helped yield crystals with higher resolution and was also a potent inhibitor of the 5-HT<sub>3A</sub> receptor (Hassaine *et al.*, 2014). All of the structures above were obtained after cleaving the entire or part of the intracellular TM3-TM4 loop, in order to obtain the high-resolution crystals.

## 1.5 FUNCTION OF NICOTINIC ACETYLCHOLINE RECEPTORS

### 1.5.1 Agonist binding

The conserved aromatic residues present in the extracellular binding site of the nAChR and the bridged cysteine residues in loop C form an electron dense structure at the subunit interface, termed the ‘aromatic box’ (Unwin, 2005) (as discussed in section 1.4.3). The binding of acetylcholine involves a cation- $\pi$  interaction, a non-covalent interaction between a cation and the electron-rich  $\pi$  system, with the conserved tryptophan residue of loop B, making the quaternary ammonium group of the agonist a key pharmacophore. The importance of the aromatic box and, particularly, Trp 149 in stabilising agonist interactions was initially demonstrated by studies substituting this residue with unnatural tryptophan derivatives (Zhong *et al.*, 1998). Furthermore, introduction of tethered quaternary ammonium groups on Trp 149 renders the receptor constitutively active. A number of additional conserved aromatic residues on the principal component and charged residues on the complementary component have been shown to stabilise acetylcholine binding (Sine *et al.*, 1994; Nowak *et al.*, 1995; Corringer *et al.*, 2000). Cation- $\pi$  interactions of ligands with the aromatic box appear to be important for agonist binding in a number of Cys-loop receptors, including the 5-HT<sub>3</sub> receptor (Beene *et al.*, 2002), the invertebrate 5-HT-gated chloride channel (MOD-1) (Mu *et al.*, 2003) and GABA receptors (Padgett *et al.*, 2007). The study on the MOD-1 receptor revealed that the ammonium moiety of 5-HT establishes a cation- $\pi$  interaction with a non-homologous Trp residue to that of the vertebrate 5-HT<sub>3</sub> receptor, suggesting that agonist binding resembles a ‘wedge’ mechanism, rather than a specific ‘lock and key’ (Mu *et al.*, 2003). In further support of this theory, the receptor becomes constitutively active if appropriate groups are tethered at any of several positions in the box (Li *et al.*, 2001).

X-ray structures demonstrating the cation- $\pi$  interactions have been reported for AChBP (Brejc *et al.*, 2001), GLIC (Bocquet *et al.*, 2009; Hilf & Dutzler, 2009), ELIC (Hilf & Dutzler, 2008), GluCl (Hibbs & Gouaux, 2011) and GABA<sub>A</sub> receptors (Miller & Aricescu, 2014). The conformation of loop C is postulated to reflect the functional state of the receptor, contracted in agonist-bound structures and open in antagonist-bound

structures (Bourne *et al.*, 2005; Hansen *et al.*, 2005; Unwin, 2005; Huang *et al.*, 2013). Overall, the mechanism of agonist binding in pentameric LGICs appears to be remarkably conserved, from bacteria to humans.

## 1.5.2 Gating

The conformational changes that take place in the receptor after agonist binding to produce an ion-conducting receptor are commonly referred to as the gating isomerisation. High-resolution structures, which provide a snapshot of the receptor in different conformational states, in combination with complementary and time-resolved analyses, such as rate-equilibrium free energy relationships (Auerbach, 2007; Lee *et al.*, 2008) and molecular dynamics stimulation (Taly *et al.*, 2005; Nury *et al.*, 2010; Calimet *et al.*, 2013) have provided information on the sequence of structural events that translate agonist binding into channel opening 60 Å away. Gating appears to be a progressive stepwise isomerisation, also referred to as a conformational wave, that starts from loops A, B and C of the orthosteric binding site, propagates to the interface of the extracellular domain and transmembrane domain via a rearrangement of the extracellular  $\beta$ -sandwich and ends at the transmembrane helices to ultimately open the gate (Grosman *et al.*, 2000; Purohit *et al.*, 2007; Calimet *et al.*, 2013; Sauguet *et al.*, 2014).

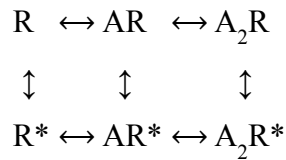
The quaternary twist model, first identified by normal mode analysis of a homology model of the  $\alpha 7$  nAChR (Taly *et al.*, 2005), was initially suggested to be directly involved in receptor gate opening, as it involves a global reorganisation with significant reshaping of subunit interfaces. This structural rearrangement is described as an opposite rotation of the extracellular domain relative to the transmembrane domain, in anticlockwise manner as viewed from the extracellular site. Indeed, comparison of the crystal structures of the prokaryotic homologues GLIC at pH 4 (open channel) and GLIC at pH 7 and ELIC (closed channels) showed a global quaternary twist occurring upon receptor activation, but also highlighted the important tertiary changes that take place; in particular a significant tilting of the TM2 helices (Hilf & Dutzler, 2008) (Bocquet *et al.*, 2009; Sauguet *et al.*, 2014). Furthermore, the structure of the locally closed conformation of GLIC, which involves a closed ion pore in a receptor containing

most of the open-channel features, indicates that the quaternary twist alone is not a sufficient mechanism to explain channel opening.

Computational analyses, based on molecular dynamics, provide evidence for an indirect coupling mechanism by monitoring the spontaneous relaxation of the open-channel structure upon agonist unbinding. The simulation of the open GLIC channel transferred to neutral pH (proton agonists removed) (Nury *et al.*, 2010) and that of GluCl with ivermectin removed (Calimet *et al.*, 2013) showed that global twisting initiates channel closing by facilitating the untilting of the TM2 helices. Furthermore, the simulation of GluCl when ivermectin was removed predicted a large outward expansion of the  $\beta$ -sandwich on the extracellular domain would be essential for communication between the agonist binding domain and the ion pore (Calimet *et al.*, 2013). Such a radial expansion or ‘blooming’ of the extracellular domain has been reported in the crystal structures of GLIC at neutral pH (Sauguet *et al.*, 2014) and for GluCl in the absence of ivermectin (Althoff *et al.*, 2014). Importantly, the reported unbound structure of GluCl appears to be 10° more twisted than the active state (Calimet *et al.*, 2013), confirming the occurrence of both twisting and blooming during structural transitions to the resting state.

Single-channel electrophysiological data show that agonist binding at the extracellular binding site modulates the opening rate of the receptor with little or no effect on closing (Jadey *et al.*, 2011), while computer simulations of the active state of GluCl showed that ivermectin binding at the transmembrane domain controls ion channel closing (Calimet *et al.*, 2013). These findings suggest that the rate determining step on gating would be mediated by different events in the forward (activation) and backward (deactivation) direction, possibly with un-blooming being the rate determining step on activation and twisting on deactivation.

In order to describe the mechanism of receptor gating, the extended del Castillo and Katz mechanism can be used. Even though the gating isomerisation consists of a wave of conformational changes, some distinct end states can be assigned, with the arrows between them describing the separating energy barrier, which equals the sum of the energy barriers for all unassigned conformational states in between.



In the scheme above, R represents the closed receptor, A the agonist molecule and R\* the receptor in the open state. An important observation is that nAChRs in the absence of an agonist can isomerise between R and R\* (Jackson, 1984, 1986) by approximately the same mechanism as with an agonist (Purohit & Auerbach, 2009). At synapses, nAChRs have a very low probability of adopting an open channel conformation in the absence of an agonist, because the equilibrium constant for unliganded, or spontaneous, gating is small. The nAChRs have at least two agonist binding sites and the equilibrium constant for gating increases as the number of bound agonist molecules increase.

Recent studies on the glycine receptor and muscle nAChR have identified a conformational state before the channel opens that could potentially explain some of the differences between full and less efficacious (partial) agonists. These studies propose that an intermediate ‘primed’ or ‘flipped’ conformation exists, where the receptor has an increased affinity for the agonist, but is still shut (Burzomato *et al.*, 2004). Electrophysiological data suggest that the shut-open isomerisation is similar for both full and partial agonists. The distinction between full and partial agonists is not due to partial agonists being inefficient at eliciting the change between shut and open states, but between shut and ‘flipped’ states (Lape *et al.*, 2008). Further studies on mutated muscle nAChRs have proposed the existence of two primed conformational states, which elicit receptor openings with different durations, depending on whether one or two agonist molecules are bound on the receptor (Mukhtasimova *et al.*, 2009).

### 1.5.3 Desensitisation

The continuous exposure of nAChRs to a high concentration of agonist elicits a decrease of ion conductance following activation, a process called desensitisation (Katz & Thesleff, 1957). Desensitisation, which is a feature of most LGICs, modulates the frequency of the conducting states of the receptor and it is thought to play an important role in shaping neuronal networks that are associated with memory and learning,

whereas altered desensitisation mechanisms are implicated in a number of pathophysiological conditions (Ochoa *et al.*, 1989; Dehaene & Changeux, 1991).

At the molecular level, the current declines because the receptor adopts stable desensitised conformations that have high affinity for the agonist, but little or no conductance. Details of the desensitisation process remain largely unknown, although single-channel electrophysiological data have helped establish some facts. These include that agonist molecules at the binding sites are not necessary for nAChRs to enter and recover from desensitisation (Purohit & Auerbach, 2009) and that, upon removal of the agonist, the desensitised receptor can return to the resting closed state without channel opening (Katz & Thesleff, 1957). However, in diliganded nAChRs, entry into the desensitised state usually occurs from the active state (Auerbach & Akk, 1998). In addition, at least four different desensitised states can be seen in the single-channel record, but it is not clear how they are interconnected (Elenes & Auerbach, 2002).

Electron microscopy and X-ray crystallography studies have largely failed to capture a receptor in a desensitised state, even though the time required for crystallisation when an agonist is present would be more likely to capture such a state. In contrast, the crystal structure of a number of prokaryotic (Bocquet *et al.*, 2009; Hilf & Dutzler, 2009) and eukaryotic receptors (Hibbs & Gouaux, 2011) has been resolved in a presumed active state, while only one structure has so far been resolved in a desensitised state (Miller & Aricescu, 2014). This latter structure captures the human homopentameric  $\beta 3$  GABA<sub>A</sub> receptor with the channel forming a closed gate at the base of the pore. This crystal structure was obtained in the presence of the agonist benzadamide and therefore it is assumed to represent a desensitised state. In addition the geometry of the pore was shown to differ from the ELIC and *Torpedo* closed conformations and resembling more the open conformations of GLIC and GluCl (Miller & Aricescu, 2014).

## 1.6 LIGANDS OF NICOTINIC ACETYLCHOLINE RECEPTORS

### 1.6.1 Orthosteric agonists

Compounds that bind at the receptor and promote ion channel opening are described as agonists. Agonists that bind at the same or overlapping site as the endogenous neurotransmitter acetylcholine are termed orthosteric agonists. The agonist binds according to its affinity for the receptor site, determined by the equilibrium association constant. Once bound, they shift the isomerisation equilibrium towards the active state, a property measured by their efficacy. The potency of an agonist, which is usually denoted by the effective concentration (EC), is a function of both affinity and efficacy (Colquhoun & Patrick, 1997). Agonists of nAChRs can exhibit different pharmacological properties, including various degrees of efficacy, leading to full (same efficacy as acetylcholine), partial (lower efficacy than acetylcholine) and super (higher efficacy than acetylcholine) agonists, as well as nicotinic subtype selectivity.

Acetylcholine is the endogenous agonist of both muscle and neuronal nAChRs. Choline, the precursor of acetylcholine, is also an endogenous agonist on the homomeric  $\alpha 7$  nAChR (Papke *et al.*, 1996). However, many other natural and synthetic agonists have been identified over the years, which have been used as medicines, as well as poisons and pesticides. Even though orthosteric agonists usually display limited subtype-selectivity, marked differences are often present in the rank order of potency for different nicotinic subtypes. Several nicotinic agonists have been isolated from natural sources, notably nicotine, cytisine and epibatidine, providing lead structures for the design of numerous synthetic agents.

Nicotine is the active compound of tobacco, which is responsible for the addictive and cognitive effects of smoking. It is an alkaloid isolated from the Solanaceae family of plants, with the species *Nicotiana tabacum* being cultivated globally for tobacco production. Neuronal heteromeric receptors, especially  $\alpha 4\beta 2$ , show the highest sensitivity for nicotine, while muscle and homomeric  $\alpha 7$  nAChRs are less sensitive (Flores *et al.*, 1992).

Cytisine is another example of a naturally occurring nAChR agonist, isolated from plants of the Fabaceae family. It has strong binding affinity for neuronal  $\beta$ 2- and  $\beta$ 4-containing nAChRs, with much lower affinity for neuronal homomeric and muscle nAChRs (Luetje & Patrick, 1991; Chavez-Noriega *et al.*, 1997). Cytisine has been used for the treatment of tobacco addiction and it exerts its effects as a partial nAChR agonist, rather than an antagonist (West *et al.*, 2011). Similarly, varenicline, a synthetic drug with structural similarities to cytisine, is also approved as a smoking cessation aid. As a partial agonist, it reduces cravings and decreases the pleasurable effects of smoking (Jorenby *et al.*, 2006).

Epibatidine is an alkaloid isolated from the poisonous dart frog *Epipedobates anthonyi*. It is an agonist on all nAChRs, but shows higher potency for the  $\alpha$ 4 $\beta$ 2 subtype. Epibatidine was found to be a potent analgesic, however its therapeutic index is very narrow (Spande *et al.*, 1992; Badio & Daly, 1994).

### 1.6.2 Competitive antagonists

Competitive antagonists are compounds that bind at the orthosteric binding site of the receptor, but do not promote channel opening. They are termed ‘competitive’ because they compete with agonists for the same binding site. Traditionally, true competitive antagonists are ligands that bind to the receptor and have no efficacy, meaning they do not affect the gating isomerisation kinetics. Antagonists that shift the gating equilibrium towards the inactive state are called inverse agonists (negative efficacy). Depending on the binding affinity of the competitive antagonist for the nAChR, the compounds bind in a reversible, or irreversible manner. The block by reversible competitive antagonists is surmountable by increasing concentrations of the agonist. As with nAChR agonists, numerous competitive antagonists have been isolated from natural sources, such as d-tubocurarine,  $\alpha$ -bungarotoxin and methyllycaconitine (MLA) (Daly, 2005).

Tubocurarine is the active ingredient of curare, which was used as a paralysing poison on tips of hunting darts by South American indigenous tribes. Tubocurarine is an alkaloid purified from the tree bark of *Chondodendron tomentosum* and it is a potent antagonist on all nAChRs (King, 1946). Muscle-type nAChRs appear to have two

binding sites with different affinities for tubocurarine (Blount & Merlie, 1989; Pedersen & Papineni, 1995).

As discussed earlier, the snake toxin  $\alpha$ -bungarotoxin, isolated from the venom of *Bungarus multicinctus*, has been useful for the purification of the *Torpedo* nAChR (Chang & Lee, 1963; Changeux *et al.*, 1970). This toxin is a very high affinity competitive antagonist on the *Torpedo* and muscle nAChR and, therefore, the block it produces is practically irreversible.  $\alpha$ -bungarotoxin is also an antagonist on the neuronal  $\alpha 7$  homomeric receptors (Séguéla *et al.*, 1993; Gopalakrishnan *et al.*, 1995). Snake neurotoxins can be radio-iodinated (Eldefrawi & Fertuck, 1974) or tritiated (Jones & Thompson, 1980) without loss of their pharmacological properties. These radioligands have played an important role in localisation and characterisation of nAChRs.

The marine snails of the genus *Conus* contain in their venom multiple classes of peptide neurotoxins, called conotoxins, targeting LGICs. The largest group of characterised conotoxins is the class of  $\alpha$ -conotoxins, which are selective competitive antagonists of the muscle and neuronal nAChRs (McIntosh *et al.*, 1999). Conotoxins display great molecular diversity and members of the family of  $\alpha$ -conotoxins have evolved to selectively target different nAChR subtypes, including  $\alpha 7$ ,  $\alpha 3\beta 2$ ,  $\alpha 3\beta 4$ ,  $\alpha 4\beta 2$ ,  $\alpha 9\alpha 10$  and  $\alpha 6$ -containing nAChRs (Lebbe *et al.*, 2014). This selectivity has significantly contributed to nAChR *in vivo* and *in vitro* characterisation, as well as the dissection of the functional role of specific receptor subtypes (Terlau & Olivera, 2004; Livett *et al.*, 2006).

MLA, an alkaloid isolated from *Delphinium* species (Aiyar *et al.*, 1979), is a potent and highly selective competitive antagonist of  $\alpha 7$  nAChRs (Macallan *et al.*, 1988; Ward *et al.*, 1990; Alkondon *et al.*, 1992). However, MLA also blocks heteromeric nAChRs at higher concentrations (Alkondon *et al.*, 1992; Drasdo *et al.*, 1992). Dihydro- $\beta$ -erythroidine (Dh $\beta$ E) and other alkaloids isolated from the coral tree and other members of the genus are examples of very potent,  $\alpha 4\beta 2$ -selective competitive antagonists (Lukas, 1989; Decker *et al.*, 1995)

### 1.6.3 Channel blockers

Channel blockers are an important category of ligands that have therapeutic value, such as local anaesthesia. They exert their effects in a manner distinct from competitive antagonists, by binding at the channel lumen and preventing the flow of ions. Channel blockers of nAChRs include chlorpromazine (CPZ), phencyclidine (PCP) and triphenylmethylphosphonium (TPMP<sup>+</sup>) (Arias, 1998). Early studies with channel blockers contributed significantly towards the characterisation of the nAChR ion pore (Heidmann & Changeux, 1984; Giraudat *et al.*, 1989). However, many molecules block the channel pore of the nAChR at high concentrations, including the orthosteric agonists acetylcholine and nicotine.

### 1.6.4 Allosteric modulators

In addition to agonists and competitive antagonists, other ligands modulate the gating process, by binding at a region distinct to the orthosteric site or the channel lumen. These compounds are termed allosteric modulators and can either potentiate the effects of an agonist on channel activation (called positive allosteric modulators or PAMs), or inhibit the agonist effects (negative allosteric modulators, or NAMs). Allosteric modulators often have no intrinsic activity and only modulate the effects of an agonist; however allosteric ligands that can induce receptor activation in the absence of an orthosteric agonist, termed allosteric agonists, have been identified recently.

#### 1.6.4.1 Positive allosteric modulators and allosteric agonists

Much of the recent work concerning nAChR PAMs has focussed on the homomeric  $\alpha 7$  receptor, one of the main nAChR subtypes expressed in the mammalian brain. It is somewhat atypical in the sense that it displays a relatively low sensitivity to acetylcholine and unusually fast desensitisation, in addition to high calcium permeability (Couturier *et al.*, 1990). In addition to potentiating agonist peak responses, some PAMs acting on  $\alpha 7$  nAChRs have been reported to cause a slowing of receptor desensitisation, whereas other PAMs have little or no effect on the rate of receptor desensitisation. As a consequence of this differing effect on desensitisation,  $\alpha 7$ -selective PAMs have been classified into two categories: type I and type II (Bertrand & Gopalakrishnan, 2007; Grønlien *et al.*, 2007). Type I PAMs increase peak current in the

presence of an orthosteric agonist, without having an effect on receptor desensitisation. Type II PAMs, on the other hand, significantly reduce the fast desensitisation of  $\alpha 7$  receptors. A further difference between  $\alpha 7$ -selective type I and type II PAMs is the ability of type II PAMs to allow receptor reactivation from the desensitised state (Hurst *et al.*, 2005; Grønlien *et al.*, 2007). However, this distinction between type I and type II PAMs is a classification that is based on observed properties, rather than a defined mechanism of action or from information about the binding site. Although classifying PAMs acting on  $\alpha 7$  nAChRs as either type I or type II can be useful in some circumstances, it is clear that this is an over-simplification and that PAMs with intermediate properties have been identified.

An early demonstration of allosteric modulation of nAChRs came from the observation that the divalent cation calcium potentiated  $\alpha 7$  nAChR currents in a voltage-independent manner (Mulle *et al.*, 1992; Vernino *et al.*, 1992). Early studies with  $\alpha 7$  nAChRs also demonstrated the ability of ivermectin, a large macrocyclic lactone, to potentiate agonist-evoked responses (Krause *et al.*, 1998). Ivermectin was found to increase acetylcholine-evoked current on  $\alpha 7$  nAChRs, reduce the half maximal effective concentration ( $EC_{50}$ ) of acetylcholine, convert the partial agonist dimethylphenylpiperazinium (DMPP) into a full agonist and modestly reduce desensitisation. In addition, the AChE inhibitor galanthamine has been reported to act as a relatively weak and non-selective PAM of  $\alpha 7$  nAChRs (Lopes *et al.*, 2007). Similarly, genistein, a tyrosine kinase inhibitor, and 5-hydroxyindole (5-HI) are also weak and relatively non-selective PAMs on  $\alpha 7$  receptors (Zwart *et al.*, 2002; Grønlien *et al.*, 2007). A number of proteins have also been reported to enhance agonist responses on the  $\alpha 7$  receptors, including a secreted mammalian Ly-6/uPAR-related protein (SLURP-1) and bovine serum albumin (BSA) (Chimienti *et al.*, 2003; Conroy *et al.*, 2003). All of these compounds have only minimal effects on the rapid desensitisation of  $\alpha 7$  nAChRs and, in most cases, do not display high selectivity for this receptor subtype.

Over the past decade there has been considerable interest from pharmaceutical companies and academic research groups in developing PAMs of  $\alpha 7$  nAChRs that display higher potency and greater subtype selectivity. PNU-120596 was the first  $\alpha 7$ -selective PAM identified that had a dramatic effect on receptor desensitisation and is classified as a type II PAM (Hurst *et al.*, 2005). PNU-120596 is one of the best-studied

PAMs in pre-clinical models of pain, ischaemia, schizophrenia and cognitive deficits (Hurst *et al.*, 2005; Thomsen *et al.*, 2011; McLean *et al.*, 2012; Callahan *et al.*, 2013; Freitas *et al.*, 2013; Kalappa *et al.*, 2013; Sun *et al.*, 2013). Other  $\alpha 7$ -selective PAMs that cause a dramatic reduction in receptor desensitisation and, consequently, have been described as type II PAMs include TQS (Grønlien *et al.*, 2007) and A-867744 (Faghieh *et al.*, 2009; Malysz *et al.*, 2009).

A feature of compounds such as PNU-120596, TQS and A-867744 is that they cause little or no receptor activation in the absence of an orthosteric agonist. However, a derivative of TQS, 4BP-TQS, has been shown to activate the receptor in the absence of an orthosteric agonist (Gill *et al.*, 2011). In contrast to the activation of  $\alpha 7$  nAChRs by acetylcholine, activation by 4BP-TQS occurs with minimal desensitisation (Gill *et al.*, 2011). In addition, the agonist dose-response curve with 4BP-TQS is steeper and maximal responses are substantially larger than observed with orthosteric agonists, all of which argues that activation by 4BP-TQS occurs by a different mechanism of action (Gill *et al.*, 2011). As will be discussed in section 1.6.4.3, there is evidence that 4BP-TQS causes receptor activation via a distinct allosteric site and, as a consequence, it has been described as an allosteric agonist (Gill *et al.*, 2011). Subsequently, a number of TQS derivatives that have agonist and PAM effects have been developed and characterised (Gill *et al.*, 2012; Ondrejcek *et al.*, 2012). Interestingly, very minor changes to ligand structure, such as altering the size of a single halogen atom or the pattern of methyl substitution of an aromatic ring, can convert type II PAMs into potent allosteric agonists (Gill *et al.*, 2012; Gill-Thind *et al.*, 2015).

In addition to allosteric modulators that reduce levels of agonist-induced desensitisation, a number of  $\alpha 7$ -selective type I PAMs have been described in recent years as a consequence of high-throughput compound screening. Amongst the first to be examined in detail were the urea derivative NS-1738 (Timmermann *et al.*, 2007) and CCMI (also described as ‘Compound 6’) (Ng *et al.*, 2007). Other compounds acting as type I PAMs of  $\alpha 7$ , but displaying less subtype selectivity, are LY-2087101, LY-2087133 and LY-1078733 (Broad *et al.*, 2006). In addition to potentiating  $\alpha 7$  nAChRs, these compounds also potentiate  $\alpha 2\beta 4$ ,  $\alpha 4\beta 2$  and  $\alpha 4\beta 4$  subtypes (Broad *et al.*, 2006).

Whilst the distinction between type I and type II PAMs can be useful, there is increasing evidence that it is an over-simplification. A number of studies have reported  $\alpha 7$ -selective PAMs with effects on desensitisation that are intermediate between classical type I and type II PAMs (Dunlop *et al.*, 2009; Dinklo *et al.*, 2011). Another  $\alpha 7$ -selective PAM, RO5126946, has effects on desensitisation that are typical of a type II PAM (Sahdeo *et al.*, 2014). However, it lacks the ability to facilitate reactivation of desensitised  $\alpha 7$  nAChRs, a feature that is normally considered to be characteristic of type II PAMs (Sahdeo *et al.*, 2014).

Heteromeric  $\alpha 4\beta 2$ -containing nAChRs are an abundant receptor subtype expressed in the human brain and have been a target for the development of orthosteric ligands, including the partial agonists varenicline and cytisine, which have been approved as aids for smoking cessation (Rollema *et al.*, 2007). There has also been considerable interest in the development of PAMs that target  $\alpha 4\beta 2$ -containing receptors.

Steroids are among compounds that act as endogenous PAMs of nAChRs.  $17\beta$ -oestradiol increases acetylcholine-evoked currents in the human  $\alpha 4\beta 2$  receptor and, more modestly, in the  $\alpha 4\beta 4$  receptor (Curtis *et al.*, 2002). Galanthamine also potentiates  $\alpha 4\beta 2$  nAChRs, in addition to a number of other nAChR subtypes including  $\alpha 6\beta 4$  and  $\alpha 3\beta 4$  nAChRs (Samochocki *et al.*, 2003). Both oestradiol and galanthamine increase the potency of the orthosteric agonist, without having a significant effect on the size of the maximum response. In contrast, desformylflustrabromine (dFBr) and some of its derivatives are  $\alpha 4\beta 2$  selective PAMs that increase the size of the maximum response and have very modest effect on the potency of the agonist (Sala *et al.*, 2005; Kim *et al.*, 2007). LY-2087101 is another relatively non-selective nAChR PAM that increases maximum response size as well as potency of acetylcholine on  $\alpha 4\beta 2$  nAChRs (Broad *et al.*, 2006). Other compounds that have been reported to potentiate  $\alpha 4\beta 2$  and  $\alpha 4\beta 4$  nAChRs include the muscarinic antagonists atropine and scopolamine (Zwart & Vijverberg, 1997; Smulders *et al.*, 2005).

Receptors containing  $\alpha 4$  and  $\beta 2$  subunits can exist in two different stoichiometries with distinct functional properties. The  $(\alpha 4)_3(\beta 2)_2$  subtype has a lower sensitivity to acetylcholine and it displays higher permeability to calcium and faster desensitisation kinetics in comparison to the  $(\alpha 4)_2(\beta 2)_3$  subtype (Zwart & Vijverberg, 1998; Buisson &

Bertrand, 2001; Nelson *et al.*, 2003; Moroni *et al.*, 2006). In addition, the two subtypes display some ligand selectivity. NS9283 (alternatively A-969933) is an  $\alpha 4\beta 2$ -selective PAM with *in vivo* efficacy in models of pain (Lee *et al.*, 2011; Zhu *et al.*, 2011). NS9283 is selective for the  $(\alpha 4)_3(\beta 2)_2$  subtype and only shifts the agonist concentration response curve to the left without an effect on maximum response (Timmermann *et al.*, 2012; Grupe *et al.*, 2013; Olsen *et al.*, 2013). NS206, a PAM thought to act through a distinct binding site, can activate both stoichiometries and increases maximum efficacy (Olsen *et al.*, 2013). In contrast, HEPES is a selective PAM for the  $(\alpha 4)_2(\beta 2)_3$  subtype (Weltzin *et al.*, 2014).

In recent years, PAMs of  $\alpha 3$ -containing nAChRs have also been reported (Levandovski *et al.*, 2003; Wu *et al.*, 2008; Bürgi *et al.*, 2014). For example, the anthelmintic compounds levamisole and morantel potentiate acetylcholine response on  $\alpha 3\beta 2$  and  $\alpha 3\beta 4$ . Zinc potentiates a number of nAChR subtypes, including both  $\alpha 3$ - and  $\alpha 4$ -containing subtypes (Hsiao *et al.*, 2001; Vázquez-Gómez & García-Colunga, 2009) but, interestingly, shows selectivity for  $\alpha 4\beta 2$  nAChRs with the  $(\alpha 4)_3(\beta 2)_2$  stoichiometry (Hsiao *et al.*, 2006; Moroni *et al.*, 2008). Recent studies aimed at identifying binding sites for modulators such as zinc and morantel are discussed in section 1.6.4.3.

#### 1.6.4.2 Negative allosteric modulators

In addition to PAMs, several endogenous and synthetic nAChR NAMs have been identified. NAMs are non-competitive antagonists that bind at an allosteric site and shift the equilibrium towards a non-conducting state. Open-channel blockers, which bind at the lumen of the open channel and sterically occlude the flow of ions, are not usually considered as NAMs, because they do not affect the gating or desensitisation equilibrium. However, it can be difficult to differentiate between open-channel block and increase in desensitisation (Gumilar *et al.*, 2003). The tricyclic antidepressants imipramine, amitriptyline and doxepin have been shown to function as NAMs on nAChRs by mainly increasing the desensitisation rate of the receptor (Gumilar *et al.*, 2003). In addition, mecamylamine is a well-characterised non-selective nAChR NAM (Varanda *et al.*, 1985; Banerjee *et al.*, 1990; Martin *et al.*, 1990; Papke *et al.*, 2001). Endogenous NAMs include progesterone and neurosteroids (Arias, 1998; Pereira *et al.*, 2002) and Lynx-1 and 2 on  $\alpha 7$  and  $\alpha 4\beta 2$  receptors (Ibañez-Tallon *et al.*, 2002; Tekinay *et al.*, 2009). Zinc inhibits responses on  $(\alpha 4)_2(\beta 2)_3$  and  $\alpha 3\beta 2$  in a voltage-dependent

manner, while it inhibits  $(\alpha 4)_3(\beta 2)_2$  subtypes at high concentrations in a voltage-independent manner (Moroni *et al.*, 2008). The endocannabinoid anandamide is also a NAM of nAChRs and other types of ligand- and voltage-gated ion channels (Oz, 2006).

#### 1.6.4.3 Allosteric binding sites

Several experimental techniques have been employed with the aim of identifying the binding sites of allosteric modulators on nAChRs. The availability of a readily purified preparation of nAChR, for example from the electric organ of the marine ray *Torpedo*, has facilitated affinity labelling experiments that have provided direct evidence for the binding of ligands to sites other than the orthosteric site. This approach has identified sites for a variety of non-competitive antagonists interacting with the transmembrane domain (Pedersen *et al.*, 1992; Middleton *et al.*, 1999; Chiara *et al.*, 2003; Ziebell *et al.*, 2004; Nirathanan *et al.*, 2008; Hamouda *et al.*, 2014). Affinity labelling studies have also identified binding sites for cholesterol within the nAChR transmembrane domain (Hamouda *et al.*, 2006). In addition, more indirect approaches, such as computer-docking studies, have been used. For example, docking studies with cholesterol have predicted binding sites in cavities within the transmembrane region (Brannigan *et al.*, 2008). Other experimental techniques aimed at identifying binding sites have included the construction of recombinant subunit chimeras, site-directed mutagenesis and SCAM. However, it is important to use a degree of caution when interpreting such studies. For example, if the mutation of an amino acid results in a change in the pharmacological properties of a ligand, it is not necessarily appropriate to conclude that this is a consequence of a change to the binding site (Colquhoun, 1998). Nevertheless, the combined use of a variety of approaches, including electrophysiological, pharmacological, biochemical and computational techniques can provide strong evidence for the location of ligand binding sites (Millar, 2009).

Various sites and amino acids have been shown to be important for allosteric modulation. Studies using  $\alpha 7/5$ -HT3 subunit chimeras, site-directed mutagenesis and docking simulations, have led to the proposal that  $\alpha 7$ -selective allosteric modulators such as LY-2087101, NS-1738 (type I PAMs) and PNU-120596 (a type II PAM) act via a binding site within an intra-subunit cavity that is located between the four transmembrane helices of a single subunit (Young *et al.*, 2008; Collins *et al.*, 2011). More recent studies have examined a series of nineteen  $\alpha 7$ -selective allosteric

modulators that differ only in methyl substitution of a single aromatic ring (Gill-Thind *et al.*, 2015). Despite relatively small changes in chemical structure, the compounds examined displayed five distinct pharmacological effects on  $\alpha 7$  nAChRs. These included effects typical of type I PAMs, type II PAMs, NAMs, silent allosteric modulators (SAMs) and allosteric agonists (Gill-Thind *et al.*, 2015) and it has been proposed that all of these pharmacological effects can arise from ligands binding to a broadly similar or overlapping site located within the previously identified intrasubunit transmembrane cavity (Gill-Thind *et al.*, 2015). Other studies are consistent with  $\alpha 7$ -selective allosteric modulators such as NS-1738, PNU-120596 and A-867744 interacting with a transmembrane site (Bertrand *et al.*, 2008; Malysz *et al.*, 2009; Sattelle *et al.*, 2009). As would be expected, allosteric modulators that have been proposed to bind in a transmembrane location do not displace the binding of orthosteric radioligands such as [ $^3$ H]-MLA or [ $^3$ H]- $\alpha$ -bungarotoxin (Timmermann *et al.*, 2007; Malysz *et al.*, 2009; Gill-Thind *et al.*, 2015). However, some unexpected results have been reported for the  $\alpha 7$ -selective PAM A-867744. Although A-867744 does not displace binding of [ $^3$ H]-MLA from  $\alpha 7$  nAChRs, in contrast to other PAMs, it has been reported to displace the binding of another agonist ([ $^3$ H]-A-585539) that is thought to interact with the orthosteric site (Malysz *et al.*, 2009).

A transmembrane binding site in nAChRs has also been proposed for monoterpine compounds such as menthol and propofol (Ashoor *et al.*, 2013a; Jayakar *et al.*, 2013) and is consistent with evidence supporting a transmembrane binding site for monoterpinines on other pentameric LGICs (Nury *et al.*, 2011; Ashoor *et al.*, 2013b; Yip *et al.*, 2013; Lynagh & Laube, 2014; Lansdell *et al.*, 2015). Affinity labelling studies with a photoreactive analogue of propofol identified three sites at which it bound within the transmembrane domain of muscle-type nAChRs, but concluded that the functionally relevant site for the inhibitory action of propofol was an intrasubunit site (Jayakar *et al.*, 2013), similar to that described earlier for  $\alpha 7$ -selective allosteric modulators such as NS-1738, PNU-120596 and 4BP-TQS (Young *et al.*, 2008; Gill *et al.*, 2011). Similarly, there is evidence for a transmembrane binding site for nAChR NAMs such as the endogenous cannabinoid anandamide (Oz *et al.*, 2004; Oz *et al.*, 2005; Jackson *et al.*, 2008) and also antihistamine compounds (Sadek *et al.*, 2015).

As discussed earlier, the  $\alpha 7$  subunit forms a homomeric nAChR. However, in addition, it can co-assemble with the  $\beta 2$  subunit to form a heteromeric  $\alpha 7\beta 2$  complex (Khiroug *et al.*, 2002). One difference that has been reported in the allosteric modulation of these two nAChR subtypes is that  $\alpha 7\beta 2$  receptors, but not  $\alpha 7$  receptors, are inhibited by the volatile anaesthetic isoflurane (Mowrey *et al.*, 2013). On the basis of mutagenesis and computer docking studies, it has been proposed that isoflurane binds to the  $\beta 2$  transmembrane domain (Mowrey *et al.*, 2013). This is consistent with evidence for a transmembrane binding site for anaesthetics on other LGICs (Olsen *et al.*, 2014b).

There is also evidence that the macrocyclic lactone ivermectin acts as a nAChR PAM by interacting with a transmembrane site (Collins & Millar, 2010). Recently, a high-resolution X-ray structure was obtained of ivermectin bound to a prokaryotic glutamate-gated chloride channel (GluCl) with close structural similarity to nAChRs (Hibbs & Gouaux, 2011). These findings are consistent with ivermectin binding to an intersubunit transmembrane site, rather than the intrasubunit transmembrane site that has been proposed for smaller allosteric modulators (Young *et al.*, 2008; Gill *et al.*, 2011; Jayakar *et al.*, 2013). Spinosad, like ivermectin, is a macrocyclic lactone pesticide that acts as an allosteric modulator of nAChRs (Kirst, 2010). Recent studies of spinosad-resistant insects has identified a resistance-associated point mutation in the nAChR transmembrane domain that is consistent with spinosad binding to nAChRs in a similar intersubunit transmembrane site to the known binding site of ivermectin in GluCl (Puinean *et al.*, 2013).

In addition to the transmembrane domain, there are many other potential sites at which allosteric modulators might potentially interact with nAChRs, as is the case with other LGICs (Hogg *et al.*, 2005; Forman & Miller, 2011). Whereas there are five potential agonist binding sites in a homomeric nAChR, there are expected to be just two or three functioning orthosteric agonist sites in heteromeric nAChRs. For example, the acetylcholine binding site in neuronal heteromeric nAChRs is at the interface between an  $\alpha$  and  $\beta$  subunit, in which the  $\alpha$ -type subunit forms the principal face and the  $\beta$ -type subunit the complementary face (designated  $\alpha(+)/\beta(-)$ ). However, it is possible that compounds can bind at equivalent positions at other subunit interfaces, for example at a  $\beta(+)/\alpha(-)$  interface. Indeed, this has been proposed as a mechanism by which compounds such as morantel and dFBr can potentiate agonist-evoked responses (Wu *et*

*al.*, 2008; Seo *et al.*, 2009; Cesa *et al.*, 2012; Short *et al.*, 2015; Weltzin & Schulte, 2015). Similarly, compounds interacting with the extracellular  $\alpha 4/\alpha 4$  interface of  $(\alpha 4)_3(\beta 2)_2$  nAChR can act as PAMs (Olsen *et al.*, 2013; Olsen *et al.*, 2014a), just as the agonist interaction with this site may explain partial agonist activity (Mazzaferro *et al.*, 2011; Mazzaferro *et al.*, 2014). In contrast, it has been proposed that HEPES acts as a potentiator of  $\alpha 4\beta 2$  nAChRs by interacting with the  $\beta(+)/\beta(-)$  interface and, as a consequence, is selective for receptors with the  $(\alpha 4)_2(\beta 2)_3$  stoichiometry (Weltzin *et al.*, 2014). Additionally, a binding site for NAMs at the  $\alpha(+)/\beta(-)$  interface of  $\alpha 3\beta 4$  and  $\alpha 4\beta 2$  nAChRs has been predicted on the basis of computer docking studies and molecular dynamic simulations (González-Cestari *et al.*, 2009; Henderson *et al.*, 2010; Pavlovicz *et al.*, 2011).

As described earlier, the AChE inhibitor galanthamine is a relatively weak PAM of  $\alpha 7$  nAChRs (Maelicke & Albuquerque, 2000) and has been proposed to bind at the extracellular domain at a site that is distinct from the acetylcholine binding site (Luttmann *et al.*, 2009; Ludwig *et al.*, 2010). Galanthamine also potentiates  $\alpha 4\beta 2$  nAChRs and a number of other nAChR subtypes including  $\alpha 6\beta 4$  and  $\alpha 3\beta 4$  nAChRs (Samochocki *et al.*, 2003), by binding at a non- $\alpha$  subunit interface (Hansen & Taylor, 2007). In addition, there is evidence that the binding site mediating the potentiating effects of calcium is located on the extracellular site of the  $\alpha 7$  nAChR (Galzi *et al.*, 1996; Pereira *et al.*, 2002). Another divalent cation, zinc, acts as a PAM of  $\alpha 4\beta 2$  nAChRs but does so selectively on receptors with the stoichiometry  $(\alpha 4)_3(\beta 2)_2$  (Moroni *et al.*, 2008). This has been explained by evidence that it interacts selectively with the  $\alpha 4(+)/\alpha 4(-)$  subunit interface, whilst inhibitory effects on  $(\alpha 4)_2(\beta 2)_3$  nAChRs are thought to be mediated by zinc binding to the  $\alpha 4(-)/\beta 2(+)$  subunit interface (Moroni *et al.*, 2008).

#### 1.6.4.4 Therapeutic uses

There is considerable interest in modulating nAChRs in order to treat a number of nervous system disorders, such as Alzheimer's disease, Parkinson's disease, schizophrenia, depression and anxiety, tobacco addiction and myasthenia gravis. A number of orthosteric agonists, partial agonists and antagonists have been developed, but allosteric ligands that modulate nAChRs potentially have significant advantages. The nAChRs are a very diverse group of receptors, distributed throughout the nervous

system and involved in a great number of physiological processes. Therefore, subunit selectivity of ligands is a vital characteristic and it is likely to be more difficult to achieve with an orthosteric ligand, because the acetylcholine binding site is very similar between receptor subtypes. In addition, spatial and temporal specificity can be achieved with allosteric modulators, as they generally have low intrinsic activity, but only potentiate acetylcholine-evoked responses and could therefore have reduced toxicity and off-target effects. Numerous disorders provide targets for nAChR drug development with some examples described in section 1.8.

## 1.7 PHYSIOLOGICAL ROLE AND DISTRIBUTION

Neuronal nAChRs are widely distributed throughout the CNS and PNS, with distinctly localised expression patterns in a region- and cell-specific manner. In the brain, the predominant subunits expressed are the  $\alpha 4$ ,  $\alpha 7$  and  $\beta 2$ , while in the periphery the  $\alpha 3$  and  $\beta 4$  are the most prevalent subunits (Paterson & Nordberg, 2000). The nAChRs are involved in numerous physiological and pathophysiological processes. In addition, the heterogeneity of the native receptors, mainly in the CNS, provides opportunities for the development of therapeutic agents that target certain populations of receptors and the functions they modulate, without affecting other aspects of cholinergic transmission. However, the identification of the exact subunit composition of native nAChR subtypes and their roles in cholinergic transmission has been complicated by the large number of neuronal nAChR subunit combinations that can form functional receptors.

### 1.7.1 Central nervous system

The predominant nAChR subunits expressed in CNS are  $\alpha 4$ ,  $\beta 2$  and  $\alpha 7$ . It is generally accepted that these subunit form the two major nAChR subtypes in the CNS, with  $\alpha 4\beta 2^*$  receptors forming most of the high affinity receptors and the  $\alpha 7^*$  receptors forming the low affinity nAChRs. Initially, the two major receptor subtypes were distinguished by using radiolabelled nicotine, cytisine or epibatidine to label  $\alpha 4\beta 2^*$  nAChRs and radiolabelled bungarotoxin to label  $\alpha 7^*$  nAChRs (Clarke *et al.*, 1985). Studies have also demonstrated that  $\alpha 4$  or  $\beta 2$  knockout mice lose most of the high affinity [ $^3\text{H}$ ]-nicotine binding sites (Picciotto *et al.*, 1995; Marubio *et al.*, 1999) and  $\alpha 7$  knockout mice lack  $\alpha$ -bungarotoxin binding (Orr-Urtreger *et al.*, 1997).

The  $\alpha 4$  and  $\beta 2$  messenger ribonucleic acid (mRNA) and protein expression patterns strongly overlap in areas such as the cortex, hippocampus and thalamic regions (Wada *et al.*, 1989). The  $\alpha 7$  subunit is also widely distributed in the brain, with the highest expression also in the cortex and hippocampus, while it is absent or expressed in low levels in thalamic regions and basal ganglia (Picciotto *et al.*, 2001). The distribution of other nAChR subunits is more limited in the brain.  $\alpha 3$  and  $\beta 4$  subunits are found in lower levels and are localised in regions such as the medial and dorsal habenula, the

interpeduncular nucleus and the locus coeruleus (Zoli *et al.*, 1998). The expression of the  $\alpha 2$  nAChR has not been studied in great detail, but this subunit appears to be expressed in very few brain regions with the highest expression in the interpeduncular nucleus, where it is believed to form  $\alpha 2\beta 4^*$  receptors (Wada *et al.*, 1989). The distribution of subunits  $\alpha 6$  and  $\beta 3$  in the CNS is also very limited, with the two subunits highly co-localised and found at high levels in the substantia nigra, ventral tegmental area, locus coeruleus, interpeduncular nucleus and medial habenula (Kuryatov *et al.*, 2000; Cui *et al.*, 2003). The  $\alpha 5$  subunit is also found in relatively few CNS regions, displaying the highest expression levels in the substantia nigra, the ventral tegmental area, the medial habenula and certain cortical regions (Picciotto *et al.*, 2001). A summary of the information collected on nAChR subtype distribution in the rodent brain is shown in Figure 1.6.

The numerous subtypes of neuronal nAChRs are located in pre- and postsynaptic regions in cholinergic neurons throughout the CNS, where they are involved in various processes connected to cognitive function, arousal, reward, learning and memory. Furthermore, presynaptic nAChRs have an essential role in modulating the release of acetylcholine and other neurotransmitters, such as noradrenaline (Clarke & Reuben, 1996), dopamine (Giorguieff *et al.*, 1977; Wonnacott *et al.*, 1989; Rapier *et al.*, 1990; Grady *et al.*, 1992), GABA (Yang *et al.*, 1996) and glutamate (Kaiser & Wonnacott, 2000). Activation of presynaptic nAChRs leads to an increase in intracellular calcium concentration, via voltage-dependent calcium channels or direct calcium influx through the nAChR channel, which leads to neurotransmitter exocytosis. The release of a particular neurotransmitter can be regulated by different nAChR subtypes in different regions of the brain. Frequently, nAChRs mediate the release of a neurotransmitter indirectly and are not actually located on the same neuron. Subtypes of nAChRs, such as  $\alpha 4\beta 2^*$ ,  $\alpha 7^*$  and  $\alpha 3\beta 4^*$  have also been found postsynaptically (Sher *et al.*, 2004). The role at postsynaptic nAChRs is not as clear as presynaptically, but their activation is thought to have a long-term effect on metabolic pathways and gene expression, through calcium influx, which activates calcium-dependent kinases, such as protein kinase C (Picciotto *et al.*, 2001).

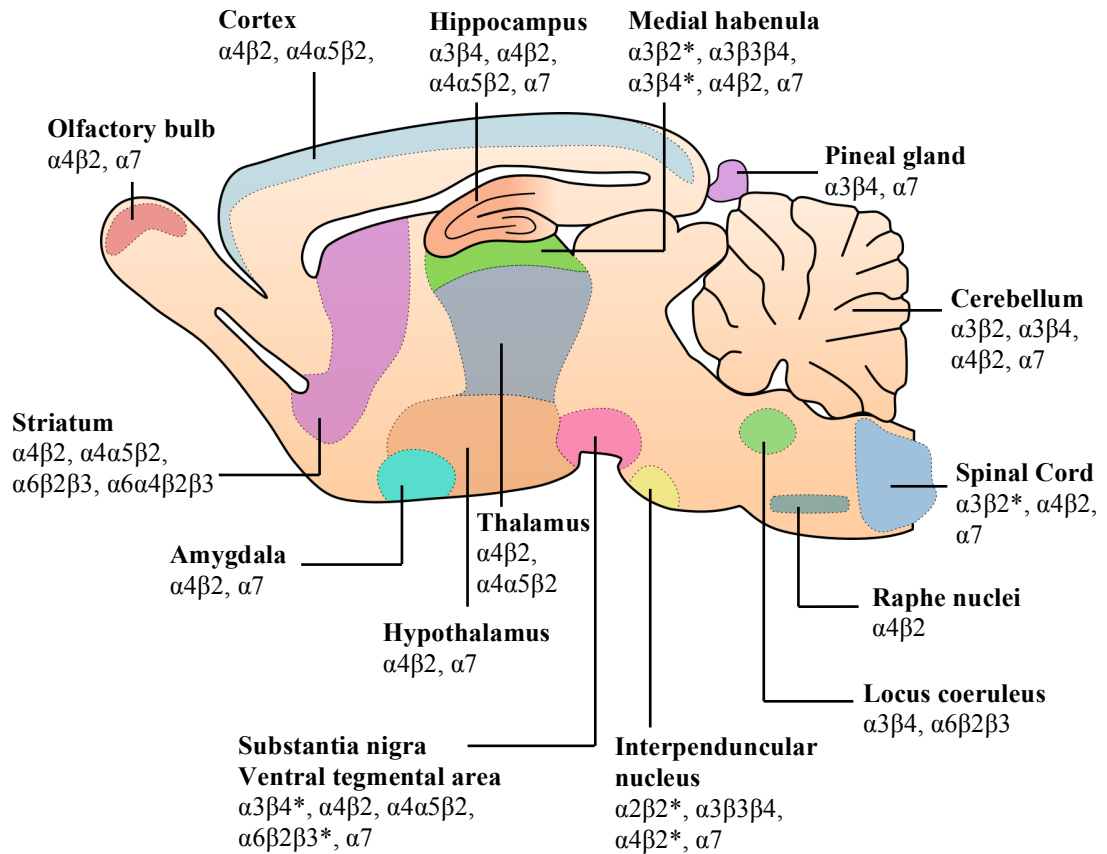


**Figure 1.6: Distribution of nAChR subtypes in the rodent brain (figure adapted from (Millar & Gotti, 2009)).**

Sagittal brain section showing nAChR subtypes expressed in different areas of the rodent CNS. The nAChR subtypes shown in the cortex, cerebellum, hippocampus, interpeduncular nucleus, medial habenula and pineal gland have been deduced from binding, immunoprecipitation and/or immunopurification assays in tissues from rat and/or from wild-type/knock-out mice. The nAChR subtypes shown in the amygdala, hypothalamus, locus coeruleus, olfactory bulb, raphe nuclei, spinal cord, thalamus and substantia nigra-ventral tegmental area have been deduced on the basis of the results of *in situ* hybridisation, single cell PCR, binding studies or functional assay of tissues obtained from rat and/or wild-type/knock-out mice (as reviewed in (Picciotto *et al.*, 2001; Drago *et al.*, 2003; Gotti & Clementi, 2004; Jensen *et al.*, 2005)).

The  $\alpha 4\beta 2^*$  nAChR subtype is expressed throughout the CNS and, like most other subtypes, is primarily located presynaptically (Wonnacott, 1997). It exhibits high affinity for nicotine, however the exact composition in the brain is not clear. Functional receptors with different  $\alpha:\beta$  subunit ratios can be formed, while other subunits, such as the  $\alpha 5$  have been shown to participate in the formation of the receptor.  $\alpha 4\beta 2$  nAChR sensitivity for agonists depends on the stoichiometry, with  $(\alpha 4)_2(\beta 2)_3$  receptors being approximately 100 times more sensitive than  $(\alpha 4)_3(\beta 2)_2$  receptors (Moroni *et al.*, 2006). The  $\alpha 4\beta 2$  receptor plays an important role in nociception, learning and memory and it directly mediates the cognitive and addictive effects of nicotine (Picciotto *et al.*, 1998). Studies with nAChR knockouts and null mutants have been very useful in determining the physiological roles of different receptor subtypes.  $\beta 2^{-/-}$  knockout mice exhibit reduced levels of nicotine self-administration and reduced nicotine-induced memory enhancement (Picciotto *et al.*, 1998; Pocivavsek *et al.*, 2006). In addition,  $\alpha 4\beta 2$  nAChRs are amongst the most susceptible receptors for nicotine-induced up-regulation (Govind *et al.*, 2009).

The other major nAChR subtype in the brain, the  $\alpha 7^*$  receptor, is characterised by low agonist sensitivity, high affinity for  $\alpha$ -bungarotoxin and fast desensitisation. It also has high calcium permeability, with  $pCa^{2+}/pNa^+$  ratio of  $\geq 10:1$  (Bertrand *et al.*, 1993). This high calcium permeability is important for the  $\alpha 7$  nAChR role in modulating gene expression and metabolic processes, while the rapid desensitisation kinetics limit calcium influx to non-toxic levels. In general,  $\beta 2$ -containing nAChRs have been found to be involved in more neurobehavioural functions than  $\alpha 7$  nAChRs. A study using  $\alpha 7^{-/-}$  knockout mice demonstrated that the mice exhibited an overall healthy phenotype with no gross abnormalities in brain development (Orr-Urtreger *et al.*, 1997). However, more recent mouse knockout studies indicate cognitive deficits and effects in chronic nicotine self-administration due to lack of  $\alpha 7$  nAChRs (Levin *et al.*, 2009). The  $\alpha 7$  nAChR is the only subunit known to form functional homomeric receptors in the mammalian brain and is thought to exist predominantly in the homomeric form. Recently, however,  $\alpha 7$  subunits were shown to co-assemble with  $\beta 2$  subunits to form functional heteromeric  $\alpha 7\beta 2$  nAChRs with different pharmacology than the homomeric receptors *in vitro* (Khiroug *et al.*, 2002; Zwart *et al.*, 2014). There is increasing evidence that  $\alpha 7\beta 2$  nAChRs exist natively in the hippocampus and basal forebrain and they exhibit increased sensitivity to modulation by amyloid peptides, an observation which could

give insight into the involvement of nAChRs in the pathophysiology of Alzheimer's disease (Liu *et al.*, 2009; Liu *et al.*, 2012; Mowrey *et al.*, 2013; Moretti *et al.*, 2014). In addition to the gene encoding the nAChR  $\alpha 7$  subunit (*CHRNA7*), a partially duplicated variant (*CHRFAM7A*) has been identified in the human genome (Gault *et al.*, 1998; Riley *et al.*, 2002) and mutations on both of these genes (*CHRNA7* and *CHRFAM7A*) have been linked to a number of pathological conditions, such as schizophrenia (Freedman *et al.*, 1997; Leonard *et al.*, 2002; Flomen *et al.*, 2006; Sinkus *et al.*, 2009). *CHRFAM7A* encodes a fusion protein (dup $\alpha 7$ ), corresponding to the ion channel domain of  $\alpha 7$  fused to an unrelated gene at its N-terminus. There is evidence, admittedly only in recombinant systems, that dup $\alpha 7$  can co-assemble with the  $\alpha 7$  subunit and exert a dominant-negative effect, resulting in reduced functional expression of  $\alpha 7$  nAChRs (Araud *et al.*, 2011; Wang *et al.*, 2014).

### 1.7.2 Peripheral nervous system

In contrast to the CNS, nAChRs in the PNS are located mainly postsynaptically and mediate fast synaptic transmission. As discussed in section 1.3.3, muscle nAChRs with the stoichiometry  $(\alpha 1)_2\beta 1\epsilon\delta$  (or  $(\alpha 1)_2\beta 1\gamma\delta$  in the foetal form) are located mainly at the postsynaptic density of the NMJ. Muscle nAChRs convert signals of the somatic PNS into skeletal muscle contractions. Activation of nAChRs by the release of acetylcholine in the synapse leads to depolarisation of the muscle cell. This depolarisation induces calcium release from the sarcoplasmic reticulum, which in turn leads to muscle contraction via the sliding filaments mechanism (Huxley, 2008).

$\alpha 3$  and  $\beta 4$  are the main nAChR neuronal subunits expressed in the PNS and the  $\alpha 3\beta 4^*$  nAChRs are thought to be the principal nAChR expressed in the periphery (Corriveau & Berg, 1993; Mandelzys *et al.*, 1994), while there is very little or no expression of the  $\alpha 4$  subunit (Rust *et al.*, 1994). The  $\alpha 3$  and  $\beta 4$  subunit co-immunoprecipitate in rat trigeminal ganglia, while other subunits such as  $\alpha 5$  and  $\beta 2$  are thought to co-assemble with the  $\alpha 3$  and  $\beta 4$  subunits to form ganglionic receptors (Vernallis *et al.*, 1993; Conroy & Berg, 1995).  $\alpha 3\beta 4^*$  nAChRs are mostly found on postsynaptic membranes of ganglionic neurons and mediate fast excitatory transmission, with the importance of these receptors demonstrated with knockout studies.  $\alpha 3$  knockout mice exhibit a severe

phenotype with high mortality rate in the first week (Xu *et al.*, 1999a). The  $\beta 4$  knockout mouse does not exhibit a dramatic phenotype, however, the double  $\beta 2$  and  $\beta 4$  knockout gives rise to a lethal phenotype and, therefore, it is thought that the  $\beta 2$  subunit participates in a compensatory mechanism in the case of  $\beta 4$  knockout (Xu *et al.*, 1999b). In addition, recent studies have demonstrated that nAChRs expressed in dorsal root ganglion neurons include  $\alpha 3\beta 4$ ,  $\alpha 6\beta 4$  and  $\alpha 7$  nAChR subtypes (Smith *et al.*, 2013).

### 1.7.3 Non-neuronal tissues

Numerous nAChR subunits are expressed outside the CNS and PNS and are thought to be involved in various important cell functions. There is evidence that nAChRs have an important role in inflammation, as  $\alpha 7$  and  $\alpha 4\beta 2$  nAChR subtypes are expressed in macrophages and their activation leads to reduction in secretion of pro-inflammatory agents (Borovikova *et al.*, 2000; Matsunaga *et al.*, 2001; Wang *et al.*, 2003). Furthermore, nAChRs are thought to be involved in angiogenesis, with a number of nAChR subtypes expressed on endothelial cells, which are necessary for the process of angiogenesis (Heeschen *et al.*, 2001). The most important subtypes are believed to be the homomeric  $\alpha 7$  and heteromeric receptors containing a combination of  $\alpha 3$ ,  $\alpha 5$ ,  $\beta 2$  and  $\beta 4$  subunits (Heeschen *et al.*, 2002; West *et al.*, 2003). Other non-neuronal tissues that express nAChRs to regulate various cellular functions include muscle, vascular tissue, lung cells, skin and lymphoid tissue (Gotti & Clementi, 2004).

## 1.8 ROLE IN DISEASE

Nicotinic receptors play an essential physiological role and both muscle and neuronal nAChRs have been implicated in numerous pathophysiological conditions. Muscle nAChRs are directly involved in neuromuscular diseases such as myasthenia gravis and congenital myasthenic syndrome, while neuronal nAChRs are implicated in neurodegenerative and neurodevelopmental disorders, including Alzheimer's disease, Parkinson's disease, schizophrenia, autism, Tourette's syndrome, anxiety, depression and epilepsy. The involvement of nAChRs in some of these disorders is summarised below.

### 1.8.1 Myasthenia gravis and congenital myasthenic syndrome

Myasthenia gravis is a debilitating autoimmune muscle weakness disease, characterised by antibodies that target the NMJ. The most common form of myasthenia gravis involves antibodies that target the postsynaptic muscle nAChRs, while some less common forms are due to antibodies against muscle specific tyrosine kinases, which are thought to be involved in the clustering of nAChRs in the postsynaptic membrane (Conti-Fine *et al.*, 2006). The trigger that initiates antibody production against nAChRs in myasthenia gravis is not clearly understood. These antibodies are thought to target a region of the extracellular N-terminus of the receptor subunits (Dellisanti *et al.*, 2007) and promote the internalisation and degradation of the receptors.

In addition to acquired myasthenia gravis, congenital myasthenic syndromes exist that exhibit similar pathophysiological profiles. These syndromes are the result of gene mutations, rather than autoimmune reaction. The mutated genes usually code for nAChR subunits, as well as proteins that regulate nAChR post-translational modification, receptor clustering and NMJ maintenance (Cruz *et al.*, 2014).

### 1.8.2 Alzheimer's disease

Alzheimer's disease (AD) is a neurodegenerative disorder characterised by progressive cognitive decline and a loss of neurons and represents the major cause of dementia for

people aged over 60. Some inherited forms of AD have provided insight into the mechanism of the disease, namely that accumulation of misfolded amyloid  $\beta$  ( $A\beta$ ) peptides is the trigger for synaptic and neural network dysfunction (Wang *et al.*, 2000; Dougherty *et al.*, 2003). AD is characterised by loss of cholinergic synapses mainly in the cerebral cortex, basal forebrain and hippocampus (Kása *et al.*, 1997) and by a reduction in muscarinic and nicotinic AChR expression (Court *et al.*, 2001).  $\alpha 7^*$  and  $\alpha 4\beta 2^*$  nAChR subtypes are particularly sensitive to  $A\beta$  peptides and the observation that  $A\beta$  preferentially accumulates in brain areas that are enriched in  $\alpha 7^*$  and  $\alpha 4\beta 2^*$  nAChRs may provide some insight into the susceptibility of the neocortex and hippocampus to  $A\beta$  toxicity (Dineley, 2007; Parri *et al.*, 2011).

The cholinergic deficit in AD has led to the use of AChE inhibitors for the symptomatic treatment of the disease. AChE inhibitors, such as galanthamine, improve memory and other cognitive functions and there is evidence that their effects are not only mediated due to an increase in acetylcholine in the synapse; for example, galanthamine has PAM effects on  $\alpha 7$  and  $\alpha 4\beta 2$  nAChRs (Maelicke *et al.*, 2001; Samochocki *et al.*, 2003). Furthermore, ligands that selectively enhance  $\alpha 4\beta 2$  and  $\alpha 7$ , such as PAMs, have been shown to improve cognitive deficits associated with Alzheimer's disease (Hurst *et al.*, 2005; Thomsen *et al.*, 2011; McLean *et al.*, 2012; Callahan *et al.*, 2013).

### 1.8.3 Parkinson's disease

Parkinson's disease is the second most common neurodegenerative disorder after AD (Mayeux, 2003). It is a movement disorder characterised by postural instability, bradykinesia, tremor and rigidity (Poewe, 2009; Schapira *et al.*, 2009). These motor symptoms are caused by degeneration of the nigrostriatal dopaminergic pathway, which is the most severely affected neurotransmitter pathway in Parkinson's disease. Other CNS systems are affected to a lesser extent, including the adrenergic, cholinergic, glutamatergic and GABAergic systems, which may underline the non-motor symptoms of Parkinson's disease, such as cognition deficits and sleep dysfunction (Poewe, 2009). A complex mixture of genetic and environmental factors is believed to be responsible for the development of Parkinson's disease, with a small minority of familial cases linked to mutations in a number of genes. Environmental factors have also been linked

to Parkinson's disease; the greatest risk factor is exposure to pesticides, while tobacco use is believed to provide some protection against Parkinson's (Quik *et al.*, 2009).

There is strong evidence for a link between nAChRs and Parkinson's disease. There is extensive anatomical and functional overlap between the nicotinic cholinergic and dopaminergic systems in the nigrostriatal pathway (Bolam *et al.*, 2000; Smith & Kieval, 2000; Misgeld, 2004; Maskos, 2008, 2010) and studies suggest that ligands modulating nAChRs, specifically  $\alpha 4\beta 2^*$  and  $\alpha 6\beta 2^*$  subtypes, such as nicotine, may protect against nigrostriatal damage, as well as alleviate motor side effects associated with dopamine replacement therapy (Quik & Wonnacott, 2011).

#### 1.8.4 Schizophrenia

Schizophrenia is a neurodevelopmental disorder characterised by symptoms of hallucinations and delusions, but also by cognitive symptoms caused by deficits in sensory gating (Sharma & Antonova, 2003). Smoking prevalence is much higher among patients with schizophrenia and may be a form of self-medication, as it may normalise some of the sensory deficits associated with the disease (Leonard *et al.*, 2007). A reported feature of schizophrenia is a decrease in the number of  $\alpha 7^*$  nAChRs in the hippocampus of patients and nicotine administration improves sensory gating, presumably through  $\alpha 7$  activation (Freedman *et al.*, 1995; Stevens & Wear, 1997; Schaaf, 2014). In addition, a direct genetic link between schizophrenia and the genes encoding the  $\alpha 7$  nAChR subunit (*CHRNA7*), as well as the truncated version of  $\alpha 7$  (*CHRFAM7A*), has been established (Freedman *et al.*, 1997; Leonard *et al.*, 2002). It has been reported that a number of type-I and type-II PAMs that target  $\alpha 7$  nAChRs, such as NS-1738 (Timmermann *et al.*, 2007), PNU-120596 (Hurst *et al.*, 2005) and A-867744 (Faghieh *et al.*, 2009), can partially restore auditory gating deficits in mutant mice. Therefore, drugs that selectively enhance  $\alpha 7$  nAChRs could potentially be used as therapeutic agents in the treatment of schizophrenia.

## 1.9 THESIS AIMS

The main aim of this thesis is to increase our understanding of neuronal nAChR function and their modulation by allosteric ligands. A series of novel PAMs have been synthesised at UCL with the aim of characterising their selectivity and pharmacological effects on  $\alpha 7$  nAChRs. These novel PAMs, in addition to classical PAMs, will be used as a tool to explore the molecular mechanisms of recombinant human  $\alpha 7$  nAChRs. More specifically, the action of PAMs will be examined on  $\alpha 7$  nAChRs with single-point mutations on residues that are potentially implicated in receptor gating and/or desensitisation (W54A, L247T and M260L). In addition, the pharmacological properties of nAChRs expressed in human neurons derived from induced pluripotent stem cells will be examined.

## CHAPTER 2

# MATERIALS AND METHODS

---

## 2.1 MOLECULAR BIOLOGY TECHNIQUES

### 2.1.1 Plasmids

Several plasmid constructs used in this thesis have been described previously. These include plasmids containing  $\alpha 7$  cDNA in pSP64GL (Broadbent *et al.*, 2006), mouse 5-HT3A in pRK5 (Harkness & Millar, 2001) and a rat  $\alpha 7$ /mouse 5-HT3A chimaera ( $\alpha 7^{4\text{TM}-5\text{-HT3A}}$ ) in pcDNA3.1 (Gee *et al.*, 2007). Human  $\alpha 3$ , human  $\alpha 4$ , human  $\beta 2$  and human  $\beta 4$  nAChR subunit cDNAs in the plasmid pSP64GL were provided by Professor Lucia Sivilotti.

### 2.1.2 Restriction digestion of DNA

Restriction digestion of DNA was usually performed under standard conditions. Enzymes were purchased from Roche or New England Biolabs. Approximately 1  $\mu\text{g}$  of plasmid DNA was incubated along with  $\sim 5$  U of restriction enzyme and 2  $\mu\text{l}$  of the appropriate 10x reaction buffer in a final volume of 20  $\mu\text{l}$  (if a larger quantity of DNA was required the above volumes were extrapolated to a final volume of 50  $\mu\text{l}$ ). The digests were mixed by gentle pipetting and incubated for 1 hour at the appropriate temperature for the restriction enzyme as recommended by the supplier (usually 37°C). Digested DNA was examined by gel electrophoresis alongside non-digested DNA to ensure the enzyme digested the DNA as expected.

### 2.1.3 DNA ligation

Ligations were performed in a final volume of 20  $\mu\text{l}$  containing  $\sim 1$  U of T4 DNA ligase (Roche) 10x T4 DNA ligase buffer and DNA (various concentrations were used when optimising ligations, with molar ratios varying from 1:2 to 1:10 vector: insert). Ligation reactions were incubated at 14°C overnight and were used directly for transformation of bacterial cells.

#### 2.1.4 Site-directed mutagenesis

Site-directed mutagenesis (SDM) was performed on human  $\alpha 7$  nAChR subunit cDNA in plasmid pSP64GL using the QuikChange mutagenesis kit (Stratagene) according to manufacturer's guidelines. Two complementary synthetic mutagenic oligonucleotide primers were synthesised (Sigma-Aldrich). The primers were designed using the following criteria:

- Typically 25 bases in length with the mutation in the middle of the primer (~10 bases of correct sequence on both sides of the mutation)
- Melting temperature greater than or equal to 78°C
- GC base content of at least 40%
- Should terminate in one or more C or G bases

All primers were purified by polyacrylamide gel electrophoresis (PAGE) to improve mutation efficiency (as recommended by the manufacturer).

The SDM reactions were performed in a final volume of 50  $\mu$ l containing 50 ng of plasmid DNA template, 125 ng of each complementary oligonucleotide primer, 1  $\mu$ l of deoxyribonucleotide triphosphate (dNTP) mix (concentration not disclosed by manufacturer), 5  $\mu$ l 10x reaction buffer and 1  $\mu$ l of *PfuTurbo* DNA polymerase (2.5 U/ $\mu$ l).

The PCR reaction was performed as follows:

- 95°C for 30 seconds (to denature the double-stranded plasmid DNA)
- 55°C for 1 minute (to anneal the oligonucleotide primers containing the mutation)
- 68°C for 1 minute per kilobase of plasmid length (to extend and incorporate the mutagenic primers)
- 12-18 PCR cycles (typically 16) were performed, depending on the number of mutated residues

The non-mutated parental DNA template was digested with *DpnI* restriction enzyme (10 U/ $\mu$ l), added directly to the amplification reaction and incubated at 37°C for 1 hour.

XL1-Blue supercompetent *Escherichia coli* (*E. coli*) cells (Stratagene) were then transformed with the remaining *DpnI*-treated DNA (section 2.1.5).

### 2.1.5 XL1-Blue supercompetent cell transformation

The XL1-Blue supercompetent *E. coli* cells were stored at  $-80^{\circ}\text{C}$  and were gently thawed on ice before use. 50  $\mu\text{l}$  of these cells were added to a pre-chilled polypropylene tube (Falcon 2059, Becton Dickinson) where 1  $\mu\text{l}$  ( $\sim 1$  ng) of *DpnI*-treated DNA was added then swirled gently to mix. This was incubated on ice for 30 minutes. The mixture was then heat shocked at  $42^{\circ}\text{C}$  for 45 s and then placed on ice for 2 minutes. The mixture was then incubated in 500  $\mu\text{l}$  of pre-warmed SOC (prepared according to manufacturer's guidelines, containing (g/l): 20 tryptone; 5 yeast extract; 0.5 NaCl; 3.6 glucose) at  $37^{\circ}\text{C}$  for 1 hour, while shaking at 225 rpm. Next, 50-100  $\mu\text{l}$  of the transformation mix was plated out into LB-ampicillin (50  $\mu\text{g}/\text{ml}$ ) agar plates and incubated at  $37^{\circ}\text{C}$  for  $\sim 16$  hours.

Bacterial colonies were used to prepare plasmid DNA (section 2.1.6 and 2.1.7) and were subsequently verified by nucleotide sequencing (section 2.1.9).

### 2.1.6 Small-scale plasmid DNA preparation

A small-scale preparation of plasmid DNA was often produced from recombinant *E. coli* cultures for sequencing the DNA using the GeneJET Plasmid Miniprep Kit (Thermo Fisher Scientific) according to the manufacturer's guidelines.

A single *E. coli* colony was transferred using a pipette tip to 3.5 ml of LB medium supplemented with ampicillin (50  $\mu\text{g}/\text{ml}$ ). The culture was then incubated for 12-16 hours at  $37^{\circ}\text{C}$ , while shaking at 225 rpm. The bacterial culture was harvested by centrifugation at 6800 g for 15 minutes at  $4^{\circ}\text{C}$ . The supernatant was then aspirated and the pelleted cells were resuspended in 250  $\mu\text{l}$  of the GeneJET Resuspension Solution (Tris-HCl, pH 8) and pipetted up and down, until no clumps remained. The cell suspension was then transferred to an Eppendorf tube, where 250  $\mu\text{l}$  of the GeneJET Lysis solution were added and mixed thoroughly by inverting the tube 6 times. 350  $\mu\text{l}$

of the GeneJET Neutralisation Solution were then added and mixed immediately by inverting the tube 6 times. The mixture was then centrifuged at 13000 g for 5 minutes at room temperature to pellet the cell debris and chromosomal DNA. The supernatant was then transferred to a GeneJET spin column by pipetting while trying to avoid disturbing the precipitate and then centrifuged for 1 minute. The flow-through was discarded and the column was placed back in the same collection tube. 500 µl of the GeneJET Wash Solution were then added to the spin column and then centrifuged for 1 minute and the flow-through was discarded and the column was placed back in the same collection tube. The procedure was repeated again using 500 µl of the Wash Solution. This was then centrifuged for an additional minute to avoid residual ethanol in the plasmid preparation. The GeneJET spin column was then transferred into a fresh Eppendorf tube and 50 µl of the GeneJET Elution Buffer (10 mM Tris-HCl, pH 8.5) were added to the centre of the spin column membrane to elute the plasmid DNA. This was incubated for 2 minutes at room temperature and then centrifuged for 2 minutes. The column was then discarded and the purified plasmid DNA was analysed by agarose gel electrophoresis (section 2.1.8) and then stored at  $-20^{\circ}\text{C}$ .

### 2.1.7 Large-scale plasmid DNA preparation

Large-scale preparation of plasmid DNA was performed using the GenElute HP Maxiprep Kit (Sigma-Aldrich) according to manufacturer's guidelines, which is a modified alkaline lysis procedure.

A single *E. coli* colony was transferred using a pipette tip to 250 ml of LB medium supplemented with ampicillin (50 µg/ml). The culture was then incubated for 12-16 hours at  $37^{\circ}\text{C}$ , while shaking at 225 rpm. The bacterial culture was then harvested by centrifugation at 6000 g for 15 minutes at  $4^{\circ}\text{C}$ . The supernatant was then aspirated and the pelleted cells were resuspended in 12 ml of chilled Resuspension buffer (50 mM Tris-HCl, pH 8; 10 mM EDTA; 100 µg/ml RNase A) and pipetted up and down until no clumps remained. 12 ml of Lysis buffer (200 mM NaOH, 1% SDS) were then added to the cell suspension and mixed by inverting the tube 6-8 times. This was then incubated at room temperature for 5 minutes. 12 ml of chilled Neutralisation buffer (3 M potassium acetate, pH 5.5) were then added and mixed by inverting the tube 4-6 times.

9 ml of Binding solution were added and mixed by inverting 1-2 times. The bacterial lysate was poured into a filter syringe and incubated at room temperature for 10 minutes. A GenElute HP Maxiprep binding column was then equilibrated by applying 12 ml Column Preparation solution (750 mM NaCl; 50 mM MOPS, pH 7; 15% isopropanol; 0.15% Triton X-100) and spinning in a swinging bucket rotor at 3000 g for 2 minutes. The plunger was inserted into the filter syringe and the lysate was filtered into the previously equilibrated binding column. The lysate was then allowed to enter the resin by spinning at 3000 g for 2 minutes. The binding column was washed with 12 ml Wash solution (1 M NaCl; 50 mM MOPS, pH 7; 15% isopropanol). After spinning at 3000 g for 2 minutes the eluate was discarded. The plasmid DNA was then eluted by adding 3 ml Elution buffer (10 mM Tris-HCl, pH 8.5) to the binding column and spinning at 1000 g for 5 minutes.

The purified plasmid DNA was analysed by agarose gel electrophoresis (section 2.1.8), quantified using a spectrophotometer (section 2.1.9) and then stored at  $-20^{\circ}\text{C}$ .

### 2.1.8 Agarose gel electrophoresis

Circular plasmid DNA, restriction fragments and SDM products were separated on an ethidium bromide-containing 1% agarose gel. The gel was prepared with 1 g electrophoresis grade agarose (Invitrogen) in 100 ml of TAE buffer solution containing (mM): 40 Tris-acetate and 0.1 ethylenediaminetetraacetic acid (EDTA) and heated until molten. The molten solution was cooled to  $\sim 50^{\circ}\text{C}$  and 5  $\mu\text{l}$  of 10 mg/ml ethidium bromide was added and swirled to mix. This mixture was then poured into a gel electrophoresis casting set and a comb was inserted to create the DNA wells. This was left to set at room temperature for  $\sim 1$  hour.

A DNA 'ladder' (1  $\mu\text{g}$  *Hind*III digested Phage  $\lambda$  DNA (Invitrogen)) was separated in parallel with the DNA samples to enable the size of the linear DNA fragments to be determined. The DNA samples were mixed with 2  $\mu\text{l}$  blue loading dye, 1x (Promega) in a final volume of 20-100  $\mu\text{l}$  and were then loaded onto the gel. Electrophoresis was performed in an electrophoresis tank filled with 1x TAE buffer under a constant voltage of 150 mV for 40 minutes. The DNA was then visualised and an image was captured

using a camera and ultraviolet (UV) transilluminator (UVP BioDock-It System) and printed with a Sony UP-895MD printer.

When purified DNA was needed from the gel for subsequent sub-cloning, a low-melt gel was made using low-melt electrophoresis grade agarose (Invitrogen). DNA was excised from gels using a flatbed UV screen to visualise the bands and a sterile scalpel. The excised bands were placed into a sterile Eppendorf tube immediately. DNA was purified from the gel using the Wizard clean up purification system (Promega), according to manufacturer's guidelines. Briefly, the agarose/DNA complex was melted and mixed with a solution of DNA-binding resin at 70°C on a hot block. The mix is then isolated on a mini-column containing DNA affinity beads, washed with ethanol and eluted from the column using 50 µl sterile water and centrifugation. A small amount (2 µl) of the purified DNA was examined by gel electrophoresis to access its purity.

### **2.1.9** Determination of DNA yield

The concentration of DNA plasmid stocks was determined by using a Nanodrop spectrophotometer (Thermo Scientific) at a wavelength of 260 nm. The sample purity was determined by the ratio of the absorbance at 260:280 nm, with a ratio of ~1.8 indicating a preparation free from contamination. If the ratio is appreciably lower, it may indicate the presence of protein or other contaminants that absorb strongly at 280 nm.

### **2.1.10** DNA nucleotide sequencing

DNA nucleotide sequencing was performed using fluorescence-based capillary sequencing with the ABI Prism BigDye Terminator Sequencing Ready Reaction Kit version 1.1 (Applied Biosystems) and ABI Prism 3100-*Avant* Genetic Analyser (Applied Biosystems) according to the manufacturer's guidelines. The reaction was carried out in a total volume of 20 µl containing 150-300 ng of DNA template, 3.2 pmol of the sequencing primer (typically 18-22 bases in length), 4 µl of 2.5x Ready Reaction Premix (dye-labelled dNTP terminators, unlabelled dNTPs, AmpiTaq DNA polymerase

and MgCl<sub>2</sub>), 2 µl BigDye Sequencing Buffer 5x and nuclease-free water to 20 µl. The thermocycling reaction was performed as follows:

- 96°C for 30 s (to denature the double-stranded plasmid DNA)
- 50°C for 15 s (to anneal the oligonucleotide primer)
- 60°C for 4 minutes per kilobase of plasmid length (to extend and incorporate the primer)
- Typically 25 cycles were performed

Following this reaction, DNA was precipitated by the addition of 2 µl sodium acetate (3 M) and 50 µl 100% ethanol. This was incubated on ice for 15 minutes, then transferred to an Eppendorf and centrifuged at 13,000 g for 15 minutes at 4°C. The supernatant was aspirated and the pellet washed in 500 µl of 70% ethanol. Residual ethanol was removed by evaporation.

Just prior to sequencing, the DNA pellet was resuspended in 10 µl of formamide and loaded into the ABI Prism 3100-*Avant* Genetic Analyser. Fluorescent DNA fragments were run on a 50 cm capillary using a POP-6 polymer (Applied Biosystems) and the sequences were digitalised using ABI Prism 3100-*Avant* Data collection version 1.0 software (Applied Biosystems). Sequence analysis was performed on MacVector 12.5.1 software.

#### 2.1.11 Linearisation of DNA

Prior to *in vitro* synthesis of cRNA, plasmid DNA needed to be linearised in order to prevent long, heterogeneous RNA transcripts. Plasmid DNA was linearised with a restriction enzyme downstream of the insert. Plasmid pSP64GL containing wild type or mutated nAChR subunit cDNA was linearised with *Bam*HI (Roche) according to manufacturer's protocol. Approximately 1 µg of plasmid was linearised with 1 U of the restriction enzyme, 2.5 µl of 10x Buffer B (100 mM Tris-HCl; 1 M NaCl; 50 mM MgCl<sub>2</sub>; 20 mM 2-mercaptoethanol, pH 8) (Roche) and an appropriate volume of distilled water was added to make the reaction volume to 25 µl. The reaction was gently mixed by pipetting and then incubated at 37°C for 1 hour.

The linearised DNA was examined using agarose gel electrophoresis to confirm that cleavage is complete and then was purified (section 2.1.12).

### 2.1.12 Purification of DNA

Following restriction, DNA was purified with the QIAquick PCR purification kit (Qiagen) according to the manufacturer's guidelines.

Buffer PB (5 volumes) was added to 1 volume of the DNA and mixed. A QIAquick column was placed in the 2 ml collection tube provided. To bind the DNA, the sample was added to the QIAquick column and centrifuged at 13000 rpm for 1 minute at room temperature. The flow-through was discarded and the QIAquick column was placed back in the same tube. To wash the DNA, 750 µl Buffer PE were added to the QIAquick column and centrifuged at 13000 rpm for 1 minute at room temperature. The flow-through was discarded and the QIAquick column was placed back in the same tube. The column was centrifuged for an additional minute at 13000 rpm. To elute the DNA, the QIAquick column was transferred to a clean Eppendorf tube and 30 µl of nuclease-free water were added to the centre of the QIAquick membrane. The column was left to stand for 1 minute and then was centrifuged at 13000 rpm for 1 minute. The DNA was examined using agarose gel electrophoresis and then stored at -20°C.

### 2.1.13 *In vitro* RNA synthesis

*In vitro* synthesis of cRNA was performed using mMessage mMachine SP6 transcription kit (Ambion) according to the manufacturer's instructions. Linear plasmid DNA (4 µl of 250 ng/µl) containing the SP6 RNA polymerase promoter was added to 10 µl of 2x NTP/CAP (a neutralised buffer solution containing (mM): 10 ATP, 10 CTP, 10 UTP, 2 GTP, 8 cap analogue), 2 µl 10x Reaction Buffer (containing salts, buffer, dithiothreitol), 2 µl of Enzyme Mix (buffered 50% glycerol containing RNA polymerase, SUPERase•In and other ingredients) and 2 µl nuclease-free water. The reaction was mixed gently and incubated at 37°C for 2 hours. Following this reaction, 1 µl TURBO DNase (2 U/µl) was added and incubated at 37°C for 15 minutes to remove the template DNA. The reaction was stopped with 15 µl ammonium acetate 'Stop

Solution' (containing: 5 M ammonium acetate and 100 mM EDTA) and 115  $\mu$ l nuclease-free water and then mixed thoroughly.

The RNA was recovered using a phenol/chloroform extraction and isopropanol precipitation. The RNA was extracted with 150  $\mu$ l phenol/chloroform. The aqueous phase was removed and transferred into a new tube. The RNA was precipitated with 150  $\mu$ l isopropanol, chilled at  $-20^{\circ}\text{C}$  for 30 minutes and then centrifuged at 13000 rpm for 15 minutes at  $4^{\circ}\text{C}$ . The supernatant was aspirated and the pellet was resuspended in 25  $\mu$ l nuclease-free water and then stored at  $-80^{\circ}\text{C}$ .

#### **2.1.14 Determination of RNA yield**

The concentration of the RNA in the samples from the in vitro RNA synthesis (section 2.1.13) was determined by using a Nanodrop spectrophotometer (Thermo Scientific) at a wavelength of 260 nm. The sample purity was determined by the ratio of the absorbance at 260:280 nm, with a ratio of  $\sim 2$  indicating a preparation free from protein contamination.

## 2.2 CELL CULTURE

### 2.2.1 Mammalian cell culture and transfection

The tsA201 cell line (a HEK-derived cell line) was obtained from Dr William Green, University of Chicago. The tsA201 cell line is a transformed human embryonic HEK293 cell line that stably expresses an SV40 temperature-sensitive T-antigen.

Cell lines were removed from long-term liquid nitrogen storage and the cryotube was immediately placed at 37°C to thaw. Cells were transferred to 15 ml polypropylene tubes (Falcon, Becton Dickinson) containing room temperature cell culture medium (Dulbecco's modified Eagle's medium (DMEM) containing 2 mM L-Glutamax (Gibco-Invitrogen), supplemented with 10% heat inactivated foetal calf serum (FCS) and 100 U/ml penicillin/100 µg/ml streptomycin (Gibco-Invitrogen)), mixed gently by pipetting and centrifuged at 900 rpm for 3 minutes. The medium was carefully removed by aspiration and the cell pellet carefully resuspended in a further 10 ml cell culture medium and centrifuged as above. The cell pellet was then resuspended in an appropriate volume of 37°C cell culture medium, transferred to 10 cm cell culture dishes (Corning) and maintained at 37°C in a humidified incubator containing 5% CO<sub>2</sub>.

Cells were passaged by aspiration of conditioned cell culture medium, washed once with 10 ml phosphate-buffered saline (PBS) and trypsinised with 500 µl trypsin:PBS (1:3) solution for 30 s at 37°C. The dishes were then tapped vigorously to dislodge the cells and 3-5 ml of 37°C cell culture medium was added to deactivate the trypsin. The cells were then passed through the constricted tip of a 1 ml pipette several times to separate cell aggregates into a homogeneous mixture of dissociated single cells. The cells were then re-seeded into fresh culture dishes at various dilutions, depending on subsequent use, and topped up with culture medium and maintained as above. Cells were discarded after 25-30 passages.

Cells were transfected using the Effectene Transfection Kit (Qiagen) using a modified manufacturer's protocol. Cells were trypsinised and re-seeded in 5 ml of medium (10

cm culture dish) 4-6 hours prior to transfection, in order to achieve ~30% confluency at the time of transfection.

Cell transfection took place in a 10 cm dish. 0.6 µg of plasmid DNA was added to 120 µl of Buffer EC and 4.8 µl of Enhancer (DNA condensing enhancer solution) in a sterile Eppendorf tube and incubated for 5 minutes. 13 µl of Effectene (non-liposomal lipid formulation that coats condensed DNA with cationic lipids) was added, mixed by pipetting and incubated for a further 10 minutes. 600 µl of 37°C conditioned cell culture medium was added and mixed by pipetting. The mixture was then added drop-wise onto the cells. After 16 hours, 5 ml of 37°C medium was added.

### 2.2.2 Human neuronal cells, derived from induced pluripotent stem cells

Human iCell neurons, which are neuronal cells, derived from induced pluripotent stem cells (iPSC), were obtained from Cellular dynamics international (CDI). The cells were removed from long-term liquid nitrogen storage and the cryotube, containing the cells in 1 ml dimethyl sulfoxide (DMSO), was immediately placed at 37°C to thaw. Cells were transferred to 15 ml polypropylene tube (Falcon, Becton Dickinson). 1 ml Neurobasal medium (without glutamine, glutamate and aspartate; Invitrogen) supplemented with B-27 supplement (5000x; Invitrogen) and L-glutamine 200 mM (2000x; PAA Laboratories), pre-warmed to 37°C, was added in the empty cryotube and then transferred drop-wise to the cells, in order to minimise osmotic shock. A further 8 ml of medium was added slowly, mixed gently and centrifuged at 900 rpm for 5 minutes. The medium was carefully removed by aspiration and the cell pellet was resuspended in 2 ml of fresh medium. The cells were counted using a haemocytometer and then resuspended to the appropriate volume for plating.

For calcium imaging experiments, cells were plated at a density of approximately  $2.5 \times 10^5$  cells/ml into Biocoat poly-D-lysine (PDL)/laminin-coated 96-well, clear bottom, black-walled plates (for single-cell calcium imaging; 100 µl/well), or into Biocoat PDL/laminin-coated half-area, 96-well, clear bottom, black-walled plates (for fluorometric imaging plate reader (FLIPR) assays; 50 µl/well).

For patch-clamp experiments, cells were plated at a density of approximately  $5 \times 10^4$  cells/ml (100  $\mu$ l/coverslip) on Biocoat PDL/laminin-coated 12 mm glass coverslips (Becton Dickinson) and placed in Biocoat 24-well clear plates.

### 2.3 *XENOPUS LAEVIS* OOCYTE PREPARATION

Adult female *Xenopus laevis* (*X. laevis*) frogs were purchased from the European Xenopus Resource Centre (University of Portsmouth). The care and use of *X. laevis* frogs were approved by the UCL Animal Research Committee and followed the guidelines of the Animal Scientific Procedures Act, 1986 (UK).

Stage V and VI *X. laevis* oocytes were removed from schedule 1 sacrificed frogs, following procedures that have been approved by both UCL's Biological Services Management Group and the UK Home Office. The ovarian lobes were washed in filter-sterilised calcium-free Barth's solution (in mM: NaCl 88; KCl 1; NaHCO<sub>3</sub> 2.4; MgCl<sub>2</sub>.6H<sub>2</sub>O 82; Tris 1.5; pH 7.5). Fine tipped tweezers were used to tear the ovarian lobe into smaller clumps containing ~50 oocytes. Oocytes were defolliculated enzymatically with collagenase type I (2 mg/ml; 250 U/mg; Worthington) in calcium-free Barth's solution in sterile 35 mm x 10 mm cell culture dishes (Nunc) by constant shaking on an orbital shaker (~100 rpm) for 2-3 hours at room temperature. After 2 hours the oocytes were subjected to mild pipetting with a Pasteur pipette to encourage separation of the oocytes and then were monitored over the next hour. When it appeared that the follicle cell layer had been removed from a sufficient number of oocytes (~30 minutes after separation) they were transferred to calcium-free Barth's solution in 90 mm x 15 mm Petri dishes (Sterlin) and washed by constant shaking for 10 minutes. The oocytes were transferred to new petri dishes with fresh calcium-free Barth's solution and washed for 10-minute cycles, until the solution was clear (~3 washes). The oocytes were then selected using binocular microscope according to health and size.

Heterologous expression of recombinant receptors was achieved by injection of either cRNA (6-12 ng) into the oocyte cytoplasm in the case of wild type and mutated nAChRs, or plasmid cDNA constructs (5-10 ng) into the oocyte nucleus in the case of chimaeras and 5-HT<sub>3A</sub>Rs. Oocytes were injected with a volume of 27-32 nl using a Nanoject Injector (Drummond Broomall). After injection, oocytes were incubated at 18°C in 48 well multidishes (Nunc) for 2-7 days in a filter-sterilised modified calcium-containing Barth's solution supplemented with antibiotics (in mM: NaCl 88; KCl 1; NaHCO<sub>3</sub> 2.4; MgCl<sub>2</sub>.6H<sub>2</sub>O 82; Tris 1.5; CaCl<sub>2</sub>.2H<sub>2</sub>O 0.77; penicillin 100 U/ml/streptomycin 100 µg/ml; tetracyclin 50 µg/ml; kanamycin 4 µg/ml; pH 7.5).

## 2.4 ELECTROPHYSIOLOGICAL TECHNIQUES

### 2.4.1 Two-electrode voltage-clamp recording

Recordings were performed 2-7 days after injection. Oocytes were placed in a recording chamber and impaled with two microelectrodes filled with 3 M KCl (0.5-2.0 M $\Omega$ ) and voltage-clamped at  $-60$  mV using an OC-725 Amplifier (Warner Instruments) PowerLab 8SP and Chart 5 software (AD Instruments). The external solution was clamped at ground potential by means of a virtual ground circuit using Ag/AgCl reference electrode and a Pt/Ir current passing electrode. The recording chamber was continuously perfused with modified Ringer solution (in mM: NaCl 115; KCl 2.4; HEPES 5; BaCl<sub>2</sub> 1.8) at a rate of  $\sim 15$  ml/min. A calcium-free solution was used in order to minimise the contribution of calcium-gated chloride channels, which are endogenous to *X. laevis* oocytes and may be activated by calcium entry through the neuronal nAChR channels (Sands *et al.*, 1993). Dilutions of drugs were prepared from frozen stocks in external Ringer solution on the day of the experiment. A rapid solution exchange was achieved using a computer-controlled eight-way solenoid valve perfusion system (BPS-8; ALA Scientific Instruments), which is controlled by pinch valves. All experiments were carried out at room temperature. Membrane currents were passed through a digital filter (low-pass) and stored for analysis.

### 2.4.2 Patch-clamp recording

Whole-cell voltage-clamp recordings were carried out 5-8 days after plating. During recordings, cells were continuously perfused with modified HBTS (Invitrogen) containing (mM): 135 NaCl, 5 KCl, 1.2 MgCl<sub>2</sub>, 2.5 CaCl<sub>2</sub>, 10 HEPES, 11 glucose, pH 7.2 at room temperature. Cells were voltage-clamped in the whole-cell configuration ( $-60$  mV holding potential) with an AxoPatch 200A patch clamp amplifier (Molecular Devices). Pipettes were pulled from borosilicate glass (Type GC150F-10, Harvard Apparatus) using a commercial puller (Model p-87, Sutter Instruments) and had resistances of 2-6 M $\Omega$  when filled with pipette solution containing (mM): 1 MgCl<sub>2</sub>, 4 MgATP, 0.5 EGTA, 10 HEPES, 140 potassium gluconate (pH adjusted to 7.3 with KOH). Current data were recorded at 10 kHz using a DA/AD interface (Digidata

1322A, Molecular Devices). Drugs were applied using a multichannel perfusion system (Model BPS-8, Scientifica) positioned 150  $\mu$ M away from the recorded cell and controlled by Clampex 9 software (Molecular Devices).

### 2.4.3 Drug application

Stock solutions of 1 M acetylcholine chloride (Sigma-Aldrich) and 10 mM MLA (Sigma-Aldrich) were prepared in sterile distilled water, while all PAMs were dissolved in DMSO (100 mM stocks for the TBS and TQS compounds, 10 mM stocks for PNU-120596 (Tocris Bioscience), NS-1738 (Tocris Bioscience) and A-867744 (Abbott)).

Orthosteric agonists were typically applied for less than 5 s before switching back to Ringer or HBTS, as during this time the receptor has already switched to its desensitised state.

For studies with allosteric agonists, the drug was usually applied until the response reached a plateau, before switching back to Ringer/HBTS.

For most of the studies on the effects of positive allosteric modulators or antagonists, a pre-application with the modulator was required in order to ensure that the drug had adequately equilibrated with the receptors, before co-application with the agonist.

In *X. laevis* oocytes and iPSC neurons, following an application of the orthosteric agonists, the receptors were allowed to recover for 2 minutes. Following exposure to allosteric compounds, the receptors were allowed to recover for 3 minutes after the response had returned to the baseline (for some compounds this was longer than 10 minutes in total).

All agonist concentration-response curve data were normalised to responses induced by a maximum effective concentration. Most potentiated and inhibited responses were normalised to a control acetylcholine response (typically an EC<sub>50</sub> concentration), unless stated otherwise.

#### 2.4.4 Data analysis

Concentration-response curves for wild type or mutated receptors were obtained by normalising the current responses to the responses elicited by a maximum or sub-maximum agonist concentration. Fits to full concentration-response curves for individual oocytes were made independently using Prism 5 (GraphPad Software) and then averaged in order to compare significant differences between groups. Data are expressed as mean  $\pm$  standard error of the mean (SEM) for  $n$  oocytes. In all cases, data were best fitted with a single-site model. Data were pooled for at least 3 separate experiments (conducted on separate oocytes).

Concentration-response curves were fitted using the following equation:

$$I/I_{\max} = 1/[1+(EC_{50}/[\text{agonist}])^{n_H}]$$

where  $I$  is the current and  $I_{\max}$  the maximum current. The  $EC_{50}$  is the concentration of the agonist that elicits 50% of the maximum response and  $n_H$  is the Hill coefficient.

Inhibition curves were fitted using the following equation:

$$I/I_{\max} = 1/[1+([\text{antagonist}]/IC_{50})^{n_H}]$$

where  $IC_{50}$  is the concentration of the antagonist that is required to inhibit the maximum response by 50%.

## 2.5 DISPLACEMENT RADIOLIGAND BINDING ASSAY

[<sup>3</sup>H]- $\alpha$ -bungarotoxin (56 Ci/mmol; Tocris Bioscience) was a gift from Syngenta (Bracknell, UK). Radioligand binding to transiently transfected tsA201 cells was performed essentially as described previously (Lansdell & Millar, 2000). Transfected cells were re-suspended in Hank's buffered saline solution (Gibco) containing 1% bovine serum albumin and incubated with [<sup>3</sup>H]- $\alpha$ -bungarotoxin for 2 hours at 22°C in a total volume of 150  $\mu$ l. Non-specific binding was determined in the presence of nicotine (1 mM) and carbamylcholine (1 mM). Competition binding experiments were performed by incubating triplicate samples of transfected cells with a fixed concentration of [<sup>3</sup>H]- $\alpha$ -bungarotoxin (typically 1 nM), together with a range of concentrations of the competing ligand. Radioligand binding was assayed by filtration onto Whatman GF/A filters (pre-soaked in 0.5% polyethylenimine), followed by rapid washing with phosphate-buffered saline (Oxoid) using a Brandel cell harvester. Bound radioligand was quantified by scintillation counting. IC<sub>50</sub> values were converted to K<sub>i</sub> values using the equation  $K_i = IC_{50}/[1 + ([L]/K_d)]$ , where [L] is the free concentration of [<sup>3</sup>H]- $\alpha$ -bungarotoxin used in the assay and K<sub>d</sub> is the dissociation constant of [<sup>3</sup>H]- $\alpha$ -bungarotoxin binding on the receptor. Curves for equilibrium binding were fitted using GraphPad Prism (GraphPad Software).

## 2.6 INTRACELLULAR CALCIUM ASSAYS

### 2.6.1 Fluorometric imaging plate reader assays

For the fluorometric imaging plate reader (FLIPR; Molecular Devices) assays, iCell neurons were plated as described above (section 2.2.2) into Biocoat PDL/laminin-coated, black-walled, clear bottom, half area 96-well plates at a density of  $2.5 \times 10^5$  cells/ml. FLIPR experiments took place 4-8 days after plating. A modified HBTS (Invitrogen) was used throughout the experiments, containing (mM): 135 NaCl, 5 KCl, 1.2 MgCl<sub>2</sub>, 2.5 CaCl<sub>2</sub>, 10 HEPES, 10 glucose, pH 7.2. Cell medium was removed and the cells were incubated in 50  $\mu$ l of 1  $\mu$ M Fluo-4 acetoxymethyl ester (Invitrogen) in HBTS with 0.05% Pluronic F-127 (Invitrogen) for 60 min at room temperature, protected from light. The Fluo-4 was then removed and 50  $\mu$ l HBTS were added in each well. The cells were then assayed using a FLIPR (Molecular Devices). Cells were excited by light at 488 nm from a 4 W Argon-ion laser and the emitted fluorescence passed through a 510-570 nm band-pass interference filter before detection with a cooled charge-coupled device (CCD) camera (Princeton Instruments). Drug dilutions in assay buffer were prepared in a separate 96-well, flat-bottom plate. Parameters for drug addition to the cell plate were pre-programmed and delivery was automated through a 96-well head pipettor. Drugs were added in 25  $\mu$ l volumes by automated pipetting. Intracellular calcium levels were monitored before and after the addition of the compounds. Fluorescence data were exported and analysed in Microsoft Excel and GraphPad Prism. Data were presented as normalised values, where the baseline fluorescence is subtracted from the peak fluorescence, in order to normalise for initial levels of fluorescence, and then expressed as a percentage of the response obtained by depolarising the cells with 30 mM KCl.

### 2.6.2 Single cell intracellular calcium imaging

Fluorescence-based calcium imaging experiments were carried out 6-10 days after plating of cells. A modified HBTS (Invitrogen) was used throughout the experiments, containing (mM): 135 NaCl, 5 KCl, 1.2 MgCl<sub>2</sub>, 2.5 CaCl<sub>2</sub>, 10 HEPES, 10 glucose, pH 7.2. Cells were loaded in the dark for 60 minutes at room temperature (22°C), in HBTS

containing 4  $\mu\text{M}$  of calcium-sensitive dye Fluo-4 AM (Invitrogen) in the presence of 0.05% Pluronic F-127 (Invitrogen). Cells were washed with HBTS and continuously perfused during the experiment. The perfusion flow rate was 3 ml/min, which results in complete replacement of the 100  $\mu\text{l}$  volume in each well every 2 seconds. Dye-loaded cells were viewed using an inverted epifluorescence microscope (Axiovert, 135TV, Zeiss). Fluo-4 fluorescence was excited by a  $480 \pm 10$  nm light source (Polychrome II, TILL-Photonics) and emission was captured by an iXon 897 EMCCD camera (Andor Technologies) after passage through a dichroic mirror (505LP nm) and a high pass barrier filter (515LP nm). Digitised images were stored and processed by using Imaging Workbench 5.0 software (INDEC Biosystems). Data were analysed by averaging individual traces collected from a large number of cells in multiple wells of the 96-well plate.  $\Delta F/F_0$  values were measured by quantifying the ratio between the change in fluorescence signal intensity ( $\Delta F$ ) and baseline fluorescence ( $F_0$ ).

## 2.7 STATISTICAL ANALYSIS

All statistical analysis was performed in Microsoft Excel and GraphPad Prism software.  $p$  values  $< 0.05$  were considered to be significant. Student's paired or unpaired  $t$ -tests were used for comparisons of two groups. For multiple comparisons, ANOVA (analysis of variance) was used and significances calculated using the Tukey-Kramer *post hoc* allowing for unequal sample sizes.

## 2.8 CHEMICAL SYNTHESIS

TBS compounds were synthesised by scientists at UCL in the Department of Chemistry (Jarryl D'Oyley and Dr Tom Sheppard). The following compounds were prepared by a modification of a literature procedure for triazole synthesis (El Kaim *et al.*, 2010): 4-(3-(4-bromophenyl)-5-phenyl-1H-1,2,4-triazol-1-yl)benzenesulfonamide (TBS-345), 4-(3-(4-bromophenyl)-5-(4-methoxyphenyl)-1H-1,2,4-triazol-1-yl) benzenesulfonamide (TBS-346), 4-(5-benzyl-3-(4-bromophenyl)-1H-1,2,4-triazol-1-yl)benzenesulfonamide (TBS-516), 4-(3-(4-bromophenyl)-5-propyl-1H-1,2,4-triazol-1-yl)benzenesulfonamide (TBS-546) and 4-(3-(4-bromophenyl)-5-phenethyl-1H-1,2,4-triazol-1-yl)benzenesulfonamide (TBS-556). Synthesis of *cis-cis*-4-(4-bromophenyl)-3a,4,5,9b-tetrahydro-3H-cyclopenta[c]quinoline-8-sulfonamide (4BP-TQS) and *cis-cis*-4-(naphthalen-1-yl)-3a,4,5,9b-tetrahydro-3H-cyclopenta[c]quinoline-8-sulfonamide (TQS) has been described previously (Gill *et al.*, 2011).

The biarylcarboxamide compound (R)-N-(1-azabicyclo[2.2.2]oct-3-yl)(5-(2-pyridyl)thiophene-2-carboxamide (compound B) was synthesised by scientists at Lilly Research Laboratories according to methods described previously (Phillips & Schmiesing, 2001).

CHAPTER 3

A NOVEL SERIES OF POSITIVE  
ALLOSTERIC MODULATORS  
WITH DIVERSE  
PHARMACOLOGICAL  
PROPERTIES

---

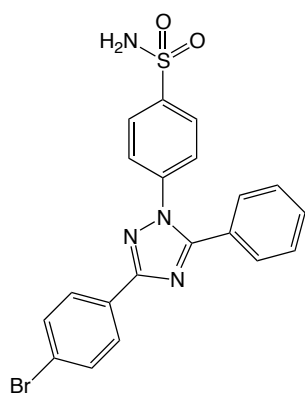
### 3.1 INTRODUCTION

Neuronal nAChRs have been implicated in a variety of cognitive and neurological disorders, including Alzheimer's disease, Parkinson's disease, epilepsy and schizophrenia (Changeux & Taly, 2008) and, as a consequence, are targets for therapeutic drug development. A number of subtype-selective orthosteric agonists, partial agonists and antagonists have been developed (Gündisch & Eibl, 2011), but it has been argued that compounds binding to allosteric sites may provide an opportunity for greater receptor subtype selectivity (Williams *et al.*, 2011b). Promising results have been obtained with nAChR allosteric modulators in pre-clinical studies examining effects on cognitive deficits (Hurst *et al.*, 2005; Ng *et al.*, 2007), nociception (Timmermann *et al.*, 2007; Zhu *et al.*, 2011; Munro *et al.*, 2012) cerebral ischemia (Kalappa *et al.*, 2013) and depression (Targowska-Duda *et al.*, 2014).

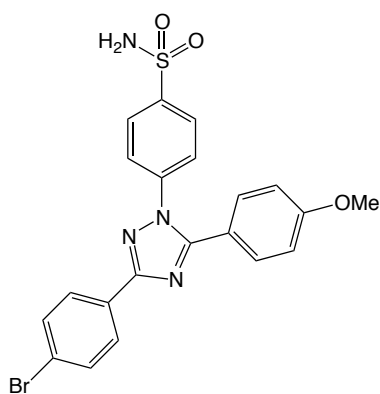
As discussed in sections 1.4.2 and 1.7, whereas most nAChRs are heteromeric combinations of more than one type of subunit (Millar & Gotti, 2009), some nAChRs, such as  $\alpha 7$ , are able to form functional homomeric nAChRs (Couturier *et al.*, 1990). Homomeric  $\alpha 7$  nAChRs undergo very rapid desensitisation in response to agonist activation. Indeed, with high concentrations of acetylcholine, almost complete inactivation of  $\alpha 7$  nAChRs is observed within milliseconds of agonist activation (Couturier *et al.*, 1990). However, rapid desensitisation of  $\alpha 7$  nAChRs is not seen with all agonists. A group of compounds, described as allosteric agonists, activate  $\alpha 7$  nAChRs with minimal levels of desensitisation (Gill *et al.*, 2011; Gill *et al.*, 2012; Papke *et al.*, 2014). In contrast to conventional orthosteric agonists such as acetylcholine, there is evidence that allosteric agonists may act via a distinct transmembrane binding site (Gill *et al.*, 2011).

Previous studies have identified an extensive series of PAMs on  $\alpha 7$  nAChRs (Faghieh *et al.*, 2008; Williams *et al.*, 2011a). As discussed in more detail in section 1.6.4,  $\alpha 7$  nAChRs PAMs have been referred to as either 'type I' or 'type II' PAMs, depending on their effects on receptor desensitisation (Bertrand & Gopalakrishnan, 2007). The convention is to describe PAMs with little or no significant effect on desensitisation as type I PAMs and those causing a dramatic reduction in desensitisation as type II PAMs.

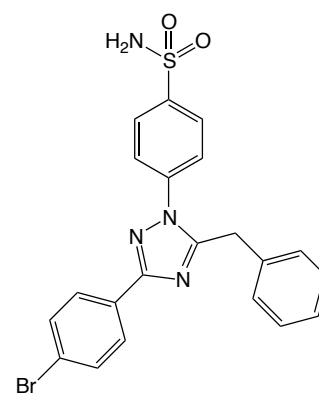
A novel series of compounds (Figure 3.1) was constructed involving a combination of structural elements from two previously described  $\alpha 7$ -selective allosteric modulators, 4BP-TQS (Gill *et al.*, 2011) and A-867744 (Faghieh *et al.*, 2008). Both 4BP-TQS and A-867744 contain an arylsulfonamide unit linked to a heterocyclic core, which has both a bromoarene and a second lipophilic group attached. Five compounds were synthesised which retained the key structural features of 4BP-TQS and A-867744 but which contained a more polar triazole group as the heterocyclic core. For convenience, these compounds are referred to here collectively as ‘TBS’ compounds to reflect the fact that they all contain triazole and benzenesulfonamide groups. In this chapter, the properties of this series of compounds are examined on nAChRs. Evidence is provided showing that the TBS compounds constitute a novel series of potent  $\alpha 7$ -selective PAMs with a range of effects on receptor desensitisation.



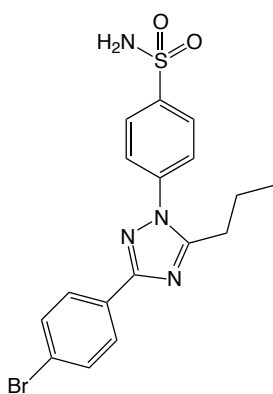
TBS-345



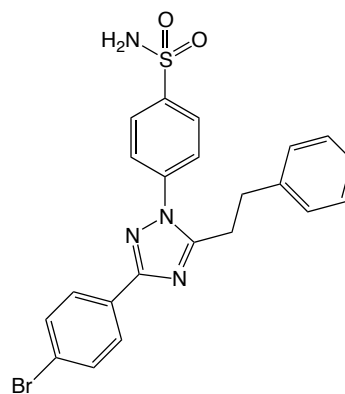
TBS-346



TBS-516



TBS-546



TBS-556

**Figure 3.1: Chemical structures of allosteric ligands examined in this chapter.**

Abbreviations: TBS-345: 4-(3-(4-bromophenyl)-5-phenyl-1*H*-1,2,4-triazol-1-yl)benzenesulfonamide; TBS-346: 4-(3-(4-bromophenyl)-5-(4-methoxyphenyl)-1*H*-1,2,4-triazol-1-yl)benzenesulfonamide; TBS-516: 4-(5-benzyl-3-(4-bromophenyl)-1*H*-1,2,4-triazol-1-yl)benzenesulfonamide; TBS-546: 4-(3-(4-bromophenyl)-5-propyl-1*H*-1,2,4-triazol-1-yl)benzenesulfonamide; TBS-556: 4-(3-(4-bromophenyl)-5-phenethyl-1*H*-1,2,4-triazol-1-yl)benzenesulfonamide.

## 3.2 RESULTS

The TBS series of compounds used for experiments in this chapter were synthesised by scientists at UCL in the Department of Chemistry (Jarryl D'Oyley and Dr Tom Sheppard). The pharmacological properties of the TBS series of compounds were examined by two-electrode voltage-clamp recordings in *Xenopus* oocytes expressing human recombinant nAChRs, unless stated otherwise, and with competition radioligand binding assays in mammalian cultured cells transiently transfected with human  $\alpha 7$  nAChRs.

### 3.2.1 Characterisation of the effects of TBS compounds on activation of $\alpha 7$ nAChRs by acetylcholine

In agreement with previous studies (Couturier *et al.*, 1990), acetylcholine activated  $\alpha 7$  nAChRs with an  $EC_{50}$  value of  $132 \pm 13 \mu\text{M}$  and Hill coefficient ( $n_H$ ) of  $1.4 \pm 0.2$ . In addition, activation by acetylcholine was associated with rapid desensitisation (Figure 3.2). None of the TBS compounds examined displayed agonist activity when applied alone to human  $\alpha 7$  nAChRs expressed in *Xenopus* oocytes but all of them potentiated responses evoked by a submaximal concentration of acetylcholine ( $100 \mu\text{M}$ ; near the  $EC_{50}$ ) (Figure 3.3–3.7 and Table 1). TBS-346 potentiated submaximal acetylcholine responses with an  $EC_{50}$  of  $2.83 \pm 1.20 \mu\text{M}$  and Hill coefficient of  $1.0 \pm 0.1$  and the maximum fold potentiation was  $5.1 \pm 0.5$  (Figure 3.3 and Table 1). TBS-546 potentiated submaximal acetylcholine responses with an  $EC_{50}$  of  $2.84 \pm 0.01 \mu\text{M}$ , Hill coefficient of  $2.4 \pm 0.3$  and maximum fold potentiation of  $3.5 \pm 0.5$  (Figure 3.4 and Table 1). TBS-345 potentiated submaximal acetylcholine responses with an  $EC_{50}$  of  $1.69 \pm 0.31 \mu\text{M}$ , Hill coefficient of  $1.2 \pm 0.2$  and maximum fold potentiation of  $8.9 \pm 1.1$  (Figure 3.5 and Table 1). TBS-556 potentiated submaximal acetylcholine responses with an  $EC_{50}$  of  $2.08 \pm 0.32 \mu\text{M}$ , Hill coefficient of  $2.8 \pm 0.9$  and maximum fold potentiation of  $6.1 \pm 0.6$  (Figure 3.6 and Table 1). TBS-516 potentiated submaximal acetylcholine responses with an  $EC_{50}$  of  $1.43 \pm 0.15 \mu\text{M}$ , Hill coefficient of  $2.4 \pm 0.4$  and maximum fold potentiation of  $17.3 \pm 3.0$  (Figure 3.7 and Table 1). Notably, despite the relatively close chemical similarity between these compounds (Figure 3.1), they displayed a diverse range of effects on the rate of desensitisation of  $\alpha 7$  nAChRs (Figure 3.3–3.7). For

example, TBS-346 caused minimal changes to desensitisation (Figure 3.3), a feature that is typical of type I PAMs, whereas TBS-516 caused a dramatic slowing of desensitisation (Figure 3.7), typical of type II PAMs. In addition, other compounds in this series (TBS-345, TBS-546 and TBS-556) had effects on receptor desensitisation that could be considered as being intermediate between those of classical type I and type II PAMs (Figure 3.4–3.6). A consistent feature in the potentiated responses by the intermediate compounds appears to be the existence of a fast-desensitising component, followed by a very slow-desensitising current. The ratio of the amplitude of the slow to fast current was determined for the TBS compounds and is shown in Table 1. TBS-516 did not evoke a detectable fast-desensitising component, so this ratio was not determined. No slow-desensitising component was detected with TBS-346 and, consequently, the slow to fast ratio was determined as 0.

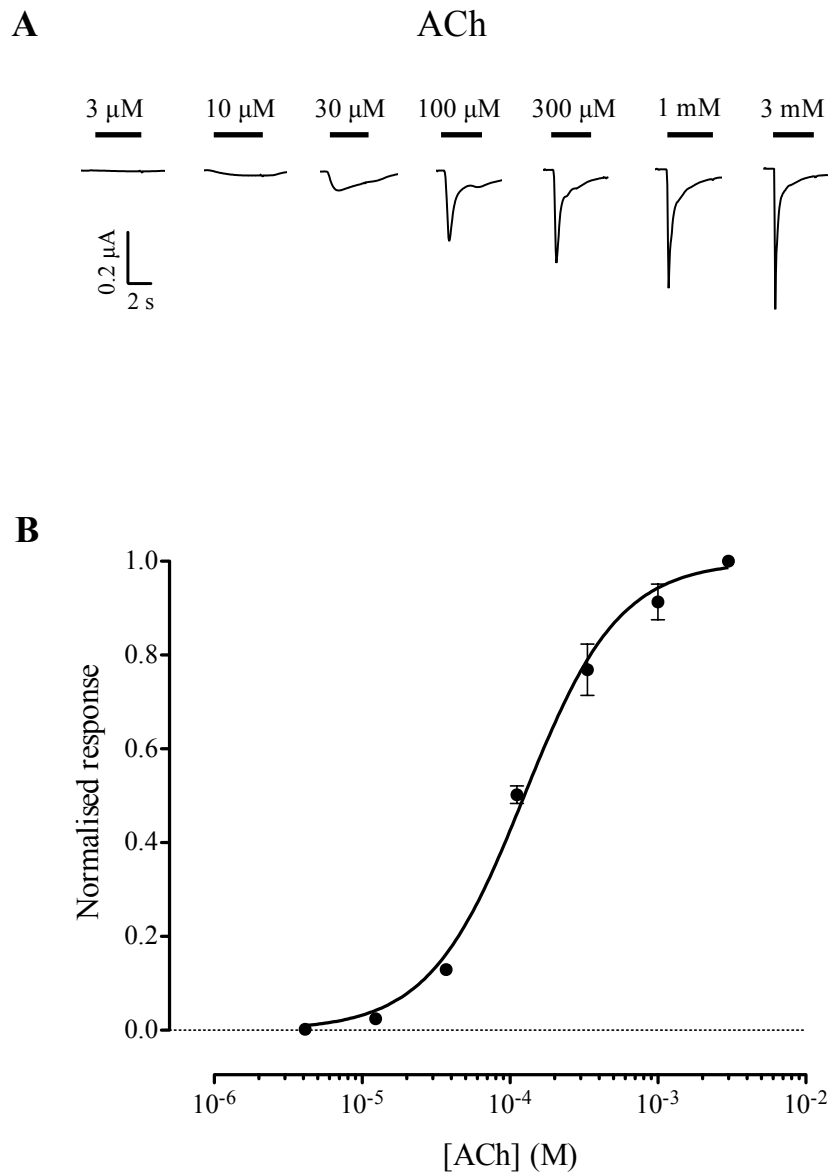


**Figure 3.2: Agonist activation of recombinant human  $\alpha 7$  nAChRs by ACh, examined by two-electrode voltage-clamp recording in *Xenopus* oocytes.**

A) Representative traces are shown illustrating responses to ACh (3  $\mu\text{M}$  – 3 mM). The horizontal bars indicate the duration of agonist application.

B) Concentration-response data are plotted for a range of concentrations of ACh. Data are means  $\pm$  SEM of six independent experiments, each from different oocytes. Data are normalised to the maximum response, obtained with 3 mM ACh.

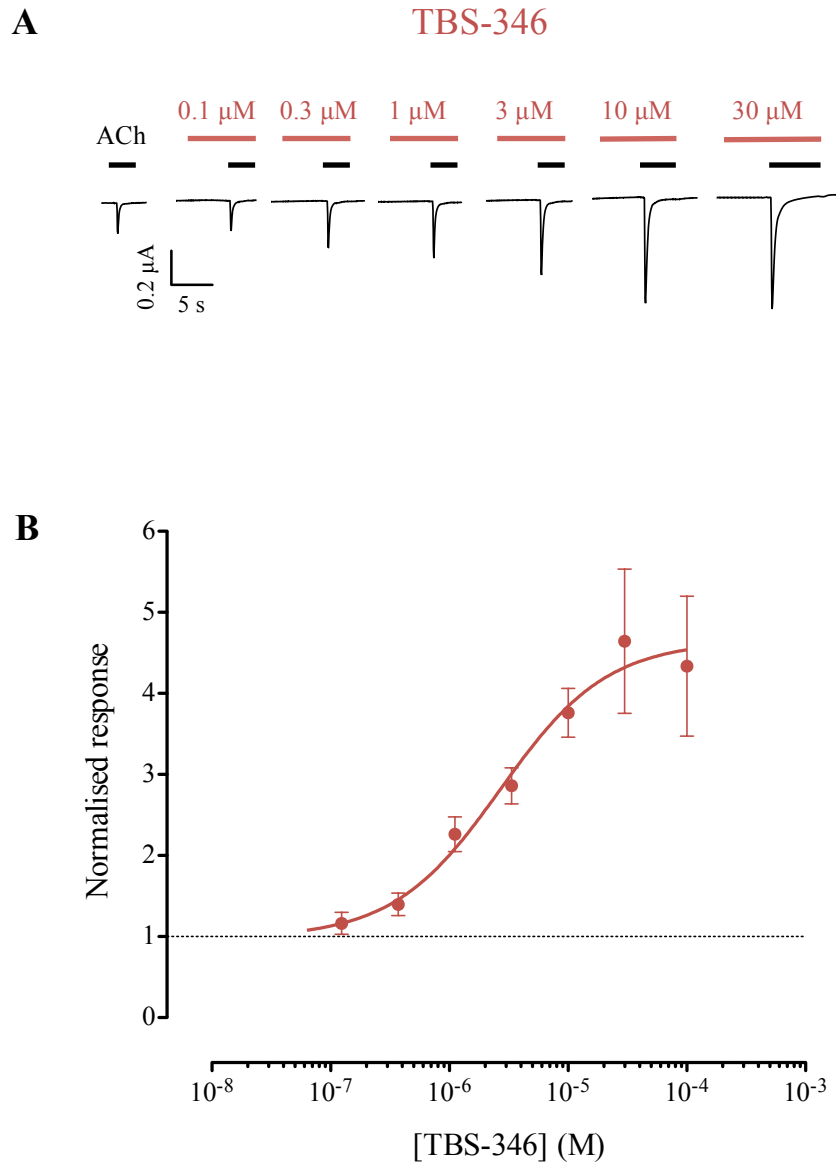


**Figure 3.3: Positive allosteric modulation of  $\alpha 7$  nAChRs by TBS-346, examined by two-electrode voltage-clamp recording in *Xenopus* oocytes.**

A) Representative traces are shown illustrating responses to an  $\text{EC}_{50}$  of ACh (100  $\mu\text{M}$ ) and of ACh (100  $\mu\text{M}$ ) co-applied with a range of concentrations of TBS-346 (0.1 – 30  $\mu\text{M}$ ). TBS-346 was pre-applied for 5 s before ACh was co-applied. The horizontal bars indicate the duration of ACh (black bars) and TBS-346 (red bars) application.

B) Concentration-response data are plotted for a range of concentrations of TBS-346 co-applied with an  $\text{EC}_{50}$  of ACh (100  $\mu\text{M}$ ). Data are means  $\pm$  SEM of four independent experiments, each from different oocytes. Data are normalised to the response obtained with 100  $\mu\text{M}$  ACh.

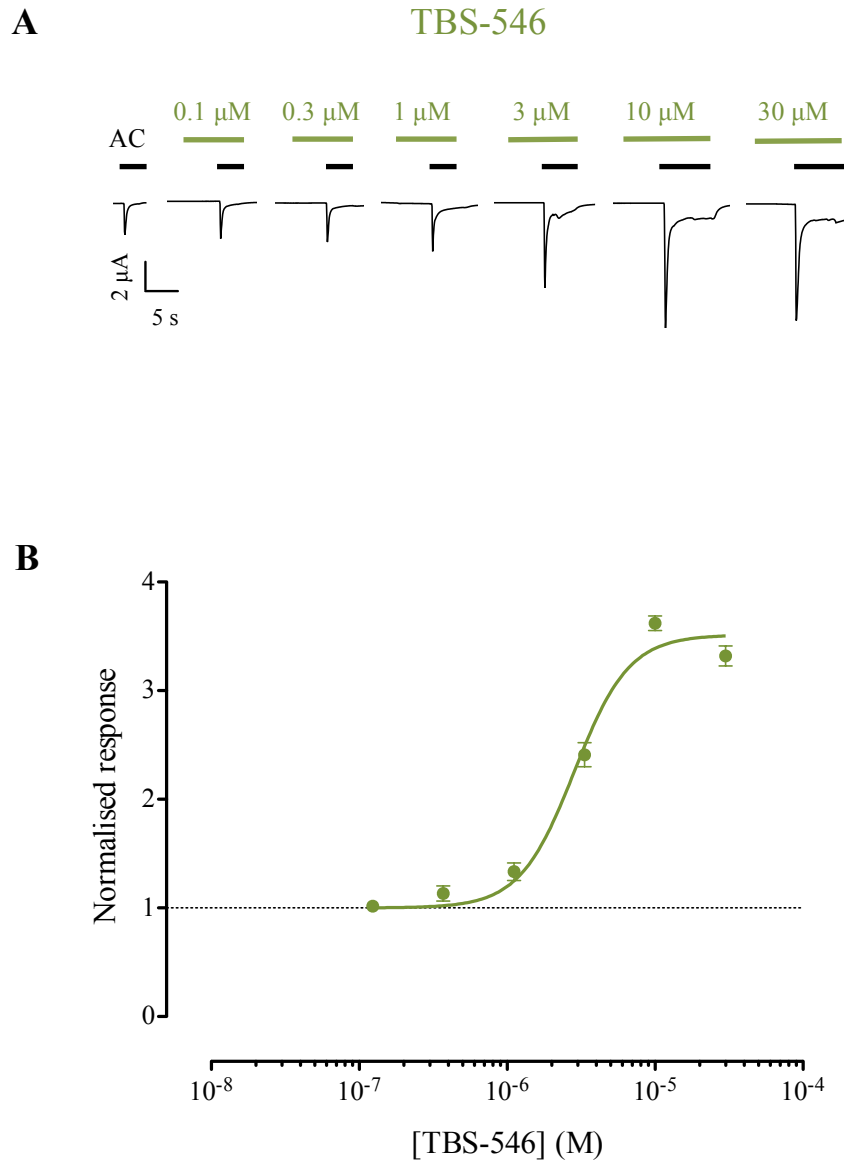


**Figure 3.4: Positive allosteric modulation of  $\alpha 7$  nAChRs by TBS-546, examined by two-electrode voltage-clamp recording in *Xenopus* oocytes.**

A) Representative traces are shown illustrating responses to an  $EC_{50}$  of ACh (100  $\mu$ M) and of ACh (100  $\mu$ M) co-applied with a range of concentrations of TBS-546 (0.1 – 30  $\mu$ M). TBS-546 was pre-applied for 5 s before ACh was co-applied. The horizontal bars indicate the duration of ACh (black bars) and TBS-546 (green bars) application.

B) Concentration-response data are plotted for a range of concentrations of TBS-546 co-applied with an  $EC_{50}$  of ACh (100  $\mu$ M). Data are means  $\pm$  SEM of three independent experiments, each from different oocytes. Data are normalised to the response obtained with 100  $\mu$ M ACh.

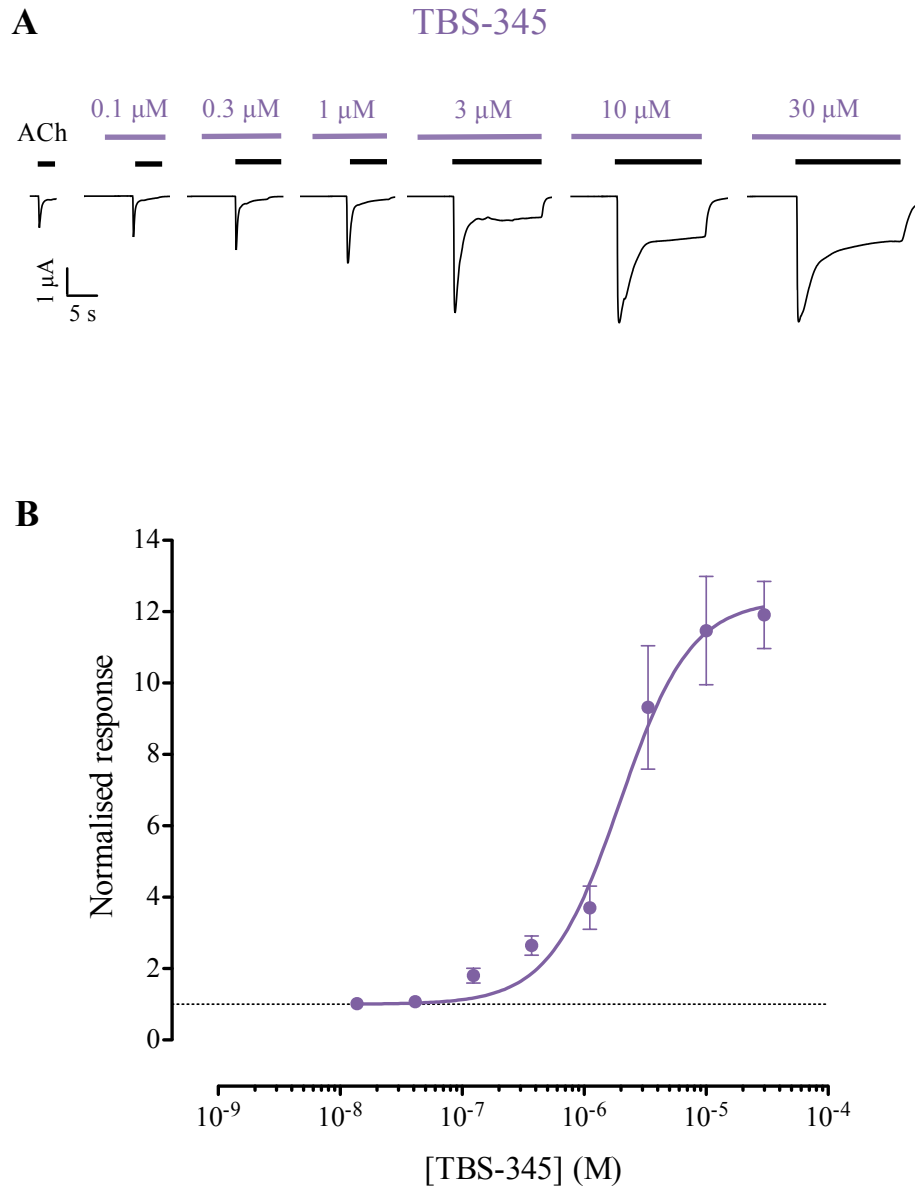


**Figure 3.5: Positive allosteric modulation of  $\alpha 7$  nAChRs by TBS-345, examined by two-electrode voltage-clamp recording in *Xenopus* oocytes.**

A) Representative traces are shown illustrating responses to an  $\text{EC}_{50}$  of ACh (100  $\mu\text{M}$ ) and of ACh (100  $\mu\text{M}$ ) co-applied with a range of concentrations of TBS-345 (0.1 – 30  $\mu\text{M}$ ). TBS-345 was pre-applied for 5 s before ACh was co-applied. The horizontal bars indicate the duration of ACh (black bars) and TBS-345 (purple bars) application.

B) Concentration-response data are plotted for a range of concentrations of TBS-345 co-applied with an  $\text{EC}_{50}$  of ACh (100  $\mu\text{M}$ ). Data are means  $\pm$  SEM of three independent experiments, each from different oocytes. Data are normalised to the response obtained with 100  $\mu\text{M}$  ACh.

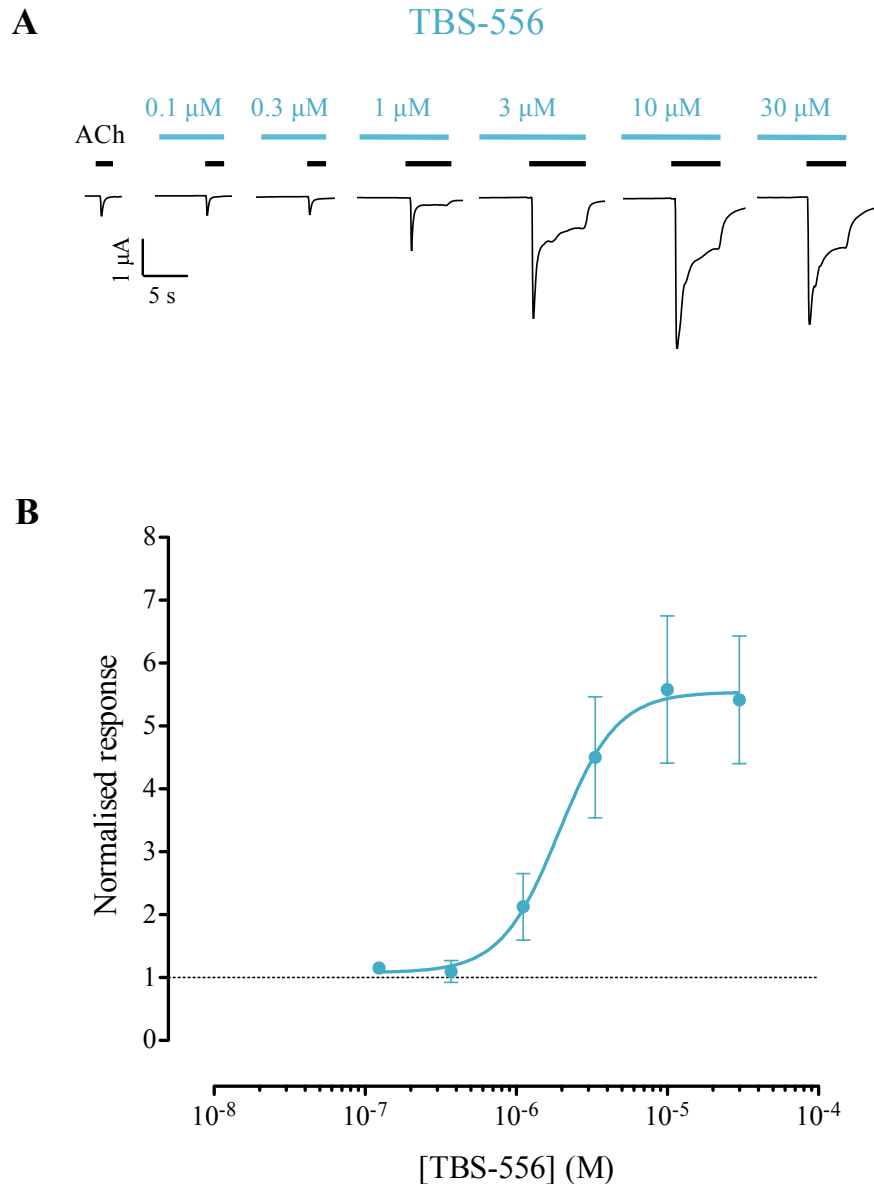


**Figure 3.6: Positive allosteric modulation of  $\alpha 7$  nAChRs by TBS-556, examined by two-electrode voltage-clamp recording in *Xenopus* oocytes.**

A) Representative traces are shown illustrating responses to an  $\text{EC}_{50}$  of ACh (100  $\mu\text{M}$ ) and of ACh (100  $\mu\text{M}$ ) co-applied with a range of concentrations of TBS-556 (0.1 – 30  $\mu\text{M}$ ). TBS-556 was pre-applied for 5 s before ACh was co-applied. The horizontal bars indicate the duration of ACh (black bars) and TBS-556 (blue bars) application.

B) Concentration-response data are plotted for a range of concentrations of TBS-556 co-applied with an  $\text{EC}_{50}$  of ACh (100  $\mu\text{M}$ ). Data are means  $\pm$  SEM of three independent experiments, each from different oocytes. Data are normalised to the response obtained with 100  $\mu\text{M}$  ACh.

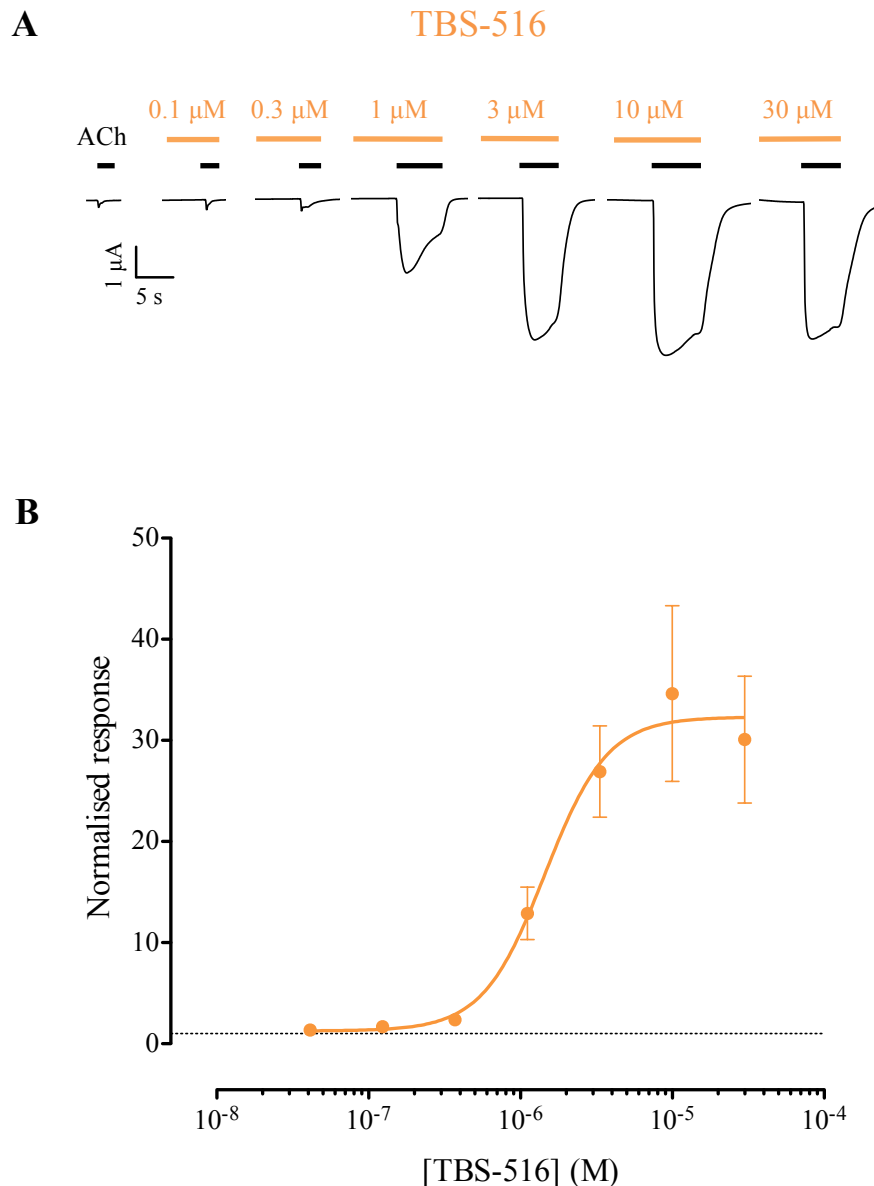


**Figure 3.7: Positive allosteric modulation of  $\alpha 7$  nAChRs by TBS-516, examined by two-electrode voltage-clamp recording in *Xenopus* oocytes.**

A) Representative traces are shown illustrating responses to an EC<sub>50</sub> of ACh (100  $\mu\text{M}$ ) and of ACh (100  $\mu\text{M}$ ) co-applied with a range of concentrations of TBS-516 (0.1 – 30  $\mu\text{M}$ ). TBS-516 was pre-applied for 5 s before ACh was co-applied. The horizontal bars indicate the duration of ACh (black bars) and TBS-516 (orange bars) application.

B) Concentration-response data are plotted for a range of concentrations of TBS-516 co-applied with an EC<sub>50</sub> of ACh (100  $\mu\text{M}$ ). Data are means  $\pm$  SEM of three independent experiments, each from different oocytes. Data are normalised to the response obtained with 100  $\mu\text{M}$  ACh.

### 3.2.2 Examination of the ability of TBS compounds to facilitate recovery from desensitisation on $\alpha 7$ nAChRs

A notable property of type II PAMs is their ability to reactivate  $\alpha 7$  nAChRs after they have been desensitised by continuous application of an orthosteric agonist (Hurst *et al.*, 2005), while type I PAMs lack this ability (Grønlien *et al.*, 2007). Figure 3.8 demonstrates the effect of TBS compounds on the recovery from desensitisation of  $\alpha 7$  nAChRs after activation and desensitisation by a submaximal concentration of acetylcholine (100  $\mu$ M). TBS-346 and TBS-546 elicited no detectable responses after the receptor had been desensitised, a feature that is characteristic of type I PAMs. In contrast, TBS-345, TBS-516 and TBS-556 caused recovery from desensitisation, albeit to differing extents (Figure 3.8 and Table 1). TBS-516 had the most profound effect, by eliciting a response that was  $3.2 \pm 0.9$  - fold larger than the response to 100  $\mu$ M acetylcholine. TBS-556 and TBS-345 elicited responses that were  $57.3 \pm 10.1\%$  and  $23.0 \pm 2.1\%$  of the response to 100  $\mu$ M acetylcholine, respectively (Figure 3.8). Where receptor reactivation was observed (when acetylcholine was co-applied with TBS-345, TBS-556 or TBS-516), no current decline was observed over a period of 30 s (Figure 3.8). The total net charge transfer (the area under the curve for the current trace) measured during a 30 s application of TBS-345, TBS-556 and TBS-516 was  $12 \pm 2$ ,  $27 \pm 6$  and  $250 \pm 71$  - fold larger than that measured during the initial application of acetylcholine alone (Figure 3.8).

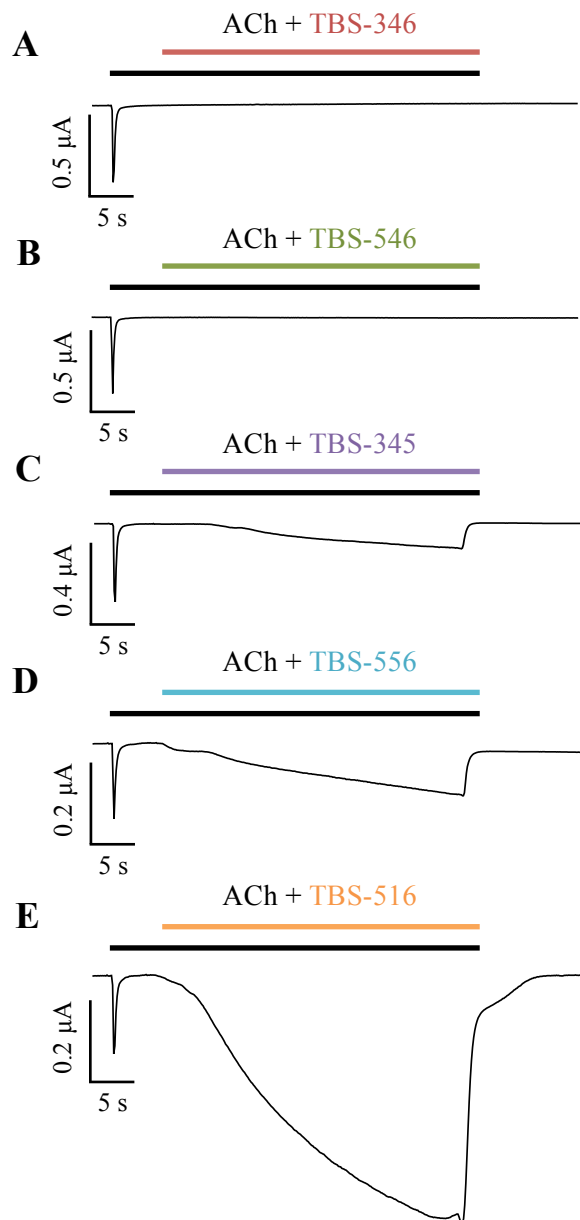


**Figure 3.8: Influence of TBS compounds on the recovery of  $\alpha 7$  nAChRs from desensitisation, examined by two-electrode voltage-clamp recording in *Xenopus* oocytes.**

Representative traces showing prolonged exposure of  $\alpha 7$  nAChRs to ACh (100  $\mu\text{M}$ ), causing activation, followed by rapid desensitisation. In the continued presence of ACh, application of (A) TBS-346 (10  $\mu\text{M}$ ) and (B) TBS-546 (10  $\mu\text{M}$ ) does not result in reactivation of the receptor. However, application of (C) TBS-345 (10  $\mu\text{M}$ ), (D) TBS-556 (10  $\mu\text{M}$ ) and (E) TBS-516 (10  $\mu\text{M}$ ) results in reactivation of desensitised receptors. Traces have been scaled to their response to ACh. Horizontal bars indicate the duration of ACh (black bar) and TBS compound (coloured bar) application.

**Table 1: Pharmacological properties of TBS PAMs on  $\alpha 7$  nAChRs.**

Data are means  $\pm$  SEM of at least three independent experiments. TBS compounds were pre-applied for 5 s and then co-applied with ACh (100  $\mu$ M). The EC<sub>50</sub> values of all TBS compounds were not significantly different to each other (ANOVA with Tukey's *post hoc*,  $p = 0.35$ ).

<sup>a</sup> Data for maximal currents ( $I_{\max}$ ) are normalised to the size of the acetylcholine response (100  $\mu$ M) in the absence of the PAM.

<sup>b</sup> The ratio of the peak amplitude of the slow-desensitising component to the peak amplitude of the fast-desensitising component of the potentiated response. No fast-desensitising component was detected with TBS-516.

<sup>c</sup> Recovery from desensitisation elicited by PAMs after a long application of acetylcholine. Peak amplitude is normalised to the initial acetylcholine response (100  $\mu$ M).

PAM	EC <sub>50</sub> ( $\mu$ M)	n <sub>H</sub>	I <sub>max</sub> <sup>a</sup>	Slow: Fast component <sup>b</sup>	Recovery from desensitisation <sup>c</sup>
TBS-345	1.69 $\pm$ 0.31	1.2 $\pm$ 0.2	8.9 $\pm$ 1.1	0.19 $\pm$ 0.04	0.2 $\pm$ 0.02
TBS-346	2.83 $\pm$ 1.20	1.0 $\pm$ 0.1	5.1 $\pm$ 0.5	0.00	0.0
TBS-516	1.43 $\pm$ 0.15	2.4 $\pm$ 0.4	17.3 $\pm$ 3.0	–	3.2 $\pm$ 0.9
TBS-546	2.84 $\pm$ 0.01	2.4 $\pm$ 0.3	3.5 $\pm$ 0.5	0.08 $\pm$ 0.01	0.0
TBS-556	2.08 $\pm$ 0.32	2.8 $\pm$ 0.9	6.1 $\pm$ 0.6	0.34 $\pm$ 0.09	0.6 $\pm$ 0.1

### 3.2.3 Displacement of [<sup>3</sup>H]- $\alpha$ -bungarotoxin by TBS compounds

Competition radioligand binding was performed to examine the ability of the TBS compounds to displace [<sup>3</sup>H]- $\alpha$ -bungarotoxin from the orthosteric binding site of  $\alpha 7$  nAChRs (Figure 3.9). As expected, the competitive antagonist MLA fully displaced specific [<sup>3</sup>H]- $\alpha$ -bungarotoxin binding in a concentration-dependent manner with a  $K_i$  of  $49.2 \pm 3.1$  nM (Figure 3.9). This is higher than what is usually reported for MLA ( $\sim 4$  nM) (Davies *et al.*, 1999; Puinean *et al.*, 2013), which could possibly be the result of MLA stock degradation. In contrast, none of the TBS compounds displayed any significant displacement of [<sup>3</sup>H]- $\alpha$ -bungarotoxin binding (Figure 3.9). These findings are consistent with TBS compounds acting as potentiators of  $\alpha 7$  nAChRs via a site other than the extracellular orthosteric binding site.

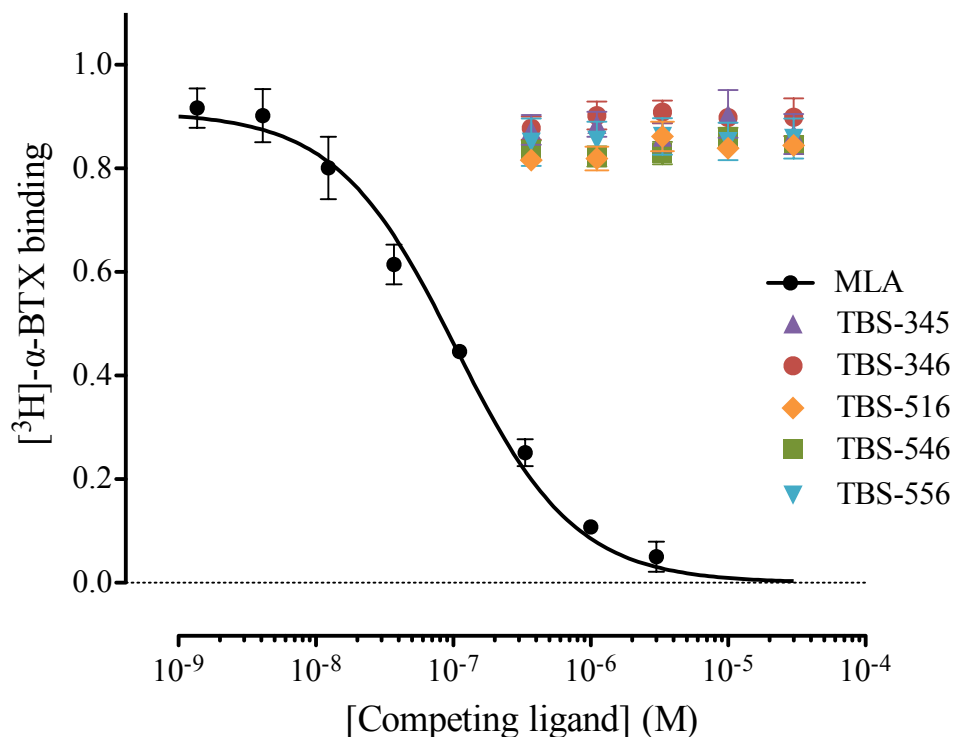


**Figure 3.9: Displacement of [<sup>3</sup>H]-α-bungarotoxin from the orthosteric site of α7 nAChRs by TBS compounds, examined by competition radioligand binding.**

Equilibrium radioligand binding was performed with [<sup>3</sup>H]-α-bungarotoxin (1 nM) with mammalian tsA201 cells transiently transfected with human α7 nAChR subunit and with human RIC-3 cDNAs (1:1 ratio). TBS-345, TBS-346, TBS-516, TBS-546 and TBS-556 (0.3 – 30 μM) cause no significant displacement of [<sup>3</sup>H]-α-bungarotoxin binding, whereas MLA causes complete displacement of specific radioligand binding ( $K_i = 49.2 \pm 3.1$  nM). This is higher than what is usually reported for MLA (~ 4 nM) (Davies *et al.*, 1999; Puinean *et al.*, 2013), which could possibly be the result of MLA stock degradation. Data points are means ( $\pm$  SEM) of three independent experiments, each done in triplicates.

### 3.2.4 Selectivity of TBS compounds

All of the TBS compounds acted as potentiators of both human and rat  $\alpha 7$  nAChRs (Figure 3.10–3.12 and Table 2). In contrast, none of the TBS compounds caused potentiation of human  $\alpha 4\beta 2$  nAChRs, human  $\alpha 3\beta 4$  nAChRs or mouse 5-HT<sub>3A</sub>Rs. Instead, all of the compounds acted as inhibitors of this diverse group of receptors (Figure 3.10–3.12 and Table 2), indicating that, to the extent that we have examined, these TBS compounds can be considered to be  $\alpha 7$ -selective PAMs. The opposing effects of the TBS compounds on  $\alpha 7$  nAChRs and 5-HT<sub>3A</sub>Rs (potentiation and inhibition, respectively) prompted us to examine the effect of these compounds on an artificial subunit chimera ( $\alpha 7/5$ -HT3A) containing the N-terminal domain of the rat  $\alpha 7$  nAChR subunit and the transmembrane/C-terminal domain of the mouse 5-HT3A subunit. For all of the TBS compounds examined, inhibition of agonist-evoked responses was observed on the  $\alpha 7/5$ -HT3A subunit chimera (Figure 3.11, 3.12 and Table 2). Together, these results are consistent with these compounds interacting with the transmembrane domain, a location that has been proposed as being the site at which several other  $\alpha 7$ -selective PAMs interact with  $\alpha 7$  nAChRs (Young *et al.*, 2008; Collins *et al.*, 2011; Gill *et al.*, 2011).

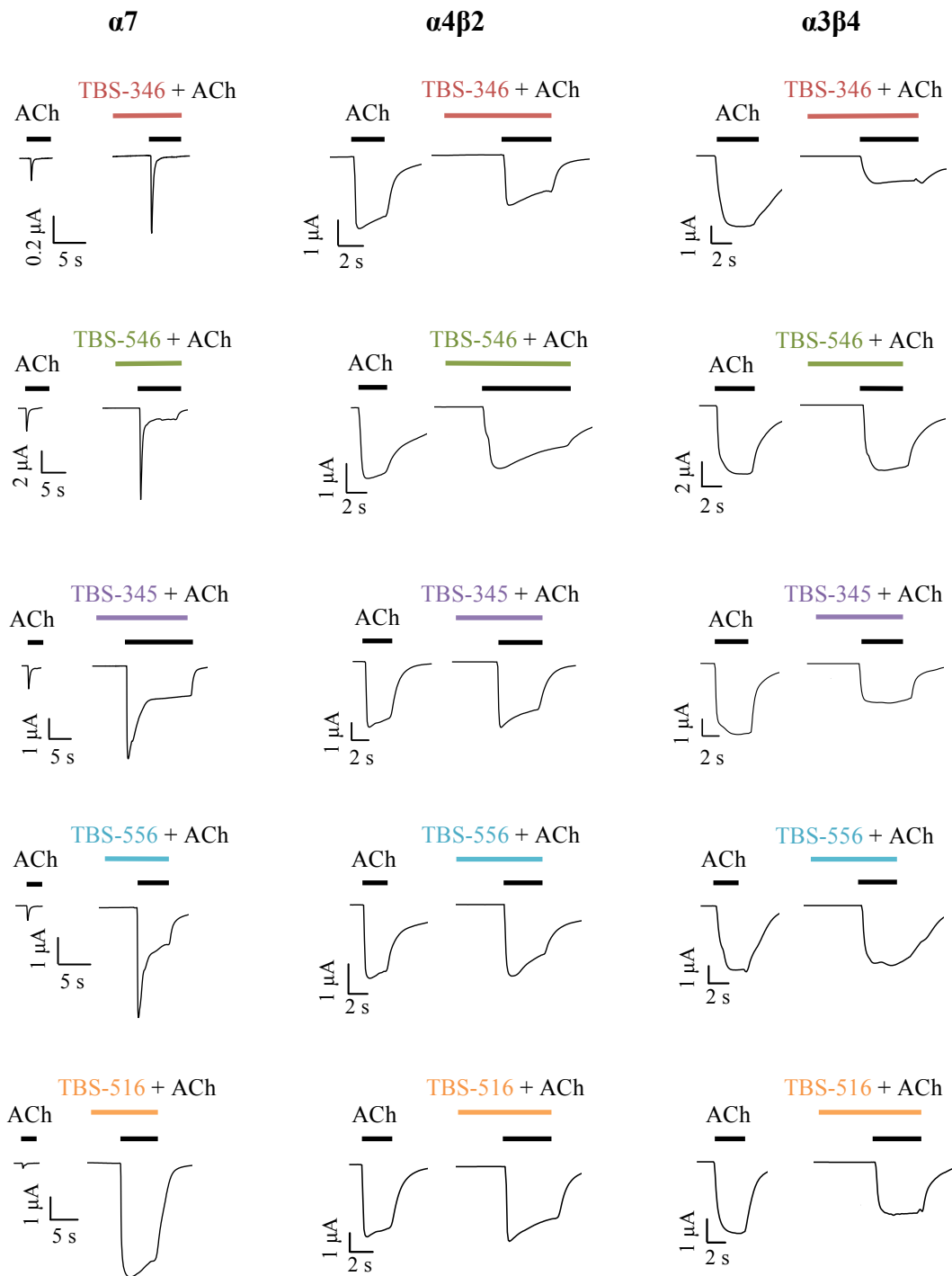


**Figure 3.10: Nicotinic subtype selectivity of TBS compounds, examined by two-electrode voltage-clamp recording in *Xenopus* oocytes.**

Representative traces illustrating responses to ACh (100  $\mu$ M; black bars) and to TBS compounds (10  $\mu$ M on  $\alpha$ 7 nAChRs; 50  $\mu$ M on other subtypes; coloured bars) pre-applied for 5 s and then co-applied with ACh (100  $\mu$ M; black bars). Left column of traces illustrates responses of  $\alpha$ 7 nAChRs, middle column illustrates responses of  $\alpha$ 4 $\beta$ 2 nAChRs (mRNA injection in 1:1 subunit ratio) and right column illustrates responses of  $\alpha$ 3 $\beta$ 4 nAChRs (mRNA injection in 1:1 subunit ratio).

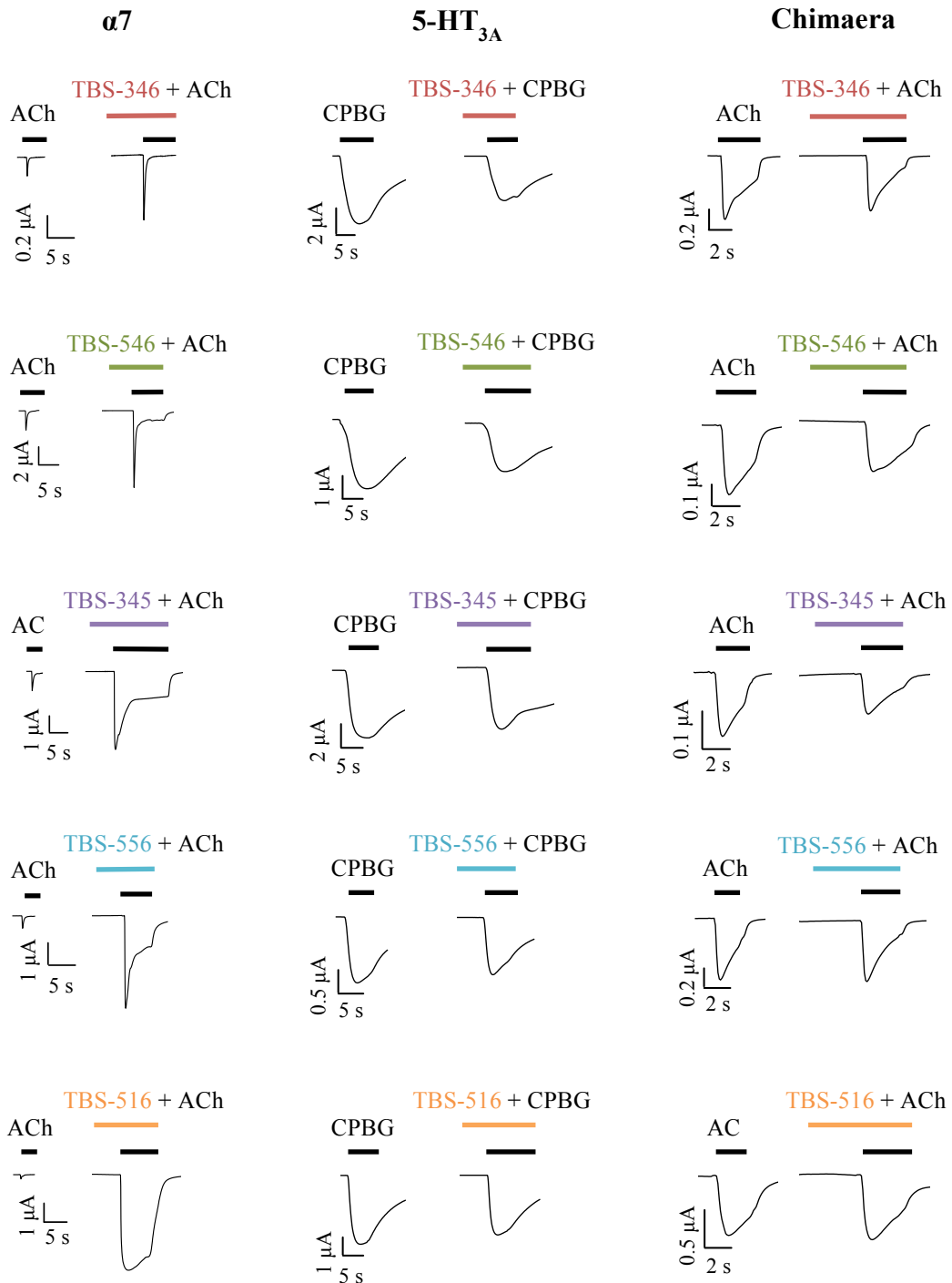


**Figure 3.11: Contrasting effects of TBS compounds between  $\alpha 7$  nAChR, 5-HT<sub>3A</sub>R and a subunit chimaera, examined by two-electrode voltage-clamp recording in *Xenopus* oocytes.**

Representative traces illustrating responses to agonist (100  $\mu$ M ACh for  $\alpha 7$  and chimaera receptors; 1  $\mu$ M CPBG for 5-HT<sub>3A</sub>Rs; black bars) and to TBS compounds (10  $\mu$ M on  $\alpha 7$  nAChRs; 50  $\mu$ M on other subtypes; coloured bars) pre-applied for 5 s and then co-applied with the agonist. Left column of traces illustrates responses of  $\alpha 7$  nAChRs, middle column illustrates responses of 5-HT<sub>3A</sub>Rs and right column illustrates responses of a subunit chimaera consisting of the  $\alpha 7$  nAChR N-terminus and 5-HT<sub>3A</sub>R TM domain and C-terminus.

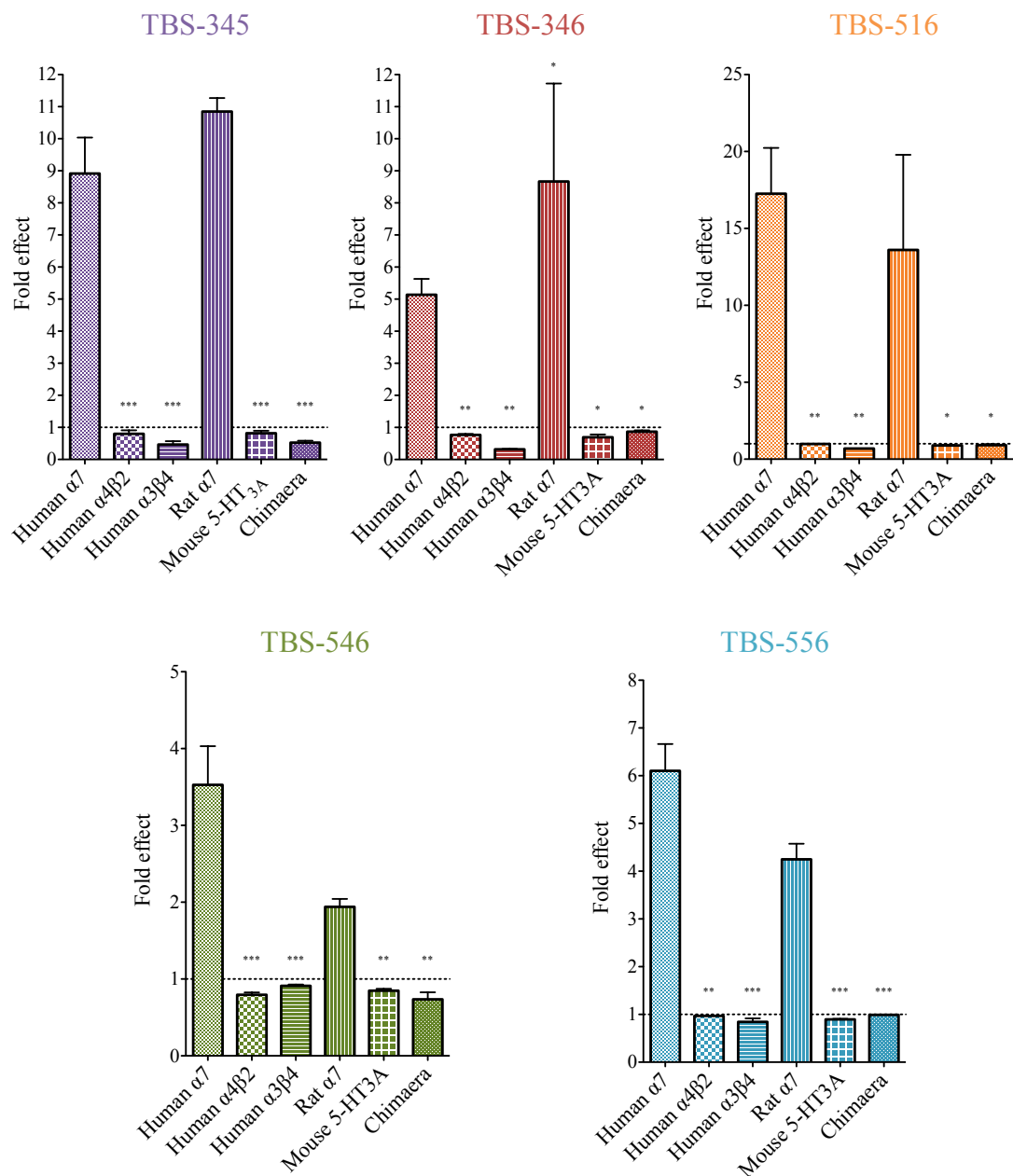


**Figure 3.12: Subtype selectivity of TBS compounds, examined by two-electrode voltage-clamp recording in *Xenopus* oocytes.**

Bar charts illustrating the effects of TBS compounds (10  $\mu$ M on  $\alpha 7$  nAChRs; 50  $\mu$ M on other subtypes) on the agonist response (100  $\mu$ M ACh for nAChRs and chimaeric receptors; 1  $\mu$ M CPBG for 5-HT<sub>3A</sub>Rs) of different receptor subtypes. Bars represent means and SEMs of at least three independent experiments. Asterisks denote significance levels between human  $\alpha 7$  and the other subtypes as determined by one-way ANOVA with Dunnett's *post hoc* (\*  $p < 0.05$ ; \*\*  $p < 0.01$ ; \*\*\*  $p < 0.001$ ).

**Table 2: Subtype selectivity of TBS compounds.**

Data are means  $\pm$  SEM of at least three independent experiments. Fold-potential and % inhibition data of TBS compounds (10  $\mu$ M on  $\alpha$ 7 nAChRs; 50  $\mu$ M on other subtypes) are normalised to control agonist responses in the absence of the TBS compounds (100  $\mu$ M acetylcholine for nAChRs and chimaeric receptors; 1  $\mu$ M CPBG for 5-HT<sub>3A</sub>Rs). TBS compounds were pre-applied for 5 s and then co-applied with the orthosteric agonist.

<sup>a</sup> Chimaeric subunit containing the rat nAChR  $\alpha$ 7 subunit N-terminal domain and mouse 5-HT<sub>3A</sub> subunit transmembrane and C-terminal domain.

Compound		Human $\alpha$ 7	Human $\alpha$ 4 $\beta$ 2	Human $\alpha$ 3 $\beta$ 4	Rat $\alpha$ 7	Mouse 5-HT <sub>3A</sub>	Chimaera <sup>a</sup>
TBS-345	fold-potential	8.9 $\pm$ 1.1	–	–	10.9 $\pm$ 0.4	–	–
	% inhibition	–	20.1 $\pm$ 11.0	53.7 $\pm$ 10.6	–	18.3 $\pm$ 7.7	47.3 $\pm$ 5.9
TBS-346	fold-potential	5.1 $\pm$ 0.5	–	–	8.7 $\pm$ 3.1	–	–
	% inhibition	–	23.1 $\pm$ 2.9	68.4 $\pm$ 1.5	–	30.8 $\pm$ 8.9	13.4 $\pm$ 4.4
TBS-516	fold-potential	17.3 $\pm$ 3.0	–	–	13.6 $\pm$ 6.2	–	–
	% inhibition	–	1.7 $\pm$ 0.2	31.1 $\pm$ 0.3	–	10.4 $\pm$ 4.3	9.3 $\pm$ 7.4
TBS-546	fold-potential	3.5 $\pm$ 0.5	–	–	1.9 $\pm$ 0.1	–	–
	% inhibition	–	20.5 $\pm$ 3.0	9.0 $\pm$ 1.7	–	15.2 $\pm$ 2.5	26.4 $\pm$ 9.2
TBS-556	fold-potential	6.1 $\pm$ 0.6	–	–	4.3 $\pm$ 0.3	–	–
	% inhibition	–	3.2 $\pm$ 0.6	15.6 $\pm$ 7.3	–	10.4 $\pm$ 1.1	1.0 $\pm$ 0.6

### 3.3 DISCUSSION

A large number of ligands have been identified in recent years that potentiate  $\alpha 7$  nAChRs through an allosteric mechanism of action (Bertrand & Gopalakrishnan, 2007; Faghieh *et al.*, 2008; Arias, 2010; Mazurov *et al.*, 2011; Williams *et al.*, 2011a). In large part, this interest in  $\alpha 7$ -selective PAMs has been a consequence of the possibility that such compounds may have therapeutic use in the treatment of various neurological and psychiatric disorders (Romanelli & Gualtieri, 2003; Moaddel *et al.*, 2007; Haydar & Dunlop, 2010; Williams *et al.*, 2011b). Traditionally,  $\alpha 7$ -selective PAMs have been characterised as either type I or type II, depending on their effect on receptor desensitisation (Bertrand & Gopalakrishnan, 2007; Grønlien *et al.*, 2007). Type I PAMs increase peak agonist-evoked currents, without altering receptor desensitisation, whereas type II PAMs reduce the fast desensitisation of the  $\alpha 7$  receptors. Evidence is accumulating to indicate that both compounds identified as type I and type II PAMs can act via a transmembrane site in  $\alpha 7$  nAChRs (Young *et al.*, 2008; Collins *et al.*, 2011).

In the present chapter, five TBS compounds with close chemical similarity to one another were demonstrated to act as PAMs on  $\alpha 7$  nAChRs but with range of effects on receptor desensitisation. For example, TBS-346 displays effects on receptor desensitisation that are typical of type I PAMs and TBS-516 displays effects that are more typical of type II PAMs. In addition, compounds with intermediate properties have been identified (TBS-546, TBS-345 and TBS-556). With several of the TBS compounds, there is evidence for two components to the rate of desensitisation of the potentiated acetylcholine-evoked response, but the proportion of the fast and slow component varied. TBS-516 did not evoke a detectable fast-desensitising component, so the ratio of the slow to fast component amplitude was not determined. The largest slow to fast component ratio of the intermediate compounds was observed with TBS-556, followed by TBS-345, followed by TBS-546. The slow-desensitising component was not detected with TBS-346 and, consequently, this ratio was determined as 0. Significantly, because of the similarity in chemical structure of these compounds, we can conclude that these differences in their ability to influence receptor desensitisation is due solely to changes in substitution at the 5-position of the triazole ring.

A notable property of type II PAMs is their ability to reactivate  $\alpha 7$  nAChRs after they have been desensitised by continuous application of an orthosteric agonist (Hurst *et al.*, 2005), while type I PAMs lack this ability (Grønlien *et al.*, 2007). A recent study has identified a compound that acts as an  $\alpha 7$  PAM, JNJ-1930942, which has properties on receptor desensitisation that resemble those of the intermediate TBS compounds. However, no significant facilitation of the recovery from desensitisation was observed with JNJ-1930942 compared to control (Dinklo *et al.*, 2011). In contrast, TBS-345, TBS-516 and TBS-556 caused recovery from desensitisation, albeit to differing extents. The proportion of the fast to slow component of the TBS compounds appears to be important in determining the ability of the PAMs to facilitate recovery from desensitisation, with TBS-516 evoking the largest current after receptor desensitisation, followed by TBS-556, followed by TBS-345. TBS-346 and TBS-546 elicited no detectable responses after the receptor had been desensitised, a feature that is characteristic of type I PAMs.

The TBS compounds are potent  $\alpha 7$  PAMs. The potentiation concentration-response curves of the TBS compounds in the presence of a submaximal concentration of acetylcholine reveal that the potencies of these compounds are relatively similar, with  $EC_{50}$  values ranging from 1.43 to 2.84  $\mu$ M. However, the maximum peak fold-potentiation of the acetylcholine response varied significantly, from 3.5-fold to 19.7-fold. In addition, these compounds lack PAM activity on other nAChR subtypes (such as  $\alpha 4\beta 2$  and  $\alpha 3\beta 4$ ) and on 5-HT<sub>3A</sub>Rs, indicating that they are relatively selective potentiators of  $\alpha 7$  nAChRs.

Competition radioligand binding assays indicate that the TBS compounds do not displace [<sup>3</sup>H]- $\alpha$ -bungarotoxin from its orthosteric-binding site on  $\alpha 7$  nAChRs, supporting the conclusion that these TBS compounds are allosteric modulators. In addition, data obtained from studies of an  $\alpha 7/5$ -HT<sub>3A</sub> subunit chimera is consistent with TBS compounds interacting with a site within the transmembrane domain. It has been proposed previously that PAMs such as PNU-120597, LY-2087101 and NS-1738 bind at the same or overlapping sites within an intrasubunit cavity in the transmembrane domain of the  $\alpha 7$  nAChR (Young *et al.*, 2008; Collins *et al.*, 2011). In addition, recent studies with methyl-substituted TQS compounds have demonstrated how compounds can exert a number of different pharmacological effects by binding at the same binding

site (Gill-Thind *et al.*, 2015). It is plausible that the TBS compounds exert their effects by binding at a similar site in the transmembrane domain of the  $\alpha 7$  nAChR.

It is hoped that the ability to develop and identify compounds with differing effects on properties such as receptor desensitisation may be useful in developing therapeutic tools for a range of disorders. There is considerable interest in modulating nicotinic receptors in order to treat nervous system disorders such as Alzheimer's disease, Parkinson's disease and schizophrenia. A number of orthosteric agonists, partial agonists and antagonists have been developed, but allosteric ligands that modulate nAChRs have potentially significant advantages in regards to subtype selectivity and spatial and temporal specificity. The availability of PAMs with properties that are intermediate between those of classical type I and type II PAMs increases the pharmacological diversity of this family of allosteric modulators. Furthermore, the development of compounds with a range of effects on receptor desensitisation, such as the TBS series of compounds, could provide the valuable balance of maximising the therapeutic effects that could be obtained from potentiating nAChRs, while minimising cytotoxicity caused from prolonged opening of the calcium-permeable neuronal nAChRs.

CHAPTER 4

EFFECT OF MUTATIONS ON  
MODULATION OF  $\alpha 7$  NICOTINIC  
ACETYLCHOLINE RECEPTORS  
BY ALLOSTERIC LIGANDS

---

## 4.1 INTRODUCTION

The discovery and characterisation of  $\alpha 7$ -selective nAChR agonists, antagonists and allosteric modulators constitutes a major goal of pharmacological research. In part, this is a consequence of these receptors being implicated in numerous neurological disorders. Activation of  $\alpha 7$  nAChRs by orthosteric agonists results in activation followed by rapid desensitisation. However, rapid desensitisation of  $\alpha 7$  nAChRs is not seen with all agonists. A group of compounds, described as allosteric agonists, activate  $\alpha 7$  nAChRs with minimal levels of desensitisation (Gill *et al.*, 2011; Gill *et al.*, 2012; Papke *et al.*, 2014). In contrast to conventional orthosteric agonists such as acetylcholine, there is evidence that allosteric agonists may act via a distinct transmembrane binding site (Gill *et al.*, 2011). In many respects, such compounds are analogous to the allosteric agonists that have been described for GPCRs (Langmead & Christopoulos, 2006; Schwartz & Holst, 2006). It is probable that nAChRs contain a variety of distinct allosteric binding sites (Taly *et al.*, 2009), but studies have provided evidence that one such site is located in an intrasubunit cavity located between the four  $\alpha$ -helical transmembrane domains of a single  $\alpha 7$  subunit (Young *et al.*, 2008). In addition, there is evidence that this is a site at which allosteric agonists, as well as both type I and type II potentiators, can act (Young *et al.*, 2008; Collins *et al.*, 2011; Gill *et al.*, 2011).

In this chapter, studies with  $\alpha 7$  nAChRs containing one of two point mutations in the second transmembrane domain (TM2) or a mutation on the N-terminal domain are conducted and the effect of these mutations on receptor activation and desensitisation is examined. Introduction of a single point mutation (L247T) in the 9' position of TM2 of the  $\alpha 7$  nAChR has been reported previously to exert dramatic and diverse effects on the functional properties of this receptor (Revah *et al.*, 1991; Bertrand *et al.*, 1992). As discussed in section 1.4.4, the effects of the L247T mutation include increased potency of agonists such as acetylcholine and reduced levels of desensitisation (Revah *et al.*, 1991; Bertrand *et al.*, 1992), which could be the result of destabilising the axial cluster of side chains that closes the channel (Labarca *et al.*, 1995). In contrast, it is shown here that mutating the M260 residue, which is located near the extracellular site of the TM2 domain (at the 22' position) and points towards an intrasubunit cavity that has been

previously proposed as a binding site for allosteric modulators of  $\alpha 7$  nAChRs (Young *et al.*, 2008; Gill *et al.*, 2011), does not result in any difference in receptor desensitisation after activation by acetylcholine compared to wild-type receptors. In addition, a mutation on a residue situated on the complementary component of the orthosteric binding site, W54A, has been recently reported to convert type II PAMs into agonists, as a result of the ‘de-coupling’ between the orthosteric and allosteric binding sites (Papke *et al.*, 2014). In this chapter, the effects of these mutations on receptor activation are examined using a variety of PAMs shown in Figure 4.1, including the ‘classical’ type I PAM, NS-1738 (Timmermann *et al.*, 2007), and type II PAM, TQS (Grønlien *et al.*, 2007), in addition to a series of novel compounds containing a substituted triazole group (Chapter 3). It is demonstrated that multiple mutations in  $\alpha 7$  nAChRs can convert PAMs into allosteric agonists. In addition, it appears that the M260L mutation has a selective effect on PAMs that reduce agonist-evoked desensitisation (type II PAMs).

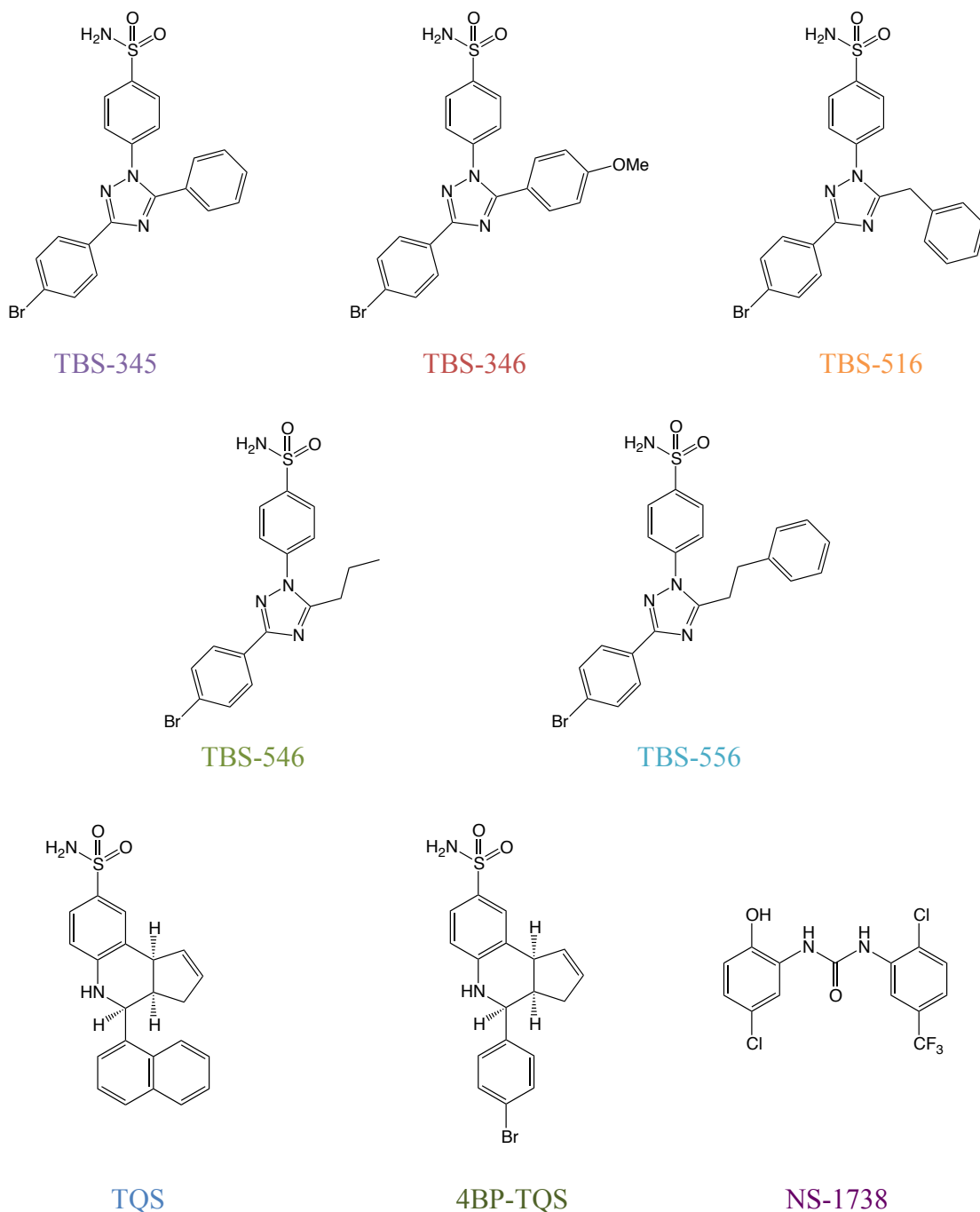


**Figure 4.1: Chemical structures of allosteric ligands examined in this chapter.**

Abbreviations: 4BP-TQS: *cis-cis*-4-(4-bromophenyl)-3*a*,4,5,9*b*-tetrahydro-3*H*-cyclopenta[*c*]quinoline-8-sulfonamide; NS-1738: 1-(5-chloro-2-hydroxyphenyl)-3-(2-chloro-5-trifluoromethylphenyl)urea; TBS-345: 4-(3-(4-bromophenyl)-5-phenyl-1*H*-1,2,4-triazol-1-yl)benzenesulfonamide; TBS-346: 4-(3-(4-bromophenyl)-5-(4-methoxyphenyl)-1*H*-1,2,4-triazol-1-yl)benzenesulfonamide; TBS-516: 4-(5-benzyl-3-(4-bromophenyl)-1*H*-1,2,4-triazol-1-yl)benzenesulfonamide; TBS-546: 4-(3-(4-bromophenyl)-5-propyl-1*H*-1,2,4-triazol-1-yl)benzenesulfonamide; TBS-556: 4-(3-(4-bromophenyl)-5-phenethyl-1*H*-1,2,4-triazol-1-yl)benzenesulfonamide; TQS: *cis-cis*-4-(naphthalen-1-yl)-3*a*,4,5,9*b*-tetrahydro-3*H*-cyclopenta[*c*]quinoline-8-sulfonamide.

## 4.2 RESULTS

The effects of  $\alpha 7$  nAChR mutations on the pharmacological properties of a number of allosteric ligands (Figure 4.1) were examined by two-electrode voltage-clamp recordings in *Xenopus* oocytes expressing wild-type and mutated human recombinant  $\alpha 7$  nAChRs.

### 4.2.1 L247T (9') and M260L (22') transmembrane mutations

There are several examples of individual point mutations in nAChR subunits that result in dramatic effects on the pharmacological properties of receptors. For example, in agreement with previous studies (Revah *et al.*, 1991), a single point mutation (L247T), located towards the middle of the second transmembrane (TM2) domain (at the 9' position) of the  $\alpha 7$  subunit (Figure 4.2) caused a dramatic slowing of receptor desensitisation and a large leftward shift (660-fold;  $p < 0.001$ ) of the concentration-response curve for acetylcholine, with the  $EC_{50}$  value for wild-type being  $132 \pm 13 \mu\text{M}$  and for L247T  $201 \pm 10 \text{ nM}$  (Figure 4.2B and C). In contrast, another point mutation (M260L), located towards the top of TM2 (at the 22' position) (Figure 4.2A) was found to have no significant effect on the rate of receptor desensitisation after activation by acetylcholine. The desensitisation time constants of the current decay after activation by 1 mM acetylcholine were  $\tau_{\text{fast}} = 53.3 \pm 8.4 \text{ ms}$  ( $n = 20$ ) for M260L and  $76.1 \pm 6.6 \text{ ms}$  ( $n = 57$ ) for wild-type ( $p = 0.06$ ) and  $\tau_{\text{slow}} = 242.5 \pm 87.5 \text{ ms}$  ( $n = 20$ ) for M260L and  $239.8 \pm 21.8 \text{ ms}$  ( $n = 57$ ) for wild-type ( $p = 0.97$ ). In addition, M260L caused a much smaller leftward shift (2.1-fold;  $p = 0.03$ ) of the acetylcholine concentration-response curve, with the  $EC_{50}$  for wild-type being  $132 \pm 13 \mu\text{M}$  and for M260L  $63 \pm 12 \mu\text{M}$  (Figure 4.2 and Table 3).

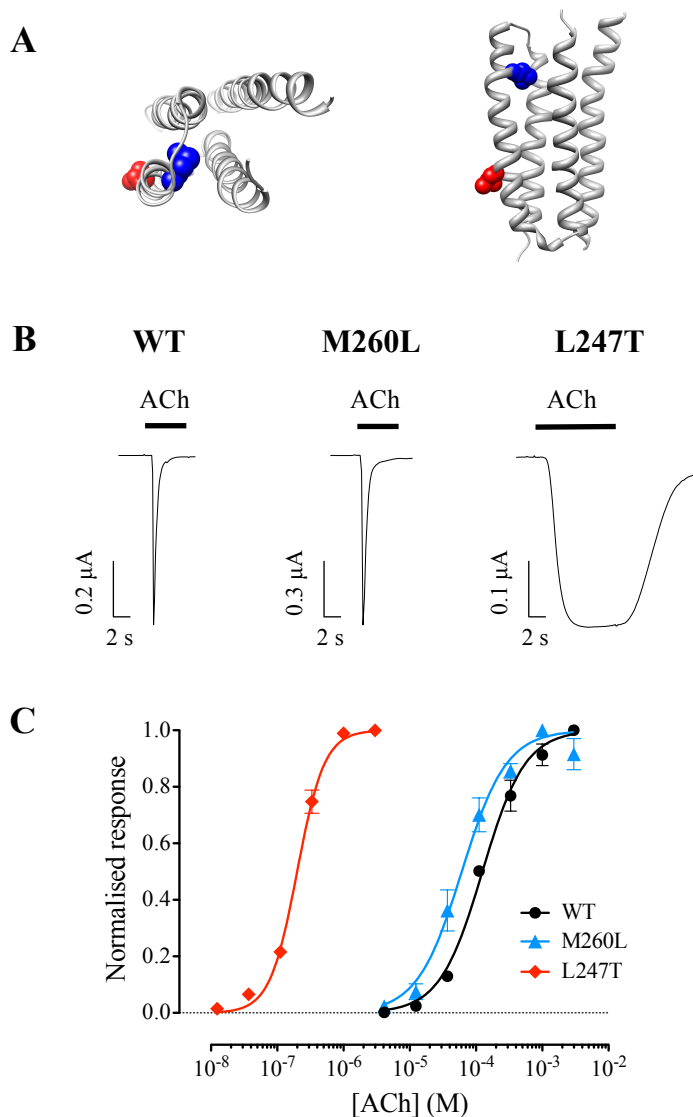


**Figure 4.2: The influence of  $\alpha 7$  nAChR mutations (L247T and M260L) on activation by ACh.**

A) The location of L247 (9') and M260 (22') residues in the  $\alpha 7$  nAChR subunit transmembrane (TM2) domain. The transmembrane region of an  $\alpha 7$  nAChR subunit homology model (Young *et al.*, 2008) is shown viewed from the top (left) and from the side (right). The  $\alpha$ -helical transmembrane regions are illustrated as ribbon structures with the side chains of the two mutated amino acids shown as space-filling models (L247 in red and M260 in blue).

B) Representative traces are shown illustrating responses to maximal concentrations of ACh on human wild-type (WT)  $\alpha 7$  nAChRs and  $\alpha 7$  nAChRs containing the M260L mutation (M260L) and the L247T mutation (L247T). ACh concentrations: 1 mM for WT and M260L and 10  $\mu$ M for L247T.

C) ACh concentration-response data are presented for wild-type  $\alpha 7$  nAChRs (circles) and for  $\alpha 7$  nAChRs containing either the M260L mutation (triangles) or the L247T mutation (diamonds). Data are means  $\pm$  SEM of at least three independent experiments and are normalised to the respective maximum response obtained with each nAChR variant.

#### 4.2.2 Effects of transmembrane mutations on modulation of $\alpha 7$ nAChRs by type I and type II PAMs

Further differences were observed between wild-type and mutated (L247T and M260L)  $\alpha 7$  nAChRs in the extent to which they are modulated by type I and type II PAMs. Initially, studies were conducted with two previously described ‘classical’ type I and type II PAMs (NS-1738 and TQS, respectively). As is illustrated, both compounds lacked agonist effects on wild-type  $\alpha 7$  nAChRs but both potentiated agonist-evoked responses on wild-type receptors (Figure 4.3A). In agreement with previous studies (Grønlien *et al.*, 2007; Timmermann *et al.*, 2007), NS-1738 caused potentiation of agonist-evoked responses with little or no effect on desensitisation, whereas TQS resulted in a dramatic loss of desensitisation (Figure 4.3A).

As has been reported previously (Gill *et al.*, 2011), one of the effects of the L247T mutation is that it converts the type II PAM TQS into a potent agonist of the mutated receptor. Here it is demonstrated that a similar effect (the conversion of a PAM into an agonist) was also observed with NS-1738, a classical type I PAM (Figure 4.3B). In contrast to L247T, the M260L mutation had a selective effect on these two PAMs. As was observed with L247T, TQS (a type II PAM) acted as a non-desensitising agonist on receptors containing the M260L mutation, whereas NS-1738 (a type I PAM) had no agonist activity on this mutated receptor (Figure 4.3C). Thus, the two TM2 mutations (L247T and M260L) have differing effects on desensitisation of  $\alpha 7$  nAChRs, when activated by acetylcholine (Figure 4.2) and also differ in their ability to convert the type I PAM into an agonist (Figure 4.3). However, they share an ability to convert the type II PAM into an agonist (Figure 4.3).

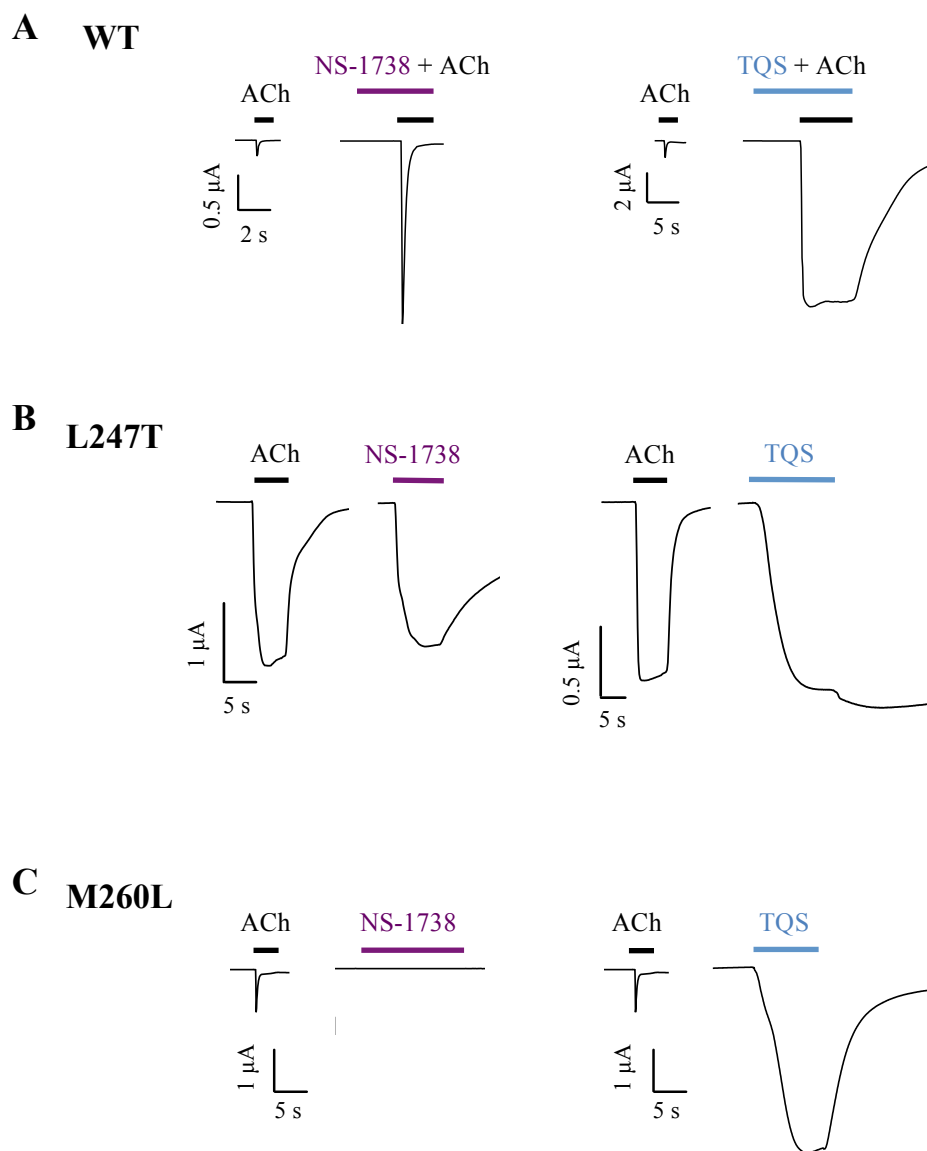


**Figure 4.3: The influence of a type I (NS-1738) and a type II PAM (TQS) on wild-type and mutated (L247T or M260L)  $\alpha 7$  nAChRs.**

A) Representative traces illustrating responses with wild-type  $\alpha 7$  nAChRs to ACh (100  $\mu\text{M}$ ) and after the pre- and co-application of either NS-1738 (10  $\mu\text{M}$ ; left pair of traces) or TQS (30  $\mu\text{M}$ ; right).

B) Representative traces illustrating responses with mutated (L247T)  $\alpha 7$  nAChRs to ACh (10  $\mu\text{M}$ ) and to NS-1738 (10  $\mu\text{M}$ ; left) or TQS (30  $\mu\text{M}$ ; right).

C) Representative traces illustrating responses with mutated (M260L)  $\alpha 7$  nAChRs to ACh (100  $\mu\text{M}$ ) and NS-1738 (10  $\mu\text{M}$ ; left) or TQS (30  $\mu\text{M}$ ; right).

### 4.2.3 Effects of transmembrane mutations on modulation of $\alpha 7$ nAChRs by TBS compounds

As described in chapter 3, a series of chemically related TBS compounds have been identified that differ in their ability to alter desensitisation of  $\alpha 7$  nAChRs (Figure 4.4A). The influence of L247T and M260L mutations on the pharmacological properties of these compounds was examined. The reason for doing so was to determine whether the differing effects of the L247T and M260L mutations in converting TQS but not NS-1738 into agonists reflect a consistent ability to discriminate between type I and type II PAMs. When examined on  $\alpha 7$  nAChRs containing the L247T mutation, all five TBS compounds acted as agonists (Figure 4.4). Thus, it appears that a feature of the L247T mutation is the conversion of all PAMs examined, irrespective of their effect on desensitisation, into agonists. In contrast, with  $\alpha 7$  nAChRs containing the M260L mutation, strong agonist activity was observed only with the two TBS compounds that had the greatest propensity to reduce desensitisation in wild-type  $\alpha 7$  nAChRs (TBS-516 and TBS-556; Figure 4.4C). Therefore, it appears that the M260L mutation has an effect on  $\alpha 7$  nAChR structure that can discriminate between PAMs that differ in their influence upon desensitisation of wild-type  $\alpha 7$  nAChRs.

The  $\alpha 7$ -selective antagonist MLA blocked responses to acetylcholine on both L247T (Figure 4.5A) and M260L  $\alpha 7$  nAChRs (Figure 4.6A). Similarly, MLA blocked responses with all of the allosteric modulators that act as agonists on these two mutated  $\alpha 7$  nAChRs (Figure 4.5 and Figure 4.6). This is consistent with previous reports indicating that, in addition to acting as a competitive antagonist of acetylcholine, MLA can block activation of wild-type  $\alpha 7$  nAChRs by allosteric agonists such as 4BP-TQS via a non-competitive mechanism (Gill *et al.*, 2011).

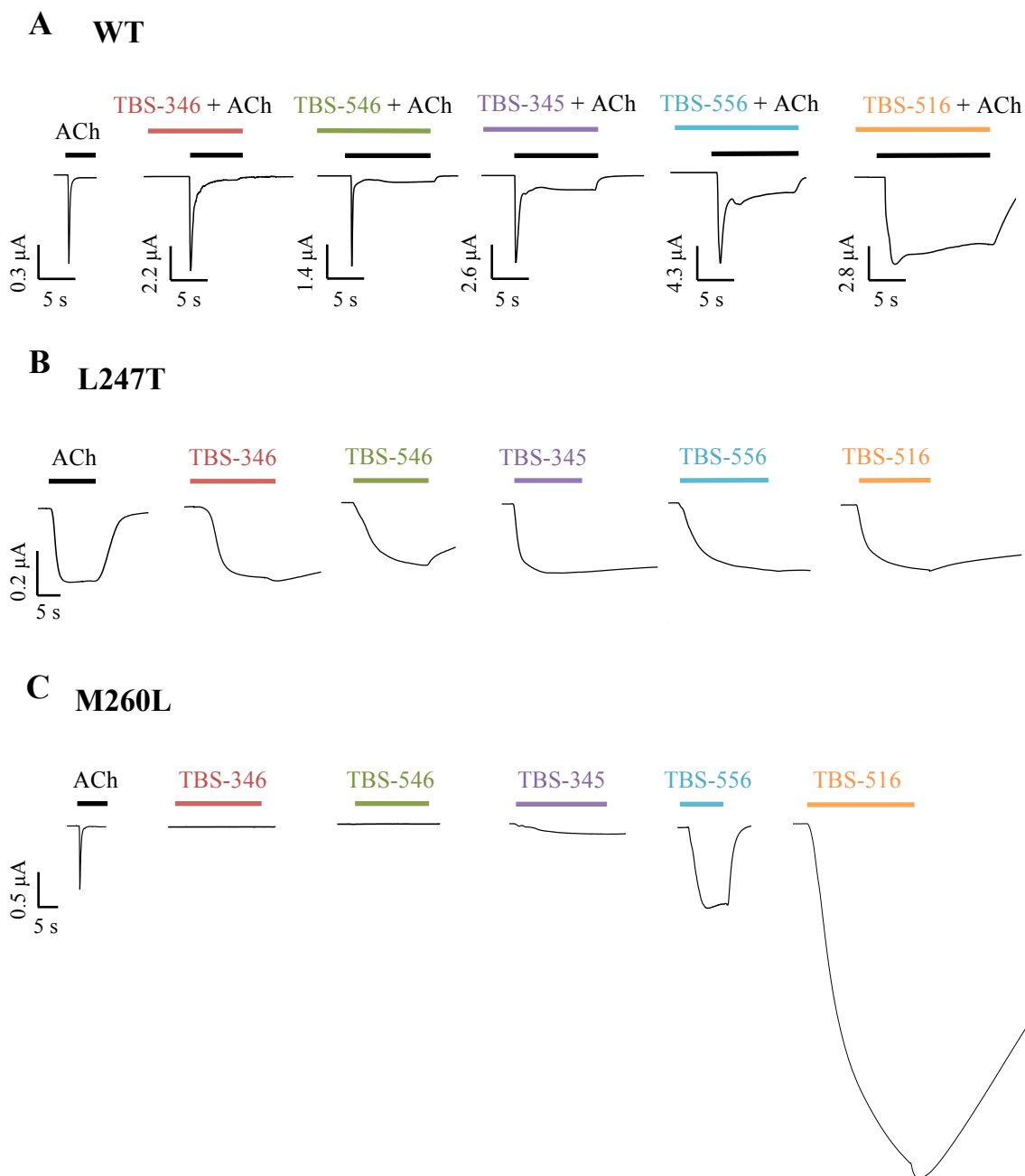


**Figure 4.4: Potentiation and agonist effects of TBS compounds on wild-type and mutated  $\alpha 7$  nAChRs.**

A) Representative traces are shown illustrating responses of wild-type  $\alpha 7$  nAChRs to ACh (100  $\mu$ M), together with responses to ACh (100  $\mu$ M) after pre- and co-application of TBS compounds (10  $\mu$ M). All responses on wild-type  $\alpha 7$  nAChRs have been normalised to their peak response, so as to illustrate differences in the rate of desensitisation.

B) Representative traces are shown illustrating agonist responses of  $\alpha 7$  nAChRs containing the L247T (9') mutation to either ACh (10  $\mu$ M) or TBS compounds (10  $\mu$ M).

C) Representative traces are shown illustrating agonist responses of  $\alpha 7$  nAChRs containing the M260L (22') mutation to either ACh (100  $\mu$ M) or TBS compounds (10  $\mu$ M).

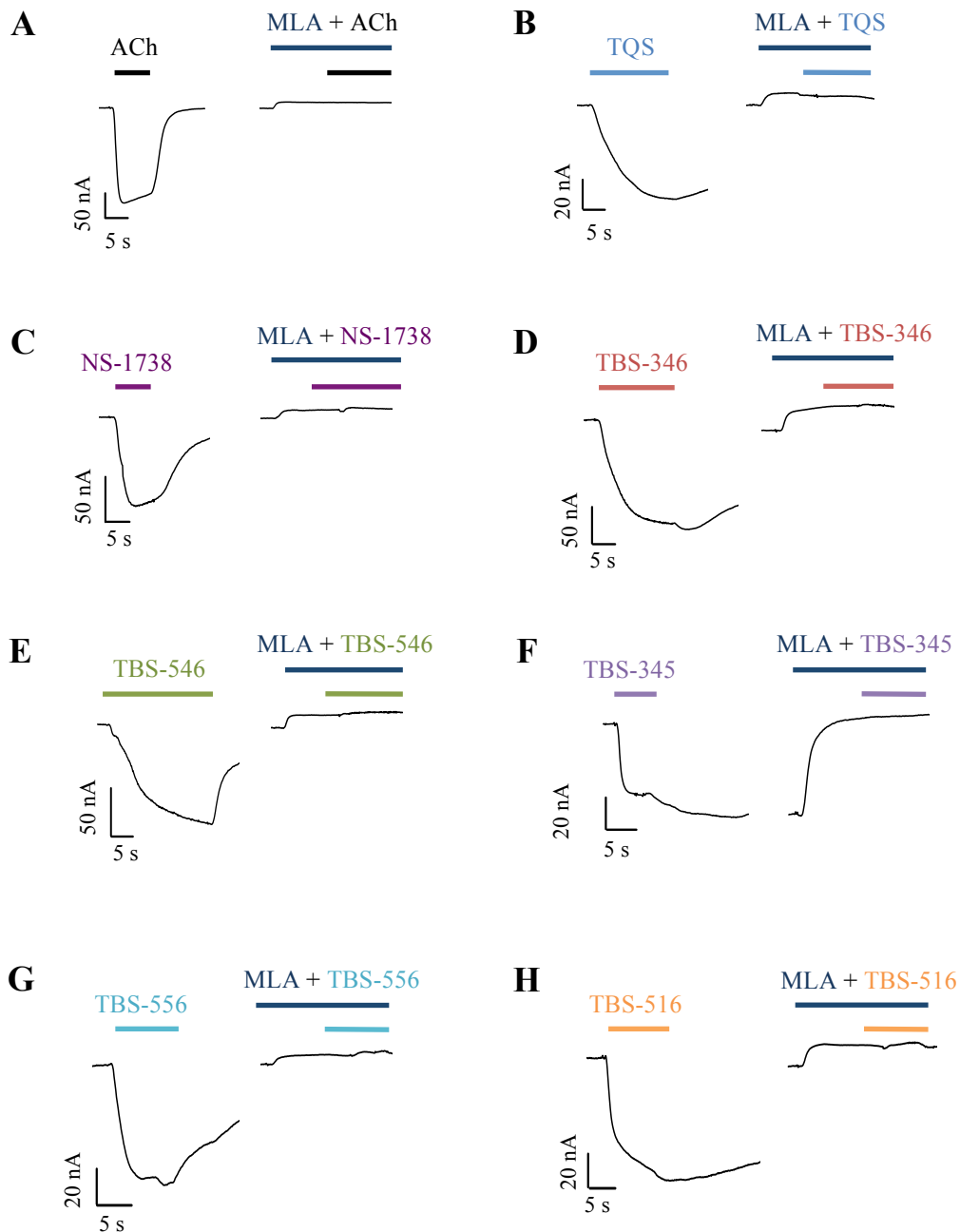


**Figure 4.5: Antagonism of agonist responses on L247T  $\alpha 7$  nAChRs by MLA.**

Representative traces with L247T  $\alpha 7$  nAChRs illustrating initial agonist responses with (A) ACh (10  $\mu$ M), (B) TQS (3  $\mu$ M), (C) NS-1738 (10  $\mu$ M), (D) TBS-346 (10  $\mu$ M), (E) TBS-546 (10  $\mu$ M), (F) TBS-345 (10  $\mu$ M), (G) TBS-556 (10  $\mu$ M) and (H) TBS-516 (10  $\mu$ M) (left) and antagonism by pre- and co-application of MLA (1  $\mu$ M) (right).

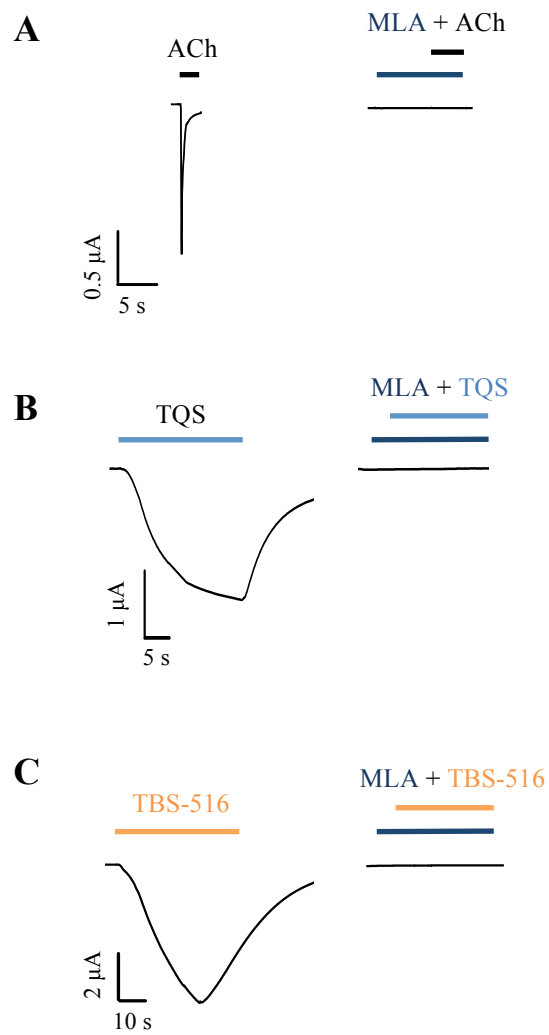


**Figure 4.6: Antagonism of agonist responses on M260L  $\alpha 7$  nAChRs by MLA.**

Representative traces with M260L  $\alpha 7$  nAChRs illustrating initial agonist responses with (A) ACh (1 mM), (B) TQS (10  $\mu$ M) and (C) TBS-516 (10  $\mu$ M) (left) and antagonism by pre- and co-application of MLA (1  $\mu$ M) (right).

For wild-type and mutated  $\alpha 7$  nAChRs, concentration-response curves were constructed for the orthosteric agonist acetylcholine and for the allosteric agonist 4BP-TQS (Figure 4.7). In addition, agonist concentration-response curves were constructed for two type I PAMs (NS-1738 and TBS-346) and for two type II PAMs (TBS-516 and TQS) (Figure 4.7). In agreement with previous studies (Gill *et al.*, 2011), the allosteric agonist 4BP-TQS generated larger maximal responses and a steeper Hill coefficient than the endogenous agonist acetylcholine on wild-type  $\alpha 7$  nAChRs, whereas none of the PAMs tested (NS-1738, TBS-346, TBS-516 or TQS) had any detectable agonist activity on wild-type receptors (Figure 4.7A and Table 3). In marked contrast, all of the compounds tested (4BP-TQS, acetylcholine, NS-1738, TBS-346, TBS-516 and TQS) generated broadly similar maximal responses and had similar Hill coefficients on  $\alpha 7$  nAChRs containing the L247T mutation (Figure 4.7B and Table 3). With  $\alpha 7$  nAChRs containing the M260L mutation, the orthosteric and allosteric agonists (acetylcholine and 4BP-TQS, respectively) differed in their maximal responses and Hill coefficients, much as they do on wild-type  $\alpha 7$  nAChRs (Figure 4.7A and C). Also, with  $\alpha 7$  nAChRs containing the M260L mutation, agonist responses were observed with the two type II PAMs (TBS-516 and TQS) but not with the two type I PAMs (NS-1738 and TBS-346). In addition, in contrast to the L247T mutation, maximal responses with TBS-516 and TQS (the type II PAMs) were much closer to that observed with acetylcholine than with 4BP-TQS (Figure 4.7C and Table 3).

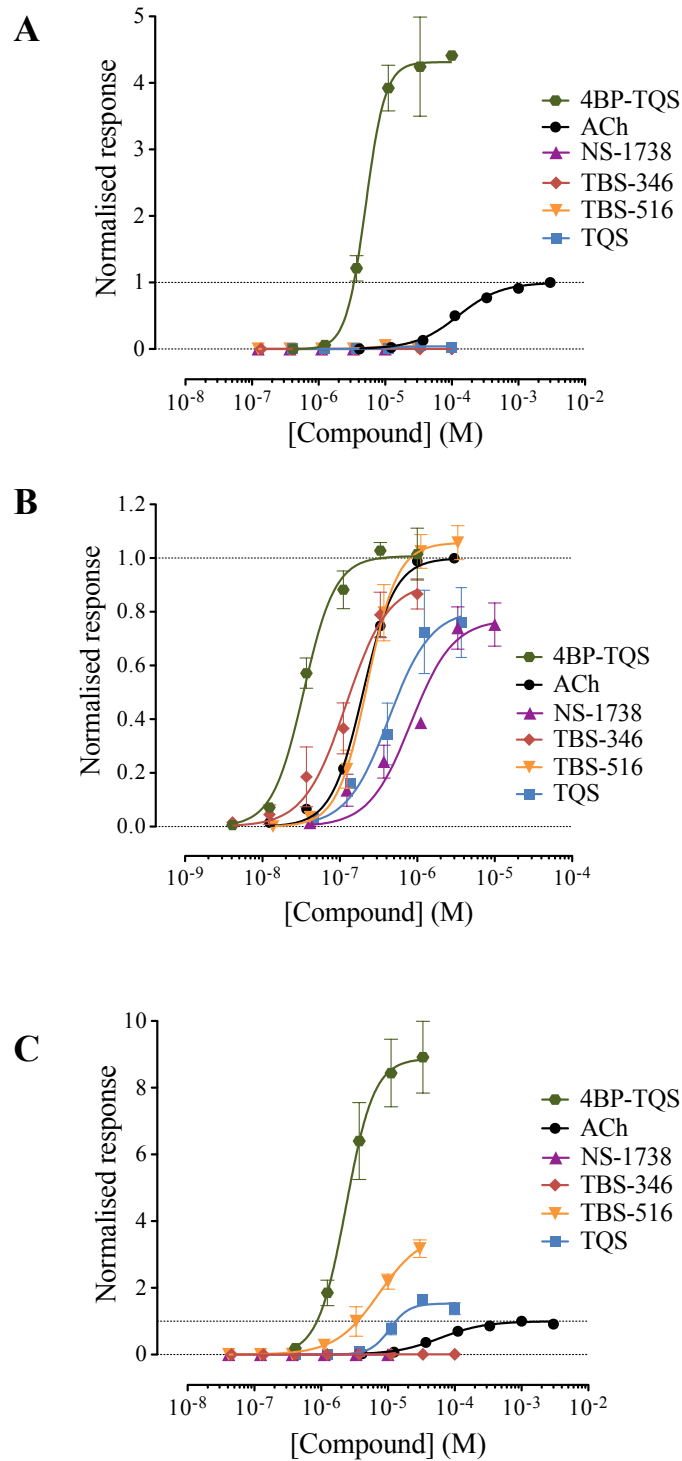


**Figure 4.7: Concentration-response curves for wild-type and mutated  $\alpha 7$  nAChRs.**

Data are shown from wild-type  $\alpha 7$  nAChRs (A),  $\alpha 7$  nAChRs containing the L247T (9') mutation (B) and  $\alpha 7$  nAChRs containing the M260L (22') mutation (C). Data are presented for a range of concentrations of ACh (circles), the allosteric agonist 4BP-TQS (hexagons), the type II PAMs, TQS (squares) and TBS-516 (inverted triangles), and the type I PAMs, NS-1738 (triangles) and TBS-346 (diamonds). Data are means  $\pm$  SEM of at least three independent experiments and are normalised to the maximum acetylcholine response.

**Table 3: Agonist properties on wild-type and mutated  $\alpha 7$  nAChRs.**

Data are means  $\pm$  SEM of at least three independent experiments.

<sup>a</sup> Data for maximal currents ( $I_{\max}$ ) are normalised to the size of the maximum acetylcholine response for each receptor type.

Receptor	Agonist	EC <sub>50</sub> ( $\mu$ M)	n <sub>H</sub>	I <sub>max</sub> <sup>a</sup>
<b><math>\alpha 7</math> WT</b>	<b>Acetylcholine</b>	132 $\pm$ 13	1.4 $\pm$ 0.2	1.0
	<b>4BP-TQS</b>	4.2 $\pm$ 0.3	5.2 $\pm$ 0.8	4.4 $\pm$ 0.3
	<b>NS-1738</b>	N/A	N/A	0.0
	<b>TBS-346</b>	N/A	N/A	0.0
	<b>TBS-516</b>	N/A	N/A	0.0
	<b>TQS</b>	N/A	N/A	0.0
<b><math>\alpha 7</math> L247T</b>	<b>Acetylcholine</b>	0.2 $\pm$ 0.01	2.1 $\pm$ 0.2	1.0
	<b>4BP-TQS</b>	0.03 $\pm$ 0.003	2.3 $\pm$ 0.2	1.0 $\pm$ 0.1
	<b>NS-1738</b>	0.8 $\pm$ 0.1	1.6 $\pm$ 0.2	0.8 $\pm$ 0.1
	<b>TBS-346</b>	0.1 $\pm$ 0.04	1.7 $\pm$ 0.3	0.9 $\pm$ 0.1
	<b>TBS-516</b>	0.2 $\pm$ 0.04	2.5 $\pm$ 0.3	1.1 $\pm$ 0.1
	<b>TQS</b>	0.4 $\pm$ 0.1	1.7 $\pm$ 0.1	0.8 $\pm$ 0.1
<b><math>\alpha 7</math> M260L</b>	<b>Acetylcholine</b>	63 $\pm$ 12	1.3 $\pm$ 0.1	1.0
	<b>4BP-TQS</b>	2.5 $\pm$ 0.4	2.3 $\pm$ 0.4	9.0 $\pm$ 1.2
	<b>NS-1738</b>	N/A	N/A	0.0
	<b>TBS-346</b>	N/A	N/A	0.0
	<b>TBS-516</b>	8.9 $\pm$ 2.5	1.8 $\pm$ 0.3	3.7 $\pm$ 0.6
	<b>TQS</b>	12 $\pm$ 1.1	3.1 $\pm$ 0.4	1.5 $\pm$ 0.1

It is notable that compounds that had no agonist effect on M260L receptors (NS-1738, TBS-346, TBS-546 and TBS-345), in addition to the compounds that were converted into agonists (TQS, TBS-556 and TBS-516), retained their ability to potentiate agonist responses when co-applied with acetylcholine (Figure 4.8). The fold-potentiation (determined on the basis of maximum peak response compared to acetylcholine alone) was  $2.5 \pm 0.3$  for NS-1738,  $5.8 \pm 3.1$  for TQS,  $2.8 \pm 0.6$  for TBS-346,  $3.6 \pm 0.6$  for TBS-546,  $6.2 \pm 1.2$  for TBS-345,  $6.6 \pm 1.0$  for TBS-556 and  $8.0 \pm 3.1$  for TBS-516 (mean  $\pm$  SEM of  $n \geq 3$ ). In contrast, on L247T  $\alpha 7$  nAChRs, upon which acetylcholine acts as a non-desensitising agonist (Figure 4.7B), the amplitude of the maximum response elicited by application of acetylcholine or by allosteric ligands was very similar (Figure 4.7B and Table 3). Co-application of acetylcholine with the allosteric modulators on L247T  $\alpha 7$  nAChRs did not potentiate or inhibit the response elicited by acetylcholine alone (data not shown).

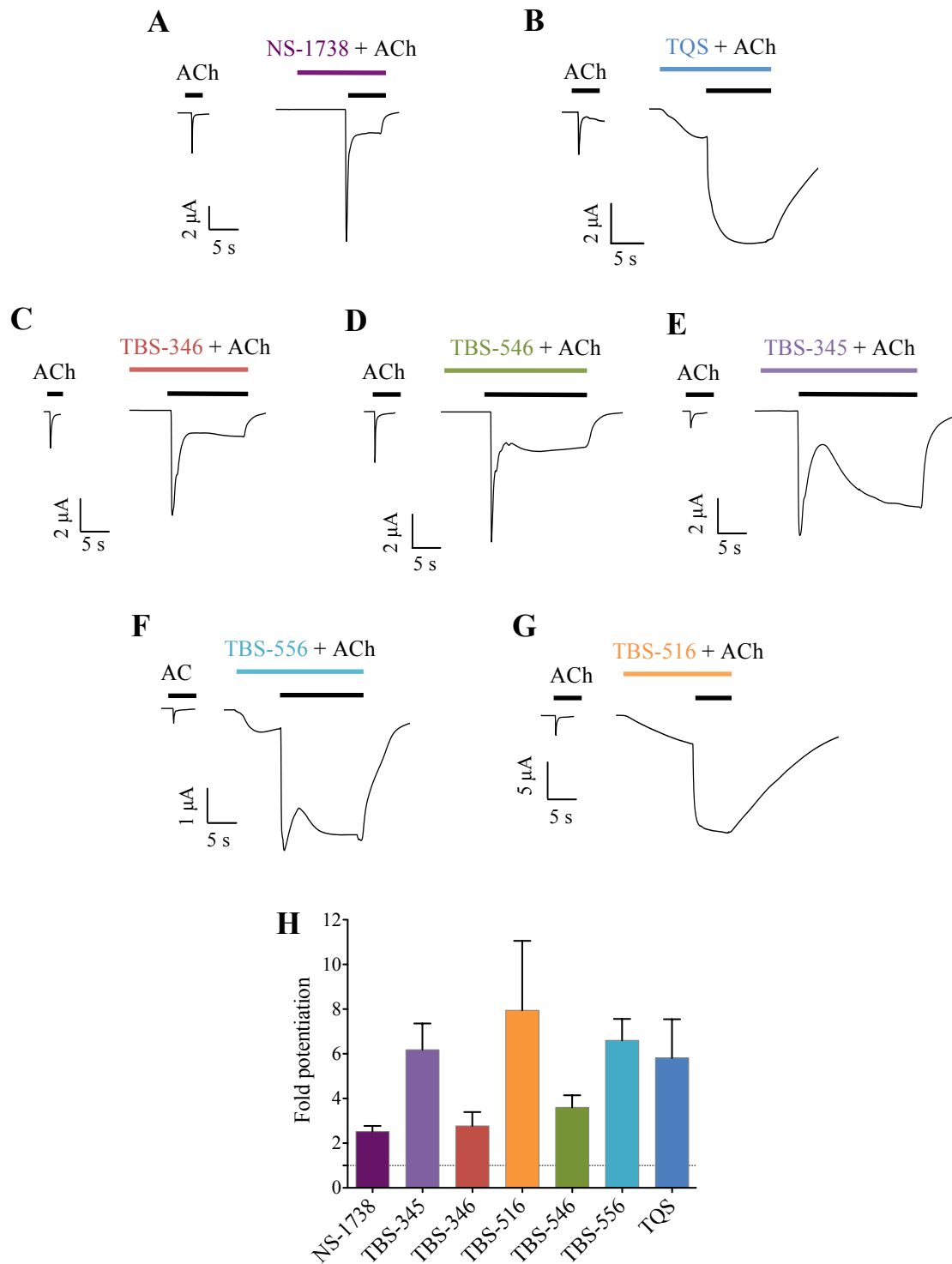


**Figure 4.8: Potentiation of ACh responses by allosteric modulators on M260L  $\alpha 7$  nAChRs.**

A-G) Representative traces are shown illustrating responses to ACh (100  $\mu$ M) (left) together with responses from the same oocyte after pre- and co-application of an allosteric modulator (10  $\mu$ M) (right). Representative traces are shown for NS-1738 (A), TQS (B), TBS-346 (C), TBS-546 (D), TBS-345 (E), TBS-556 (F) and TBS-516 (G).

H) Bar chart showing fold potentiation of responses to ACh (100  $\mu$ M) by PAMs on M260L  $\alpha 7$  nAChRs (mean and SEM of at least three independent experiments).

#### 4.2.4 Type I PAMs block agonist effects of type II PAMs on M260L in a surmountable manner

Previous studies have concluded that type I and type II PAMs, despite their differing effects on desensitisation, can bind competitively at a common allosteric transmembrane site (Collins *et al.*, 2011). Therefore, although the type I PAMs (NS-1738 and TBS-346) did not act as agonists on  $\alpha 7$  nAChRs containing the M260L mutation (Figure 4.7C) it is possible that they may block the agonist response observed with type II PAMs on this mutated receptor. When either of the type I PAMs (NS-1738 and TBS-346 at 10  $\mu\text{M}$ ) was pre- and co-applied with either of the type II PAMs (TQS or TBS-516 at 10  $\mu\text{M}$ ), an inhibition of agonist responses was observed (Figure 4.9A-D). NS-1738 completely blocked responses to TQS, while TBS-346 blocked responses to TQS by  $95.7 \pm 1.1\%$ . NS-1738 blocked responses to TBS-516 by  $92.7 \pm 2.3\%$ , while TBS-346 blocked responses to TBS-516 by  $83.4 \pm 4.1\%$  ( $n = 3$ ).

The antagonism caused would be expected to be surmountable at high concentrations of the type II PAM, if type I PAMs are causing antagonism by binding competitively with type II PAMs on  $\alpha 7$  nAChRs containing the M260L mutation. This possibility was investigated by constructing an agonist concentration-response curve of TQS in the absence and the presence of a fixed concentration of NS-1738 (Figure 4.9E). The  $\text{EC}_{50}$  for TQS was  $11.5 \pm 1.1 \mu\text{M}$  ( $n = 4$ ) in the absence of NS-1738 and  $45.4 \pm 5.4 \mu\text{M}$  ( $n = 5$ ) in the presence of NS-1738 (Figure 4.9E). This corresponds to a significant rightward shift (4.0-fold;  $p < 0.001$ ) of the concentration-response curve in the presence of NS-1738. However, the two curves had similar maxima (Figure 4.9E), which suggests that NS-1738 is blocking responses to TQS by a competitive mechanism of action. A notable feature of the data is that the concentration-response curve is significantly less steep ( $p < 0.01$ ) in the presence of NS-1738 (a Hill coefficient of  $1.5 \pm 0.2$ ), than in the absence of NS-1738 ( $3.1 \pm 0.4$ ), which may be a consequence of NS-1738 acting as a potentiator of the TQS response, at low TQS concentrations, when not all sites of the receptor are occupied by TQS.

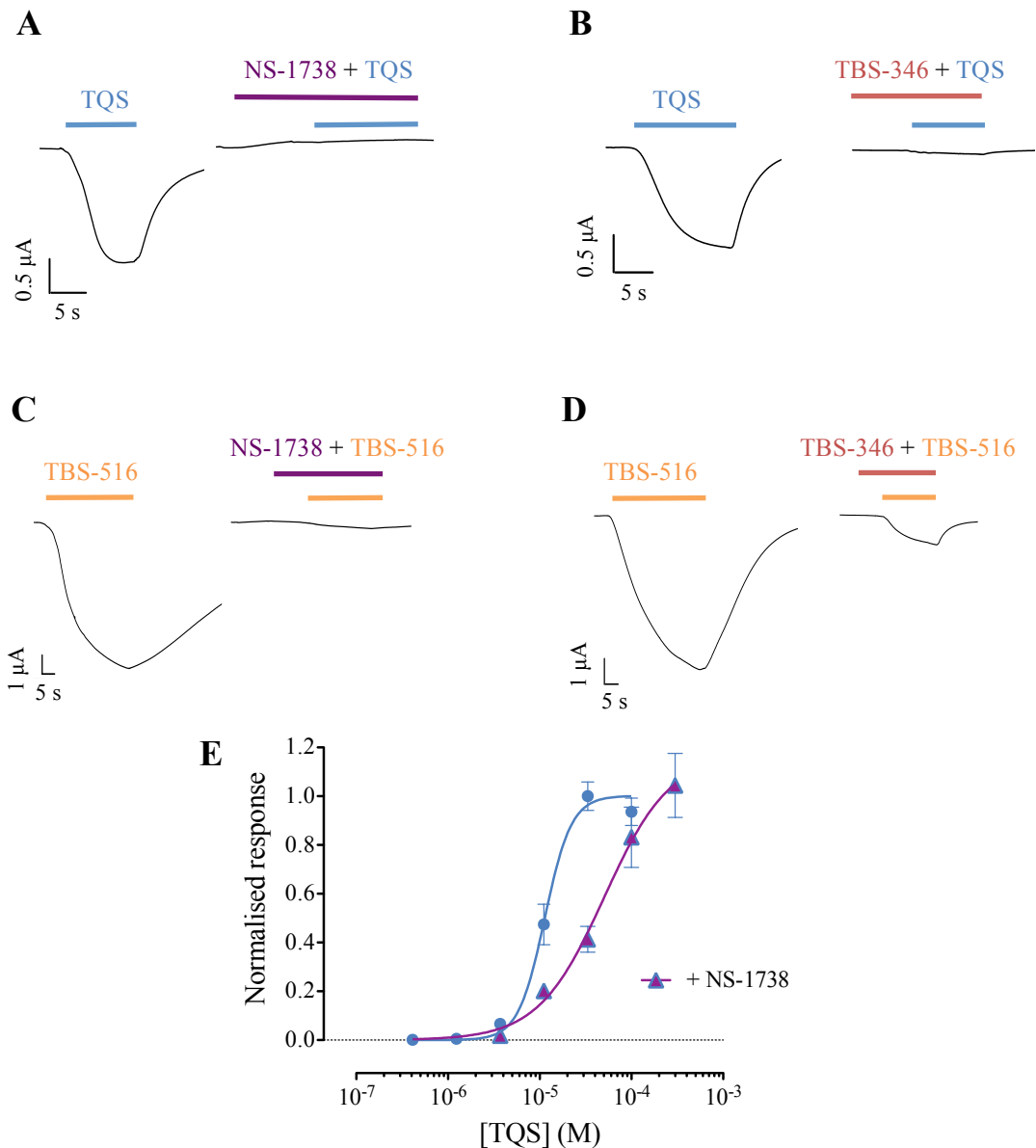


**Figure 4.9: Type I PAMs block agonist activity of TQS and TBS-516 on  $\alpha 7$  nAChRs containing the M260L mutation.**

Representative traces are shown, obtained by two-electrode voltage-clamp recording in oocytes expressing  $\alpha 7$  nAChRs containing the M260L mutation, in which a type I PAM (NS-1738 or TBS-346) is pre-applied for 10 s and then co-applied with a type II PAM (TQS or TBS-516) (A-D). A) NS-1738 (10  $\mu$ M) completely blocks responses to TQS (10  $\mu$ M). B) TBS-346 (10  $\mu$ M) blocks responses to TQS (10  $\mu$ M) by  $95.7 \pm 1.1\%$  (n = 3). C) NS-1738 (10  $\mu$ M) blocks responses to TBS-516 (10  $\mu$ M) by  $92.7 \pm 2.3\%$  (n = 3). D) TBS-346 (10  $\mu$ M) blocks responses to TBS-516 (10  $\mu$ M) by  $83.4 \pm 4.1\%$  (n = 3).

E) The agonist concentration-response curve for TQS on  $\alpha 7$  nAChRs containing the M260L mutation is shifted to the right in the presence of NS-1738 (2  $\mu$ M, pre-applied for 10 s and then co-applied with TQS). The antagonism by NS-1738 is surmountable at high concentrations of TQS. Data are means and SEM of at least three independent experiments. Data are normalised to the maximum response obtained with TQS in the absence of NS-1738.

#### 4.2.5 Effects of the W54A mutation on modulation of $\alpha 7$ nAChRs by allosteric ligands

A residue on the extracellular domain of the nAChR, W54, has previously been implicated in determining the efficacy and selectivity of specific orthosteric ligands in both  $\alpha 7$  and heteromeric receptors (Williams *et al.*, 2009). W54 is situated on the complementary surface of the orthosteric binding site (Corringer *et al.*, 1995). It has been reported recently that the mutation W54A in  $\alpha 7$  nAChRs also converts TQS and PNU-120596 (both type II PAMs) into agonists (Papke *et al.*, 2014). In addition, agonism by allosteric ligands has been reported to not be susceptible to block by MLA, suggesting a de-coupling of the orthosteric and allosteric binding site on this mutated receptor (Papke *et al.*, 2014). The influence of the W54A mutation on NS-1738 and TBS-346 (type I PAMs) and on TBS-516 and TQS (type II PAMs) was examined in order to determine whether this mutation also discriminates between PAMs that have differing effects on desensitisation.

There was no significant difference in the potency of acetylcholine between wild-type and W54A  $\alpha 7$  nAChRs. The  $EC_{50}$  for wild-type was  $132.3 \pm 12.7 \mu\text{M}$  ( $n = 6$ ) and for W54A  $155.3 \pm 31.6 \mu\text{M}$  ( $n = 4$ ;  $p = 0.46$ ), while the Hill coefficient was  $1.4 \pm 0.2$  ( $n = 6$ ) for wild-type and  $1.6 \pm 0.1$  for W54A ( $n = 4$ ;  $p = 0.36$ ). In addition, very rapid desensitisation was observed after activation by acetylcholine, similar to the profile observed with wild-type  $\alpha 7$  nAChRs. Figure 4.10 shows that all the PAMs tested elicited slow-desensitising agonist responses on the W54A receptor, albeit to different levels. The response to TQS ( $10 \mu\text{M}$ ) was  $2.4 \pm 0.3$  - fold larger than the maximum acetylcholine response ( $1 \text{ mM}$ ) (Figure 4.10A) and the response to TBS-516 ( $10 \mu\text{M}$ ) was  $3.4 \pm 0.5$  - fold larger (Figure 4.10B). Peak responses to type I PAMs were smaller than acetylcholine, with NS-1738 ( $10 \mu\text{M}$ ) eliciting a response with amplitude of  $16.9 \pm 0.7\%$  of the maximum acetylcholine response (Figure 4.10C) and TBS-346 ( $10 \mu\text{M}$ ) eliciting a response with amplitude of  $10.1 \pm 2.4\%$  of the acetylcholine response (Figure 4.10D). Concentration-response data collected for acetylcholine, the type I PAMs, NS-1738 and TBS-346, and the type II PAMs, TQS and TBS-516, are shown in Figure 4.10E and 4.10F. NS-1738 activated W54A  $\alpha 7$  nAChRs with an  $EC_{50}$  of  $5.7 \pm 0.7 \mu\text{M}$  ( $n = 3$ ) and TBS-346 with an  $EC_{50}$  of  $7.6 \pm 0.9 \mu\text{M}$  ( $n = 3$ ). TQS activated W54A  $\alpha 7$  nAChRs with an  $EC_{50}$  of  $4.1 \pm 0.6 \mu\text{M}$  ( $n = 3$ ) and TBS-516 with an  $EC_{50}$  of  $1.5 \pm 0.5$

$\mu\text{M}$  ( $n = 3$ ). The Hill coefficients were not significantly different ( $p = 0.64$ ; Tukey's *post hoc*) between NS-1738, TBS-346, TBS-516 and TQS ( $3.0 \pm 0.4$ ,  $2.6 \pm 0.4$ ,  $2.6 \pm 0.3$  and  $3.4 \pm 0.7$ , respectively;  $n = 3$ ).

It has been reported previously that activation of  $\alpha 7$  nAChRs containing the W54A mutation by the allosteric agonist 4BP-TQS is insensitive to the competitive antagonist MLA (Papke et al., 2014). Here, the effect of MLA on activation of W54A  $\alpha 7$  nAChRs by acetylcholine and allosteric ligands was examined (Figure 4.11). As expected, 1  $\mu\text{M}$  MLA completely blocked responses to 1 mM acetylcholine (Figure 4.11A). In agreement to previous studies (Papke et al., 2014), the agonist response elicited by 10  $\mu\text{M}$  TQS was largely insensitive to block by 1  $\mu\text{M}$  MLA ( $94.8 \pm 5.0\%$  of the TQS response;  $n = 4$ ) (Figure 4.11B). However, responses to TBS-516, NS-1738 and TBS-346 were blocked to different extent. 1  $\mu\text{M}$  MLA reduced the response to 10  $\mu\text{M}$  TBS-516 to  $34.6 \pm 5.3\%$  ( $n = 4$ ) of the control response in the absence of MLA (Figure 4.11C). The response to 10  $\mu\text{M}$  NS-1738 was reduced to  $18.3 \pm 1.3\%$  ( $n = 5$ ) of control (Figure 4.11D) and the response to 10  $\mu\text{M}$  TBS-346 was reduced to  $41.4 \pm 7.6$  ( $n = 4$ ) of control (Figure 4.11E).

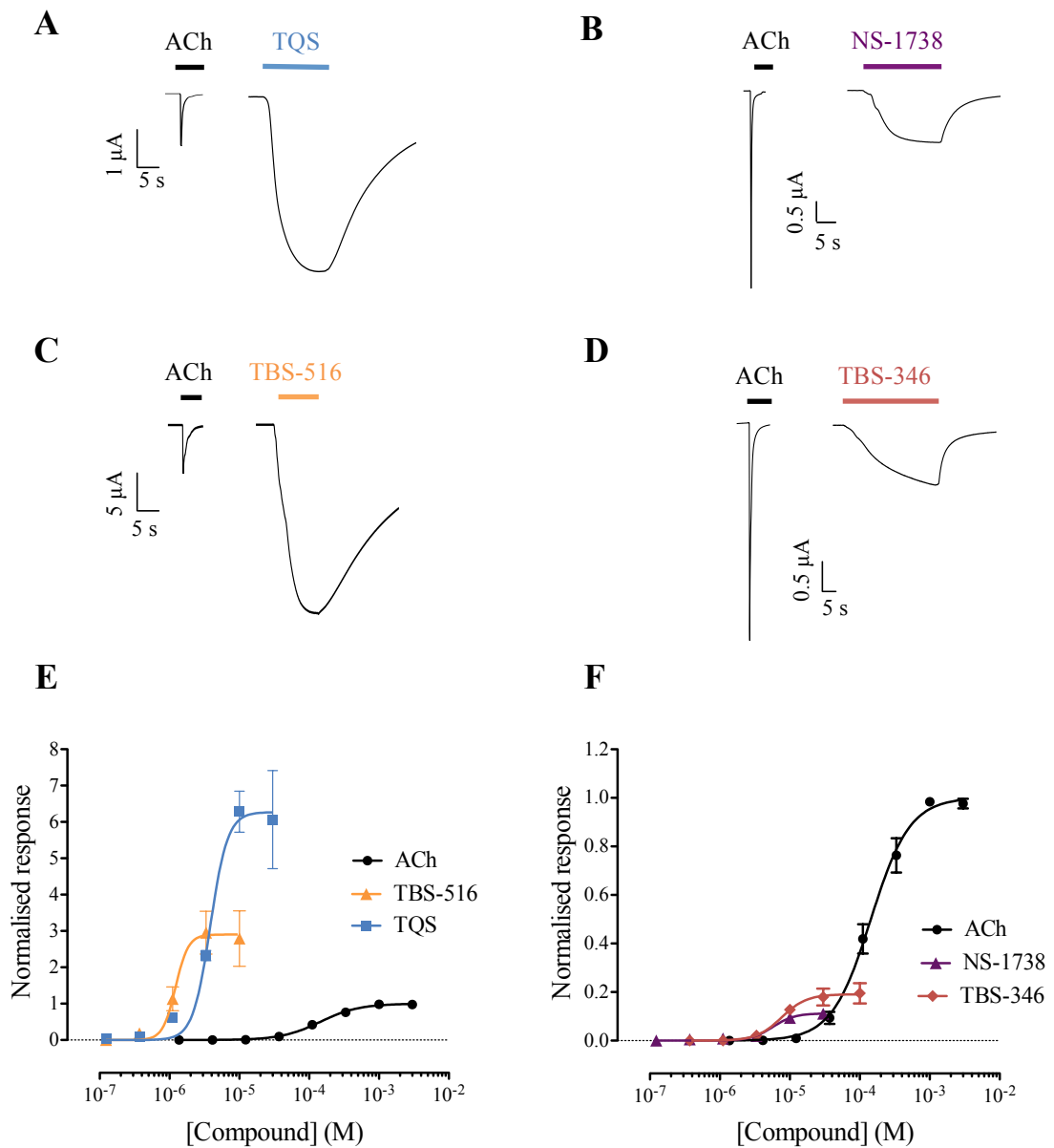


**Figure 4.10: Agonist activation of recombinant human  $\alpha 7$  nAChRs containing the W54A mutation.**

A-D) Representative traces, obtained by two-electrode voltage-clamp recording in oocytes expressing  $\alpha 7$  nAChRs containing the W54A mutation, showing responses to (A) ACh (1 mM; left) and TQS (10  $\mu$ M; right), (B) ACh (1 mM; left) and NS-1738 (10  $\mu$ M; right), (C) ACh (1 mM; left) and TBS-516 (10  $\mu$ M; right) and (D) ACh (1 mM; left) and TBS-346 (10  $\mu$ M; right).

E-F) Agonist concentration-response curves for ACh, TBS-516 and TQS (E) and ACh, NS-1738 and TBS-346 (F) obtained with oocytes expressing W54A  $\alpha 7$  nAChRs. Data are means and SEM of at least three independent experiments. Data are normalised to the maximum response obtained with ACh.

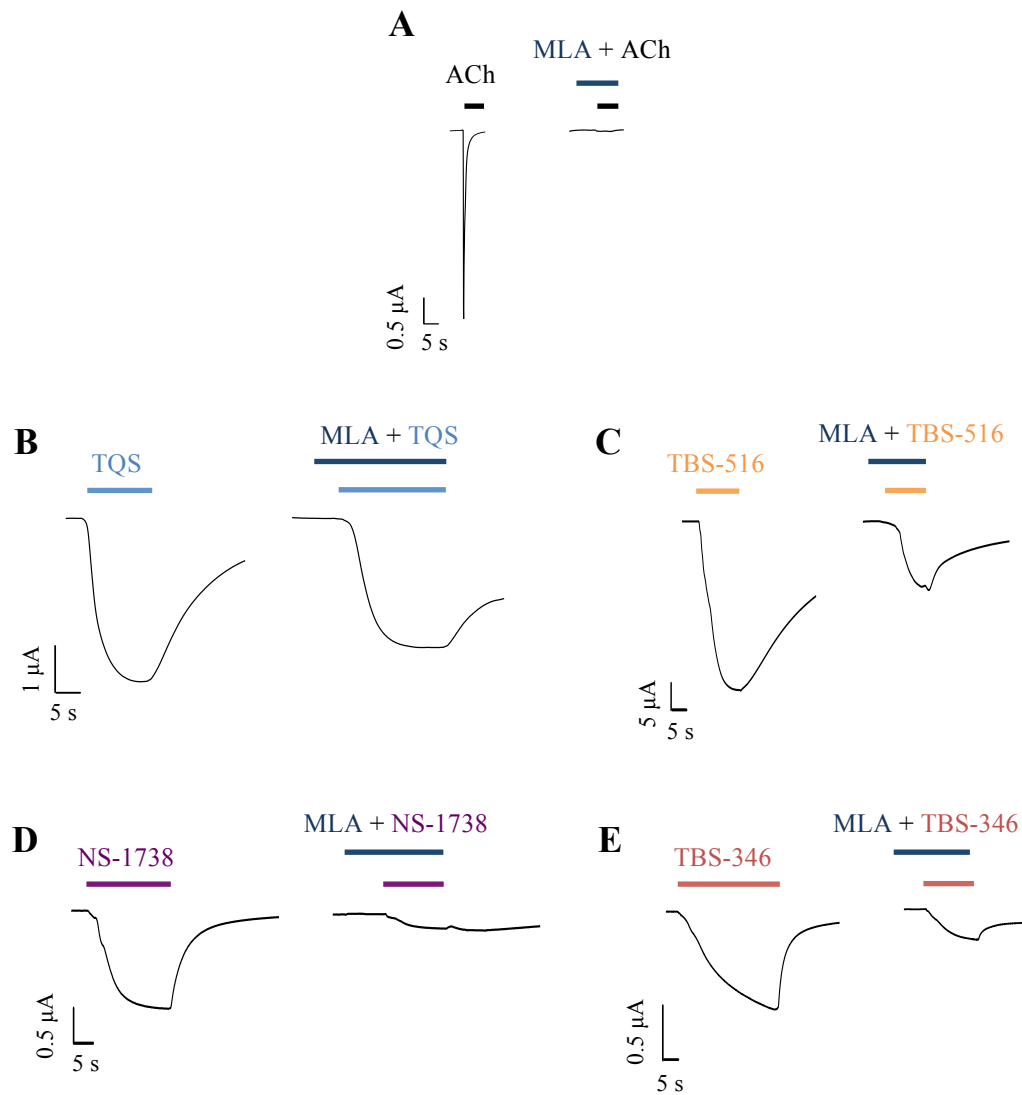


**Figure 4.11: Antagonism of agonist responses on W54A  $\alpha$ 7 nAChRs by MLA.**

Representative traces obtained by two-electrode voltage-clamp recording in oocytes expressing  $\alpha$ 7 nAChRs containing the W54A mutation, illustrating initial agonist responses with (A) ACh (1 mM), (B) TQS (10  $\mu$ M), (C) TBS-516 (10  $\mu$ M), (D) NS-1738 (10  $\mu$ M) and (E) TBS-346 (10  $\mu$ M) and antagonism by pre- and co-application of MLA (1  $\mu$ M) (right).

### 4.3 DISCUSSION

It is well established that orthosteric agonists, such as acetylcholine, bind to an extracellular site at the interface between two subunits (Arias, 2000). In contrast, evidence is accumulating to support that certain PAMs, such as PNU-120596, TQS and NS-1738, bind at an intrasubunit site in the nAChR transmembrane domain (Young *et al.*, 2008; Collins *et al.*, 2011). In addition, allosteric agonists have been identified that appear to bind at a similar transmembrane site but, in doing so, can activate  $\alpha 7$  nAChRs in the absence of an orthosteric agonist (Gill *et al.*, 2011; Gill *et al.*, 2012; Gill *et al.*, 2013; Papke *et al.*, 2014). Similarly, there is evidence for agonist activation, via an allosteric transmembrane site, for other pentameric LGICs (Amin & Weiss, 1993; Cully *et al.*, 1996; Lansdell *et al.*, 2015).

Although previous studies have demonstrated that the L247T mutation can convert a type II PAM into an allosteric agonist (Gill *et al.*, 2011), this finding has now been extended by demonstrating that this is a feature conferred by the L247T mutation on type I PAMs, type II PAMs and also on PAMs that can be considered to have intermediate (type I/II) properties. Based on structural studies from a variety of pentameric LGICs, the amino acid located at a position analogous to L247 (position 9') in the  $\alpha 7$  nAChR is located close to the gate of the channel pore (Unwin, 2005; Beckstein & Sansom, 2006; Althoff *et al.*, 2014; Hassaine *et al.*, 2014). This may help to explain the profound effects that have been observed when this amino acid is mutated. It seems plausible that mutating this amino acid might disrupt the gate of the channel and mutations have been shown to increase the opening rate. Indeed, higher frequency of spontaneous openings has been reported in receptors containing the L247T mutation (Labarca *et al.*, 1995; Bertrand *et al.*, 1997) as well as other changes in pharmacological properties (Revah *et al.*, 1991; Bertrand *et al.*, 1992; Palma *et al.*, 1996). In contrast, the M260L mutation, which is located towards the extracellular site of the TM2 domain (position 22'), has a more selective effect on PAMs. With this mutation, agonist activation was observed only with PAMs that substantially reduced the levels of desensitisation in wild-type  $\alpha 7$  nAChRs. This effect of the M260L mutation is unlikely to be due to it preventing the binding of type I PAMs because, even though type I PAMs are not converted into agonists on the mutated receptor, they retain their PAM activity in the presence of acetylcholine. In addition, type I PAMs block

agonist activation by type II PAMs in receptors containing the M260L mutation. It is thought that type I PAMs increase peak current in the presence of an agonist by facilitating the transition of the receptor from the resting to open state upon activation by the agonist without having an effect on receptor desensitisation. On the other hand, type II PAMs significantly reduce the fast desensitisation of the  $\alpha 7$  nAChRs and may allow receptor reactivation from the desensitised state, perhaps by destabilising the desensitised state or converting the desensitised state into a new conducting state.

As is illustrated in Figure 4.2, M260 is located near the extracellular site of the TM2 domain, whereas L247 is located towards the intracellular site (at positions 22' and 9', respectively). It is also notable that the side chain of L247 is predicted to point towards the ion channel pore, whereas that of M260 points towards an intrasubunit cavity that has been proposed previously as a binding site for allosteric modulators of  $\alpha 7$  nAChRs (Young *et al.*, 2008; Gill *et al.*, 2011). It is possible that these mutations may facilitate direct receptor activation by PAMs by altering the energy barrier for transitions between the closed, open and desensitised states of the receptor. Direct allosteric activation appears to be associated with a loss of rapid desensitisation. In the case of the M260L mutation, which has no significant effect on desensitisation, allosteric activation occurs only with type II PAMs (which themselves cause a loss of agonist-induced desensitisation). In contrast, the L247T mutation, which itself cause a loss of desensitisation, facilitates agonist activation by type I PAMs (which do not alter receptor desensitisation). The M260 residue is located towards the extracellular end of the TM2 domain in a region that has been referred to as the 'M2-cap' (Bafna *et al.*, 2008). Previous studies have indicated that a stretch of 10 amino acids this region can influence allosteric modulation of an  $\alpha 7/5$ -HT3A subunit chimera (Bertrand *et al.*, 2008). In addition, studies of this region (18'-28') on the  $\alpha 1$  subunit of the muscle-type nAChR, indicate that mutations in this region have large effects on gating but smaller effects on channel conductance and desensitisation (Bafna *et al.*, 2008). However, mutating the isoleucine on the 22' position to a leucine (which corresponds to M260 on the human  $\alpha 7$  subunit) increased the apparent rate for entry into long-lived desensitised states by  $\sim 10$ -fold (Bafna *et al.*, 2008). It is plausible that this mutation in the corresponding residue of the  $\alpha 7$  subunit could have an effect on the rate of receptor desensitisation, which could alter its modulation by type II PAMs.

Numerous mutations on the  $\alpha 7$  nAChR have been reported to alter the properties of orthosteric and allosteric ligands. As discussed above, the L247T mutation has been reported to dramatically alter the properties of various ligands, possibly due to its significance in receptor gating (Revah *et al.*, 1991; Labarca *et al.*, 1995; Palma *et al.*, 1996). In addition, M260L points to an intrasubunit cavity, proposed to be the binding site of a number of PAMs, including TQS (Young *et al.*, 2008; Gill *et al.*, 2011). In contrast, a mutation located at a distant site to the proposed binding site of these PAMs, W54A, has been reported to influence receptor modulation by allosteric ligands (Papke *et al.*, 2014). This mutation is situated on a highly conserved residue at the complementary component of the orthosteric binding site (Corringer *et al.*, 1995). It has been reported recently that the type II PAMs TQS and PNU-120596 are converted into agonists on  $\alpha 7$  nAChRs containing the W54A mutation. In addition, agonism by allosteric ligands was reported to be insensitive to MLA block, suggesting a ‘de-coupling’ of the orthosteric and allosteric binding sites (Papke *et al.*, 2014). Here, it has been shown that, similar to L247T, both type I and type II PAMs are converted into non-desensitising agonists. However, type I PAMs activated the receptor to a lesser degree than type II PAMs. In addition, even though TQS was largely insensitive to MLA block (in agreement with previous studies (Papke *et al.*, 2014)), the other PAMs tested were not. This would suggest a compound-selective effect of MLA block, rather than a generalised de-coupling of the orthosteric and allosteric binding sites in  $\alpha 7$  nAChRs containing the W54A mutation.

In conclusion, evidence for mutations located at different positions in the receptor subunit having distinct effects on allosteric modulation helps to provide a greater insight into the pharmacological diversity of these compounds.

## CHAPTER 5

# ATYPICAL PHARMACOLOGICAL PROPERTIES OF A-867744

---

## 5.1 INTRODUCTION

As discussed previously, numerous allosteric ligands that potentiate nAChRs have been identified in recent years. A-867744 (4-(5-(4-chlorophenyl)-2-methyl-3-propionyl-1H-pyrrol-1-yl) benzenesulfonamide) (Figure 5.1) is a compound first developed and characterised by Abbott as an  $\alpha 7$ -selective type II PAM (Faghih *et al.*, 2009; Malysz *et al.*, 2009). Similar to other type II PAMs, such as PNU-120596 and TQS, A-867744 does not activate the receptor when applied alone, but, when co-applied with an orthosteric agonist, it potentiates peak agonist response and dramatically reduces the fast desensitisation observed with  $\alpha 7$  nAChRs (Malysz *et al.*, 2009). There is also evidence from subunit chimaeras that A-867744 exhibits its effect by binding at a transmembrane site. However, some unexpected results have been reported. Although A-867744 does not displace binding of [ $^3$ H]-MLA from  $\alpha 7$  nAChRs, it has been reported to displace the binding of another agonist ([ $^3$ H]-A-585539) that is thought to interact with the orthosteric site (Malysz *et al.*, 2009).

Previous studies with receptors containing site-directed point mutations have identified critical residues for the functioning of orthosteric and allosteric ligands of  $\alpha 7$  nAChRs. The orthosteric binding site has been extensively mapped (Corringer *et al.*, 1998), and critical residues like Y188 and W149 have been identified (Akk, 2001; Stewart *et al.*, 2006; Horenstein *et al.*, 2007; Williams *et al.*, 2009). Likewise, residue M253 in the transmembrane domain has been identified to be essential for the function of allosteric potentiators and agonists, with the M253L mutation reducing or abolishing the effect of allosteric ligands such as PNU-120596, TQS and 4BP-TQS (Young *et al.*, 2008; Gill *et al.*, 2011). In contrast, the M260L mutation, which is situated near the same intrasubunit cavity as M253, was shown to convert PAMs that reduce the rate of desensitisation into agonists (Chapter 4). In addition, the L247T and W54A mutations have also been shown to convert PAMs, irrespective of their effect on desensitisation, into non-desensitising agonists ((Papke *et al.*, 2014) and Chapter 4).

In this chapter, the effects of A-867744 are examined on  $\alpha 7$  nAChRs containing mutations proposed to be significant for allosteric modulation, in order to investigate whether this compound behaves differently than other allosteric ligands examined previously.

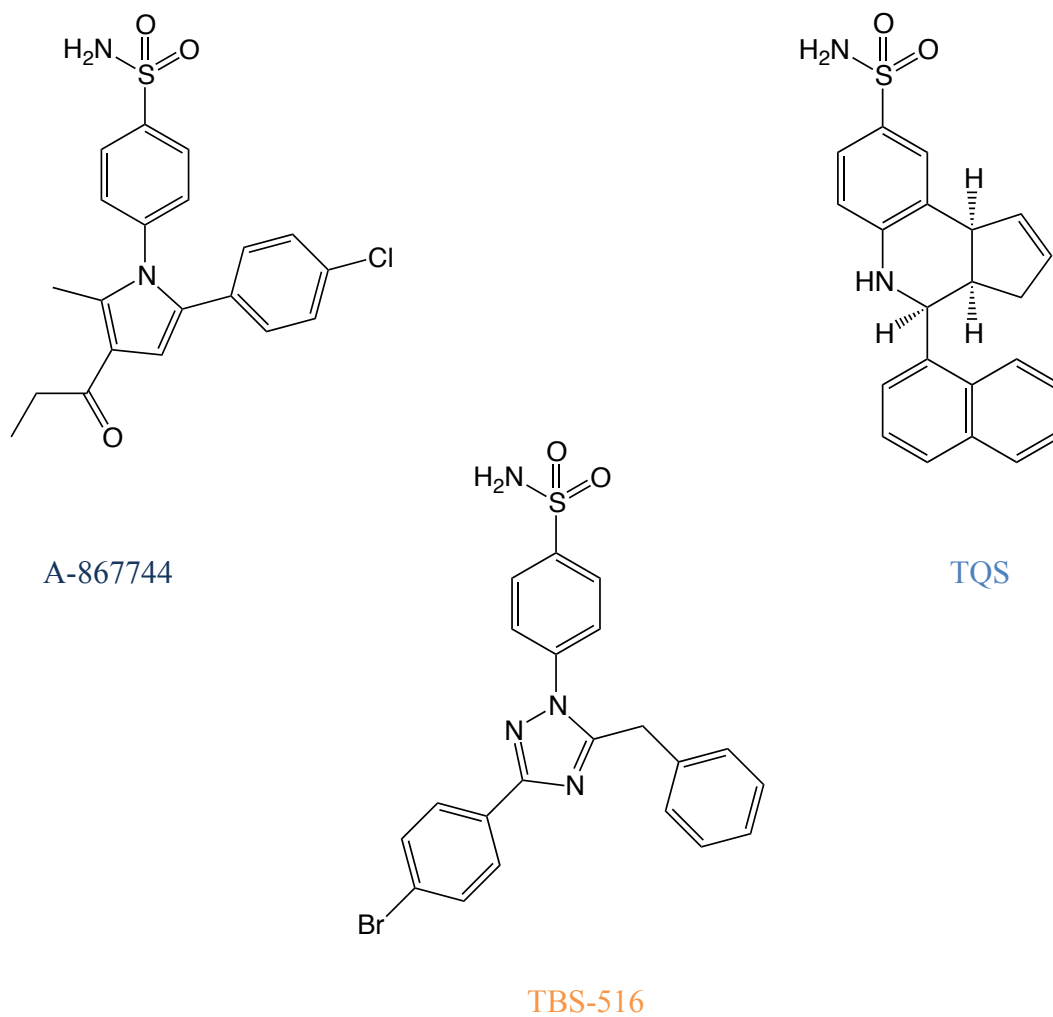


**Figure 5.1: Chemical structures of allosteric ligands examined in this chapter.**

Abbreviations: A-867744: 4-(5-(4-chlorophenyl)-2-methyl-3-propionyl-1H-pyrrol-1-yl)benzenesulfonamide; TBS-516: 4-(5-benzyl-3-(4-bromophenyl)-1H-1,2,4-triazol-1-yl)benzenesulfonamide; TQS: *cis-cis*-4-(naphthalen-1-yl)-3*a*,4,5,9*b*-tetrahydro-3*H*-cyclopenta[*c*]quinoline-8-sulfonamide.

## 5.2 RESULTS

The pharmacological properties of A-867744 were examined on wild-type and mutated human recombinant  $\alpha 7$  nAChRs expressed in *Xenopus* oocytes by two-electrode voltage-clamp recordings and on mammalian cultured cells transiently transfected with human  $\alpha 7$  nAChRs by competition radioligand binding assays.

### 5.2.1 A-867744 is a type II PAM of $\alpha 7$ nAChRs

In agreement with previous studies (Malysz *et al.*, 2009), A-867744 did not evoke responses when applied on  $\alpha 7$  nAChRs in the absence of an orthosteric agonist. However, it potentiated responses to acetylcholine and dramatically reduced the fast desensitisation kinetics of the  $\alpha 7$  nAChR at higher concentrations (Figure 5.2). Concentration-response data obtained for a range of A-867744 concentrations pre- and co-applied with 100  $\mu$ M acetylcholine confirmed that A-867744 is a potent PAM, with an  $EC_{50}$  of  $115 \pm 21$  nM and Hill coefficient of  $1.4 \pm 0.2$  (Figure 5.2;  $n = 6$ ). In addition, the maximum potentiation of a submaximal acetylcholine response (100  $\mu$ M) was  $17.1 \pm 2.7$  fold ( $n = 7$ ).

Competition radioligand binding was performed in order to examine the ability of A-867744 to displace [ $^3$ H]- $\alpha$ -bungarotoxin from the orthosteric binding site of  $\alpha 7$  nAChRs (Figure 5.3). It has been reported previously that A-867744 does not displace the binding of [ $^3$ H]-MLA, though, surprisingly, it displaces the binding of another agonist that is thought to interact with the orthosteric binding site (Malysz *et al.*, 2009). Here it is demonstrated that A-867744 did not elicit any significant displacement of [ $^3$ H]- $\alpha$ -bungarotoxin binding (Figure 5.3). These findings are consistent with A-867744 acting as potentiator of  $\alpha 7$  nAChRs via a site other than the extracellular orthosteric binding site.

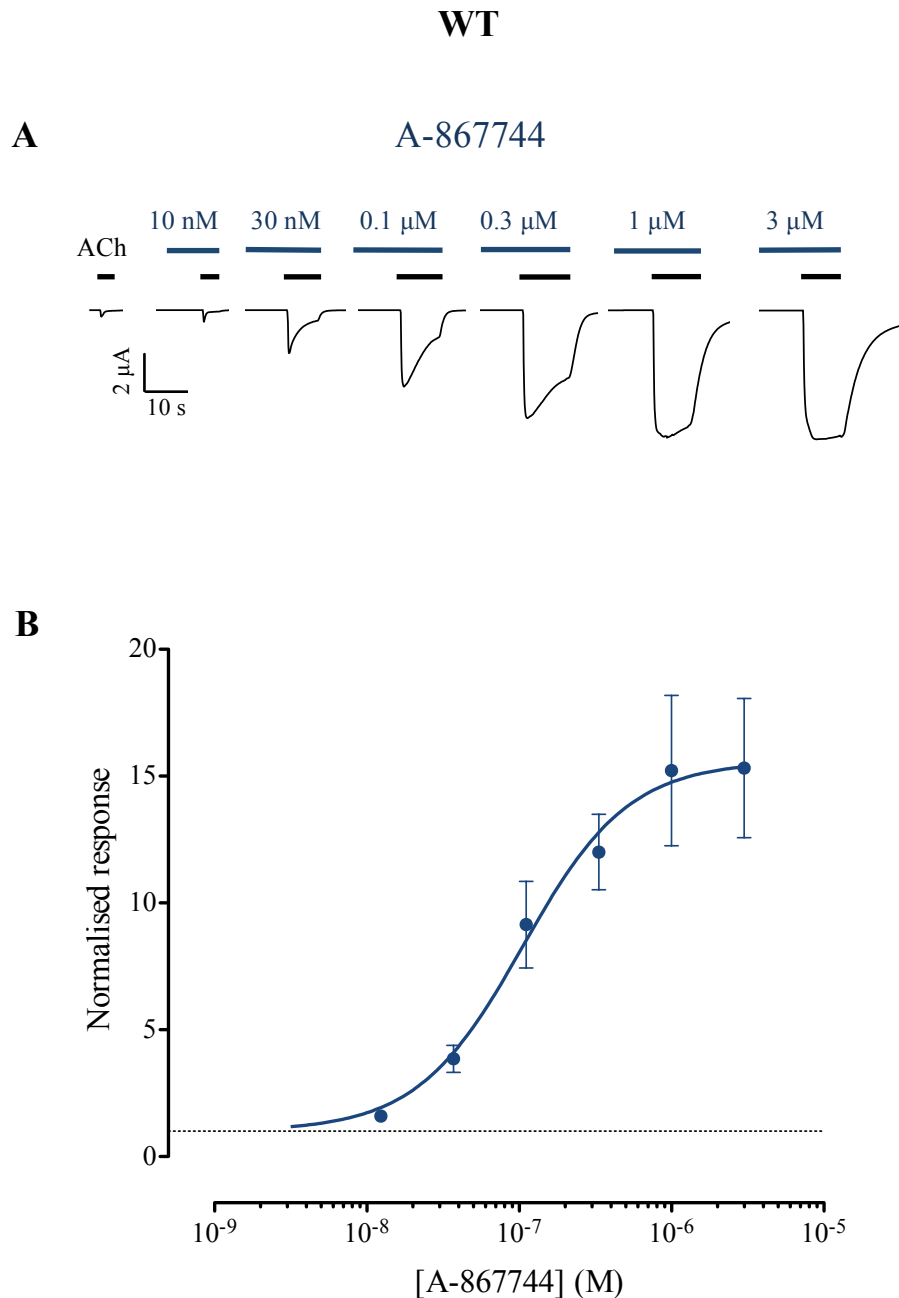


**Figure 5.2: Positive allosteric modulation of wild-type  $\alpha 7$  nAChRs by A-867744, examined by two-electrode voltage-clamp recording in *Xenopus* oocytes.**

A) Representative traces are shown illustrating responses to an  $\text{EC}_{50}$  of ACh (100  $\mu\text{M}$ ) and to ACh (100  $\mu\text{M}$ ) co-applied with a range of concentrations of A-867744 (0.01 – 3  $\mu\text{M}$ ). A-867744 was pre-applied for 5 s before ACh was co-applied. The horizontal bars indicate the duration of ACh (black bars) and A-867744 (blue bars) application.

B) Concentration-response data are plotted for a range of concentrations of A-867744 co-applied with an  $\text{EC}_{50}$  of ACh (100  $\mu\text{M}$ ). Data are means  $\pm$  SEM of six independent experiments, each from different oocytes. Data are normalised to the response obtained with 100  $\mu\text{M}$  ACh.

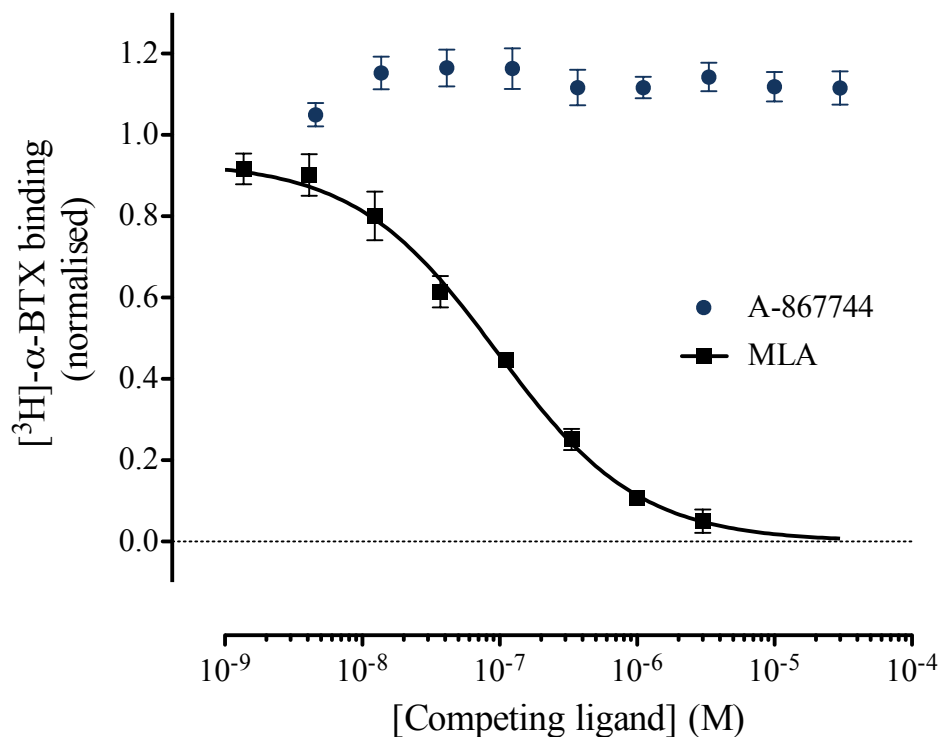


**Figure 5.3: Displacement of [3H]-α-bungarotoxin from the orthosteric site of α7 nAChRs by A-867744, examined by competition radioligand binding.**

Equilibrium radioligand binding was performed with [3H]-α-bungarotoxin (1 nM) with mammalian tsA201 cells transiently transfected with human α7 nAChR subunit and with human RIC-3 cDNAs (1:1 ratio). A-867744 (3 nM – 30 μM) causes no significant displacement of [3H]-α-bungarotoxin binding, whereas MLA causes complete displacement of specific radioligand binding. Data points are means (± SEM) of three independent experiments, each done in triplicates.

### 5.2.2 The influence of M260L on the pharmacological properties of A-867744

As described in chapter 4, PAMs that have a profound effect on  $\alpha 7$  nAChR desensitisation were converted into agonists on  $\alpha 7$  nAChRs containing the M260L mutation. A-867744 is an  $\alpha 7$  PAM that dramatically reduces the fast desensitisation observed after activation with acetylcholine (Figure 5.2) and is classified as a type II PAM. However, A-867744 failed to evoke any responses when up to 100  $\mu\text{M}$  were applied in the absence of an agonist on  $\alpha 7$  nAChRs containing the M260L mutation (Figure 5.4), in marked contrast to the type II PAMs TQS and TBS-516, which evoked non-desensitising currents (Chapter 4). In addition, even though A-867744 was not converted into an agonist on M260L receptors, it retained its type II PAM activity (Figure 5.4B). The maximum fold potentiation of the response to 100  $\mu\text{M}$  acetylcholine on M260L by 1  $\mu\text{M}$  A-867744 was  $14.9 \pm 5.1$  ( $n = 5$ ), which is not significantly different to that observed with wild-type ( $17.1 \pm 2.7$ ;  $n = 7$ ;  $p = 0.69$ ). Furthermore, 1  $\mu\text{M}$  A-867744 completely blocked the agonist responses elicited by 30  $\mu\text{M}$  TQS (Figure 5.4C).

### 5.2.3 The influence of W54A on the pharmacological properties of A-867744

$\alpha 7$  nAChRs containing the W54A mutation convert type II and also type I PAMs into non-desensitising agonists (Chapter 4 and (Papke *et al.*, 2014)). However, similar to M260L, A-867744 was not converted into an agonist when tested up to 100  $\mu\text{M}$  on W54A receptors (Figure 5.5). A-867744 retained its activity as a type II PAM (Figure 5.5B). The maximum fold potentiation of the response to 100  $\mu\text{M}$  acetylcholine by 1  $\mu\text{M}$  A-867744 was  $15.1 \pm 1.8$  ( $n = 12$ ), which is not significantly different to that observed with wild-type ( $17.1 \pm 2.7$ ;  $n = 7$ ;  $p = 0.54$ ). In addition, 1  $\mu\text{M}$  A-867744 completely blocked the agonist responses elicited by 10  $\mu\text{M}$  TQS (Figure 5.5C).

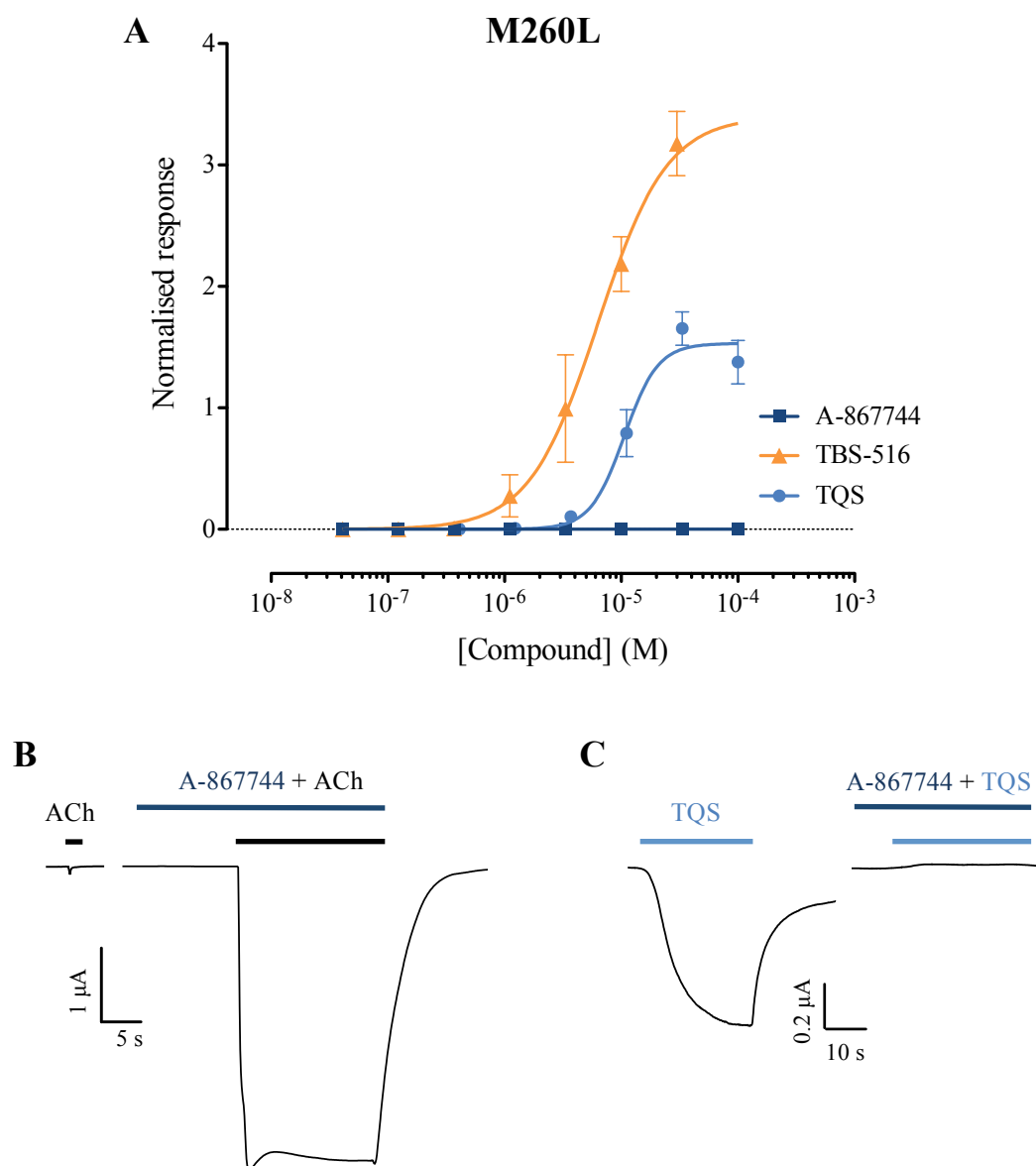


**Figure 5.4: The effects of A-867744 on  $\alpha 7$  nAChRs containing the M260L mutation.**

A) Concentration-response data are plotted for a range of concentrations of the type II PAMs A-867744, TBS-516 and TQS. Data are means  $\pm$  SEM of three independent experiments, each from different oocytes. Data are normalised to the maximum acetylcholine response.

B) Representative traces illustrating responses to ACh (100  $\mu$ M; left) together with ACh responses from the same oocyte after pre- and co-application of A-867744 (1  $\mu$ M; right). A-867744 was pre-applied for 10 s.

C) Representative traces illustrating responses to TQS (30  $\mu$ M; left) together with TQS responses from the same oocyte after pre- and co-application of A-867744 (1  $\mu$ M; right). A-867744 was pre-applied for 10 s.

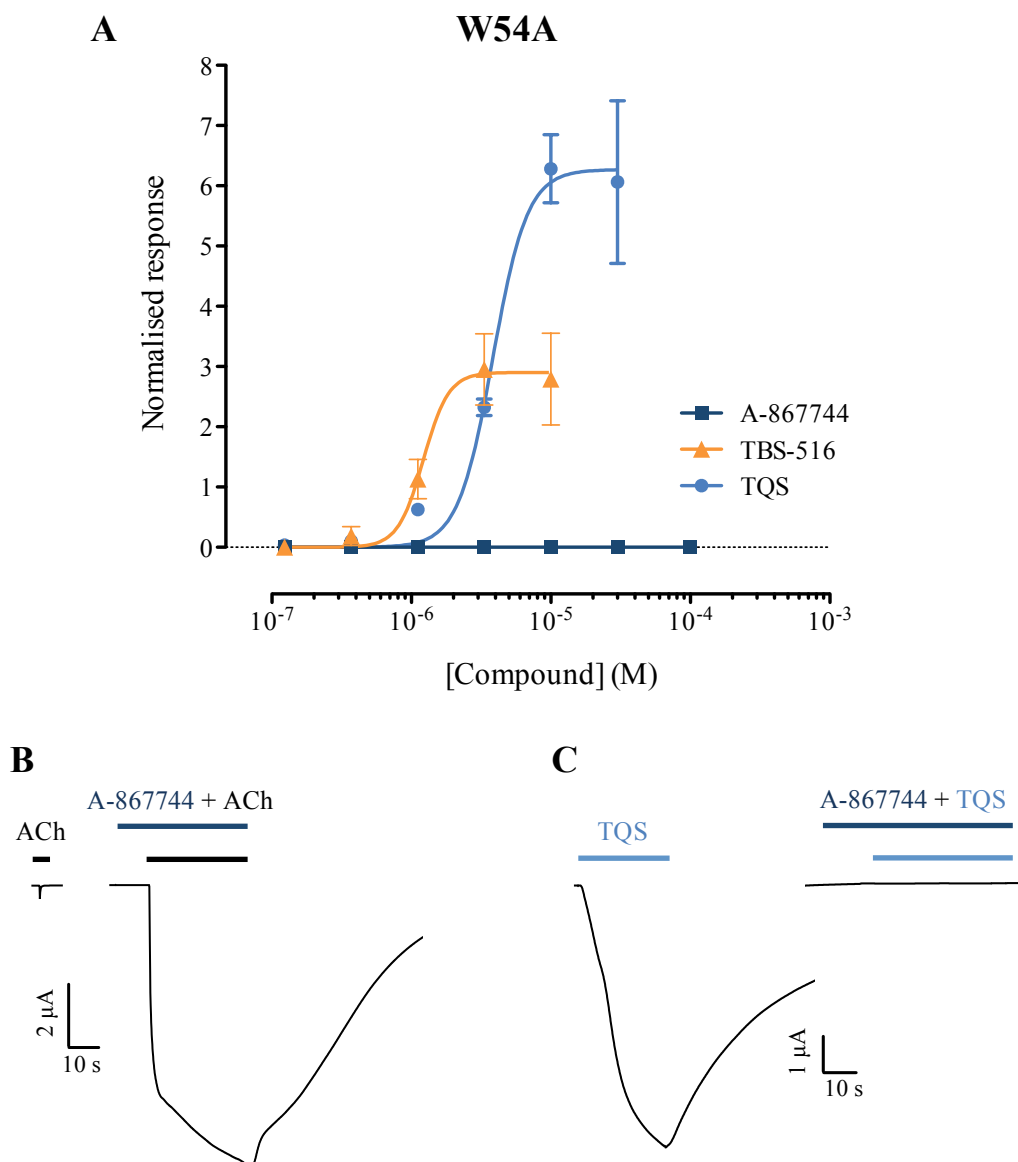


**Figure 5.5: The effects of A-867744 on  $\alpha 7$  nAChRs containing the W54A mutation.**

A) Concentration-response data are plotted for a range of concentrations of the type II PAMs A-867744, TBS-516 and TQS. Data are means  $\pm$  SEM of three independent experiments, each from different oocytes. Data are normalised to the maximum acetylcholine response.

B) Representative traces illustrating responses to ACh (100  $\mu$ M; left) together with ACh responses from the same oocyte after pre- and co-application of A-867744 (1  $\mu$ M; right). A-867744 was pre-applied for 10 s.

C) Representative traces illustrating responses to TQS (10  $\mu$ M; left) together with TQS responses from the same oocyte after pre- and co-application of A-867744 (1  $\mu$ M; right). A-867744 was pre-applied for 10 s.

#### 5.2.4 The influence of L247T on the pharmacological properties of A-867744

As demonstrated in chapter 4 and in previous studies (Revah *et al.*, 1991; Bertrand *et al.*, 1992; Palma *et al.*, 1996; Gill *et al.*, 2011),  $\alpha 7$  nAChRs containing the L247T mutation display dramatic differences in their pharmacological profile compared to wild-type receptors. These include converting all PAMs, irrespective of their effects on receptor desensitisation, into potent and efficacious non-desensitising agonists (Chapter 4). However, the type II PAM A-867744 was not converted into an agonist on L247T receptors (Figure 5.6A). In contrast, 1  $\mu$ M A-867744 inhibited maximum acetylcholine responses (10  $\mu$ M) by  $66.3 \pm 1.2\%$  (Figure 5.6B). In addition, the same concentration of A-867744 completely blocked agonist responses to a maximum TQS concentration (10  $\mu$ M) (Figure 5.6C). It is notable that when A-867744 was applied on  $\alpha 7$  receptors containing the L247T mutation, a decrease in the baseline current was observed, which can be interpreted as inhibition of the more frequent spontaneously opened receptors (a feature of the L247T mutation (Bertrand *et al.*, 1997)) by A-867744.

#### 5.2.5 The influence of M253L on the pharmacological properties of A-867744

The M253L mutation on  $\alpha 7$  nAChRs has been reported to reduce or abolish the effect of allosteric ligands such as PNU-120596, TQS and 4BP-TQS (Young *et al.*, 2008; Gill *et al.*, 2011). In agreement with previous studies (Gill *et al.*, 2011), co-application of TQS (10  $\mu$ M) with acetylcholine (100  $\mu$ M) on M253L receptors did not result in an increase in peak current, while only very modest changes in desensitisation kinetics were observed (Figure 5.7A). In contrast, 1  $\mu$ M A-867744 completely blocked the acetylcholine response (Figure 5.7B). This block was very persistent and the acetylcholine response could not be recovered even after a long wash (10 minutes) (Figure 5.7B). Interestingly, when TQS (10  $\mu$ M) was pre-applied before co-application of A-867744 (1  $\mu$ M) and acetylcholine (100  $\mu$ M), the A-867744 block was not observed and there was no reduction in the acetylcholine response (Figure 5.7C). However, after TQS and A-867744 wash, no acetylcholine response could be detected, even after a prolonged wash (Figure 5.7C), suggesting a very high affinity block by A-867744.

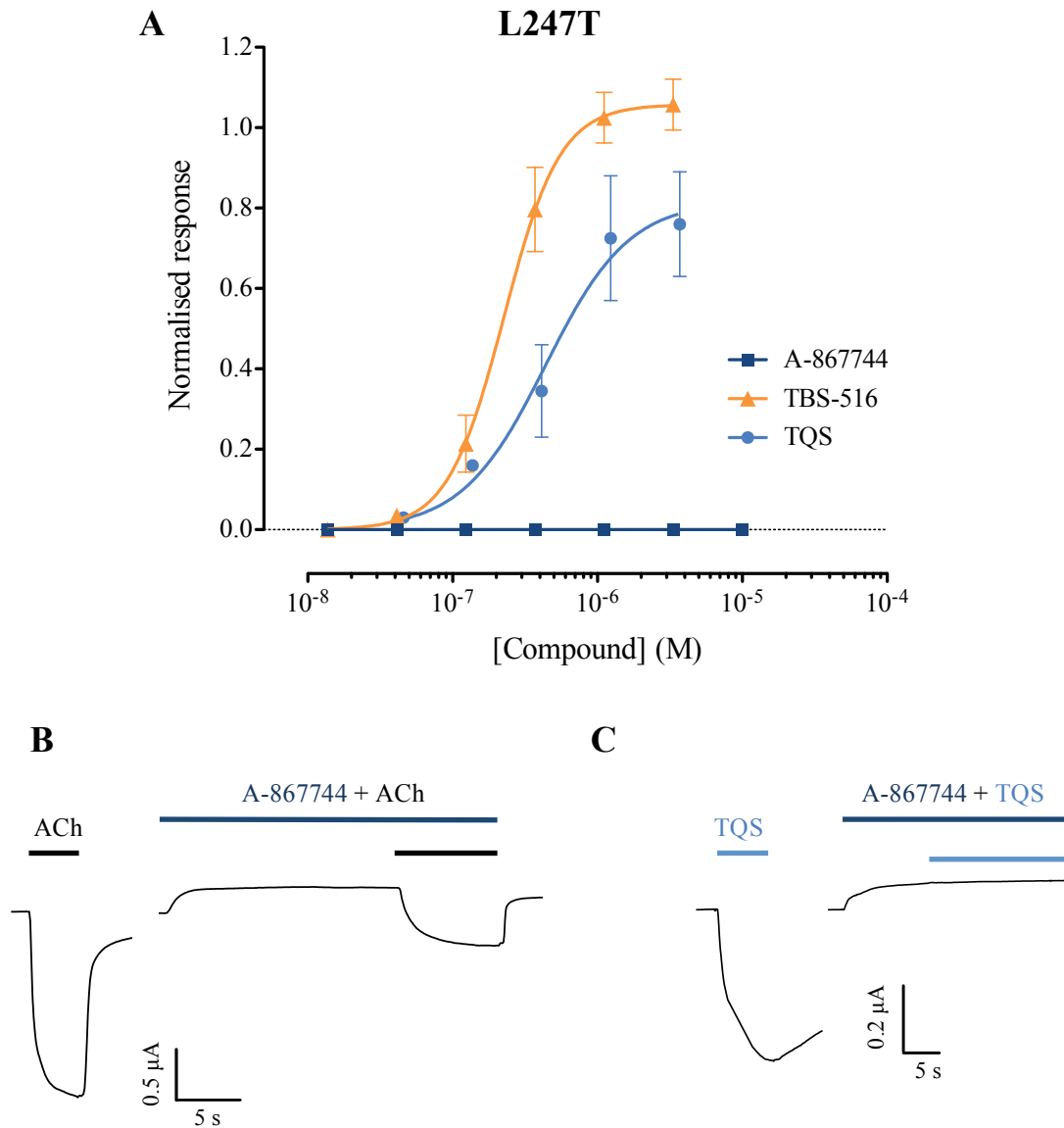


**Figure 5.6: The effects of A-86774 on  $\alpha 7$  nAChRs containing the L247T mutation.**

A) Concentration-response data are plotted for a range of concentrations of the type II PAMs A-86774, TBS-516 and TQS. Data are means  $\pm$  SEM of three independent experiments, each from different oocytes. Data are normalised to the maximum acetylcholine response.

B) Representative traces illustrating responses to ACh (10  $\mu$ M; left) together with ACh responses from the same oocyte after pre- and co-application A-86774 (1  $\mu$ M; right). A-86774 was pre-applied for 10 s.

C) Representative traces illustrating responses to TQS (10  $\mu$ M; left) together with TQS responses from the same oocyte after pre- and co-application of A-86774 (1  $\mu$ M; right). A-86774 was pre-applied for 10 s.

## M253L

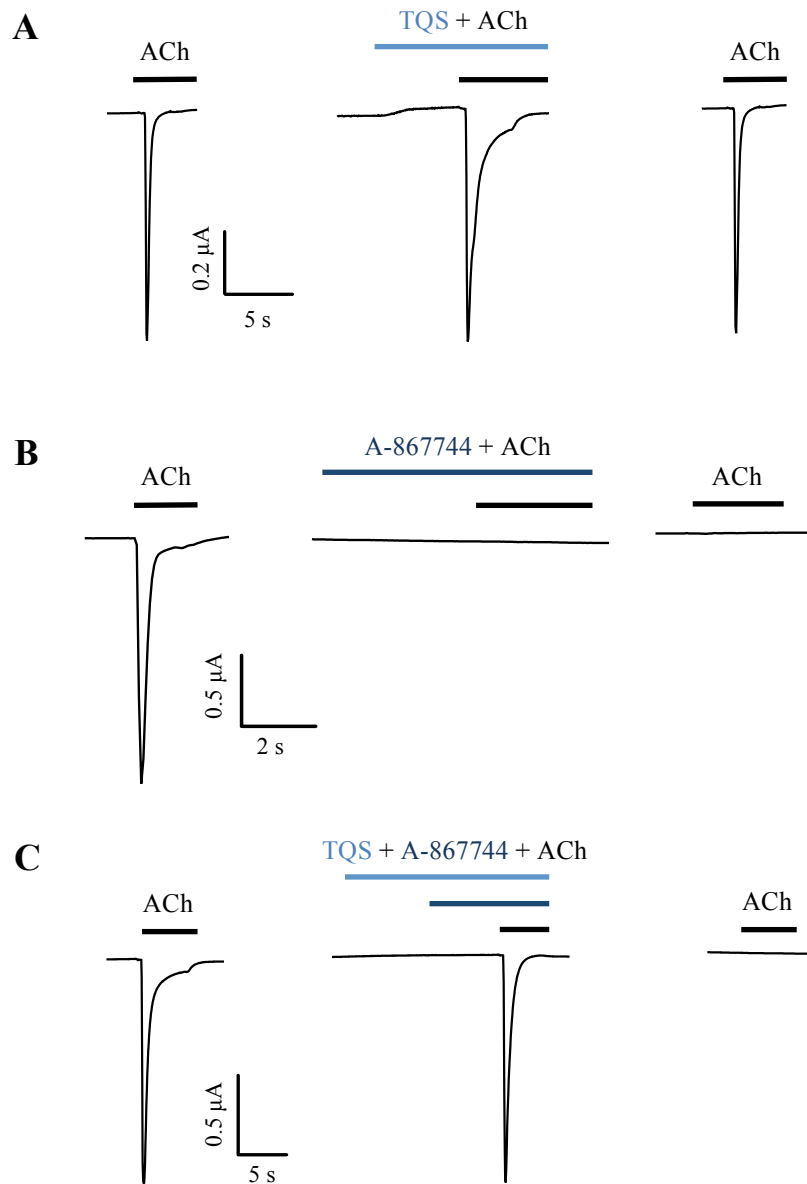


**Figure 5.7: The effects of A-867744 on  $\alpha 7$  nAChRs containing the M253L mutation.**

A) Representative traces illustrating response to ACh (100  $\mu$ M; left), response to ACh after pre- and co-application of TQS (10  $\mu$ M; middle) and then response to ACh after TQS wash (right).

B) Representative traces illustrating responses to ACh (100  $\mu$ M; left) and block of ACh responses after pre- and co-application of A-867744 (1  $\mu$ M; middle). The ACh response does not recover after A-867744 wash (10 minutes; right).

C) Representative traces illustrating responses to ACh (100  $\mu$ M; left) and ACh responses after pre- and co-application of TQS (10  $\mu$ M) and A-867744 (1  $\mu$ M) (middle). TQS was pre-applied for 10 s and A-867744 for 5 s. The ACh response does not recover after A-867744 wash (10 minutes; right).

### 5.3 DISCUSSION

In this chapter, the pharmacological properties of A-867744 (Figure 5.1) were examined on wild-type and mutated  $\alpha 7$  nAChRs. As described previously (Faghieh *et al.*, 2009; Malysz *et al.*, 2009), A-867744 potentiated agonist responses on wild-type  $\alpha 7$  nAChRs both by increasing peak current and strongly slowing down the desensitisation kinetics. It has been demonstrated in previous studies that A-867744, similar to other PAMs, such as PNU-120596, TQS and NS-1738, does not displace [<sup>3</sup>H]-MLA. However, A-867744 (in contrast to the other PAMs tested) displaces the binding of [<sup>3</sup>H]-A-585539 (Malysz *et al.*, 2009), an  $\alpha 7$ -selective agonist thought to bind at the orthosteric binding site (Anderson *et al.*, 2008).

Studies with subunit chimaeras suggest that A-867744 exerts its potentiating effects by binding at a site in the transmembrane domain. A-867744 does not potentiate responses on 5-HT<sub>3A</sub>Rs, or chimaeric  $\alpha 7/5$ -HT<sub>3A</sub> receptors, composed of the N-terminal domain and TM2-3 loop of the  $\alpha 7$  nAChRs and the TM domains of 5-HT<sub>3A</sub>Rs (Malysz *et al.*, 2009). It has been proposed that the same allosteric binding site interaction is involved in positive modulation effects and displacement of [<sup>3</sup>H]-A-585539 on  $\alpha 7$  nAChRs, although it is recognised that A-867744 could exert its effects by binding at two distinct sites (Malysz *et al.*, 2009). Indeed, it is possible that A-867744 induces the displacement of [<sup>3</sup>H]-A-585539 via an allosteric mechanism and not competitive binding.

[<sup>3</sup>H]-A-585539 has been reported to be an  $\alpha 7$ -selective agonist with unusually fast dissociation rate at room temperature (Anderson *et al.*, 2008), which could contribute to an increased sensitivity of displacement by A-867744 via an allosteric mechanism of action. Displacement of [<sup>3</sup>H]-A-585539, however, is not observed with other allosteric ligands, which suggests that A-867744 displays different properties to PAMs, such as TQS (Malysz *et al.*, 2009). Here, it is confirmed that A-867744 does not displace [<sup>3</sup>H]- $\alpha$ -bungarotoxin binding and the effects of A-867744 have been examined on  $\alpha 7$  nAChRs containing mutations that are known to affect modulation by allosteric ligands.

In chapter 4,  $\alpha 7$  nAChRs containing the M260L mutation, located towards the extracellular site of the TM2 domain, were shown to convert PAMs with a significant

effect on desensitisation into agonists, while PAMs with no significant effect on desensitisation retained their PAM activity, but were not converted into agonists. The effects of A-867744 on  $\alpha 7$  nAChRs containing the M260L mutation were somewhat unexpected. Even though A-867744 displays a dramatic reduction in desensitisation kinetics when co-applied with acetylcholine in wild-type  $\alpha 7$  nAChRs, it displayed no agonist activity on M260L receptors even at the highest concentrations tested. In addition, A-867744 blocked TQS agonist responses on M260L. However, when A-867744 was co-applied with acetylcholine it potentiated responses with a type II profile and fold-potential that was not significantly different to wild-type nAChRs.

The M260 residue is located near an intrasubunit cavity that has been proposed to be the binding site for ligands such as PNU-120596, TQS and 4BP-TQS (Young *et al.*, 2008; Gill *et al.*, 2011) and it can be argued that, depending on the interaction of the various ligands with the side chain, the M260L mutation can influence the ligand effects in a different way. However, W54A, a mutation located on the complementary component of the orthosteric binding site (Corringer *et al.*, 1995) is not located near the proposed transmembrane binding sites of the ligands tested. The W54A mutation has been previously shown to convert both type I and type II PAMs into non-desensitising agonists (Chapter 4 and (Papke *et al.*, 2014)). However, A-867744 failed to elicit any agonist responses on W54A receptors. In addition, similarly to M260L, A-867744 potentiated agonist responses with no significant difference to wild-type receptors and it also blocked agonist responses to TQS. Considering these two contrasting properties on both M260L and W54A (potentiation of acetylcholine response and inhibition of TQS response), it is proposed that inhibition of TQS by A-867744 is due to a competitive mechanism of action. However, it is possible that A-867744 binds at a distinct place from TQS, or it exerts its effects on TQS and acetylcholine responses by binding at multiple sites on the receptor.

Perhaps a more surprising difference in the properties of A-867744 compared to other PAMs comes from analysis of the influence of the L247T mutation on A-867744. Mutating this residue on the TM2 domain, which has been reported to have an important role in receptor gating, produces a receptor with very dramatic differences in its properties compared to wild-type receptors. As shown in chapter 4 and in previous studies (Palma *et al.*, 1996; Bertrand *et al.*, 1997; Gill *et al.*, 2011),  $\alpha 7$  nAChRs

containing the L247T mutation convert numerous ligands, including some competitive antagonists and all PAMs, irrespective of their effect on desensitisation, into potent, efficacious and non-desensitising agonists. However, A-867744 had no agonist activity on L247T receptors. In addition, A-867744 inhibited both acetylcholine and TQS responses. Application of A-867744 also induced a reduction on the base current, which can be due to block of spontaneously open receptors (Labarca *et al.*, 1995; Bertrand *et al.*, 1997).

The M253 residue is located near the same intrasubunit cavity as M260 and the mutation M253L on  $\alpha 7$  nAChRs has been reported to significantly reduce or completely abolish the effect of PAMs and allosteric agonists (Young *et al.*, 2008; Gill *et al.*, 2011). Even though TQS had no significant effect on the peak current of acetylcholine-induced responses as reported previously (Gill *et al.*, 2011), A-867744 completely blocked responses to acetylcholine. It appears that A-867744 induces a high affinity block, since the antagonism was irreversible, even after a prolonged wash. However, although TQS does not affect peak acetylcholine responses, it appears to be able to rescue the acetylcholine response from A-867744 block.

In summary, evidence is presented from four different mutations on the  $\alpha 7$  nAChRs to illustrate the different properties displayed by A-867744 compared to other PAMs. In addition, it is demonstrated that A-867744 antagonises the effects of TQS on M260L, W54A and L247T receptors, while TQS blocks the effect of A-867744 on the M253L receptors. Taken in combination, these results suggest that A-867744 elicits its effects on  $\alpha 7$  nAChRs by binding at the same or overlapping site as TQS. However, this has not been demonstrated unambiguously and multiple binding sites may exist.

CHAPTER 6

CHARACTERISATION OF NATIVE  
NICOTINIC ACETYLCHOLINE  
RECEPTORS ON NEURONS  
DERIVED FROM INDUCED  
PLURIPOTENT STEM CELLS

---

## 6.1 INTRODUCTION

Neuronal nAChRs have been implicated in a variety of neurological and psychiatric disorders, including Alzheimer's disease, schizophrenia, depression and attention deficit hyperactivity disorder (Wilens & Decker, 2007; Steinlein & Bertrand, 2008; Haydar & Dunlop, 2010; Parri *et al.*, 2011). As a consequence, there has been a considerable interest, from both academic laboratories and pharmaceutical companies, in developing novel subtype-selective nAChR ligands (Gündisch & Eibl, 2011; Hurst *et al.*, 2013). For this reason, the identification of novel cellular assays, in particular those providing access to native human nAChRs, is an important discovery role.

As discussed above, most nAChRs contain more than one type of subunit (heteromeric nAChRs) whereas some subunits, such as  $\alpha 7$ , are capable of forming homomeric receptors, containing five copies of a single subunit (Millar & Gotti, 2009). In addition to the gene encoding the nAChR  $\alpha 7$  subunit (*CHRNA7*) a partially duplicated variant (*CHRFAM7A*) has been identified in the human genome (Gault *et al.*, 1998; Riley *et al.*, 2002) and both of these genes (*CHRNA7* and *CHRFAM7A*) have been linked to schizophrenia (Freedman *et al.*, 1997; Leonard *et al.*, 2002; Flomen *et al.*, 2006; Sinkus *et al.*, 2009). *CHRFAM7A* encodes a fusion protein (dup $\alpha 7$ ), corresponding to the ion channel domain of  $\alpha 7$  fused to an unrelated gene at its N-terminus. There is evidence, admittedly only in recombinant systems, that dup $\alpha 7$  can co-assemble with the  $\alpha 7$  subunit, and exert a dominant-negative effect, resulting in reduced functional expression of  $\alpha 7$  nAChRs (Araud *et al.*, 2011; Wang *et al.*, 2014).

Induced pluripotent stem cells (iPSCs) can be generated from somatic cells by retroviral expression of reprogramming factors (Takahashi *et al.*, 2007) and, by using a combination of growth factors and culture conditions, iPSCs can be further differentiated into a large variety of cellular types, including CNS-like neurons and glial cells (Dimos *et al.*, 2008; Chambers *et al.*, 2009). Although it is possible to study the pharmacological properties of receptors expressed in naturally occurring neuronal preparations (for example, those obtained from neuronal tissues ablations), iPSC-derived neurons provide a more readily available source and have the potential to increase our understanding of how native human receptors function. In addition, iPSC-derived neurons can be generated from patients carrying a specific genetic background,

corresponding to a particular neuropsychiatric disease. Indeed, recent studies using iPSC-derived neurons generated from patients have been successful in demonstrating phenotypes associated with a variety of diseases, such as Phelan–McDermid, Timothy, and Rett syndromes (Park *et al.*, 2008; Marchetto *et al.*, 2010; Dolmetsch & Geschwind, 2011; Grskovic *et al.*, 2011; Paşca *et al.*, 2011; Shcheglovitov *et al.*, 2013; Wen *et al.*, 2014).

Many of the initial studies on human iPSC-derived neurons focused on the assessment of the expression of specific neuronal markers (Dimos *et al.*, 2008; Chambers *et al.*, 2009). However, subsequent studies have demonstrated the functional expression of a variety of ion channels and neurotransmitter receptors (Haythornthwaite *et al.*, 2012). The human iPSC-derived neurons used in this study have been characterised previously, both in terms of their general gene expression profile and the functional expression of various ion channels (Dage *et al.*, 2014). In addition, other studies have examined the electrophysiology profile of these cells (Haythornthwaite *et al.*, 2012). The microarray data reported previously point to a gene expression profile that closely resembles that observed in neonatal prefrontal cortex tissue. In particular, genes which are known to be associated with neurite outgrowth, synaptic development or neuronal function were clearly expressed and upregulated in the iPSC-derived neurons (Dage *et al.*, 2014). The nAChR gene expression profile has been recently characterised (Chatzidaki *et al.*, 2015). Quantitative PCR was performed on cDNA that was prepared from iPSC-derived neurons. Using gene-specific primers, the abundance of mRNA for individual nAChR subunits was determined (Figure 6.1<sup>a</sup>). The muscle-type nAChR subunits and neuronal nAChR subunit transcripts  $\alpha 2$ ,  $\alpha 9$ ,  $\alpha 10$  and  $\beta 3$  were either not present or detected at only low levels. All other human nAChR subunit transcripts ( $\alpha 3$ – $\alpha 7$ ,  $\beta 1$ ,  $\beta 2$  and  $\beta 4$  subunits, were detected at broadly similar levels. In addition, transcripts of *CHRFAM7A*, encoding dup $\alpha 7$ , a partially duplicated variant of the  $\alpha 7$  subunit gene *CHRNA7* (Gault *et al.*, 1998; Riley *et al.*, 2002) were also identified (Figure 6.1).

In this chapter, the functional properties of nAChRs expressed in the iPSC-derived neurons have been characterised by means of calcium flux assays, performed at either the single cell level or by a higher-throughput 96-well assay. In addition, it has been confirmed that functional nAChRs are expressed in these cells by use of the patch-clamp electrophysiological technique.

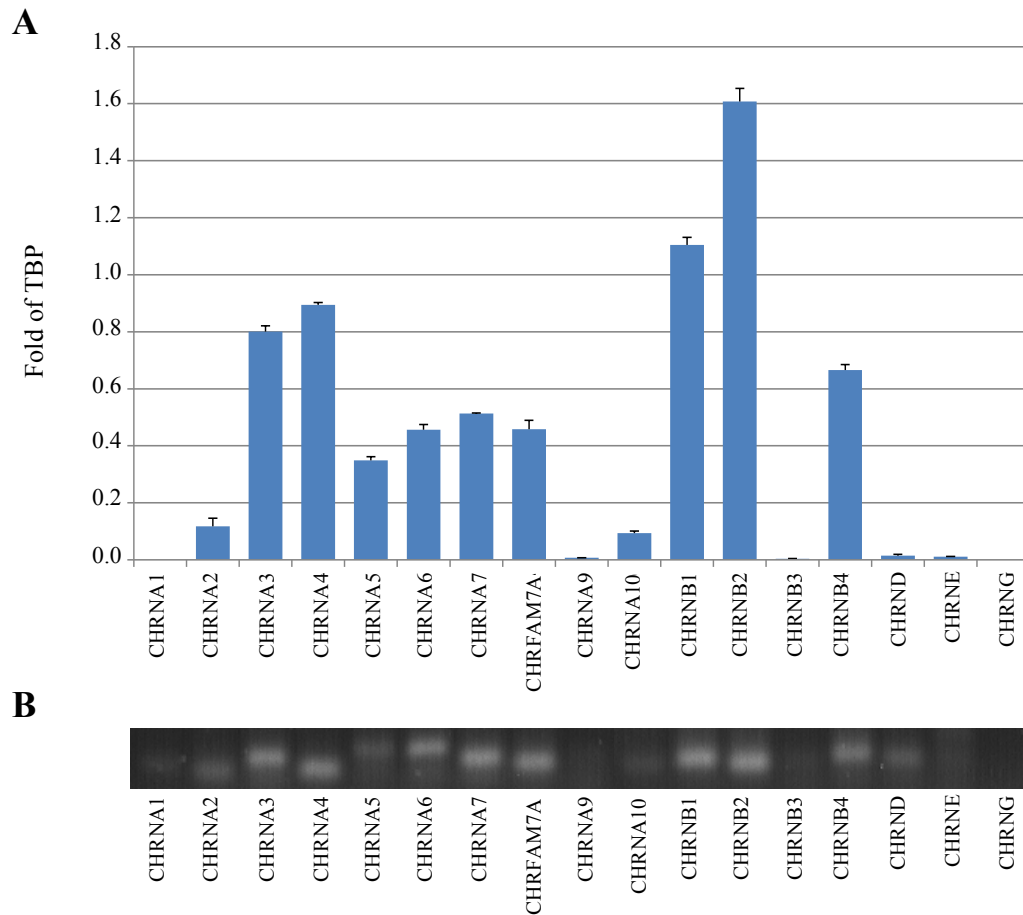


**Figure 6.1: Relative Expression of nAChR subunits in iPSC-derived neurons examined by RT-PCR (from (Chatzidaki *et al.*, 2015)<sup>a</sup>).**

A) Levels of gene expression relative to TBP, using data generated from 10 ng RNA input. The following transcripts were either undetectable or detected only at very low levels at 10 ng input RNA: *CHRNA1* (encoding the  $\alpha 1$  nAChR subunit), *CHRNA2* ( $\alpha 2$ ), *CHRNA9* ( $\alpha 9$ ), *CHRNA10* ( $\alpha 10$ ), *CHRNB3* ( $\beta 3$ ), *CHRNG* ( $\gamma$ ), *CHRND* ( $\delta$ ) and *CHRNE* ( $\epsilon$ ). Note, all of the CT values at lower input levels were near 35 or not detected. In contrast, the following transcripts were detected at relatively high levels: *CHRNA3-CHRNA7* ( $\alpha 3$ - $\alpha 7$ ), *CHRNB1* ( $\beta 1$ ), *CHRNB2* ( $\beta 2$ ), *CHRNB4* ( $\beta 4$ ) and the partially duplicated gene *CHRFA7A*.

B) Agarose gel electrophoresis using PCR products from the 50 ng input.

<sup>a</sup> The results presented in this figure were generated by Li J. and Dage J. and published in (Chatzidaki *et al.*, 2015).

## 6.2 RESULTS

### 6.2.1 Characterisation of nAChRs with a FLIPR-based assay

Based on the evidence obtained from quantitative PCR experiments, indicating that iPSC-derived neurons express a variety of nAChR subunit mRNAs, the expression of functional nAChRs was examined by a fluorescence-based calcium assay (Figure 6.2). Cells were loaded with a calcium-sensitive fluorescent dye (Fluo-4) and examined in a 96-well format fluorescent imaging plate reader (FLIPR). No agonist-induced intracellular calcium responses were detected with the  $\alpha 7$ -selective orthosteric agonist compound B (Figure 6.2A). This is in agreement with previous studies of  $\alpha 7$  nAChRs examined by fluorescence-based methods (Gill *et al.*, 2013) and is likely to be a consequence of the low open probability and fast desensitisation of  $\alpha 7$  nAChRs that is observed in response to activation by orthosteric agonists (Couturier *et al.*, 1990; Gill *et al.*, 2013). In contrast to  $\alpha 7$  nAChRs, which display very rapid desensitisation, most nAChRs desensitise relatively slowly during prolonged agonist applications and are expected to be more easily detected in fluorescence assays using conventional orthosteric agonists. Application of epibatidine, a non-selective agonist of neuronal nAChRs, resulted in a detectable fluorescence response in iPSC-derived neurons (Figure 6.2B). However, although a response to epibatidine was detectable in these cells, it generated a relatively small signal, being only  $1 \pm 0.2\%$  of a control response obtained by depolarisation of cells with KCl (Figure 6.2B;  $n = 3$ ). Responses evoked by compound B ( $1 \mu\text{M}$ ) and epibatidine ( $1 \mu\text{M}$ ) were also studied at different culture times (4 days and 28 days) (Figure 6.2C and D). The data obtained at longer time in culture failed to show a significant increase in response amplitude. For compound B, the response was  $0.2 \pm 0.1\%$  of the positive control after 4 days in culture, while after 28 days in culture the response was  $0.5 \pm 0.5\%$  of the positive control ( $p = 0.65$ ,  $n = 3$ ). For epibatidine, the response was  $1.0 \pm 0.1\%$  of the positive control after 4 days in culture and  $1.4 \pm 0.4\%$  of the positive control after 28 days in culture ( $p = 0.38$ ,  $n = 3$ ). In contrast to the small responses observed when nicotinic agonists were applied alone, a strong increase in intracellular calcium signal was observed when either compound B or epibatidine were co-applied with the  $\alpha 7$ -selective PAM PNU-120596 (Figure 6.2E and F). As reported previously, PNU-120596 dramatically reduces desensitisation kinetics

of  $\alpha 7$  nAChRs (Hurst *et al.*, 2005; Young *et al.*, 2008; Gill *et al.*, 2013). When co-applied with PNU-120596, large responses were observed with both compound B and epibatidine ( $119 \pm 2\%$  and  $110 \pm 5\%$  of control KCl responses, respectively;  $n = 3-5$ ).

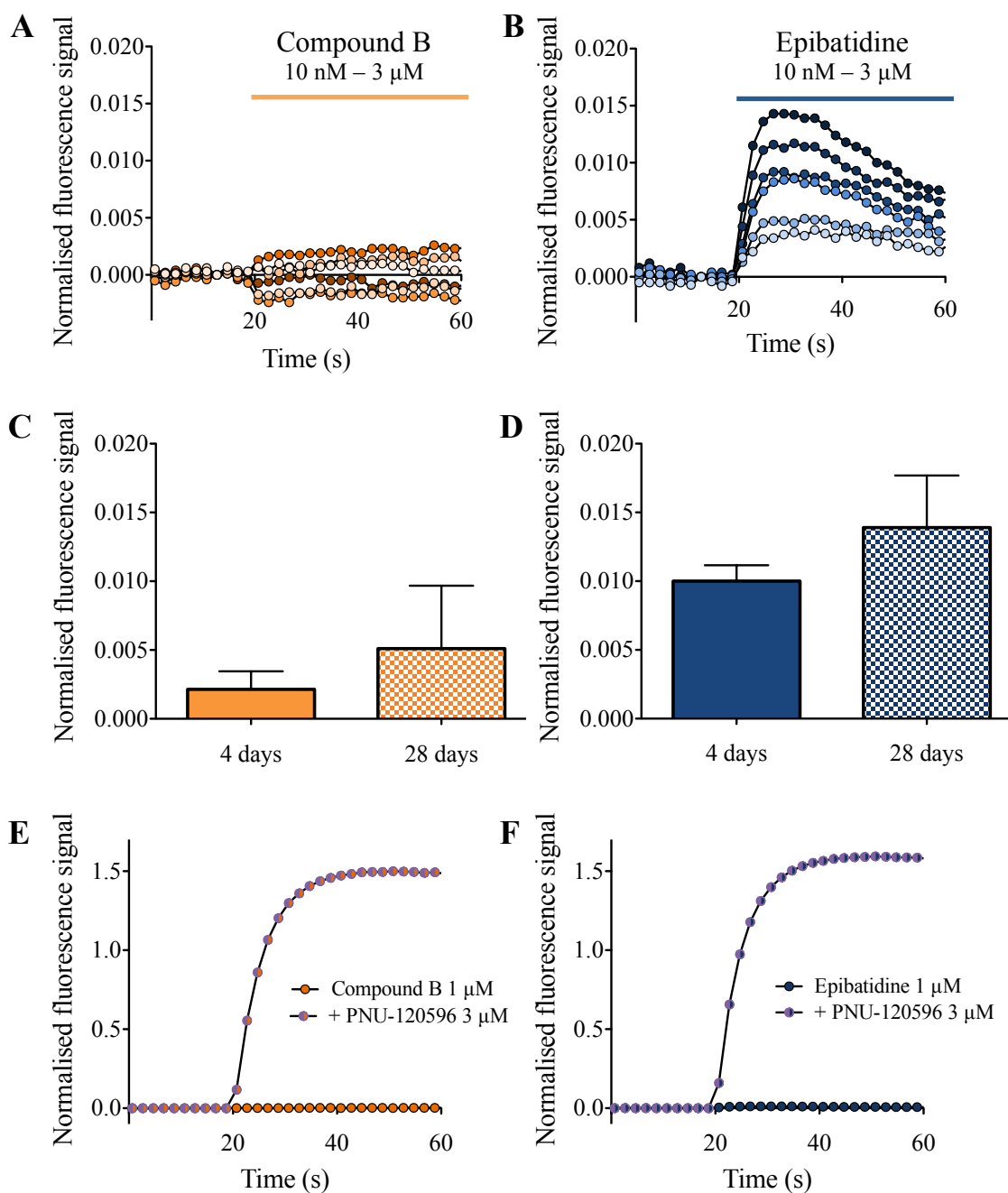


**Figure 6.2: Nicotinic agonist-induced responses in iPSC-derived neurons, examined by FLIPR.**

A) and B) Representative examples of changes in fluorescence detected in iPSC-derived neurons with a range of concentrations of compound B (10 nM – 3 μM; A) and epibatidine (10 nM – 3 μM; B).

C) and D) Average data for agonist induced responses by compound B (1 μM; C) and epibatidine (1 μM; D) in experiments performed at 4 and 28 days in culture. Data represent mean of replicates ± SEM.

E) and F) Co-application of the  $\alpha 7$ -selective PAM PNU-120596 (3 μM; pre-applied for 60 s) with either compound B (1 μM; E) or epibatidine (1 μM; F) resulted in large fluorescence responses. Data are means ± SEMs from 3 experiments. All values are normalised to a control response to application of KCl (30 mM).

### 6.2.2 Characterisation of nAChRs by single-cell calcium imaging

In order to obtain information about the heterogeneity of nicotinic responses in iPSC-derived neurons at the single-cell level, cell monolayers were examined by fluorescence-based intracellular calcium imaging (Figure 6.3). In agreement with FLIPR-based measurements (Figure 6.2), no response was detected to compound B when applied alone, whereas a large change in fluorescence was observed when compound B was co-applied with PNU-120596 (Figure 6.3A and B). In contrast to the absence of response to compound B, a small proportion of cells (4.9%) responded to application of epibatidine (Figure 6.3C). As illustrated in a representative example (Figure 6.3C), the second application of epibatidine did not cause an increase in calcium in the cells that had responded after the first application, presumably because of residual desensitisation to the initial agonist application. Similarly, only a very small number of cells (3.7%) responded to the  $\alpha 4\beta 2$ -selective agonist 5-Iodo-A-85380 (Figure 6.3D), suggesting that there are only a small population of cells expressing functional  $\alpha 4\beta 2$  nAChRs.

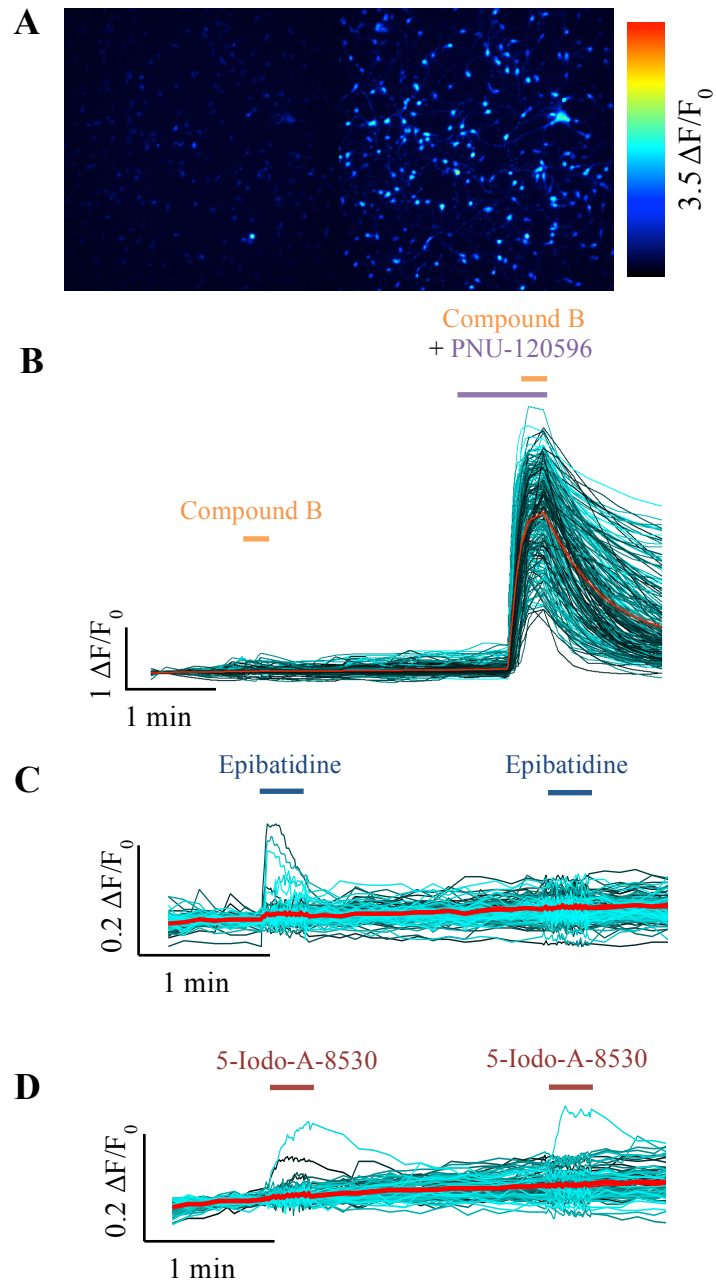


**Figure 6.3: Characterisation of nAChRs in iPSC-derived neurons, examined by single-cell intracellular calcium imaging.**

A) Pseudocolour images of human iPSC-derived neurons corresponding to low initial resting calcium levels (left panel) and higher calcium levels after co-application of compound B (1  $\mu$ M) with PNU-120596 (3  $\mu$ M) (right panel).

B) Single-cell traces for neurons present in the optical field, showing the effects of application of compound B (1  $\mu$ M) followed by co-application of compound B (1  $\mu$ M) with PNU-120596 (3  $\mu$ M).

C) Single-cell traces in response to two consecutive applications of epibatidine (1  $\mu$ M).

D) Single-cell traces in response to two consecutive applications of 5-Iodo-A-85380 (1  $\mu$ M). In B-D, individual single-cell traces are displayed in cyan, whereas a mean response (average of multiple cells) is shown in red.

### 6.2.3 Effect of temperature on agonist-induced nAChR responses

The FLIPR and single-cell imaging experiments described previously were all performed with cells maintained at room temperature during agonist application. However, previous studies with recombinant nAChRs expressed in *Xenopus* oocytes have indicated that the magnitude of nAChR responses can be influenced by temperature (Sitzia *et al.*, 2011; Jindrichova *et al.*, 2012; Williams *et al.*, 2012). When such experiments are performed at physiological temperature (37°C), rather than at room temperature, increased responses have been observed for  $\alpha 4\beta 2$  nAChRs (Jindrichova *et al.*, 2012) and decreased responses for  $\alpha 7$  nAChRs (Sitzia *et al.*, 2011; Jindrichova *et al.*, 2012; Williams *et al.*, 2012). For this reason, FLIPR assays with iPSC-derived neurons were compared at room temperature and at 37°C. No significant differences were observed in responses to either compound B or epibatidine when applied alone. However, responses of reduced magnitude and different kinetics were observed at 37°C when compound B was co-applied with PNU-120596 (Figure 6.4). The maximum potentiated response at 37°C was significantly lower than that at room temperature ( $63.5 \pm 5.4\%$ ,  $P = 0.04$ ,  $n = 4$ ) (Figure 6.4B), in agreement with previous studies (Sitzia *et al.*, 2011; Jindrichova *et al.*, 2012; Williams *et al.*, 2012). Because of the relatively low proportion of cells expressing functional non- $\alpha 7$  receptors and the inability to enhance levels of functional expression in studies conducted at higher temperature, subsequent studies were focused on understanding in greater detail the pharmacological properties of the nAChRs expressed in these neurons that were activated by the  $\alpha 7$ -selective agonist compound B.

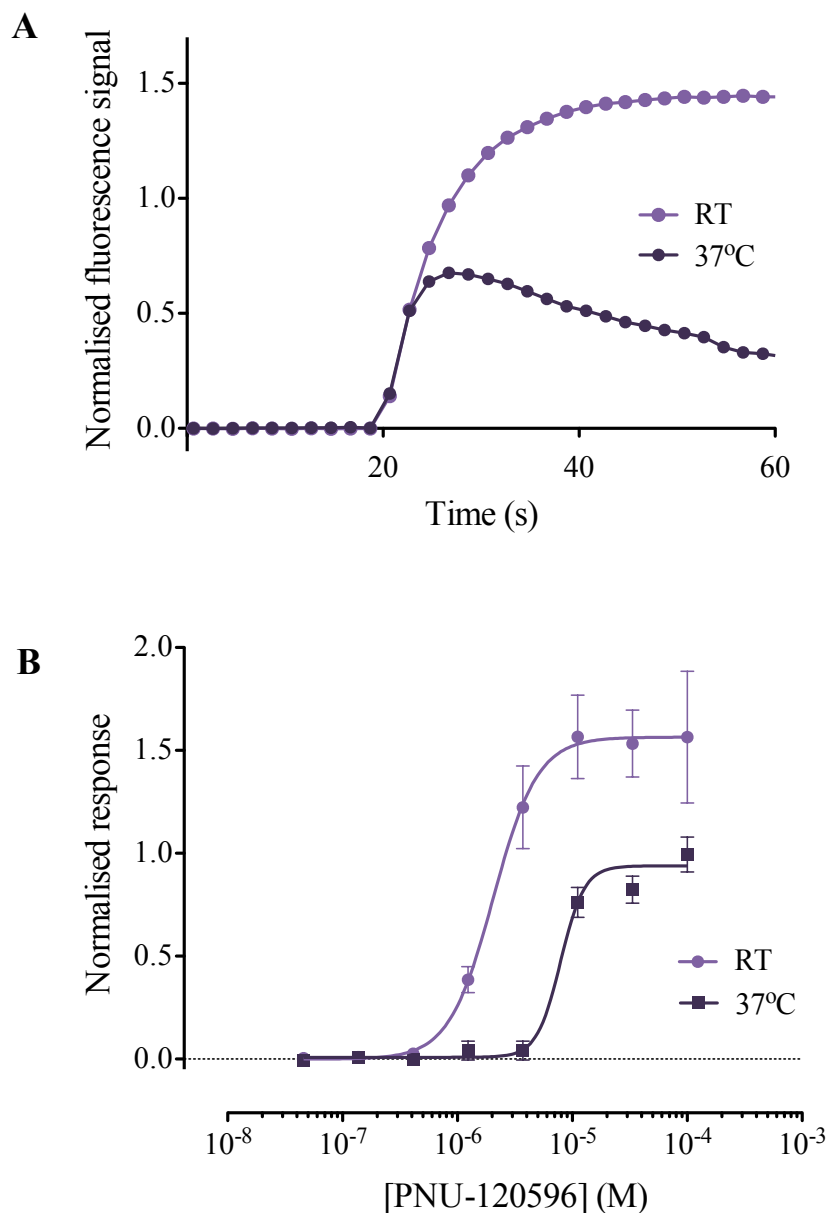


**Figure 6.4: Influence of temperature on potentiation of compound B responses by PNU-120596, examined by FLIPR.**

A) Representative FLIPR traces showing the change in fluorescence observed when compound B (1  $\mu\text{M}$ ) and PNU-120596 (100  $\mu\text{M}$ ) were co-applied to iPSC-derived neurons at room temperature (RT) and at 37°C.

B) Concentration-response relationship of PNU-120596 in the presence of compound B (1  $\mu\text{M}$ ) at room temperature (RT) and at 37°C. Data points are means of 4 independent experiments, each of which generated paired data from the same batch of cells incubated at two temperatures.

#### 6.2.4 Characterisation of $\alpha 7$ nAChRs expressed in iPSC-derived neurons

The data described previously (Figure 6.2–6.4) are consistent with the conclusion that  $\alpha 7$  nAChRs are the major functional nAChR subtype expressed in iPSC-derived neurons. Further studies were performed to examine in more detail the pharmacological properties of nAChRs in these cells. As discussed earlier,  $\alpha 7$  nAChRs are characterised by very fast desensitisation kinetics and, therefore, agonist responses alone are not easily detected using calcium imaging. For this reason, responses to a range of concentrations of three agonists (compound B, epibatidine and choline) were examined in the presence of a fixed concentration of the  $\alpha 7$ -selective PAM PNU-120596 (3  $\mu\text{M}$ ; near maximal). Representative FLIPR traces and concentration-response relationships are illustrated in Figure 6.5 and the mean  $\pm$  SEM of the  $\text{EC}_{50}$ , maximum response and Hill coefficient values for 3–5 independent experiments are summarized in Table 4. Further evidence that these agonist-evoked responses in iPSC-derived neurons are due to activation of  $\alpha 7$  nAChRs was provided by the  $\alpha 7$ -selective antagonist MLA. Responses to compound B in the presence of PNU-120596 were blocked completely and in a concentration-dependent manner by MLA (Figure 6.5C) with an  $\text{IC}_{50}$  value of  $0.7 \pm 0.1 \mu\text{M}$  ( $n = 3$ ). This is very similar to the  $\text{IC}_{50}$  value for MLA ( $0.8 \pm 0.1 \mu\text{M}$ ) that has been determined previously for recombinant  $\alpha 7$  nAChRs in the presence of PNU-120596 (Collins *et al.*, 2011).

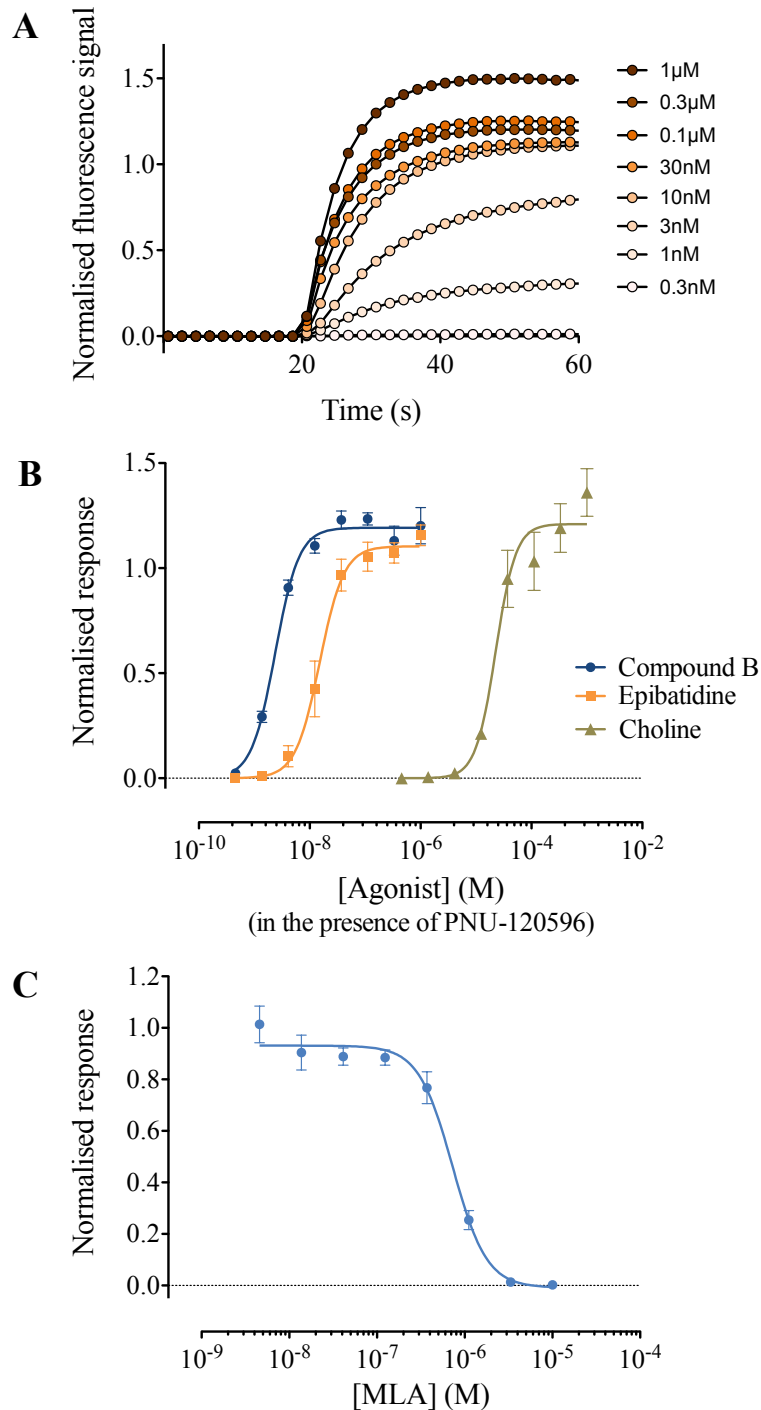


**Figure 6.5: Potentiation and antagonism of nAChR agonist responses in iPSC-derived neurons, examined by FLIPR.**

A) Representative of FLIPR traces produced with a range of compound B concentrations (0.3 nM – 1  $\mu$ M) in the presence of PNU-120596 (3  $\mu$ M).

B) Concentration-response curves for the agonists compound B (circles), epibatidine (squares) and choline (triangles), in the presence of PNU-120596 (3  $\mu$ M). Data represent the maximum change in fluorescence during a 40 s co-application and are means  $\pm$  SEM of 3 – 5 experiments.

C) Responses to compound B (1  $\mu$ M) in the presence of PNU-120596 (3  $\mu$ M) were blocked completely in a concentration-dependent manner by the  $\alpha$ 7-selective antagonist MLA. Data are means  $\pm$  SEM of 5 independent experiments.

Additional FLIPR experiments were performed to compare a series of  $\alpha 7$ -selective PAMs, including those classified as type I PAMs, or as type II PAMs. Concentration-response curves were constructed (Figure 6.6A) using a range of concentrations of compound B in the presence of either a fixed concentration of a type I PAM (NS-1738) or in the presence of one of three different type II PAMs (PNU-120596, A-867744 and TQS). As illustrated in Figure 6.6A, significantly larger increases in fluorescence were observed in the presence of type II PAMs (PNU-120596, A-867744 and TQS) than in the presence of the type I PAM NS-1738 (Table 4). A similar series of FLIPR experiments were performed in which a range of concentrations of the four  $\alpha 7$ -selective PAMs was examined in the presence of a fixed concentration of compound B (Figure 6.6B and 6.6C). As found previously, significantly larger maximal responses were observed with the type II PAMs than with the type I PAM (Figure 6.6 and Table 4).

In contrast to orthosteric agonists, such as acetylcholine, which induce rapid desensitisation of  $\alpha 7$  nAChRs, 4BP-TQS is an example of an  $\alpha 7$ -selective allosteric agonist that has been reported to interact with a transmembrane binding site and cause receptor activation associated with minimal desensitisation (Gill *et al.*, 2011; Gill *et al.*, 2013). In contrast to  $\alpha 7$ -selective orthosteric agonists (such as compound B) when applied alone, clear concentration-dependent agonist responses were observed with 4BP-TQS (Figure 6.7 and Table 4). The  $EC_{50}$  value for activation by 4BP-TQS was  $4.3 \pm 3.4 \mu\text{M}$  and responses to 4BP-TQS were blocked by MLA (Figure 6.7). Furthermore, block by MLA was not surmountable (Figure 6.7B), which is consistent with evidence that 4BP-TQS and MLA bind non-competitively at distinct allosteric and orthosteric binding sites (Gill *et al.*, 2011).

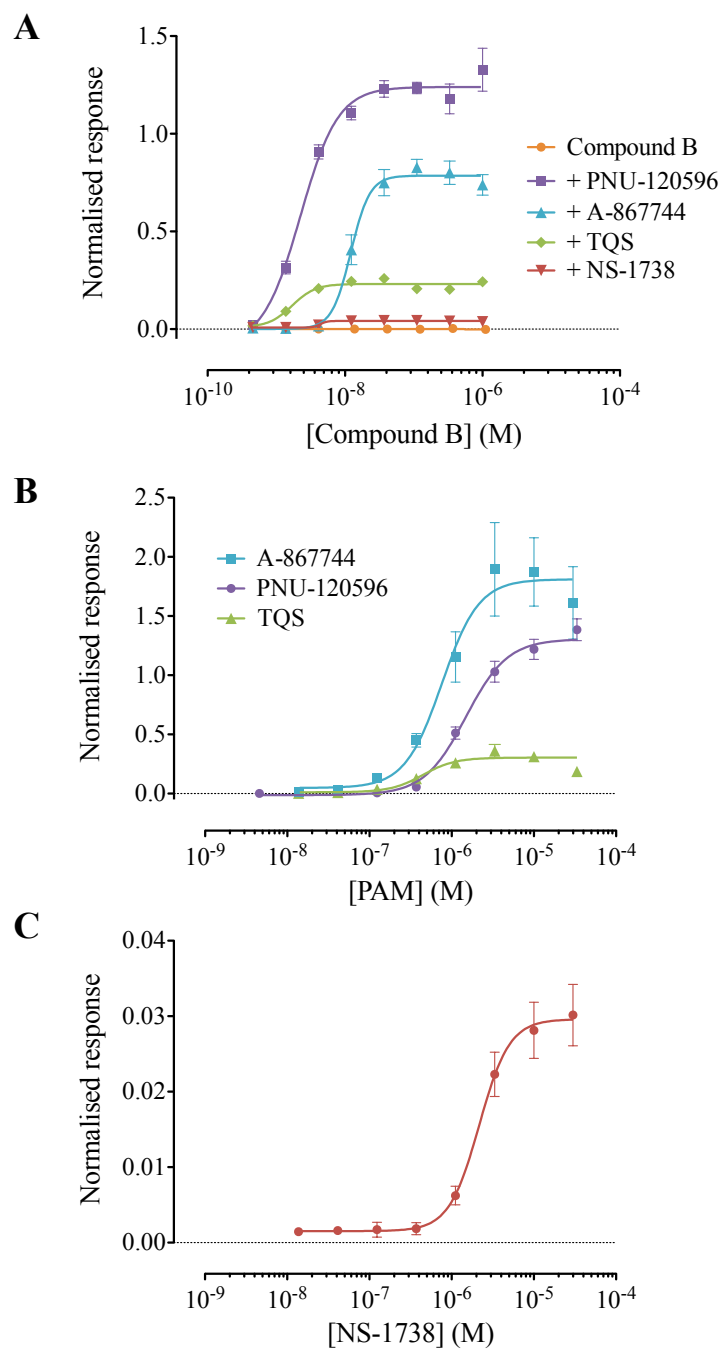


**Figure 6.6: Characterisation of  $\alpha 7$ -selective type I and type II PAMs in iPSC-derived neurons, examined by FLIPR.**

A) Concentration-response curves of compound B in the presence of PNU-120596 (3  $\mu\text{M}$ ; squares), A-867744 (10  $\mu\text{M}$ ; triangles), TQS (10  $\mu\text{M}$ ; diamonds), NS-1738 (30  $\mu\text{M}$ ; inverted triangles) and in the absence of a PAM (circles). Data are means  $\pm$  SEM of 3 – 5 independent experiments.

B) Concentration-response curves of the type II PAMs A-867744 (squares), PNU-120596 (circles) and TQS (triangles), in the presence of maximum concentration of compound B (1  $\mu\text{M}$ ). Data are means  $\pm$  SEM of 3 – 5 independent experiments.

C) Concentration-response relationship of the type I PAM NS-1738 in the presence of compound B (1  $\mu\text{M}$ ). Data are means  $\pm$  SEM of 3 independent experiments.

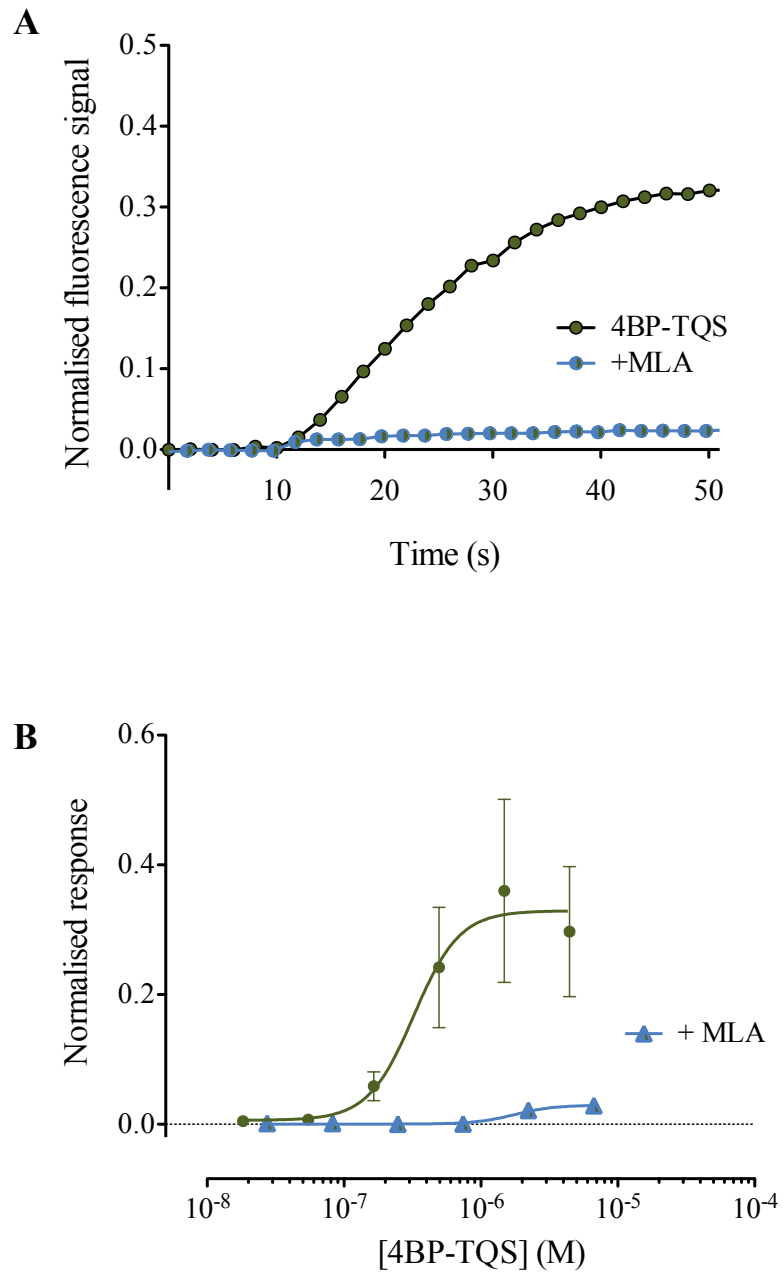


**Figure 6.7: Agonist activity of 4BP-TQS in iPSC-derived neurons, examined by FLIPR.**

A) Representative examples of FLIPR traces with the  $\alpha 7$ -selective allosteric agonist 4BP-TQS (10  $\mu$ M). Responses to 4BP-TQS are inhibited by the  $\alpha 7$ -selective antagonist MLA (1  $\mu$ M).

B) Concentration-response curve for 4BP-TQS (circles) and 4BP-TQS in the presence of the  $\alpha 7$ -selective antagonist MLA (1  $\mu$ M; triangles). Data are means  $\pm$  SEM of 3 independent experiments.

**Table 4: Pharmacological properties of nAChR ligands on iPSC-derived neurons, as examined by FLIPR.**

Data are means  $\pm$  SEM of 3 – 5 independent experiments.

<sup>a</sup> Data for maximal currents ( $I_{\max}$ ) are normalised to the fluorescence response to 30 mM KCl.

Compound	EC <sub>50</sub> ( $\mu$ M)	n <sub>H</sub>	I <sub>max</sub> <sup>a</sup>
Epibatidine	0.38 $\pm$ 0.27 $\mu$ M	1.8 $\pm$ 2.1	0.01 $\pm$ 0.002
Epibatidine (+ 3 $\mu$ M PNU-120596)	14.2 $\pm$ 5.6 nM	2.0 $\pm$ 0.4	1.10 $\pm$ 0.05
Choline (+ 3 $\mu$ M PNU-120596)	26.1 $\pm$ 3.2 $\mu$ M	2.4 $\pm$ 0.5	1.21 $\pm$ 0.05
Compound B (+ 3 $\mu$ M PNU-120596)	2.6 $\pm$ 0.3 nM	2.0 $\pm$ 0.2	1.19 $\pm$ 0.02
Compound B (+ 10 $\mu$ M A-867744)	13.7 $\pm$ 3.1 nM	3.1 $\pm$ 1.3	0.79 $\pm$ 0.02
Compound B (+ 10 $\mu$ M TQS)	1.6 $\pm$ 0.3 nM	2.3 $\pm$ 0.7	0.23 $\pm$ 0.01
Compound B (+ 30 $\mu$ M NS-1738)	10.2 $\pm$ 5.0 nM	2.6 $\pm$ 1.6	0.04 $\pm$ 0.003
PNU-120596 (+ 1 $\mu$ M Compound B)	1.5 $\pm$ 0.2 $\mu$ M	1.7 $\pm$ 0.3	1.31 $\pm$ 0.03
A-867744 (+ 1 $\mu$ M Compound B)	0.8 $\pm$ 0.1 $\mu$ M	1.9 $\pm$ 0.9	1.81 $\pm$ 0.14
TQS (+ 1 $\mu$ M Compound B)	0.6 $\pm$ 0.1 $\mu$ M	2.2 $\pm$ 1.2	0.30 $\pm$ 0.02
NS-1738 (+ 1 $\mu$ M Compound B)	2.3 $\pm$ 0.2 $\mu$ M	2.8 $\pm$ 0.5	0.03 $\pm$ 0.001
4BP-TQS	4.3 $\pm$ 3.4 nM	2.2 $\pm$ 0.5	0.33 $\pm$ 0.06

### 6.2.5 Potentiated nAChR responses detected by patch-clamp recording

The ability of nicotinic agonists to activate nAChRs expressed in iPSC-derived neurons was also examined by patch-clamp recordings. Surprisingly, no agonist-evoked currents could be detected when acetylcholine was applied alone. However, in the experiments where acetylcholine was co-applied with PNU-120596, a large inward current was observed with a value of  $225.2 \pm 85.9$  pA ( $n = 5$ ; Figure 6.8). Figure 6.8A shows a representative patch-clamp trace from iPSC-derived neurons, illustrating the absence of a response to acetylcholine and a slowly desensitising current in response to the co-application of acetylcholine (1 mM) with PNU-120596 (3  $\mu$ M). The pooled data from 5 different recorded cells are presented in Figure 6.8B.

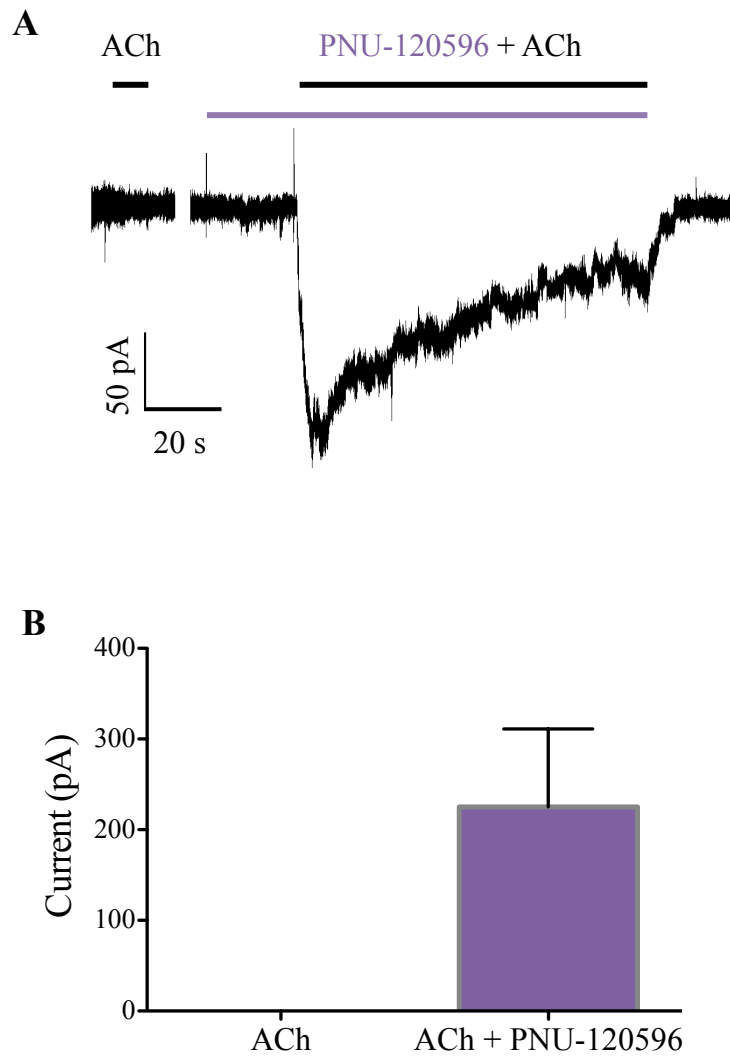


**Figure 6.8: Agonist-induced responses in iPSC-derived neurons, examined by patch-clamp electrophysiology.**

A) Representative recording showing no detectable currents with acetylcholine (1 mM) (Left) and a slow-desensitising current in response to co-application of acetylcholine (1 mM; black bar) and PNU-120596 (3  $\mu$ M; purple bar) (Right). PNU-120596 was pre-applied for 20 s before co-application with acetylcholine.

B) The average response data from n=5 cells was 225.2  $\pm$  85.9 pA, when acetylcholine (1 mM) was co-applied with PNU-120596 (3  $\mu$ M).

### 6.3 DISCUSSION

iPSC-derived neurons provide a readily available supply of human cells with which to study endogenous neuronal nAChRs and also provide several opportunities for both pharmaceutical drug-discovery and academic research. In this chapter, previous studies of iPSC-derived neurons (Gill *et al.*, 2013; Dage *et al.*, 2014) have been extended with a detailed pharmacological characterisation of nAChR subtypes expressed in these cells.

Quantitative PCR experiments indicated that the iPSC-derived neurons examined in this study express mRNA for a variety of nAChR subunits. However, despite this finding, functional characterisation (performed by FLIPR, calcium imaging and patch-clamp recording), suggests that  $\alpha 7$  nAChRs are the predominant subtype of functional nicotinic receptor in these cells.

Initially, FLIPR assays were used to investigate the composition of the nAChR population expressed in these neurons. Application of the  $\alpha 7$ -selective agonist, compound B, did not elicit any detectable fluorescence responses. However, large responses were observed when compound B was co-applied with PNU-120596, an  $\alpha 7$ -selective PAM that reduces agonist-evoked desensitisation of  $\alpha 7$  nAChRs. As has been discussed previously (Roncarati *et al.*, 2008; Gill *et al.*, 2013) difficulties in detecting responses to  $\alpha 7$ -selective agonists such as compound B using fluorescence-based assays are likely to be due to the very fast desensitisation of  $\alpha 7$  nAChRs. In contrast, small, concentration-dependent responses were observed with epibatidine, a non-selective nicotinic agonist, which are likely to be due to the activation of heteromeric non- $\alpha 7$  nAChRs that desensitise more slowly.

Single-cell calcium imaging was used with the aim of examining the proportion of iPSC-derived neurons responding to nicotinic agonists. As was found with the FLIPR-based assay,  $\alpha 7$  responses could only be detected when orthosteric agonists were co-applied with a PAM. While almost all cells in the optical field showed a large increase in intracellular calcium when compound B was co-applied with PNU-120596 (assumed to be cells expressing functional  $\alpha 7$  nAChRs), fluorescence responses were detected in only a very small number of cells when the non-selective agonist epibatidine was applied alone. In addition, the  $\alpha 4\beta 2$ -selective agonist, 5-Iodo-A-85380, gave similar

results to epibatidine, suggesting that only a small number of cells express functional  $\alpha 4\beta 2$  nAChRs.

Previous studies have indicated that changes in temperature can influence the magnitude of agonist responses with neuronal nAChRs (Sitzia *et al.*, 2011; Jindrichova *et al.*, 2012; Williams *et al.*, 2012). Experiments conducted with recombinant nAChRs have indicated an increase in responses with  $\alpha 4\beta 2$  nAChRs and a decrease in responses with  $\alpha 7$  nAChRs when performed at physiological temperature (37°C), rather than at room temperature (Sitzia *et al.*, 2011; Jindrichova *et al.*, 2012; Williams *et al.*, 2012). For this reason, functional responses in iPSC-derived neurons were examined at both room temperature (22°C; the standard experimental conditions used for the experiments reported in this study) and also at physiological temperature (37°C). No significant difference was observed when agonists such as compound B or epibatidine were applied alone but responses to agonists in the presences of  $\alpha 7$ -selective PAMs were lower at 37°C. This is consistent with heteromeric nAChRs such as  $\alpha 4\beta 2$  being a minor component in these cells and  $\alpha 7$  nAChRs being the predominant nAChR subtype in iPSC-derived neurons

Perhaps not unexpectedly, the mRNA expression profile determined in the quantitative PCR study is not in direct agreement with the functional data. Although the expression profile suggests that mRNA for many neuronal nAChR subunits is expressed by these cells, the majority of functional nAChRs detected in these studies have pharmacological properties that are characteristic of the  $\alpha 7$  receptor subtype. It appears therefore that the expression profile of nAChR subunit mRNAs does not reflect the profile of functional nAChRs in these cells. A more detailed pharmacological characterisation, with a variety of agonists, antagonists and PAMs, was consistent with  $\alpha 7$  receptors being the predominant functional nAChR subtype in iPSC-derived neurons.

Patch-clamp recordings were performed with the aim of investigating in more detail the properties of nAChRs expressed in iPSC-derived neurons. Responses to a variety of nicotinic agonists (acetylcholine, epibatidine, choline or compound B) applied alone were not detected. However, when these agonists were co-applied with PNU-120596, large, slow-desensitising inward currents were detected. This is consistent with previous evidence that  $\alpha 7$  nAChRs have a low open probability and desensitise rapidly when

activated by conventional orthosteric agonists, but have greater open probability and reduced desensitisation when orthosteric agonists are co-applied with type II PAMs (daCosta *et al.*, 2011; Williams *et al.*, 2011a; Pałczyńska *et al.*, 2012). The lack of agonist-induced  $\alpha 7$  responses in the patch-clamp experiments can be also attributed to the general low expression of ion channels and receptors observed in the iPSC-derived neurons. Under identical experimental conditions and with similarly fast drug applications, nicotinic currents could be detected in other cell types, such as rodent hippocampal neurons in culture (Gill *et al.*, 2013).

In addition to transcripts for the  $\alpha 7$  subunit (encoded by *CHRNA7*), the gene expression analysis has provided evidence for expression in iPSC-derived neurons of the partially duplicated gene *CHRFAM7A*. Interestingly, both *CHRNA7* and *CHRFAM7A* have been implicated in cognitive disorders such as schizophrenia (Flomen *et al.*, 2006; Sharp *et al.*, 2008; Miller *et al.*, 2009; Sinkus *et al.*, 2009). *CHRFAM7A* encodes a truncated version of the nAChR  $\alpha 7$  subunit (Riley *et al.*, 2002), which does not itself form a functional ion channel but it can reduce functional expression of  $\alpha 7$  nAChRs via a dominant negative effect (Araud *et al.*, 2011; Wang *et al.*, 2014). Evidence for the expression of *CHRFAM7A* transcripts in iPSC-derived neurons indicates that these readily available human neuronal cells may provide a valuable tool for studies aimed at investigating the role of *CHRFAM7A*. This is even more valuable considering that *CHRFAM7A* is only expressed in humans.

In summary, evidence is provided showing that the predominant nAChR expressed as a functional receptor in iPSC-derived neurons has pharmacological properties typical of  $\alpha 7$  nAChRs. These results have important implications for the development of drug-discovery focused screening assays on native receptors that could be used to identify new modulators of nAChRs in the quest to develop novel therapies for psychiatric and neurodegenerative disorders.

## CHAPTER 7

# FINAL CONCLUSIONS AND FUTURE DIRECTIONS

---

The aim of this thesis was to characterise the pharmacological properties of neuronal nAChRs and particularly the action of allosteric ligands on the homomeric  $\alpha 7$  nAChR. The major findings to emerge from this work include the characterisation of a novel series of compounds that act as selective  $\alpha 7$  nAChR PAMs with a range of effects in receptor desensitisation and the identification of selective mutations throughout the  $\alpha 7$  nAChR (Figure 7.1) that can convert PAMs into allosteric agonists (Table 5). Furthermore, it was shown that, even though most PAMs tested had similar effect on nAChRs containing these mutations, A-867744 (a type II PAM) behaved differently (Table 5). Although initial studies were performed using recombinant receptors expressed in *Xenopus* oocytes, a pharmacological characterisation of native human nAChRs was also performed, using iPSC-derived neurons. It was demonstrated that these cells, which represent a valuable tool for therapeutic drug discovery, predominantly express functional  $\alpha 7$  nAChRs.

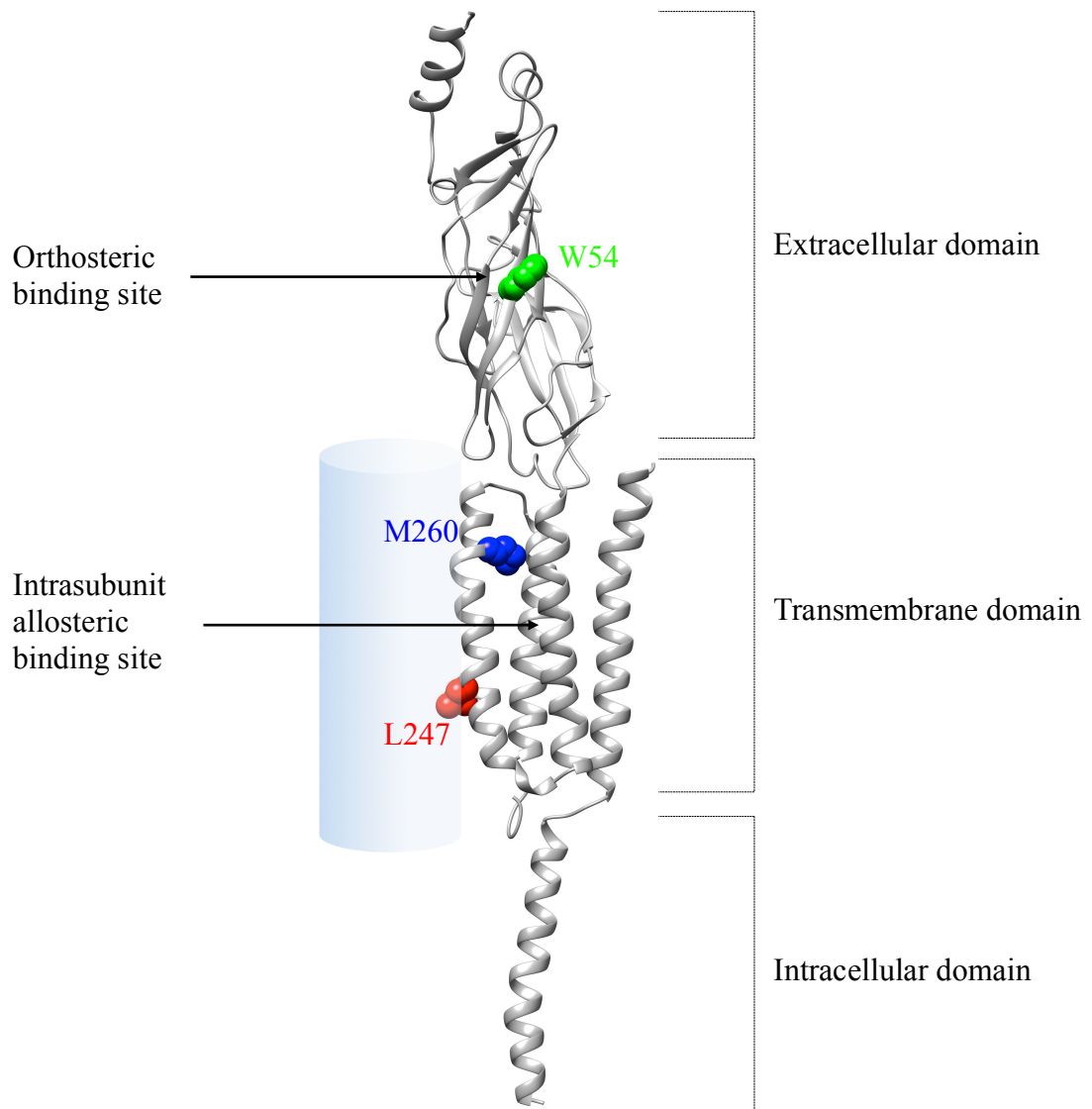


**Figure 7.1: Homology model of the  $\alpha 7$  nAChR subunit highlighting the position of the mutated residues in relation to the orthosteric and allosteric binding sites.**

Side view of the homology model of a single  $\alpha 7$  nAChR subunit (Cheng *et al.* 2006), based on the 4 Å structure of the *Torpedo* nAChR (Unwin, 2005). The backbone of the subunit is shown in grey and the side chains of the mutated amino acids examined in this thesis are shown in green (W54), red (L247) and blue (M260). The approximate locations of the orthosteric binding site and the proposed transmembrane allosteric binding site (Young *et al.*, 2008) are also highlighted. The blue cylinder indicates the approximate location of the channel pore.

**Table 5: Summary of compound effects on wild-type and mutated human  $\alpha 7$  nAChRs.**

PAM: Potentiates effects of acetylcholine without displaying any agonist activity; with type I (I), type II (II) or intermediate profiles (I/II).

Inhibitor: Inhibits the response to acetylcholine.

N.D.: Not determined

Compound	Receptor			
	WT	W54A	L247T	M260L
<b>NS-1738</b>	PAM (I)	Agonist	Agonist	PAM (I/II)
<b>TBS-346</b>	PAM (I)	Agonist	Agonist	PAM (I/II)
<b>TBS-546</b>	PAM (I/II)	N.D.	Agonist	PAM (I/II)
<b>TBS-345</b>	PAM (I/II)	N.D.	Agonist	Agonist
<b>TBS-556</b>	PAM (I/II)	N.D.	Agonist	Agonist
<b>TBS-516</b>	PAM (II)	Agonist	Agonist	Agonist
<b>TQS</b>	PAM (II)	Agonist	Agonist	Agonist
<b>A-867744</b>	PAM (II)	PAM (II)	Inhibitor	PAM (II)

The main goal of chapter 3 was to characterise the pharmacological properties of a series of novel compounds on nAChRs (TBS compounds). The five TBS compounds have close chemical similarity to one another and are shown to act as PAMs on  $\alpha 7$  nAChRs. Traditionally,  $\alpha 7$  PAMs have been characterised as either type I or type II, depending on their effect on receptor desensitisation (Bertrand & Gopalakrishnan, 2007; Grønlien *et al.*, 2007). Type I PAMs increase peak agonist-evoked currents, without altering receptor desensitisation, whereas type II PAMs reduce the fast desensitisation of the  $\alpha 7$  receptors. Here, evidence is provided of  $\alpha 7$  PAMs having a range of effects on receptor desensitisation. For example, TBS-346 displays effects on receptor desensitisation that are typical of type I PAMs and TBS-516 displays effects that are more typical of type II PAMs. In addition, compounds with intermediate properties (TBS-546, TBS-345 and TBS-556) have been identified. With several of the TBS compounds, there is evidence for two components to the rate of desensitisation of the potentiated acetylcholine-evoked response, but the proportion of the fast and slow component varied. The TBS compounds were shown to potentiate  $\alpha 7$  nAChRs with similarly high potency, with  $EC_{50}$  values at the low  $\mu M$  range. However, the maximum peak fold-potentiation of the acetylcholine response varied significantly, from 3.5-fold to 19.7-fold. These compounds were shown to lack PAM activity on other nAChR subtypes (such as  $\alpha 4\beta 2$  and  $\alpha 3\beta 4$ ) and on 5-HT<sub>3A</sub>Rs, indicating that they are relatively selective potentiators of  $\alpha 7$  nAChRs. Competition radioligand binding assays demonstrated that the TBS compounds do not displace [<sup>3</sup>H]- $\alpha$ -bungarotoxin from its orthosteric-binding site on  $\alpha 7$  nAChRs, supporting the conclusion that these compounds are allosteric modulators. In addition, data obtained from studies of an  $\alpha 7/5$ -HT<sub>3A</sub> subunit chimera is consistent with TBS compounds interacting with a site within the transmembrane domain. This conclusion could be further verified by the use of radiolabelled allosteric ligands that bind at the transmembrane domain. Currently, no radiolabelled versions of nAChR PAMs are commercially available. Such compounds would be useful in displacement radioligand binding assays, in order to examine if novel allosteric ligands, such as the TBS series, or allosteric ligands with different pharmacological profiles exert their effects by binding at an overlapping site.

In chapter 4, the series of TBS compounds, together with two ‘classical’  $\alpha 7$  PAMs, were used in order to examine the influence of  $\alpha 7$  nAChR mutations on modulation by allosteric ligands. The main finding in this chapter was that the M260L and L247T

mutations on the transmembrane domain, as well the W54A mutation on the orthosteric binding site, can convert  $\alpha 7$  PAMs into allosteric agonists. Although previous studies have demonstrated that the L247T mutation can convert a type II PAM into an allosteric agonist (Gill *et al.*, 2011), this finding has now been extended by demonstrating that this is a feature conferred by the L247T mutation on type I PAMs, type II PAMs and also on PAMs that can be considered to have intermediate (type I/II) properties. It seems plausible that mutating this amino acid might disrupt the closed state of the channel and therefore allow PAMs to activate the receptor in the absence of an orthosteric agonist. Indeed, increased opening rate and higher frequency of spontaneous openings has been reported in receptors containing the L247T mutation (Labarca *et al.*, 1995; Bertrand *et al.*, 1997) as well as other changes in pharmacological properties (Revah *et al.*, 1991; Bertrand *et al.*, 1992; Palma *et al.*, 1996).

In contrast to the effects of the L247T mutation, the M260L mutation, which is located towards the extracellular side of the TM2 domain, has a more selective effect on PAMs. With this mutation, agonist activation was observed only with PAMs that substantially reduced the levels of desensitisation in wild-type  $\alpha 7$  nAChRs. This effect of the M260L mutation is unlikely to be due to it preventing the binding of type I PAMs because, even though type I PAMs are not converted into agonists on the mutated receptor, they retain their PAM activity in the presence of acetylcholine. In addition, type I PAMs block agonist activation by type II PAMs in receptors containing the M260L mutation. The M260 residue is located near an intrasubunit cavity (Figure 7.1) that has been proposed to be the binding site of certain allosteric ligands (Young *et al.*, 2008). This residue is also situated towards the extracellular end of the TM2 domain in a region that has been referred to as the 'M2-cap' (Bafna *et al.*, 2008). Previous studies have indicated that a stretch of 10 amino acids in this region can influence allosteric modulation of an  $\alpha 7/5$ -HT3A subunit chimera (Bertrand *et al.*, 2008). In addition, studies on the  $\alpha 1$  subunit of the muscle-type nAChR, indicate that mutations in this region have large effects on gating but smaller effects on channel conductance and desensitisation (Bafna *et al.*, 2008). However, mutating the isoleucine on the 22' position to a leucine (which corresponds to M260 on the human  $\alpha 7$  subunit) increased the apparent rate for entry into long-lived desensitised states by  $\sim 10$ -fold (Bafna *et al.*, 2008). It is plausible that this mutation in the corresponding residue of the  $\alpha 7$  subunit could shift the equilibrium in the absence of an orthosteric agonist towards a desensitised state that is converted to

a conducting state in the presence of the type II PAMs. Single-channel recordings with  $\alpha 7$  nAChRs containing the M260L mutation can be performed in the future in order to investigate this theory. In addition, this work could be expanded further by examining additional mutations on the TM2-3 loop and the transmembrane domain of the  $\alpha 7$  nAChRs. Examining the influence of other mutations in the ‘M2-cap’ on PAMs with differing effects on desensitisation may increase our understanding of the  $\alpha 7$  nAChRs desensitisation mechanisms. Furthermore, previous studies (Young *et al.*, 2008) have identified a number of residues in an intrasubunit cavity of the rat  $\alpha 7$  nAChRs that are important in the modulation of the receptor by PNU-120596. Even though mutating these residues (S222M, A225D, M253L, F455A and C459Y) has a significant effect on the effects of PNU-120596, this may not be the case for the series of TBS compounds.

Interestingly, a mutation located at a distant site to the proposed binding site of these PAMs, W54A, has been reported to influence receptor modulation by allosteric ligands (Papke *et al.*, 2014). This mutation is situated on a highly conserved residue at the complementary component of the orthosteric binding site (Corringer *et al.*, 1995). It has been reported recently that the type II PAMs TQS and PNU-120596 are converted into agonists on  $\alpha 7$  nAChRs containing the W54A mutation. In addition, agonism by allosteric ligands was reported to be insensitive to MLA block, suggesting a ‘de-coupling’ of the orthosteric and allosteric binding sites (Papke *et al.*, 2014). Here, it has been shown that, similar to L247T, both type I and type II PAMs are converted into non-desensitising agonists. However, type I PAMs activated the receptor to a lesser degree than type II PAMs. In addition, even though TQS was largely insensitive to MLA block (in agreement with previous studies (Papke *et al.*, 2014)), the other PAMs tested were not. This would suggest a compound-selective effect of MLA block, rather than a generalised de-coupling of the orthosteric and allosteric binding sites in  $\alpha 7$  nAChRs containing the W54A mutation.

Chapter 5 provides evidence from four different mutations on the  $\alpha 7$  nAChR to illustrate the atypical properties displayed by the PAM A-867744 compared to other PAMs. The effects of A-867744 on  $\alpha 7$  nAChRs containing the M260L mutation were somewhat unexpected. As discussed above, the M260L mutation converts PAMs that substantially reduce the levels of desensitisation on  $\alpha 7$  nAChRs into agonists. However, even though A-867744 displays a dramatic reduction in desensitisation kinetics when

co-applied with acetylcholine in wild-type  $\alpha 7$  nAChRs, it displayed no agonist activity on M260L receptors. In addition, A-867744 blocked TQS agonist responses on M260L. However, when A-867744 was co-applied with acetylcholine it potentiated responses with a type II profile and fold-potentiation that was not significantly different to wild-type nAChRs. In addition, A-867744 failed to elicit any agonist responses on  $\alpha 7$  nAChRs containing the W54A mutation. Similar to M260L, A-867744 potentiated agonist responses on W54A receptors with no significant difference to wild-type and it also blocked TQS agonist responses. More surprisingly, A-867744 also failed to activate L247T receptors. As discussed above, mutating this residue on the TM2 domain, which has been reported to have an important role in receptor gating, produces a receptor with very dramatic differences in its properties compared to wild-type receptors. As shown in chapter 4 and in previous studies (Palma *et al.*, 1996; Bertrand *et al.*, 1997; Gill *et al.*, 2011),  $\alpha 7$  nAChRs containing the L247T mutation convert numerous ligands, including some competitive antagonists and all PAMs, irrespective of their effect on desensitisation, into potent, efficacious and non-desensitising agonists. However, A-867744 had no agonist activity on L247T receptors. In addition, A-867744 inhibited both acetylcholine and TQS responses. Another difference in the profile of A-867744 comes from examining the M253L mutation. The M253 residue is located near the same intrasubunit cavity as M260 and the mutation M253L on  $\alpha 7$  nAChRs has been reported to significantly reduce or completely abolish the effect of PAMs and allosteric agonists (Young *et al.*, 2008; Gill *et al.*, 2011). Even though TQS had no significant effect on the peak current of acetylcholine-induced responses, as reported previously (Gill *et al.*, 2011), A-867744 completely blocked responses to acetylcholine. It appears that A-867744 induces a high affinity block, since the antagonism was irreversible, even after a prolonged wash. However, although TQS does not affect peak acetylcholine responses, it appears to be able to rescue the response from A-867744 block. In summary, the mutations shown in chapter 4 to convert other PAMs into allosteric agonists did not have this effect on the type II PAM A-867744. It is also demonstrated that A-867744 antagonises the effects of TQS on M260L, W54A and L247T receptors, while TQS blocks the effect of A-867744 on the M253L receptors. Taken in combination, these results suggest that A-867744 elicits its effects on  $\alpha 7$  nAChRs by binding at the same or overlapping site as TQS. However, this has not been demonstrated unambiguously. A useful extension to this study would therefore be the construction of TQS agonist concentration-response curves on the M260L and W54A

$\alpha 7$  nAChRs in the presence and absence of A-867744, in order to examine if the block observed is surmountable. In addition, computer-docking experiments with A-867744 and other PAMs on a homology model of the  $\alpha 7$  nAChR may provide some indication on the differences in binding sites and interactions of the PAMs with the amino acid side chains, which could explain the unusual effects observed with A-867744.

The chapters above describe pharmacological properties of recombinant nAChRs expressed in *Xenopus* oocytes and transfected mammalian cells. In chapter 6, the pharmacological properties of nAChRs were examined in a native environment, using human iPSC-derived neurons. iPSC-derived neurons provide a readily available supply of human cells with which to study endogenous neuronal nAChRs and also provide several opportunities for both pharmaceutical drug-discovery and academic research. Here, previous studies of iPSC-derived neurons (Gill *et al.*, 2013; Dage *et al.*, 2014) have been extended with a detailed pharmacological characterisation of nAChR subtypes expressed in these cells. Quantitative PCR experiments have indicated that the iPSC-derived neurons express mRNA for a variety of nAChR subunits. However, despite this finding, functional characterisation (performed by FLIPR, calcium imaging and patch-clamp recording), suggests that  $\alpha 7$  nAChRs are the predominant subtype of functional nicotinic receptor in these cells. Initially, FLIPR assays and single-cell calcium imaging assays were used to investigate the composition of the nAChR population expressed in these neurons. In summary, evidence has been provided showing that the predominant nAChR subtype expressed in these cells is  $\alpha 7$ -containing nAChRs. Perhaps not unexpectedly, the mRNA expression profile determined in the quantitative PCR study is not in direct agreement with the functional data. Although the expression profile suggests that mRNA for many neuronal nAChR subtypes is expressed by these cells, the majority of functional nAChRs detected in these studies have pharmacological properties that are characteristic of the  $\alpha 7$  receptor subtype. A more detailed pharmacological characterisation, with a variety of agonists, antagonists and PAMs, was consistent with  $\alpha 7$  receptors being the predominant functional nAChR subtype in iPSC-derived neurons.

## CHAPTER 8

# REFERENCES

---

- Aiyar VN, Benn MH, Hanna T, Jacyno J, Roth SH & Wilkens JL. (1979). The principal toxin of *Delphinium brownii* Rydb., and its mode of action. *Experientia* **35**, 1367-1368.
- Akabas MH, Kaufmann C, Archdeacon P & Karlin A. (1994). Identification of acetylcholine receptor channel-lining residues in the entire M2 segment of the  $\alpha$  subunit. *Neuron* **13**, 919-927.
- Akabas MH, Stauffer DA, Xu M & Karlin A. (1992). Acetylcholine receptor channel structure probed in cysteine-substitution mutants. *Science* **258**, 307-310.
- Akk G. (2001). Aromatics at the murine nicotinic receptor agonist binding site: mutational analysis of the  $\alpha$ Y93 and  $\alpha$ W149 residues. *J Physiol* **535**, 729-740.
- Alkondon M, Pereira EF, Wonnacott S & Albuquerque EX. (1992). Blockade of nicotinic currents in hippocampal neurons defines methyllycaconitine as a potent and specific receptor antagonist. *Mol Pharmacol* **41**, 802-808.
- Althoff T, Hibbs RE, Banerjee S & Gouaux E. (2014). X-ray structures of GluCl in apo states reveal a gating mechanism of Cys-loop receptors. *Nature* **512**, 333-337.
- Amin J & Weiss DS. (1993). GABAA receptor needs two homologous domains of the  $\beta$ -subunit for activation by GABA but not by pentobarbital. *Nature* **366**, 565-569.
- Anderson DJ, Bunnelle W, Surber B, Du J, Surowy C, Tribollet E, Marguerat A, Bertrand D & Gopalakrishnan M. (2008). [3H]A-585539 [(1S,4S)-2,2-dimethyl-5-(6-phenylpyridazin-3-yl)-5-aza-2-azoniabicyclo[2.2.1]heptane], a novel high-affinity  $\alpha$ 7 neuronal nicotinic receptor agonist: radioligand binding characterization to rat and human brain. *J Pharm Exp Ther* **324**, 179-187.
- Araud T, Graw S, Berger R, Lee M, Neveu E, Bertrand D & Leonard S. (2011). The chimeric gene *CHRFAM7A*, a partial duplication of the *CHRNA7* gene, is a dominant negative regulator of  $\alpha$ 7\*nAChR function. *Biochem Pharmacol* **82**, 904-914.
- Arias HR. (1998). Binding sites for exogenous and endogenous non-competitive inhibitors of the nicotinic acetylcholine receptor. *Biochim Biophys Acta* **1376**, 173-220.
- Arias HR. (2000). Localization of agonist and competitive antagonist binding sites on nicotinic acetylcholine receptors. *Neurochem Int* **36**, 595-645.

- Arias HR. (2010). Positive and negative modulation of nicotinic receptors. *Adv Protein Chem Struct Biol* **80**, 153-203.
- Ashoor A, Nordman JC, Veltri D, Yang K-HS, Kury LA, Shuba Y, Mahgoub M, Howarth FC, Sadek B, Shehu A, Kabbani N & Oz M. (2013a). Menthol binding and inhibition of  $\alpha 7$ -nicotinic acetylcholine receptors. *PLOS ONE* **8**, e67674.
- Ashoor A, Nordman JC, Veltri D, Yang K-HS, Shuba Y, Kury LA, Sadek B, Howarth FC, Shehu A, Kabbani N & Oz M. (2013b). Menthol inhibits 5-HT<sub>3</sub> receptor-mediated currents. *J Pharm Exp Ther* **247**, 398-409.
- Auerbach A. (2007). How to turn the reaction coordinate into time. *J Gen Physiol* **130**, 543-546.
- Auerbach A & Akk G. (1998). Desensitization of mouse nicotinic acetylcholine receptor channels. A two-gate mechanism. *J Gen Physiol* **112**, 181-197.
- Badio B & Daly JW. (1994). Epibatidine, a potent analgetic and nicotinic agonist. *Mol Pharmacol* **45**, 563-569.
- Bafna PA, Purohit PG & Auerbach A. (2008). Gating at the mouth of the acetylcholine receptor channel: energetic consequences of mutations in the  $\alpha$ M2-cap. *PLOS ONE* **3**, e2515.
- Banerjee S, Punzi JS, Kreilick K & Abood LG. (1990). [<sup>3</sup>H]mecamylamine binding to rat brain membranes. Studies with mecamylamine and nicotine analogues. *Biochem Pharmacol* **40**, 2105-2110.
- Beckstein O & Sansom MS. (2006). A hydrophobic gate in an ion channel: the closed state of the nicotinic acetylcholine receptor. *Phys Biol* **3**, 147-159.
- Beene DL, Brandt GS, Zhong W, Zacharias NM, Lester HA & Dougherty DA. (2002). Cation- $\pi$  interactions in ligand recognition by serotonergic (5-HT<sub>3A</sub>) and nicotinic acetylcholine receptors: the anomalous binding properties of nicotine. *Biochemistry* **41**, 10262-10269.
- Bernard C. (1850). Action de curare et de la nicotine sur le système nerveux et sur le système musculaires. *C R Soc Biol* **2**, 195.
- Bertrand D, Bertrand S, Casser S, Gubbins E, Li J & Gopalakrishnan M. (2008). Positive allosteric modulation of the  $\alpha 7$  nicotinic acetylcholine receptor: ligand interactions with distinct binding sites and evidence for a prominent role of the M2-M3 segment. *Mol Pharmacol* **74**, 1407-1416.

- Bertrand D, Devillers-Thiery A, Revah F, Galzi JL, Hussy N, Mulle C, Bertrand S, Ballivet M & Changeux JP. (1992). Unconventional pharmacology of a neuronal nicotinic receptor mutated in the channel domain. *Proc Natl Acad Sci USA* **89**, 1261-1265.
- Bertrand D, Galzi JL, Devillers-Thiery A, Bertrand S & Changeux JP. (1993). Mutations at two distinct sites within the channel domain M2 alter calcium permeability of neuronal  $\alpha 7$  nicotinic receptor. *Proc Natl Acad Sci USA* **90**, 6971-6975.
- Bertrand D & Gopalakrishnan M. (2007). Allosteric modulation of nicotinic acetylcholine receptors. *Biochem Pharmacol* **74**, 1155-1163.
- Bertrand S, Devillers-Thiéry A, Palma E, Buisson B, Edelstein SJ, Corringer P-J, Changeux J-P & Bertrand D. (1997). Paradoxical allosteric effects of competitive inhibitors on neuronal  $\alpha 7$  nicotinic receptor mutants. *NeuroReport* **8**, 3591-3596.
- Blount P & Merlie JP. (1989). Molecular basis of the two nonequivalent ligand binding sites of the muscle nicotinic acetylcholine receptor. *Neuron* **3**, 349-357.
- Bocquet N, Nury H, Baaden M, Le Poupon C, Changeux JP, Delarue M & Corringer PJ. (2009). X-ray structure of a pentameric ligand-gated ion channel in an apparently open conformation. *Nature* **457**, 111-114.
- Bocquet N, Prado de Carvalho L, Cartaud J, Neyton J, Le Poupon C, Taly A, Grutter T, Changeux JP & Corringer PJ. (2007). A prokaryotic proton-gated ion channel from the nicotinic acetylcholine receptor family. *Nature* **445**, 116-119.
- Bolam JP, Hanley JJ, Booth PA & Bevan MD. (2000). Synaptic organisation of the basal ganglia. *J Anat* **196 ( Pt 4)**, 527-542.
- Borovikova LV, Ivanova S, Zhang M, Yang H, Botchkina GI, Watkins LR, Wang H, Abumrad N, Eaton JW & Tracey KJ. (2000). Vagus nerve stimulation attenuates the systemic inflammatory response to endotoxin. *Nature* **405**, 458-462.
- Bourne Y, Talley TT, Hansen SB, Taylor P & Marchot P. (2005). Crystal structure of a Cbtx-AChBP complex reveals essential interactions between snake  $\alpha$ -neurotoxins and nicotinic receptors. *EMBO J* **24**, 1512-1522.
- Brannigan G, Hénin J, Law R, Eckenhoff R & Klein ML. (2008). Embedded cholesterol in the nicotinic acetylcholine receptor. *Proc Natl Acad Sci USA* **105**, 14418-14423.

- Brejč K, van Dijk WJ, Klaassen RV, Schuurmans M, van der Oost J, Smit AB & Sixma TK. (2001). Crystal structure of an ACh-binding protein reveals the ligand-binding domain of nicotinic receptors. *Nature* **411**, 269-276.
- Brisson A & Unwin PNT. (1985). Quaternary structure of the acetylcholine receptor. *Nature* **315**, 474-477.
- Broad LM, Zwart R, Pearson KH, Lee M, Wallace L, McPhie GI, Emkey R, Hollinshead SP, Dell CP, Baker SR & Sher E. (2006). Identification and pharmacological profile of a new class of selective nicotinic acetylcholine receptor potentiators. *J Pharm Exp Ther* **318**, 1108-1117.
- Broadbent S, Groot-Kormelink PJ, Krashia PA, Harkness PC, Millar NS, Beato M & Sivilotti LG. (2006). Incorporation of the  $\beta 3$  subunit has a dominant-negative effect on the function of recombinant central-type neuronal nicotinic receptors. *Mol Pharmacol* **70**, 1350-1356.
- Buisson B & Bertrand D. (2001). Chronic exposure to nicotine upregulates the human  $\alpha 4\beta 2$  nicotinic acetylcholine receptor function. *J Neurosci* **21**, 1819-1829.
- Burzomato V, Beato M, Groot-Kormelink PJ, Colquhoun D & Sivilotti LG. (2004). Single-channel behavior of heteromeric  $\alpha 1\beta$  glycine receptors: an attempt to detect a conformational change before the channel opens. *J Neurosci* **24**, 10924-10940.
- Bürgi JJ, Awale M, Boss SD, Schaer T, Marger F, Viveros-Paredes JM, Bertrand S, Gertsch J, Bertrand D & Reymond JL. (2014). Discovery of potent positive allosteric modulators of the  $\alpha 3\beta 2$  nicotinic acetylcholine receptor by a chemical space walk in ChEMBL. *ACS Chem Neurosci* **5**, 346-359.
- Calimet N, Simoes M, Changeux JP, Karplus M, Taly A & Cecchini M. (2013). A gating mechanism of pentameric ligand-gated ion channels. *Proc Natl Acad Sci USA* **110**, E3987-3996.
- Callahan PM, Hutchings EJ, Kille NJ, Chapman JM & Terry AV. (2013). Positive allosteric modulator of  $\alpha 7$  nicotinic-acetylcholine receptors, PNU-120596 augments the effects of donepezil on learning and memory in aged rodents and non-human primates. *Neuropharmacol* **67**, 201-212.
- Celie PH, Klaassen RV, van Rossum-Fikkert SE, van Elk R, van Nierop P, Smit AB & Sixma TK. (2005). Crystal structure of acetylcholine-binding protein from *Bulinus truncatus* reveals the conserved structural scaffold and sites of variation in nicotinic acetylcholine receptors. *J Biol Chem* **280**, 26457-26466.

- Celie PH, van Rossum-Fikkert SE, van Dijk WJ, Brejc K, Smit AB & Sixma TK. (2004). Nicotine and carbamylcholine binding to nicotinic acetylcholine receptors as studied in AChBP crystal structures. *Neuron* **41**, 907-914.
- Cesa LC, Higgins CA, Sando SR, Kuo DW & Levandoski MM. (2012). Specificity determinants of allosteric modulation in the neuronal nicotinic acetylcholine receptor: a fine line between inhibition and potentiation. *Mol Pharmacol* **81**, 239-249.
- Chambers SM, Fasano CA, Papapetrou EP, Tomishima M, Sadelain M & Studer L. (2009). Highly efficient neural conversion of human ES and iPS cells by dual inhibition of SMAD signaling. *Nat Biotechnol* **27**, 275-280.
- Chang CC & Lee CY. (1963). Isolation of neurotoxins from the venom of *Bungarus multicinctus* and their modes of neuromuscular blocking action. *Arch Int Pharmacodyn Ther* **144**, 241-257.
- Changeux JP, Kasai M & Lee CY. (1970). Use of a snake venom toxin to characterize the cholinergic receptor protein. *Proc Natl Acad Sci USA* **67**, 1241-1247.
- Changeux JP & Taly A. (2008). Nicotinic receptors, allosteric proteins and medicine. *Trends Mol Med* **14**, 93-102.
- Chatzidaki A, Fouillet A, Li J, Dage J, Millar NS, Sher E & Ursu D. (2015). Pharmacological characterisation of nicotinic acetylcholine receptors expressed in human iPSC-derived neurons. *PLOS ONE* **10**, e0125116.
- Chavez-Noriega LE, Crona JH, Washburn MS, Urrutia A, Elliott KJ & Johnson EC. (1997). Pharmacological characterization of recombinant human neuronal nicotinic acetylcholine receptors  $\alpha 2\beta 2$ ,  $\alpha 2\beta 4$ ,  $\alpha 3\beta 2$ ,  $\alpha 3\beta 4$ ,  $\alpha 4\beta 2$ ,  $\alpha 4\beta 4$  and  $\alpha 7$  expressed in *Xenopus* oocytes. *J Pharm Exp Ther* **280**, 346-356.
- Cheng X, Lu B, Grant B, Law RJ, McCammon JA. (2006). Channel opening motion of  $\alpha 7$  nicotinic acetylcholine receptor as suggested by normal mode analysis. *J Mol Biol* **355**, 310-324
- Chiara DC, Dangott LJ, Eckenhoff RG & Cohen JB. (2003). Identification of nicotinic acetylcholine receptor amino acids photolabeled by the volatile anesthetic halothane. *Biochemistry* **42**, 13457-13467.
- Chimienti F, Hogg RC, Plantard L, Lehmann C, Brakch N, Fischer J, Huber M, Bertrand D & Hohl D. (2003). Identification of SLURP-1 as an epidermal neuromodulator explains the clinical phenotype of Mal de Meleda. *Hum Mol Genet* **12**, 3017-3024.

- Clarke PB & Reuben M. (1996). Release of [3H]-noradrenaline from rat hippocampal synaptosomes by nicotine: mediation by different nicotinic receptor subtypes from striatal [3H]-dopamine release. *Br J Pharmacol* **117**, 595-606.
- Clarke PB, Schwartz RD, Paul SM, Pert CB & Pert A. (1985). Nicotinic binding in rat brain: autoradiographic comparison of [3H]acetylcholine, [3H]nicotine, and [125I]- $\alpha$ -bungarotoxin. *J Neurosci* **5**, 1307-1315.
- Cohen BN, Labarca C, Czyzyk L, Davidson N & Lester HA. (1992). Tris<sup>+</sup>/Na<sup>+</sup> permeability ratios of nicotinic acetylcholine receptors are reduced by mutations near the intracellular end of the M2 region. *J Gen Physiol* **99**, 545-572.
- Collins T & Millar NS. (2010). Nicotinic acetylcholine receptor transmembrane mutations convert ivermectin from a positive to a negative allosteric modulator. *Mol Pharmacol* **78**, 198-204.
- Collins T, Young GT & Millar NS. (2011). Competitive binding at a nicotinic receptor transmembrane site of two  $\alpha$ 7-selective positive allosteric modulators with differing effects on agonist-evoked desensitization. *Neuropharmacol* **61**, 1306-1313.
- Colquhoun D. (1998). Binding, gating, affinity and efficacy: the interpretation of structure-activity relationships for agonists and of the effects of mutating receptors. *Br J Pharmacol* **125**, 924-947.
- Colquhoun D & Ogden DC. (1988). Activation of ion channels in the frog end-plate by high concentrations of acetylcholine. *J Physiol* **395**, 131-159.
- Colquhoun LM & Patrick JW. (1997). Pharmacology of neuronal nicotinic acetylcholine receptor subtypes. *Advances Pharmacol* **39**, 191-220.
- Conroy WG & Berg DK. (1995). Neurons can maintain multiple classes of nicotinic acetylcholine receptors distinguished by different subunit compositions. *J Biol Chem* **270**, 4424-4431.
- Conroy WG, Liu Q-S, Nai Q, Margiotta JF & Berg DK. (2003). Potentiation of  $\alpha$ 7-containing nicotinic acetylcholine receptors by select albumins. *Mol Pharmacol* **63**, 419-428.
- Conti-Fine BM, Milani M & Kaminski HJ. (2006). Myasthenia gravis: past, present, and future. *J Clin Invest* **116**, 2843-2854.

- Corringer PJ, Bertrand S, Bohler S, Edelstein SJ, Changeux JP & Bertrand D. (1998). Critical elements determining diversity in agonist binding and desensitization of neuronal nicotinic acetylcholine receptors. *J Neurosci* **18**, 648-657.
- Corringer PJ, Galzi JL, Elisel  JL, Bertrand S, Changeux JP & Bertrand D. (1995). Identification of a new component of the agonist binding site of the nicotinic  $\alpha 7$  homooligomeric receptor. *J Biol Chem* **270**, 11749-11752.
- Corringer PJ, Le Nov re N & Changeux JP. (2000). Nicotinic receptors at the amino acid level. *Ann Rev Pharmacol Toxicol* **40**, 431-458.
- Corriveau RA & Berg DK. (1993). Coexpression of multiple acetylcholine receptor genes in neurons: quantification of transcripts during development. *J Neurosci* **13**, 2662-2671.
- Court J, Martin-Ruiz C, Piggott M, Spurden D, Griffiths M & Perry E. (2001). Nicotinic receptor abnormalities in Alzheimer's disease. *Biol Psychiatry* **49**, 175-184.
- Couturier S, Bertrand D, Matter JM, Hernandez MC, Bertrand S, Millar N, Valera S, Barkas T & Ballivet M. (1990). A neuronal nicotinic acetylcholine receptor subunit ( $\alpha 7$ ) is developmentally regulated and forms a homo-oligomeric channel blocked by  $\alpha$ -BTX. *Neuron* **5**, 847-856.
- Cruz PM, Palace J & Beeson D. (2014). Congenital myasthenic syndromes and the neuromuscular junction. *Curr Opin Neurol* **27**, 566-575.
- Cui C, Booker TK, Allen RS, Grady SR, Whiteaker P, Marks MJ, Salminen O, Tritto T, Butt CM, Allen WR, Stitzel JA, McIntosh JM, Boulter J, Collins AC & Heineman SF. (2003). The  $\beta 3$  nicotinic receptor subunit: a component of  $\alpha$ -conotoxin MII-binding nicotinic acetylcholine receptors that modulate dopamine release and related behaviors. *J Neurosci* **23**, 11045-11053.
- Cully DF, Paress PS, Liu KK, Schaeffer JM & Arena JP. (1996). Identification of a *Drosophila melanogaster* glutamate-gated chloride channel sensitive to the antiparasitic agent avermectin. *J Biol Chem* **271**, 20187-20191.
- Curtis L, Buisson B, Bertrand S & Bertrand D. (2002). Potentiation of human  $\alpha 4\beta 2$  neuronal nicotinic acetylcholine receptor by estradiol. *Mol Pharmacol* **61**, 127-135.
- daCosta CJ, Free CR, Corradi J, Bouzat C & Sine SM. (2011). Single-channel and structural foundations of neuronal  $\alpha 7$  acetylcholine receptor potentiation. *J Neurosci* **31**, 13870-13879.

- Dage JL, Colvin EM, Fouillet A, Langron E, Roell WC, Li J, Mathur SX, Mogg AJ, Schmitt MG, Felder CC, Merchant KM, Isaac J, Broad LM, Sher E & Ursu D. (2014). Pharmacological characterisation of ligand- and voltage-gated ion channels expressed in human iPSC-derived forebrain neurons. *Psychopharmacology (Berl)* **231**, 1105-1124.
- Dale HH. (1914). The action of certain esters and ethers of choline and their relation to muscarine. *J Pharm Exp Ther* **6**, 147-190.
- Dale HH & Feldberg W. (1934). The chemical transmitter of vagus effects to the stomach. *J Physiol* **81**, 320-334.
- Dale HH, Feldberg W & Vogt M. (1936). Release of acetylcholine at voluntary motor nerve endings. *J Physiol* **86**, 353-380.
- Daly JW. (2005). Nicotinic agonists, antagonists, and modulators from natural sources. *Cell Mol Neurobiol* **25**, 513-552.
- Davies AR, Hardick DJ, Blagbrough IS, Potter BV, Wolstenholme AJ & Wonnacott S. (1999). Characterisation of the binding of [<sup>3</sup>H]methyllycaconitine: a new radioligand for labelling  $\alpha 7$ -type neuronal nicotinic acetylcholine receptors. *Neuropharmacol* **38**, 679-690.
- Decker MW, Anderson DJ, Brioni JD, Donnelly-Roberts DL, Kang CH, O'Neill AB, Piattoni-Kaplan M, Swanson S & Sullivan JP. (1995). Erysodine, a competitive antagonist at neuronal nicotinic acetylcholine receptors. *Eur J Pharmacol* **280**, 79-89.
- Dehaene S & Changeux JP. (1991). The Wisconsin Card Sorting Test: theoretical analysis and modeling in a neuronal network. *Cereb Cortex* **1**, 62-79.
- Del Castillo J & Katz B. (1955). On the localization of acetylcholine receptors. *J Physiol* **128**, 157-181.
- Dellisanti CD, Yao Y, Stroud JC, Wang Z-Z & Chen L. (2007). Crystal structure of the extracellular domain of nAChR  $\alpha 1$  bound to  $\alpha$ -bungarotoxin at 1.94Å resolution. *Nat Neurosci* **10**, 953-962.
- Dimos JT, Rodolfa KT, Niakan KK, Weisenthal LM, Mitsumoto H, Chung W, Croft GF, Saphier G, Leibel R, Goland R, Wichterle H, Henderson CE & Eggan K. (2008). Induced pluripotent stem cells generated from patients with ALS can be differentiated into motor neurons. *Science* **321**, 1218-1221.

- Dineley KT. (2007).  $\beta$ -amyloid peptide-nicotinic acetylcholine receptor interaction: the two faces of health and disease. *Front Biosci* **12**, 5030-5038.
- Dinklo T, Shaban H, Thuring JW, Lavreysen H, Stevens KE, Zheng L, Mackie C, Grantham C, Vandenberg I, Meulders G, Peeters L, Verachtert H, De Prins E & Lesange ASJ. (2011). Characterization of 2-[[4-fluoro-3-(trifluoromethyl)phenyl]amino]-4-(4-pyridinyl)-5-thiazolethanol (JNJ-1930942), a novel positive allosteric modulator of the  $\alpha 7$  nicotinic acetylcholine receptor. *J Pharm Exp Ther* **336**, 560-574.
- Dolmetsch R & Geschwind DH. (2011). The human brain in a dish: the promise of iPSC-derived neurons. *Cell* **145**, 831-834.
- Dougherty JJ, Wu J & Nichols RA. (2003).  $\beta$ -amyloid regulation of presynaptic nicotinic receptors in rat hippocampus and neocortex. *J Neurosci* **23**, 6740-6747.
- Drago J, McColl CD, Horne MK, Finkelstein DI & Ross SA. (2003). Neuronal nicotinic receptors: insights gained from gene knockout and knockin mutant mice. *Cell Mol Life Sci* **60**, 1267-1280.
- Drasdo A, Caulfield M, Bertrand D, Bertrand S & Wonnacott S. (1992). Methyllaconitine: a novel nicotinic antagonist. *Mol Cell Neurosci* **3**, 237-243.
- Du Bois-Reymond E. (1877). *Gesammelte Aehandlung zur Allgemeinen Muskel-und Nervenphysiol.*
- Dunlop J, Lock T, Jow B, Sitzia F, Grauer S, Jow F, Kramer A, Bowlby MR, Randall A, Kowal D, Gilbert A, Comery TA, LaRocque J, Soloveva V, Brown J & Roncarati R. (2009). Old and new pharmacology: positive allosteric modulation of the  $\alpha 7$  nicotinic acetylcholine receptor by the 5-hydroxytryptamine2B/C receptor antagonist SB-206553 (3,5-dihydro-5-methyl-N-3-pyridinylbenzo[1,2-b:4,5-b']di pyrrole-1(2H)-carboxamide). *J Pharm Exp Ther* **328**, 766-776.
- El Kaim L, Gizzi M & Grimaud L. (2010). 1,2,4-Triazole synthesis via amidrazones. *Synlett*, 1771-1774.
- Eldefrawi ME & Fertuck HC. (1974). A rapid method for the preparation of [ $^{125}$ I] $\alpha$ -bungarotoxin. *Anal Biochem* **58**, 63-70.
- Elenes S & Auerbach A. (2002). Desensitization of diliganded mouse muscle nicotinic acetylcholine receptor channels. *J Physiol* **541**, 367-383.
- Faghieh R, Gopalakrishnan M & Briggs CA. (2008). Allosteric modulators of the  $\alpha 7$  nicotinic acetylcholine receptor. *J Med Chem* **51**, 701-712.

- Faghieh R, Gopalakrishnan SM, Gronlien JH, Malysz J, Briggs CA, Wetterstrand C, Ween H, Curtis MP, Sarris KA, Gfesser GA, El-Kouhen R, Robb HM, Radek RJ, Marsh KC, Bunnelle WH & Gopalakrishnan M. (2009). Discovery of 4-(5-(4-chlorophenyl)-2-methyl-3-propionyl-1H-pyrrol-1-yl)benzenesulfonamide (A-867744) as a novel positive allosteric modulator of the  $\alpha 7$  nicotinic acetylcholine receptor. *J Med Chem* **52**, 3377-3384.
- Feldberg W & Fessard A. (1942). The cholinergic nature of the nerves to the electric organ of the Torpedo (Torpedo marmorata). *J Physiol* **101**, 200-216.
- Filatov GN & White MM. (1995). The role of conserved leucines in the M2 domain of the acetylcholine receptor in channel gating. *Mol Pharmacol* **48**, 379-384.
- Flomen RH, Collier DA, Osborne S, Munro J, Breen G, St Clair D & Makoff AJ. (2006). Association study of CHRFAM7A copy number and 2 bp deletion polymorphisms with schizophrenia and bipolar affective disorder. *Am J Med Genet B Neuropsychiatr Genet* **141B**, 571-575.
- Flores CM, Rogers SW, Pabreza LA, Wolfe BB & Kellar KJ. (1992). A subtype of nicotinic cholinergic receptor in rat brain is composed of  $\alpha 4$  and  $\beta 2$  subunits and is up-regulated by chronic nicotine treatment. *Mol Pharmacol* **41**, 31-37.
- Forman SA & Miller KW. (2011). Anesthetic sites and allosteric mechanisms of action on Cys-loop ligand-gated ion channels. *Can J Anaesth* **58**, 191-205.
- Freedman R, Coon H, Myles-Worsley M, Orr-Urtreger A, Olincy A, Davis A, Polymeropoulos M, Holik J, Hopkins J, Hoff M, Rosenthal J, Waldo MC, Reimherr F, Wender P, Yaw J, Young DA, Breese CR, Adams C, Patterson D, Adler LE, Kruglyak L, Leonard S & Byerley W. (1997). Linkage of a neurophysiological deficit in schizophrenia to a chromosome 15 locus. *Proc Natl Acad Sci USA* **94**, 587-592.
- Freedman R, Hall M, Adler LE & Leonard S. (1995). Evidence in postmortem brain tissue for decreased numbers of hippocampal nicotinic receptors in schizophrenia. *Biol Psychiatry* **38**, 22-33.
- Freitas K, Negus SS, Carroll FI & Damaj MI. (2013). In vivo pharmacological interactions between a type II positive allosteric modulator of  $\alpha 7$  nicotinic ACh receptors and nicotinic agonists in a murine tonic pain model. *Br J Pharmacol* **169**, 567-579.
- Froehner SC, Reiness CG & Hall ZW. (1977). Subunit structure of the acetylcholine receptor from denervated rat skeletal muscle. *J Biol Chem* **252**, 8589-8596.

- Galzi JL, Bertrand S, Corringer PJ, Changeux JP & Bertrand D. (1996). Identification of calcium binding sites that regulate potentiation of a neuronal nicotinic acetylcholine receptor. *EMBO J* **15**, 5824-5832.
- Galzi JL, Devillers-Thiéry A, Hussy N, Bertrand S, Changeux JP & Bertrand D. (1992). Mutations in the channel domain of a neuronal nicotinic receptor convert ion selectivity from cationic to anionic. *Nature* **359**, 500-505.
- Gault J, Robinson M, Berger R, Drebing C, Logel J, Hopkins J, Moore T, Jacobs S, Meriwether J, Choi M-J, Kim E-J, Walton K, Buiting K, Davis A, Breese C, Freedman R & Leonard S. (1998). Genomic organization and partial duplication of the human  $\alpha 7$  neuronal nicotinic acetylcholine receptor gene (CHRNA7). *Genomics* **52**, 173-185.
- Gee VJ, Kracun S, Cooper ST, Gibb AJ & Millar NS. (2007). Identification of domains influencing assembly and ion channel properties in  $\alpha 7$  nicotinic receptor and 5-HT3 receptor subunit chimeras. *Brit J Pharmacol* **152**, 501-512.
- Gibson RE, O'Brien RD, Edelstein SJ & Thompson WR. (1976). Acetylcholine receptor oligomers from electroplax of Torpedo species. *Biochemistry* **15**, 2377-2383.
- Gill JK, Chatzidaki A, Ursu D, Sher E & Millar NS. (2013). Contrasting properties of  $\alpha 7$ -selective orthosteric and allosteric agonists examined on native nicotinic acetylcholine receptors. *PLOS ONE* **8**, e55047.
- Gill JK, Dhankher P, Sheppard TD, Sher E & Millar NS. (2012). A series of  $\alpha 7$  nicotinic acetylcholine receptor allosteric modulators with close chemical similarity but diverse pharmacological properties. *Mol Pharmacol* **81**, 710-718.
- Gill JK, Savolainen M, Young GT, Zwart R, Sher E & Millar NS. (2011). Agonist activation of  $\alpha 7$  nicotinic acetylcholine receptors via an allosteric transmembrane site. *Proc Natl Acad Sci USA* **108**, 5867-5872.
- Gill-Thing JK, Dhankher P, D'Oyley JM, Sheppard TD & Millar NS. (2015). Structurally similar allosteric modulators of  $\alpha 7$  nicotinic acetylcholine receptors exhibit five distinct pharmacological effects. *J Biol Chem* **290**, 3552-3562.
- Giorguieff MF, Le Floc'h ML, Glowinski J & Besson MJ. (1977). Involvement of cholinergic presynaptic receptors of nicotinic and muscarinic types in the control of the spontaneous release of dopamine from striatal dopaminergic terminals in the rat. *J Pharm Exp Ther* **200**, 535-544.
- Giraudat J, Gali J, Revah F, Changeux J, Haumont P & Lederer F. (1989). The noncompetitive blocker [(3)H]chlorpromazine labels segment M2 but not

segment M1 of the nicotinic acetylcholine receptor alpha-subunit. *Febs Lett* **253**, 190-198.

González-Cestari TF, Henderson BJ, Pavlovicz RE, McKay SB, El-Hajj RA, Pulipaka AB, Orac CM, Reed DD, Boyd RT, Zhu MX, Li C, Bergmeier SC & McKay DB. (2009). Effect of novel negative allosteric modulators of neuronal nicotinic receptors on cells expressing native and recombinant nicotinic receptors: implications for drug discovery. *J Pharm Exp Ther* **328**, 504-515.

Gopalakrishnan M, Buisson B, Touma E, Giordano T, Campbell JE, Hu IC, Donnelly-Roberts D, Arneric SP, Bertrand D & Sullivan JP. (1995). Stable expression and pharmacological properties of the human  $\alpha 7$  nicotinic acetylcholine receptor. *Eur J Pharmacol* **290**, 237-246.

Gotti C & Clementi F. (2004). Neuronal nicotinic receptors: from structure to pathology. *Prog Neurobiol* **74**, 363-396.

Govind AP, Vezina P & Green WN. (2009). Nicotine-induced upregulation of nicotinic receptors: underlying mechanisms and relevance to nicotine addiction. *Biochem Pharmacol* **78**, 756-765.

Grady S, Marks MJ, Wonnacott S & Collins AC. (1992). Characterization of nicotinic receptor-mediated [3H]dopamine release from synaptosomes prepared from mouse striatum. *J Neurochem* **59**, 848-856.

Groot-Kormelink PJ, Luyten WHML, Colquhoun D & Sivilotti LG. (1998). A reporter mutation approach shows incorporation of the "orphan" subunit  $\beta 3$  into a functional nicotinic receptor. *J Biol Chem* **273**, 15317-15320.

Grosman C, Zhou M & Auerbach A. (2000). Mapping the conformational wave of acetylcholine receptor channel gating. *Nature* **403**, 773-776.

Grskovic M, Javaherian A, Strulovici B & Daley GQ. (2011). Induced pluripotent stem cells--opportunities for disease modelling and drug discovery. *Nat Rev Drug Discov* **10**, 915-929.

Grupe M, Jensen AA, Ahring PK, Christensen JK & Grunnet M. (2013). Unravelling the mechanism of action of NS9283, a positive allosteric modulator of  $(\alpha 4)\beta 2$  nicotinic ACh receptors. *Br J Pharmacol* **168**, 2000-2010.

Grønlien JH, Håkerud M, Ween H, Thorin-Hagene K, Briggs CA, Gopalakrishnan M & Malysz J. (2007). Distinct profiles of  $\alpha 7$  nAChR positive allosteric modulation revealed by structurally diverse chemotypes. *Mol Pharmacol* **72**, 715-724.

- Gumilar F, Arias HR, Spitzmaul G & Bouzat C. (2003). Molecular mechanisms of inhibition of nicotinic acetylcholine receptors by tricyclic antidepressants. *Neuropharmacol* **45**, 964-976.
- Gündisch D & Eibl C. (2011). Nicotinic acetylcholine receptor ligands, a patent review (2006-2011). *Expert Opin Ther Pat* **21**, 1867-1896.
- Hamouda AK, Chiara DC, Sauls D, Cohen JB & Blanton MP. (2006). Cholesterol interacts with transmembrane alpha-helices M1, M3, and M4 of the Torpedo nicotinic acetylcholine receptor: photolabeling studies using [3H]Azicholesterol. *Biochemistry* **45**, 976-986.
- Hamouda AK, Jayakar SS, Chiara DC & Cohen JB. (2014). Photoaffinity labeling of nicotinic receptors: diversity of drug binding sites! *J Mol Neurosci* **53**, 480-486.
- Hansen SB, Sulzenbacher G, Huxford T, Marchot P, Taylor P & Bourne Y. (2005). Structures of Aplysia AChBP complexes with nicotinic agonists and antagonists reveal distinctive binding interfaces and conformations. *EMBO J* **24**, 3635-3646.
- Hansen SB & Taylor P. (2007). Galanthamine and non-competitive inhibitor binding to ACh-binding protein: evidence for a binding site on non- $\alpha$ -subunit interfaces of heteromeric neuronal nicotinic receptors. *J Mol Biol* **369**, 895-901.
- Harkness PC & Millar NS. (2001). Inefficient cell-surface expression of hybrid complexes formed by the co-assembly of neuronal nicotinic acetylcholine receptor and serotonin receptor subunits. *Neuropharmacol* **41**, 79-87.
- Hassaine G, Deluz C, Grasso L, Wyss R, Tol MB, Hovius R, Graff A, Stahlberg H, Tomizaki T, Desmyter A, Moreau C, Li XD, Poitevin F, Vogel H & Nury H. (2014). X-ray structure of the mouse serotonin 5-HT<sub>3</sub> receptor. *Nature* **512**, 276-281.
- Haydar SN & Dunlop J. (2010). Neuronal nicotinic acetylcholine receptors - targets for the development of drugs to treat cognitive impairment associated with schizophrenia and Alzheimer's disease. *Curr Top Med Chem* **10**, 144-152.
- Haythornthwaite A, Stoelzle S, Hasler A, Kiss A, Mosbacher J, George M, Brüggemann A & Fertig N. (2012). Characterizing human ion channels in induced pluripotent stem cell-derived neurons. *J Biomol Screen* **17**, 1264-1272.
- Heeschen C, Jang JJ, Weis M, Pathak A, Kaji S, Hu RS, Tsao PS, Johnson FL & Cooke JP. (2001). Nicotine stimulates angiogenesis and promotes tumor growth and atherosclerosis. *Nat Med* **7**, 833-839.

- Heeschen C, Weis M, Aicher A, Dimmeler S & Cooke JP. (2002). A novel angiogenic pathway mediated by non-neuronal nicotinic acetylcholine receptors. *J Clin Invest* **110**, 527-536.
- Heidmann T & Changeux JP. (1984). Time-resolved photolabeling by the noncompetitive blocker chlorpromazine of the acetylcholine receptor in its transiently open and closed ion channel conformations. *Proc Natl Acad Sci USA* **81**, 1897-1901.
- Henderson BJ, Pavlovicz RE, Allen JD, González-Cestari TF, Orac CM, Bonnell AB, Zhu MX, Boyd RT, Li C, Bergmeier SC & McKay DB. (2010). Negative allosteric modulators that target human  $\alpha 4\beta 2$  neuronal nicotinic receptors. *J Pharm Exp Ther* **334**, 761-774.
- Hibbs RE & Gouaux E. (2011). Principles of activation and permeation in an anion-selective Cys-loop receptor. *Nature* **474**, 54-60.
- Hilf RJ & Dutzler R. (2008). X-ray structure of a prokaryotic pentameric ligand-gated ion channel. *Nature* **452**, 375-379.
- Hilf RJ & Dutzler R. (2009). Structure of a potentially open state of a proton-activated pentameric ligand-gated ion channel. *Nature* **457**, 115-118.
- Hogg RC, Buisson B & Bertrand D. (2005). Allosteric modulation of ligand-gated ion channels. *Biochem Pharmacol* **70**, 1267-1276.
- Horenstein NA, McCormack TJ, Stokes C, Ren K & Papke RL. (2007). Reversal of agonist selectivity by mutations of conserved amino acids in the binding site of nicotinic acetylcholine receptors. *J Biol Chem* **282**, 5899-5909.
- Hsiao B, Dweck D & Luetje CW. (2001). Subunit-dependent modulation of neuronal nicotinic receptors by zinc. *J Neurosci* **21**, 1848-1856.
- Hsiao B, Mihalak KB, Repicky SE, Everhart D, Mederos AH, Malhotra A & Luetje CW. (2006). Determinants of zinc potentiation on the  $\alpha 4$  subunit of neuronal nicotinic receptors. *Mol Pharmacol* **69**, 27-36.
- Huang S, Li SX, Bren N, Cheng K, Gomoto R, Chen L & Sine SM. (2013). Complex between  $\alpha$ -bungarotoxin and an  $\alpha 7$  nicotinic receptor ligand-binding domain chimera. *Biochem J* **454**, 303-310.
- Hucho F, Layer P, Kiefer HR & Bandini G. (1976). Photoaffinity labeling and quaternary structure of the acetylcholine receptor from *Torpedo californica*. *Proc Natl Acad Sci USA* **73**, 2624-2628.

- Huganir RL & Greengard P. (1990). Regulation of neurotransmitter receptor desensitization by protein phosphorylation. *Neuron* **5**, 555-567.
- Hurst R, Rollema H & Bertrand D. (2013). Nicotinic acetylcholine receptors: from basic science to therapeutics. *Pharmacol Ther* **137**, 22-54.
- Hurst RS, Hajós M, Raggenbass M, Wall TM, Higdon NR, Lawson JA, Rutherford-Root KL, Berkenpas MB, Hoffmann WE, Piotrowski DW, Groppi VE, Allaman G, Ogier R, Bertrand S, Bertrand D & Arneric SP. (2005). A novel positive allosteric modulator of the  $\alpha 7$  neuronal nicotinic acetylcholine receptor: in vitro and in vivo characterization. *J Neurosci* **25**, 4396-4405.
- Huxley HE. (2008). Memories of early work on muscle contraction and regulation in the 1950's and 1960's. *Biochem Biophys Res Commun* **369**, 34-42.
- Ibañez-Tallon I, Miwa JM, Wang HL, Adams NC, Crabtree GW, Sine SM & Heintz N. (2002). Novel modulation of neuronal nicotinic acetylcholine receptors by association with the endogenous prototoxin lynx1. *Neuron* **33**, 893-903.
- Ishii M & Kurachi Y. (2006). Muscarinic acetylcholine receptors. *Curr Pharm Des* **12**, 3573-3581.
- Jackson MB. (1984). Spontaneous openings of the acetylcholine receptor channel. *Proc Natl Acad Sci USA* **81**, 3901-3904.
- Jackson MB. (1986). Kinetics of unliganded acetylcholine receptor channel gating. *Biophys J* **49**, 663-672.
- Jackson SN, Singhal SK, Woods AS, Morales M, Shippenberg T, Zhang L & Oz M. (2008). Volatile anesthetics and endogenous cannabinoid anandamide have additive and independent inhibitory effects on  $\alpha 7$ -nicotinic acetylcholine receptor-mediated responses in *Xenopus* oocytes. *Eur J Pharmacol* **582**, 42-51.
- Jadey SV, Purohit P, Bruhova I, Gregg TM & Auerbach A. (2011). Design and control of acetylcholine receptor conformational change. *Proc Natl Acad Sci USA* **108**, 4328-4333.
- Jayakar SS, Dailey WP, Eckenhoff RG & Cohen JB. (2013). Identification of propofol binding sites in a nicotinic acetylcholine receptor with a photoreactive propofol analog. *J Biol Chem* **288**, 6178-6189.

- Jensen AA, Frolund B, Liljefors T & Krogsgaard-Larsen P. (2005). Neuronal nicotinic acetylcholine receptors: structural revelations, target identification, and therapeutic inspirations. *J Med Chem* **48**, 4705-4745.
- Jindrichova M, Lansdell SJ & Millar NS. (2012). Changes in temperature have opposing effects on current amplitude in  $\alpha 7$  and  $\alpha 4\beta 2$  nicotinic acetylcholine receptors. *PLOS ONE* **7**, e32073.
- Jones SW & Thompson WR. (1980). Preparation and characterization of 3H-labeled  $\alpha$ -bungarotoxin. *Anal Biochem* **101**, 261-270.
- Jorenby DE, Hays JT, Rigotti NA, Azoulay S, Watsky EJ, Williams KE, Billing CB, Gong J, Reeves KR & Group VPS. (2006). Efficacy of varenicline, an  $\alpha 4\beta 2$  nicotinic acetylcholine receptor partial agonist, vs placebo or sustained-release bupropion for smoking cessation: a randomized controlled trial. *JAMA* **296**, 56-63.
- Kaiser S & Wonnacott S. (2000).  $\alpha$ -bungarotoxin-sensitive nicotinic receptors indirectly modulate [3H]dopamine release in rat striatal slices via glutamate release. *Mol Pharmacol* **58**, 312-318.
- Kalappa BI, Sun F, Johnson SR, Jin K & Uteshev VV. (2013). A positive allosteric modulator of  $\alpha 7$  nAChRs augments neuroprotective effects of endogenous nicotinic agonists in cerebral ischaemia. *Br J Pharmacol* **169**, 1862-1878.
- Katz B & Miledi R. (1972). The statistical nature of the acetylcholine potential and its molecular components. *J Physiol* **224**, 665-699.
- Katz B & Thesleff S. (1957). A study of the desensitization produced by acetylcholine at the motor end-plate. *J Physiol* **138**, 63-80.
- Khiroug SS, Harkness PC, Lamb PW, Sudweeks SN, Khiroug L, Millar NS & Yakel JL. (2002). Rat nicotinic ACh receptor  $\alpha 7$  and  $\beta 2$  subunits co-assemble to form functional heteromeric nicotinic receptor channels. *J Physiol* **540**, 425-434.
- Kim JS, Padnya A, Weltzin M, Edmonds BW, Schulte MK & Glennon RA. (2007). Synthesis of desformylflustrabromine and its evaluation as an  $\alpha 4\beta 2$  and  $\alpha 7$  nACh receptor modulator. *Bioorg Med Chem Lett* **17**, 4855-4860.
- King H. (1946). Botanical origin of tube-curare. *Nature* **158**, 515.
- Kirst HA. (2010). The spinosyn family of insecticides: realizing the potential of natural products research. *J Antibiot (Tokyo)* **63**, 101-111.

- Krause RM, Buisson B, Bertrand S, Corringer P-J, Galzi J-L, Changeux J-P & Bertrand D. (1998). Ivermectin: a positive allosteric effector of the  $\alpha 7$  neuronal nicotinic acetylcholine receptor. *Mol Pharmacol* **53**, 283-294.
- Kuryatov A, Olale F, Cooper J, Choi C & Lindstrom J. (2000). Human  $\alpha 6$  AChR subtypes: subunit composition, assembly, and pharmacological responses. *Neuropharmacol* **39**, 2570-2590.
- Kása P, Rakonczay Z & Gulya K. (1997). The cholinergic system in Alzheimer's disease. *Prog Neurobiol* **52**, 511-535.
- Labarca C, Nowak MW, Zhang H, Tang L, Deshpande P & Lester HA. (1995). Channel gating governed symmetrically by conserved leucine residues in the M2 domain of nicotinic receptors. *Nature* **376**, 514-516.
- Langley JN. (1907). On the contraction of muscle, chiefly in relation to the presence of "receptive" substances: Part I. *J Physiol* **36**, 347-384.
- Langmead CL & Christopoulos A. (2006). Allosteric agonists of 7TM receptors: expanding the pharmacological toolbox. *Trends Pharmacol Sci* **27**, 475-481.
- Lansdell SJ & Millar NS. (2000). The influence of nicotinic receptor subunit composition upon agonist,  $\alpha$ -bungarotoxin and insecticide (imidacloprid) binding affinity. *Neuropharmacol* **39**, 671-679.
- Lansdell SJ, Sathyaprakash C, Doward A & Millar NS. (2015). Activation of human 5-hydroxytryptamine type 3 receptors via an allosteric transmembrane site. *Mol Pharmacol* **87**, 87-95.
- Lape R, Colquhoun D & Sivilotti LG. (2008). On the nature of partial agonism in the nicotinic receptor superfamily. *Nature* **454**, 722-727.
- Le Novère N, Corringer PJ & Changeux JP. (2002). The diversity of subunit composition in nAChRs: evolutionary origins, physiologic and pharmacologic consequences. *J Neurobiol* **53**, 447-456.
- Lebbe EK, Peigneur S, Wijesekara I & Tytgat J. (2014). Conotoxins targeting nicotinic acetylcholine receptors: an overview. *Mar Drugs* **12**, 2970-3004.
- Lee CH, Zhu C, Malysz J, Campbell T, Shaughnessy T, Honore P, Polakowski J & Gopalakrishnan M. (2011).  $\alpha 4\beta 2$  neuronal nicotinic receptor positive allosteric modulation: an approach for improving the therapeutic index of  $\alpha 4\beta 2$  nAChR agonists in pain. *Biochem Pharmacol* **82**, 959-966.

- Lee CY & Chang CC. (1966). Modes of actions of purified toxins from elapid venoms on neuromuscular transmission. *Mem Inst Butantan* **33**, 555-572.
- Lee CY, Tseng LF & Chiu TH. (1967). Influence of denervation on localization of neurotoxins from elapid venoms in rat diaphragm. *Nature* **215**, 1177-1178.
- Lee WY, Free CR & Sine SM. (2008). Nicotinic receptor interloop proline anchors  $\beta$ 1- $\beta$ 2 and Cys loops in coupling agonist binding to channel gating. *J Gen Physiol* **132**, 265-278.
- Leonard S, Gault J, Hopkins J, Logel J, Vianzon R, Short M, Drebing C, Berger R, Venn D, Sirota P, Zerbe G, Olincy A, Ross RG, Adler LE & Freedman R. (2002). Association of promoter variants in the  $\alpha$ 7 nicotinic acetylcholine receptor subunit gene with an inhibitory deficit found in schizophrenia. *Arch Gen Psychiatry* **59**, 1085-1096.
- Leonard S, Mexas S & Freedman R. (2007). Smoking, Genetics and Schizophrenia: Evidence for Self Medication. *J Dual Diagn* **3**, 43-59.
- Lester HA, Dibas MI, Dahan DS, Leite JF & Dougherty DA. (2004). Cys-loop receptors: new twists and turns. *Trends Neurosci* **27**, 329-336.
- Levandoski MM, Pickett B & Chang J. (2003). The anthelmintic levamisole is an allosteric modulator of human neuronal nicotinic acetylcholine receptors. *Eur J Pharmacol* **471**, 9-20.
- Levin ED, Petro A, Rezvani AH, Pollard N, Christopher NC, Strauss M, Avery J, Nicholson J & Rose JE. (2009). Nicotinic  $\alpha$ 7- or  $\beta$ 2-containing receptor knockout: effects on radial-arm maze learning and long-term nicotine consumption in mice. *Behav Brain Res* **196**, 207-213.
- Li L, Zhong W, Zacharias N, Gibbs C, Lester HA & Dougherty DA. (2001). The tethered agonist approach to mapping ion channel proteins--toward a structural model for the agonist binding site of the nicotinic acetylcholine receptor. *Chem Biol* **8**, 47-58.
- Liu Q, Huang Y, Shen J, Steffensen S & Wu J. (2012). Functional  $\alpha$ 7 $\beta$ 2 nicotinic acetylcholine receptors expressed in hippocampal interneurons exhibit high sensitivity to pathological level of amyloid  $\beta$  peptides. *BMC Neurosci* **13**, 155.
- Liu Q, Huang Y, Xue F, Simard A, DeChon J, Li G, Zhang J, Lucero L, Wang M, Sierks M, Hu G, Chang Y, Lukas RJ & Wu J. (2009). A novel nicotinic

acetylcholine receptor subtype in basal forebrain cholinergic neurons with high sensitivity to amyloid peptides. *J Neurosci* **29**, 918-929.

Livett BG, Sandall DW, Keays D, Down J, Gayler KR, Satkunanathan N & Khalil Z. (2006). Therapeutic applications of conotoxins that target the neuronal nicotinic acetylcholine receptor. *Toxicon* **48**, 810-829.

Loewi O. (1921). Über humorale Übertragbarkeit der Herznervenwirkung. **193**, 201-213.

Lopes C, Pereira FR, Wu H-Q, Purushottamachar P, Njar V, Schwarcz R & Albuquerque EX. (2007). Competitive antagonism between the nicotinic allosteric potentiating ligand galantamine and kynurenic acid at  $\alpha 7^*$  nicotinic receptors. *J Pharm Exp Ther* **322**, 48-58.

Ludwig J, Höffle-Maas A, Samochocki M, Luttmann E, Albuquerque EX, Fels G & Maelicke A. (2010). Localization by site-directed mutagenesis of a galantamine binding site on  $\alpha 7$  nicotinic acetylcholine receptor extracellular domain. *J Recept Signal Transduct Res* **30**, 469-483.

Luetje CW & Patrick J. (1991). Both  $\alpha$ - and  $\beta$ -subunits contribute to the agonist sensitivity of neuronal nicotinic acetylcholine receptors. *J Neurosci* **11**, 837-845.

Lukas RJ. (1989). Pharmacological distinctions between functional nicotinic acetylcholine receptors on the PC12 rat pheochromocytoma and the TE671 human medulloblastoma. *J Pharm Exp Ther* **251**, 175-182.

Luttmann E, Ludwig J, Höffle-Maas A, Samochocki M, Maelicke A & Fels G. (2009). Structural model for the binding sites of allosterically potentiating ligands on nicotinic acetylcholine receptors. *ChemMedChem* **4**, 1874-1882.

Lynagh T & Laube B. (2014). Opposing effects of the anesthetic propofol at pentameric ligand-gated ion channels mediated by a common site. *J Neurosci* **34**, 2155-2159.

Macallan DR, Lunt GG, Wonnacott S, Swanson KL, Rapoport H & Albuquerque EX. (1988). Methyllycaconitine and (+)-anatoxin-a differentiate between nicotinic receptors in vertebrate and invertebrate nervous systems. *FEBS Lett* **226**, 357-363.

Maelicke A & Albuquerque EX. (2000). Allosteric modulation of nicotinic acetylcholine receptors as a treatment strategy for Alzheimer's disease. *Eur J Pharmacol* **393**, 165-170.

- Maelicke A, Samochocki M, Jostock R, Fehrenbacher A, Ludwig J, Albuquerque EX & Zerlin M. (2001). Allosteric sensitization of nicotinic receptors by galantamine, a new treatment strategy for Alzheimer's disease. *Biol Psychiatry* **49**, 279-288.
- Malysz J, Grønlien JH, Anderson DJ, Håkerud M, Thorin-Hagene K, Ween H, Wetterstrand C, Briggs CA, Faghieh R, Bunnelle WH & Gopalakrishnan M. (2009). In vitro pharmacological characterization of a novel allosteric modulator of the  $\alpha 7$  neuronal acetylcholine receptor, 4-(5-(4-chlorophenyl)-2-methyl-3-propionyl-1H-pyrrol-1-yl)benzenesulfonamide (A-867744), exhibiting unique pharmacological profile. *J Pharm Exp Ther* **330**, 257-267.
- Mandelzys A, Pié B, Deneris ES & Cooper E. (1994). The developmental increase in ACh current densities on rat sympathetic neurons correlates with changes in nicotinic ACh receptor  $\alpha$ -subunit gene expression and occurs independent of innervation. *J Neurosci* **14**, 2357-2364.
- Marchetto MC, Carroneu C, Acab A, Yu D, Yeo GW, Mu Y, Chen G, Gage FH & Muotri AR. (2010). A model for neural development and treatment of Rett syndrome using human induced pluripotent stem cells. *Cell* **143**, 527-539.
- Martin TJ, Suchocki J, May EL & Martin BR. (1990). Pharmacological evaluation of the antagonism of nicotine's central effects by mecamylamine and pempidine. *J Pharm Exp Ther* **254**, 45-51.
- Marubio LM, del Mar Arroyo-Jimenez M, Cordero-Erausquin M, Léna C, Le Novère N, de Kerchove d'Exaerde A, Huchet M, Damaj MI & Changeux JP. (1999). Reduced antinociception in mice lacking neuronal nicotinic receptor subunits. *Nature* **398**, 805-810.
- Maskos U. (2008). The cholinergic mesopontine tegmentum is a relatively neglected nicotinic master modulator of the dopaminergic system: relevance to drugs of abuse and pathology. *Br J Pharmacol* **153 Suppl 1**, S438-445.
- Maskos U. (2010). Role of endogenous acetylcholine in the control of the dopaminergic system via nicotinic receptors. *J Neurochem* **114**, 641-646.
- Matsunaga K, Klein TW, Friedman H & Yamamoto Y. (2001). Involvement of nicotinic acetylcholine receptors in suppression of antimicrobial activity and cytokine responses of alveolar macrophages to Legionella pneumophila infection by nicotine. *J Immunol* **167**, 6518-6524.
- Mayeux R. (2003). Epidemiology of neurodegeneration. *Annu Rev Neurosci* **26**, 81-104.

- Mazurov AA, Speake JD & Yohannes D. (2011). Discovery and development of  $\alpha 7$  nicotinic acetylcholine receptor modulators. *J Med Chem* **54**, 7943-7961.
- Mazzaferro S, Benallegue N, Carbone A, Gasparri F, Vijayan R, Biggin PC, Moroni M & Bermudez I. (2011). Additional acetylcholine (ACh) binding site at alpha4/alpha4 interface of (alpha4beta2)2alpha4 nicotinic receptor influences agonist sensitivity. *J Biol Chem* **286**, 31043-31054.
- Mazzaferro S, Gasparri F, New K, Alcaino C, Faundez M, Iturriaga Vasquez P, Vijayan R, Biggin PC & Bermudez I. (2014). Non-equivalent ligand selectivity of agonist sites in ( $\alpha 4\beta 2$ ) $2\alpha 4$  nicotinic acetylcholine receptors: a key determinant of agonist efficacy. *J Biol Chem* **289**, 21795-21806.
- McIntosh JM, Santos AD & Olivera BO. (1999). Conus peptides targeted to specific nicotinic acetylcholine receptor subtypes. *Ann Rev Biochem* **68**, 59-88.
- McLean SL, Idris NF, Grayson B, Gendle DF, Mackie C, Lesage AS, Pemberton DJ & Neill JC. (2012). PNU-120596, a positive allosteric modulator of  $\alpha 7$  nicotinic acetylcholine receptors, reverses a sub-chronic phencyclidine-induced cognitive deficit in the attentional set-shifting task in female rats. *J Psychopharmacol* **26**, 1265-1270.
- Middleton RE, Strnad NP & Cohen JB. (1999). Photoaffinity labeling the torpedo nicotinic acetylcholine receptor with [(3)H]tetracaine, a nondesensitizing noncompetitive antagonist. *Mol Pharmacol* **56**, 290-299.
- Miledi R, Molinoff P & Potter LT. (1971). Isolation of the cholinergic receptor protein of Torpedo electric tissue. *Nature* **229**, 554-557.
- Millar NS. (2002). Assembly and targeting of neuronal nicotinic acetylcholine receptors. In *Receptor and Ion-channel Trafficking*, ed. Henley J & Moss S, pp. 109-127. Oxford University Press, Oxford.
- Millar NS. (2003). Assembly and subunit diversity of nicotinic acetylcholine receptors. *Biochem Soc Trans* **31**, 869-874.
- Millar NS. (2009). A review of experimental techniques used for the heterologous expression of nicotinic acetylcholine receptors. *Biochem Pharmacol* **78**, 766-776.
- Millar NS & Denholm I. (2007). Nicotinic acetylcholine receptors: targets for commercially important insecticides. *Invert Neurosci* **7**, 53-66.

- Millar NS & Gotti C. (2009). Diversity of vertebrate nicotinic acetylcholine receptors. *Neuropharmacol* **56**, 237-246.
- Millar NS & Lansdell SJ. (2010). Characterisation of insect nicotinic acetylcholine receptors by heterologous expression. *Adv Exp Med Biol* **683**, 65-73.
- Miller C. (1989). Genetic manipulation of ion channel: a new approach to structure and mechanism. *Neuron* **2**, 1195-1205.
- Miller DT, Shen Y, Weiss LA, Korn J, Anselm I, Bridgemohan C, Cox GF, Dickinson H, Gentile J, Harris DJ, Hegde V, Hundley R, Khwaja O, Kothare S, Luedke C, Nasir R, Poduri A, Prasad K, Raffalli P, Reinhard A, Smith SE, Sobeih MM, Soul JS, Stoler J, Takeoka M, Tan WH, Thakuria J, Wolff R, Yusupov R, Gusella JF, Daly MJ & Wu BL. (2009). Microdeletion/duplication at 15q13.2q13.3 among individuals with features of autism and other neuropsychiatric disorders. *J Med Genet* **46**, 242-248.
- Miller PS & Aricescu AR. (2014). Crystal structure of a human GABA<sub>A</sub> receptor. *Nature* **512**, 270-275.
- Misgeld U. (2004). Innervation of the substantia nigra. *Cell Tissue Res* **318**, 107-114.
- Mishina M, Takai T, Imoto K, Noda M, Takahashi T, Numa S, Methfessel C & Sakman B. (1986). Molecular distinction between fetal and adult forms of muscle acetylcholine receptor. *Nature* **313**, 364-369.
- Missias AC, Chu GC, Klocke BJ, Sanes JR & Merlie JP. (1996). Maturation of the acetylcholine receptor in skeletal muscle: regulation of the AChR  $\gamma$ -to- $\epsilon$  switch. *Dev Biol* **179**, 223-238.
- Missias AC, Mudd J, Cunningham JM, Steinbach JH, Merlie JP & Sanes JR. (1997). Deficient development and maintenance of postsynaptic specializations in mutant mice lacking an 'adult' acetylcholine receptor subunit. *Development* **124**, 5075-5086.
- Moaddel R, Jozwiak K & Wainer IW. (2007). Allosteric modifiers of neuronal nicotinic acetylcholine receptors: new methods, new opportunities. *Med Res Rev* **27**, 723-753.
- Moretti M, Zoli M, George AA, Lukas RJ, Pistillo F, Maskos U, Whiteaker P & Gotti C. (2014). The novel  $\alpha\beta 2$ -nicotinic acetylcholine receptor subtype is expressed in mouse and human basal forebrain: biochemical and pharmacological characterization. *Mol Pharmacol* **86**, 306-317.

- Moroni M, Vijayan R, Carbone A-L, Zwart R, Biggin PC & Bermudez I. (2008). Non-agonist-binding subunit interfaces confer distinct functional signatures to the alternate stoichiometries of the  $\alpha 4\beta 2$  nicotinic receptor: an  $\alpha 4$ - $\alpha 4$  interface is required for  $Zn^{2+}$  potentiation. *J Neurosci* **28**, 6884-6894.
- Moroni M, Zwart R, Sher E, Cassels BK & Bermudez I. (2006).  $\alpha 4\beta 2$  nicotinic receptors with high and low acetylcholine sensitivity: pharmacology, stoichiometry, and sensitivity to long-term exposure to nicotine. *Mol Pharmacol* **70**, 755-768.
- Mowrey DD, Liu Q, Bondarenko V, Chen Q, Seyoum E, Xu Y, Wu J & Tang P. (2013). Insights into distinct modulation of  $\alpha 7$  and  $\alpha 7\beta 2$  nicotinic acetylcholine receptors by the volatile anesthetic isoflurane. *J Biol Chem* **288**, 35793-35800.
- Mu TW, Lester HA & Dougherty DA. (2003). Different binding orientations for the same agonist at homologous receptors: a lock and key or a simple wedge? *J Am Chem Soc* **125**, 6850-6851.
- Mukhtasimova N, Lee WY, Wang HL & Sine SM. (2009). Detection and trapping of intermediate states priming nicotinic receptor channel opening. *Nature* **459**, 451-454.
- Mulle C, Lena C & Changeux JP. (1992). Potentiation of nicotinic receptor response by external calcium in rat central neurons. *Neuron* **8**, 937-945.
- Munro G, Hansen RR, Erichsen HK, Timmermann DB, Christensen JK & Hansen HH. (2012). The  $\alpha 7$  nicotinic ACh receptor agonist compound B and positive allosteric modulator PNU-120596 both alleviate inflammatory hyperalgesia and cytokine release in the rat. *Br J Pharmacol* **167**, 421-435.
- Nelson ME, Kuryatov A, Choi CH, Zhou Y & Lindstrom J. (2003). Alternate stoichiometries of  $\alpha 4\beta 2$  nicotinic acetylcholine receptors. *Mol Pharmacol* **63**, 332-341.
- Ng HJ, Whittemore ER, Tran MB, Hogenkamp DJ, Broide RS, Johnstone TB, Zheng L, Stevens KE & Gee KW. (2007). Nootropic  $\alpha 7$  nicotinic receptor allosteric modulator derived from GABA<sub>A</sub> receptor modulators. *Proc Natl Acad Sci USA* **104**, 8059-8064.
- Nirathanan S, Garcia G, Chiara DC, Husain SS & Cohen JB. (2008). Identification of binding sites in the nicotinic acetylcholine receptor for TDBzl-etomidate, a photoreactive positive allosteric effector. *J Biol Chem* **283**, 22051-22062.
- Noda M, Takahashi H, Tanabe T, Toyosato M, Furutani Y, Hirose T, Asai M, Inayama S, Miyata T & Numa S. (1982). Primary structure of  $\alpha$ -subunit precursor of

- Torpedo californica acetylcholine receptor deduced from cDNA sequence. *Nature* **299**, 793-797.
- Noda M, Takahashi H, Tanabe T, Toyosato M, Kikuyotani S, Furutana Y, Hirose T, Takashima H, Inayama S, Miyata T & Numa S. (1983a). Structural homology of Torpedo californica acetylcholine receptor subunits. *Nature* **302**, 528-532.
- Noda M, Takahashi H, Tanabe T, Toyosato M, Kikuyotani S, Hirose T, Asai M, Takashima H, Inayama S, Miyata T & Numa S. (1983b). Primary structures of  $\beta$ - and  $\delta$ -subunit precursors of Torpedo californica acetylcholine receptor deduced from cDNA sequences. *Nature* **301**, 251-255.
- Nowak MW, Kearney PC, Sampson JR, Saks ME, Labarca CG, Silverman SK, Zhong W, Thorson J, Abelson JN, Davidson N, Schultz PG, Dougherty DA & Lester HA. (1995). Nicotinic receptor binding site probed with unnatural amino acids incorporated in intact cells. *Science* **268**, 439-442.
- Nury H, Poitevin F, Van Renterghem C, Changeux JP, Corringer PJ, Delarue M & Baaden M. (2010). One-microsecond molecular dynamics simulation of channel gating in a nicotinic receptor homologue. *Proc Natl Acad Sci USA* **107**, 6275-6280.
- Nury H, Van Renterghem C, Weng Y, Tran A, Baaden M, Dufresne V, Changeux J-P, Sonner JM, Delarue M & Corringer P-J. (2011). X-ray structures of general anaesthetics bound to a pentameric ligand-gated ion channel. *Nature* **469**, 428-431.
- Ochoa EL, Chattopadhyay A & McNamee MG. (1989). Desensitization of the nicotinic acetylcholine receptor: molecular mechanisms and effect of modulators. *Cell Mol Neurobiol* **9**, 141-178.
- Olsen JA, Ahring PK, Kastrup JS, Gajhede M & Balle T. (2014a). Structural and functional studies of the modulator NS9283 reveal agonist-like mechanism of action at  $\alpha 4\beta 2$  nicotinic acetylcholine receptors. *J Biol Chem* **289**, 24911-24921.
- Olsen JA, Kastrup JS, Peters D, Gajhede M, Balle T & Ahring PK. (2013). Two distinct allosteric binding sites at  $\alpha 4\beta 2$  nicotinic acetylcholine receptors revealed by NS206 and NS9283 give unique insights to binding activity-associated linkage at Cys-loop receptors. *J Biol Chem* **288**, 35997-36006.
- Olsen RW, Li GD, Wallner M, Trudell JR, Bertaccini EJ, Lindahl E, Miller KW, Alkana RL & Davies DL. (2014b). Structural models of ligand-gated ion channels: sites of action for anesthetics and ethanol. *Alcohol Clin Exp Res* **38**, 595-603.

- Ondrejcek T, Wang Q, Kew JN, Virley DJ, Upton N, Anwyl R & Rowan MJ. (2012). Activation of  $\alpha 7$  nicotinic acetylcholine receptors persistently enhances hippocampal synaptic transmission and prevents A $\beta$ -mediated inhibition of LTP in the rat hippocampus. *Eur J Pharmacol* **677**, 63-70.
- Orr-Urtreger A, Göldner FM, Saeki M, Lorenzo I, Goldberg L, De Biasi M, Dani JA, Patrick JW & Beaudet AL. (1997). Mice deficient in the  $\alpha 7$  neuronal nicotinic acetylcholine receptor lack  $\alpha$ -bungarotoxin binding sites and hippocampal fast nicotinic currents. *J Neurosci* **17**, 9165-9171.
- Ortells MO & Lunt GG. (1995). Evolutionary history of the ligand-gated ion-channel superfamily of receptors. *Trends Neurosci* **18**, 121-127.
- Oz M. (2006). Receptor-independent effects of endocannabinoids on ion channels. *Curr Pharm Des* **12**, 227-239.
- Oz M, Jackson SN, Woods AS, Morales M & Zhang L. (2005). Additive effects of endogenous cannabinoid anandamide and ethanol on  $\alpha 7$ -nicotinic acetylcholine receptor-mediated responses in *Xenopus* oocytes. *J Pharm Exp Ther* **313**, 1272-1280.
- Oz M, Zhang L, Ravindran A, Morales M & Lupica CR. (2004). Differential effects of endogenous and synthetic cannabinoids on  $\alpha 7$ -nicotinic acetylcholine receptor-mediated responses in *Xenopus* oocytes. *J Pharm Exp Ther* **310**, 1152-11160.
- Padgett CL, Hanek AP, Lester HA, Dougherty DA & Lummis SC. (2007). Unnatural amino acid mutagenesis of the GABA(A) receptor binding site residues reveals a novel cation- $\pi$  interaction between GABA and beta 2Tyr97. *J Neurosci* **27**, 886-892.
- Palma E, Mileo AM, Eusebi F & Miledi R. (1996). Threonine-for-leucine mutation within domain M2 of the neuronal  $\alpha 7$  nicotinic receptor converts 5-hydroxytryptamine from antagonist to agonist. *Proc Natl Acad Sci USA* **93**, 11231-11235.
- Papke RL, Bencherif M & Lippiello P. (1996). An evaluation of neuronal nicotinic acetylcholine receptor activation by quaternary nitrogen compounds indicates that choline is selective for the  $\alpha 7$  subtype. *Neurosci Lett* **213**, 201-204.
- Papke RL, Horenstein NA, Kulkarni AR, Stokes C, Corrie LW, Maeng CY & Thakur GA. (2014). The activity of GAT107, an allosteric activator and positive modulator of  $\alpha 7$  nAChR, is regulated by aromatic amino acids that span the subunit interface. *J Biol Chem* **289**, 4515-4531.

- Papke RL, Sanberg PR & Shytle RD. (2001). Analysis of mecamylamine stereoisomers on human nicotinic receptor subtypes. *J Pharm Exp Ther* **297**, 646-656.
- Park IH, Arora N, Huo H, Maherali N, Ahfeldt T, Shimamura A, Lensch MW, Cowan C, Hochedlinger K & Daley GQ. (2008). Disease-specific induced pluripotent stem cells. *Cell* **134**, 877-886.
- Parri HR, Hernandez CM & Dineley KT. (2011). Research update:  $\alpha 7$  nicotinic acetylcholine receptor mechanisms in Alzheimer's disease. *Biochem Pharmacol* **82**, 931-942.
- Paterson D & Nordberg A. (2000). Neuronal nicotinic receptors in the human brain. *Prog Neurobiol* **61**, 75-111.
- Pavlovicz RE, Henderson BJ, Bonnell AB, Boyd RT, McKay DB & Li C. (2011). Identification of a negative allosteric site on human  $\alpha 4\beta 2$  and  $\alpha 3\beta 4$  neuronal nicotinic acetylcholine receptors. *PLOS ONE* **6**, e24949.
- Pałczyńska MM, Jindrichova M, Gibb AJ & Millar NS. (2012). Activation of  $\alpha 7$  nicotinic receptors by orthosteric and allosteric agonists: influence on single-channel kinetics and conductance. *Mol Pharmacol* **82**, 910-917.
- Paşca SP, Portmann T, Voineagu I, Yazawa M, Shcheglovitov A, Paşca AM, Cord B, Palmer TD, Chikahisa S, Nishino S, Bernstein JA, Hallmayer J, Geschwind DH & Dolmetsch RE. (2011). Using iPSC-derived neurons to uncover cellular phenotypes associated with Timothy syndrome. *Nat Med* **17**, 1657-1662.
- Pedersen SE & Cohen JB. (1990). d-Tubocurarine binding sites are located at alpha-gamma and alpha-delta subunit interfaces of the nicotinic acetylcholine receptor. *Proc Natl Acad Sci USA* **87**, 2785-2789.
- Pedersen SE & Papineni RV. (1995). Interaction of d-tubocurarine analogs with the Torpedo nicotinic acetylcholine receptor. Methylation and stereoisomerization affect site-selective competitive binding and binding to the noncompetitive site. *J Biol Chem* **270**, 31141-31150.
- Pedersen SE, Sharp SD, Liu WS & Cohen JB. (1992). Structure of the noncompetitive antagonist-binding site of the Torpedo nicotinic acetylcholine receptor. [3H]meproadifen mustard reacts selectively with alpha-subunit Glu-262. *J Biol Chem* **267**, 10489-10499.
- Peper K, Bradley RJ & Dreyer F. (1982). The acetylcholine receptor at the neuromuscular junction. *Physiol Rev* **62**, 1271-1340.

- Pereira EF, Hilmas C, Santos MD, Alkondon M, Maelicke A & Albuquerque EX. (2002). Unconventional ligands and modulators of nicotinic receptors. *J Neurobiol* **53**, 479-500.
- Phillips E & Schmiesing R. (2001). Novel biarylcarboxamides. International patent number: WO 01/60821.
- Picciotto MR, Caldarone BJ, Brunzell DH, Zachariou V, Stevens TR & King SL. (2001). Neuronal nicotinic acetylcholine receptor subunit knockout mice: physiological and behavioral phenotypes and possible clinical implications. *Pharmacol Ther* **92**, 755-768.
- Picciotto MR, Zoli M, Léna C, Bessis A, Lallemand Y, LeNovère N, Vincent P, Pich EM, Brûlet P & Changeux JP. (1995). Abnormal avoidance learning in mice lacking functional high-affinity nicotine receptor in the brain. *Nature* **374**, 65-67.
- Picciotto MR, Zoli M, Rimondini R, Léna C, Marubio LM, Pich EM, Fuxe K & Changeux JP. (1998). Acetylcholine receptors containing the  $\beta 2$  subunit are involved in the reinforcing properties of nicotine. *Nature* **391**, 173-177.
- Pocivavsek A, Icenogle L & Levin ED. (2006). Ventral hippocampal  $\alpha 7$  and  $\alpha 4\beta 2$  nicotinic receptor blockade and clozapine effects on memory in female rats. *Psychopharmacology (Berl)* **188**, 597-604.
- Poewe W. (2009). Clinical measures of progression in Parkinson's disease. *Mov Disord* **24 Suppl 2**, S671-676.
- Prevost MS, Sauguet L, Nury H, Van Renterghem C, Huon C, Poitevin F, Baaden M, Delarue M & Corringer PJ. (2012). A locally closed conformation of a bacterial pentameric proton-gated ion channel. *Nat Struct Mol Biol* **19**, 642-649.
- Puinean AM, Lansdell SJ, Collins T, Bielza P & Millar NS. (2013). A nicotinic acetylcholine receptor transmembrane point mutation (G275E) associated with resistance to spinosad in *Frankliniella occidentalis*. *J Neurochem* **124**, 590-601.
- Purohit P & Auerbach A. (2009). Unliganded gating of acetylcholine receptor channels. *Proc Natl Acad Sci USA* **106**, 115-120.
- Purohit P, Mitra A & Auerbach A. (2007). A stepwise mechanism for acetylcholine receptor channel gating. *Nature* **446**, 930-933.
- Quik M, Huang LZ, Parameswaran N, Bordia T, Campos C & Perez XA. (2009). Multiple roles for nicotine in Parkinson's disease. *Biochem Pharmacol* **78**, 677-685.

- Quik M & Wonnacott S. (2011).  $\alpha 6\beta 2^*$  and  $\alpha 4\beta 2^*$  nicotinic acetylcholine receptors as drug targets for Parkinson's disease. *Pharmacol Rev* **63**, 938-966.
- Ramirez-Latorre J, Yu CR, Qu F, Perin F, Karlin A & Role L. (1996). Functional contributions of  $\alpha 5$  subunit to neuronal acetylcholine receptor channels. *Nature* **380**, 347-351.
- Rapier C, Lunt GG & Wonnacott S. (1990). Nicotinic modulation of [3H]dopamine release from striatal synaptosomes: pharmacological characterisation. *J Neurochem* **54**, 937-945.
- Revah F, Bertrand D, Galzi JL, Devillers-Thiéry A, Mulle C, Hussy N, Bertrand S, Ballivet M & Changeux JP. (1991). Mutations in the channel domain alter desensitization of a neuronal nicotinic receptor. *Nature* **353**, 846-849.
- Revah F, Galzi JL, Giraudat J, Haumont PY, Lederer F & Changeux JP. (1990). The noncompetitive blocker [3H]chlorpromazine labels three amino acids of the acetylcholine receptor  $\gamma$  subunit: implications for the  $\alpha$ -helical organization of regions MII and for the structure of the ion channel. *Proc Natl Acad Sci USA* **87**, 4675-4679.
- Reynolds JA & Karlin A. (1978). Molecular weight in detergent solution of acetylcholine receptor from *Torpedo californica*. *Biochemistry* **17**, 2035-2038.
- Riley B, Williamson M, Collier D, Wilkie H & Makoff A. (2002). A 3-Mb map of a large segmental duplication overlapping the  $\alpha 7$ -nicotinic acetylcholine receptor gene (CHRNA7) at human 15q13-q14. *Genomics* **79**, 197-209.
- Rollema H, Coe JW, Chambers LK, Hust RS, Stahl SM & Williams KE. (2007). Rationale, pharmacology and clinical efficacy of partial agonists of  $\alpha 4\beta 2$  nACh receptors for smoking cessation. *Trends Pharmacol Sci* **28**, 316-325.
- Romanelli MN & Gualtieri F. (2003). Cholinergic nicotinic receptors: competitive ligands, allosteric modulators, and their potential applications. *Med Res Rev* **23**, 393-426.
- Roncarati R, Seredenina T, Jow B, Jow F, Papini S, Kramer A, Bothmann H, Dunlop J & Terstappen GC. (2008). Functional properties of  $\alpha 7$  nicotinic acetylcholine receptors co-expressed with RIC-3 in a stable recombinant CHO-K1 cell line. *Assay Drug Dev Technol* **6**, 181-193.
- Rust G, Burgunder JM, Lauterburg TE & Cachelin AB. (1994). Expression of neuronal nicotinic acetylcholine receptor subunit genes in the rat autonomic nervous system. *Eur J Neurosci* **6**, 478-485.

- Sadek B, Khanian SS, Ashoor A, Prytkova T, Ghattas MA, Atatreh N, Nurulain SM, Yang KH, Howarth FC & Oz M. (2015). Effects of antihistamines on the function of human  $\alpha 7$ -nicotinic acetylcholine receptors. *Eur J Pharmacol* **746**, 308-316.
- Sahdeo S, Wallace T, Hirakawa R, Knoflach F, Bertrand D, Maag H, Misner D, Tombaugh GC, Santarelli L, Brameld K, Milla ME & Button DC. (2014). Characterization of RO5126946, a Novel  $\alpha 7$  nicotinic acetylcholine receptor-positive allosteric modulator. *J Pharm Exp Ther* **350**, 455-468.
- Sakmann B & Neher E. (1984). Patch clamp techniques for studying ionic channels in excitable membranes. *Annu Rev Physiol* **46**, 455-472.
- Sala F, Mulet J, Reddy KP, Bernal JA, Wikman P, Valor LM, Peters L, König GM, Criado M & Sala S. (2005). Potentiation of human  $\alpha 4\beta 2$  neuronal nicotinic receptors by a *Flustra foliacea* metabolite. *Neurosci Lett* **373**, 144-149.
- Samochocki M, Höffle A, Fehrenbacher A, Jostock R, Ludwig J, Vhrstner C, Radina M, Zerlin M, Ullmer C, Pereira EFR, Lübbert H, Albuquerque EX & Maelicke A. (2003). Galantamine is an allosterically potentiating ligand of neuronal nicotinic but not of muscarinic acetylcholine receptors. *J Pharm Exp Ther* **305**, 1024-1036.
- Sands SB, Costa AC & Patrick JW. (1993). Barium permeability of neuronal nicotinic receptor  $\alpha 7$  expressed in *Xenopus* oocytes. *Biophys J* **65**, 2614-2621.
- Sattelle DB, Buckingham SD, Akamatsu M, Matsuda K, Pienarr I, Jones AK, Sattelle BM, Almond A & Blundell CD. (2009). Comparative pharmacology and computational modelling yields insights into allosteric modulation of human  $\alpha 7$  nicotinic acetylcholine receptors. *Biochem Pharmacol* **78**, 836-843.
- Sauguet L, Shahsavari A, Poitevin F, Huon C, Menny A, Nemečz À, Haouz A, Changeux JP, Corringer PJ & Delarue M. (2014). Crystal structures of a pentameric ligand-gated ion channel provide a mechanism for activation. *Proc Natl Acad Sci USA* **111**, 966-971.
- Schaaf CP. (2014). Nicotinic acetylcholine receptors in human genetic disease. *Genet Med* **16**, 649-656.
- Schapira AH, Agid Y, Barone P, Jenner P, Lemke MR, Poewe W, Rascol O, Reichmann H & Tolosa E. (2009). Perspectives on recent advances in the understanding and treatment of Parkinson's disease. *Eur J Neurol* **16**, 1090-1099.

- Schoepfer R, Conroy WG, Whiting P, Gore M & Lindstrom J. (1990). Brain  $\alpha$ -bungarotoxin binding protein cDNAs and mAbs reveal subtypes of this branch of the ligand-gated ion channel gene superfamily. *Neuron* **5**, 35-48.
- Schwartz TW & Holst B. (2006). Allosteric modulation and other types of allostery in dimeric 7TM receptors. *J Recept Signal Trans* **26**, 107-128.
- Sealock R. (1982). Visualization at the mouse neuromuscular junction of a submembrane structure in common with Torpedo postsynaptic membranes. *J Neurosci* **2**, 918-923.
- Seo S, Henry JT, Lewis AH, Wang N & Levandoski MM. (2009). The positive allosteric modulator morantel binds at noncanonical subunit interfaces of neuronal nicotinic acetylcholine receptors. *J Neurosci* **29**, 8734-8742.
- Sgard F, Charpantier E, Bertrand S, Walker N, Caput D, Graham D, Bertrand D & Besnard F. (2002). A novel human nicotinic receptor subunit,  $\alpha 10$ , that confers functionality to the  $\alpha 9$ -subunit. *Mol Pharmacol* **61**, 150-159.
- Sharma T & Antonova L. (2003). Cognitive function in schizophrenia. Deficits, functional consequences, and future treatment. *Psychiatr Clin North Am* **26**, 25-40.
- Sharp AJ, Mefford HC, Li K, Baker C, Skinner C, Stevenson RE, Schroer RJ, Novara F, De Gregori M, Ciccone R, Brooker A, Casuga I, Wang Y, Xiao C, Barbacioru C, Gimelli G, Bernardina BD, Torniero C, Giorda R, Regan R, Murday V, Mansour S, Fichera M, Castiglia L, Failla P, Ventura M, Jiang Z, Cooper GM, Knight SJ, Romano C, Zuffardi O, Chen C, Schwartz CE & Eichler EE. (2008). A recurrent 15q13.3 microdeletion syndrome associated with mental retardation and seizures. *Nat Genet* **40**, 322-328.
- Shcheglovitov A, Shcheglovitova O, Yazawa M, Portmann T, Shu R, Sebastiano V, Krawisz A, Froehlich W, Bernstein JA, Hallmayer JF & Dolmetsch RE. (2013). SHANK3 and IGF1 restore synaptic deficits in neurons from 22q13 deletion syndrome patients. *Nature* **503**, 267-271.
- Sher E, Chen Y, Sharples TJ, Broad LM, Benedetti G, Zwart R, McPhie GI, Pearson KH, Baldwinson T & De Filippi G. (2004). Physiological roles of neuronal nicotinic receptor subtypes: new insights on the nicotinic modulation of neurotransmitter release, synaptic transmission and plasticity. *Curr Top Med Chem* **4**, 283-297.
- Short CA, Cao AT, Wingfield MA, Doers ME, Jobe EM, Wang N & Levandoski MM. (2015). Subunit interfaces contribute differently to activation and allosteric

- modulation of neuronal nicotinic acetylcholine receptors. *Neuropharmacol* **91**, 157-168.
- Sine SM & Engel AG. (2006). Recent advances in Cys-loop receptor structure and function. *Nature* **440**, 448-455.
- Sine SM, Quiram P, Papanikolaou F, Kreienkamp H-J & Taylor P. (1994). Conserved tyrosines in the  $\alpha$  subunit of the nicotinic acetylcholine receptor stabilize quaternary ammonium groups of agonists and antagonists. *J Biol Chem* **269**, 8808-8816.
- Sinkus ML, Lee MJ, Gault J, Logel J, Short M, Freedman R, Christian SL, Lyon J & Leonard S. (2009). A 2-base pair deletion polymorphism in the partial duplication of the  $\alpha 7$  nicotinic acetylcholine gene (CHRFAM7A) on chromosome 15q14 is associated with schizophrenia. *Brain Res* **1291**, 1-11.
- Sitzia F, Brown JT, Randall AD & Dunlop J. (2011). Voltage- and temperature-dependent allosteric modulation of  $\alpha 7$  nicotinic receptors by PNU120596. *Front Pharmacol* **2:81**, doi: 10.3389/fphar.2011.00081.
- Smit AB, Syed NI, Schaap D, van Minnen J, Klumperman J, Kits KS, Lodder H, van der Schors RC, van Elk R, Sorgedraeger B, Brejc K, Sixma T & Geraerts WPM. (2001). A glia-derived acetylcholine-binding protein that modulates synaptic transmission. *Nature* **411**, 261-268.
- Smith NJ, Hone AJ, Memon T, Bossi S, Smith TE, McIntosh JM, Olivera BM & Teichert RW. (2013). Comparative functional expression of nAChR subtypes in rodent DRG neurons. *Front Cell Neurosci* **7**, 225.
- Smith Y & Kieval JZ. (2000). Anatomy of the dopamine system in the basal ganglia. *Trends Neurosci* **23**, S28-33.
- Smulders CJ, Zwart R, Bermudez I, van Kleef RG, Groot-Kormelink PJ & Vijverberg HP. (2005). Cholinergic drugs potentiate human nicotinic  $\alpha 4\beta 2$  acetylcholine receptors by a competitive mechanism. *Eur J Pharmacol* **509**, 97-108.
- Spande TF, Garraffo HM, Edwards MW, Yeh HJC, Pannell L & Daly JW. (1992). Epibatidine: a novel (chloropyridyl)azabicycloheptane with potent analgesic activity from an Ecuadorian poison frog. *J Am Chem Soc* **114**, 3475-3478.
- Steinlein OK & Bertrand D. (2008). Neuronal nicotinic acetylcholine receptors: from the genetic analysis to neurological diseases. *Biochem Pharmacol* **76**, 1175-1183.

- Stevens KE & Wear KD. (1997). Normalizing effects of nicotine and a novel nicotinic agonist on hippocampal auditory gating in two animal models. *Pharmacol Biochem Behav* **57**, 869-874.
- Stewart DS, Chiara DC & Cohen JB. (2006). Mapping the structural requirements for nicotinic acetylcholine receptor activation by using tethered alkyltrimethylammonium agonists and antagonists. *Biochemistry* **45**, 10641-10653.
- Sun F, Jin K & Uteshev VV. (2013). A type-II positive allosteric modulator of  $\alpha 7$  nAChRs reduces brain injury and improves neurological function after focal cerebral ischemia in rats. *PLOS ONE* **8**, e73581.
- Séguéla P, Wadiche J, Dineley-Miller K, Dani JA & Patrick JW. (1993). Molecular cloning, functional properties, and distribution of rat brain  $\alpha 7$ : a nicotinic cation channel highly permeable to calcium. *J Neurosci* **13**, 596-604.
- Takahashi K, Tanabe K, Ohnuki M, Narita M, Ichisaka T, Tomoda K & Yamanaka S. (2007). Induction of pluripotent stem cells from adult human fibroblasts by defined factors. *Cell* **131**, 861-872.
- Takai T, Noda M, Mishina M, Shimizu S, Furutani Y, Kayano T, Ikeda T, Kubo T, Takahashi H, Takahashi T, Kuno M & Numa S. (1985). Cloning, sequencing and expression of cDNA for a novel subunit of acetylcholine receptor from calf muscle. *Nature* **315**, 761-764.
- Taly A, Corringer PJ, Guedin D, Lestage P & Changeux JP. (2009). Nicotinic receptors: allosteric transitions and therapeutic targets in the nervous system. *Nat Rev Drug Discov* **8**, 733-750.
- Taly A, Delarue M, Grutter T, Nilges M, Le Novère N, Corringer PJ & Changeux JP. (2005). Normal mode analysis suggests a quaternary twist model for the nicotinic receptor gating mechanism. *Biophys J* **88**, 3954-3965.
- Targowska-Duda KM, Feuerbach D, Biala G, Jozwiak K & Arias HR. (2014). Antidepressant activity in mice elicited by 3-furan-2-yl-N-p-tolyl-acrylamide, a positive allosteric modulator of the  $\alpha 7$  nicotinic acetylcholine receptor. *Neurosci Lett* **569**, 126-130.
- Tasneem A, Iyer LM, Jakobsson E & Aravind L. (2005). Identification of the prokaryotic ligand-gated ion channels and their implications for the mechanisms and origins of animal Cys-loop ion channels. *Genome Biol* **6**, R4.

- Tekinay AB, Nong Y, Miwa JM, Lieberam I, Ibanez-Tallon I, Greengard P & Heintz N. (2009). A role for LYNX2 in anxiety-related behavior. *Proc Natl Acad Sci USA* **106**, 4477-4482.
- Terlau H & Olivera BM. (2004). Conus venoms: a rich source of novel ion channel-targeted peptides. *Physiol Rev* **84**, 41-68.
- Thomsen MS, El-Sayed M & Mikkelsen JD. (2011). Differential immediate and sustained memory enhancing effects of  $\alpha 7$  nicotinic receptor agonists and allosteric modulators in rats. *PLOS ONE* **6**, e27014.
- Timmermann DB, Grønlien JH, Kohlhaas KL, Nielsen EØ, Dam E, Jørgensen TD, Ahring PK, Peters D, Holst D, Chrsitensen JK, Malysz J, Briggs CA, Gopalakrishnan M & Olsen GM. (2007). An allosteric modulator of the  $\alpha 7$  nicotinic acetylcholine receptor possessing cognition-enhancing properties in vivo. *J Pharm Exp Ther* **323**, 294-307.
- Timmermann DB, Sandager-Nielsen K, Dyhring T, Smith M, Jacobsen AM, Nielsen E, Grunnet M, Christensen JK, Peters D, Kohlhaas K, Olsen GM & Ahring PK. (2012). Augmentation of cognitive function by NS9283, a stoichiometry-dependent positive allosteric modulator of  $\alpha 2$ - and  $\alpha 4$ -containing nicotinic acetylcholine receptors. *Br J Pharmacol* **167**, 164-182.
- Toyoshima C & Unwin N. (1990). Three-dimensional structure of the acetylcholine receptor by cryoelectron microscopy and helical image reconstruction. *J Cell Biol* **111**, 2623-2635.
- Ulens C, Hogg RC, Celie PH, Bertrand D, Tsetlin V, Smit AB & Sixma TK. (2006). Structural determinants of selective  $\alpha$ -conotoxin binding to a nicotinic acetylcholine receptor homolog AChBP. *Proc Natl Acad Sci USA* **103**, 3615-3620.
- Unwin N. (1993). Nicotinic acetylcholine receptor at 9 Å resolution. *J Mol Biol* **229**, 1101-1124.
- Unwin N. (1995). Acetylcholine receptor channel imaged in the open state. *Nature* **373**, 37-43.
- Unwin N. (2005). Refined structure of the nicotinic acetylcholine receptor at 4 Å resolution. *J Mol Biol* **346**, 967-989.
- van Nierop P, Keramidas A, Bertrand S, van Minnen J, Gouwenberg Y, Bertrand D & Smit AB. (2005). Identification of molluscan nicotinic acetylcholine receptor (nAChR) subunits involved in formation of cation- and anion-selective nAChRs. *J Neurosci* **25**, 10617-10626.

- Varanda WA, Aracava Y, Sherby SM, VanMeter WG, Eldefrawi ME & Albuquerque EX. (1985). The acetylcholine receptor of the neuromuscular junction recognizes mecamylamine as a noncompetitive antagonist. *Mol Pharmacol* **28**, 128-137.
- Vernallis AB, Conroy WG & Berg DK. (1993). Neurons assemble acetylcholine receptors with as many as three kinds of subunits while maintaining subunit segregation among receptor subtypes. *Neuron* **10**, 451-464.
- Vernino S, Amador M, Luetje CW, Patrick J & Dani JA. (1992). Calcium modulation and high calcium permeability of neuronal nicotinic acetylcholine receptors. *Neuron* **8**, 127-134.
- Villarroel A, Herlitz S, Koenen M & Sakmann B. (1991). Location of a threonine residue in the  $\alpha$ -subunit M2 transmembrane segment that determines the ion flow through the acetylcholine receptor channel. *Proc R Soc Lond B* **243**, 69-74.
- Vulprian EF. (1866). Leçons sur la physiologie generale et comparée du systeme nerveux. Bailliere, Paris.
- Vázquez-Gómez E & García-Colunga J. (2009). Neuronal nicotinic acetylcholine receptors are modulated by zinc. *Neuropharmacol* **56**, 1035-1040.
- Wada E, Wada K, Boulter J, Deneris E, Heinemann S, Patrick J & Swanson LW. (1989). Distribution of  $\alpha 2$ ,  $\alpha 3$ ,  $\alpha 4$ , and  $\beta 2$  neuronal nicotinic receptor subunit mRNAs in the central nervous system: a hybridization histochemical study in the rat. *J Comp Neurol* **284**, 314-335.
- Wang H, Yu M, Ochani M, Amella CA, Tanovic M, Susaria S, Li JH, Yang H, Ulloa L, Al-Abed Y, Czura CJ & Tracey KJ. (2003). Nicotinic acetylcholine receptor  $\alpha 7$  subunit is an essential regulator of inflammation. *Nature* **421**, 384-388.
- Wang HL, Cheng X, Taylor P, McCammon JA & Sine SM. (2008). Control of cation permeation through the nicotinic receptor channel. *PLOS Comput Biol* **4**, e41.
- Wang HY, Lee DH, Davis CB & Shank RP. (2000). Amyloid peptide A $\beta$ (1-42) binds selectively and with picomolar affinity to  $\alpha 7$  nicotinic acetylcholine receptors. *J Neurochem* **75**, 1155-1161.
- Wang Y, Xiao C, Indersmitten T, Freedman R, Leonard S & Lester HA. (2014). The duplicated  $\alpha 7$  subunits assemble and form functional nicotinic receptors with the full-length  $\alpha 7$ . *J Biol Chem* **289**, 26451-26463.

- Ward JM, Cockcroft VB, Lunt GG, Smillie FS & Wonnacott S. (1990). Methyllycaconitine: a selective probe for neuronal  $\alpha$ -bungarotoxin binding sites. *FEBS Letters* **270**, 45-48.
- Weltzin MM, Huang Y & Schulte MK. (2014). Allosteric modulation of  $\alpha 4\beta 2$  nicotinic acetylcholine receptors by HEPES. *Eur J Pharmacol* **732**, 159-168.
- Weltzin MM & Schulte MK. (2015). Desformylflustrabromine modulates  $\alpha 4\beta 2$  nAChR high- and low- sensitivity isoforms at allosteric clefts containing the  $\beta 2$  subunit. *J Pharm Exp Ther* **354**, 184-194.
- Wen Z, Nguyen HN, Guo Z, Lalli MA, Wang X, Su Y, Kim NS, Yoon KJ, Shin J, Zhang C, Makri G, Nauen D, Yu H, Guzman E, Chiang CH, Yoritomo N, Kaibuchi K, Zou J, Christian KM, Cheng L, Ross CA, Margolis RL, Chen G, Kosik KS, Song H & Ming GL. (2014). Synaptic dysregulation in a human iPS cell model of mental disorders. *Nature* **515**, 414-418.
- West KA, Brognard J, Clark AS, Linnoila IR, Yang X, Swain SM, Harris C, Belinsky S & Dennis PA. (2003). Rapid Akt activation by nicotine and a tobacco carcinogen modulates the phenotype of normal human airway epithelial cells. *J Clin Invest* **111**, 81-90.
- West R, Zatonski W, Cedzynska M, Lewandowska D, Pazik J, Aveyard P & Stapleton J. (2011). Placebo-controlled trial of cytisine for smoking cessation. *N Engl J Med* **365**, 1193-1200.
- Wilens TE & Decker MW. (2007). Neuronal nicotinic receptor agonists for the treatment of attention-deficit/hyperactivity disorder: focus on cognition. *Biochem Pharmacol* **74**, 1212-1223.
- Williams BM, Temburni MK, Levey MS, Bertrand S, Bertrand D & Jacob MH. (1998). The long internal loop of the  $\alpha 3$  subunit targets nAChRs to subdomains within individual synapses on neurones in vivo. *Nature Neurosci* **1**, 557-562.
- Williams DK, Peng C, Kimbrell MR & Papke RL. (2012). Intrinsically low open probability of  $\alpha 7$  nicotinic acetylcholine receptors can be overcome by positive allosteric modulation and serum factors leading to the generation of excitotoxic currents at physiological temperatures. *Mol Pharmacol* **82**, 746-759.
- Williams DK, Stokes C, Horenstein NA & Papke RL. (2009). Differential regulation of receptor activation and agonist selectivity by highly conserved tryptophans in the nicotinic acetylcholine receptor binding site. *J Pharm Exp Ther* **330**, 40-53.

- Williams DK, Wang J & Papke RL. (2011a). Investigation of the molecular mechanism of the  $\alpha 7$  nAChR positive allosteric modulator PNU-120596 provides evidence for two distinct desensitized states. *Mol Pharmacol* **80**, 1013-1032.
- Williams DK, Wang J & Papke RL. (2011b). Positive allosteric modulators as an approach to nicotinic acetylcholine receptor-targeted therapeutics: advantages and limitations. *Biochem Pharmacol* **82**, 915-930.
- Wilson GG & Karlin A. (1998). The location of the gate in the acetylcholine receptor channel. *Neuron* **20**, 1269-1281.
- Wonnacott S. (1997). Presynaptic nicotinic ACh receptors. *Trends Neurosci* **20**, 92-98.
- Wonnacott S, Irons J, Rapier C, Thorne B & Lunt GG. (1989). Presynaptic modulation of transmitter release by nicotinic receptors. *Prog Brain Res* **79**, 157-163.
- Wu TY, Smith CM, Sine SM & Levandoski MM. (2008). Morantel allosterically enhances channel gating of neuronal nicotinic acetylcholine  $\alpha 3\beta 2$  receptors. *Mol Pharmacol* **74**, 466-475.
- Xu J, Zhu Y & Heinemann SF. (2006). Identification of sequence motifs that target neuronal nicotinic receptors to dendrites and axons. *J Neurosci* **26**, 9780-9793.
- Xu W, Gelber S, Orr-Urtreger A, Armstrong D, Lewis RA, Ou C-N, Patrick J, Role L, De Biasi M & Beaudet AL. (1999a). Megacystis, mydriasis, and ion channel defect in mice lacking the  $\alpha 3$  neuronal nicotinic acetylcholine receptor. *Proc Natl Acad Sci USA* **96**, 5746-5751.
- Xu W, Orr-Urtreger A, Nigro F, Gelber S, Sutcliffe CB, Armstrong D, Patrick J, Role LW, Beaudet AL & De Biasi M. (1999b). Multiorgan autonomic dysfunction in mice lacking the  $\beta 2$  and the  $\beta 4$  subunits of neuronal nicotinic acetylcholine receptors. *J Neurosci* **19**, 9298-9305.
- Yang X, Criswell HE & Breese GR. (1996). Nicotine-induced inhibition in medial septum involves activation of presynaptic nicotinic cholinergic receptors on  $\gamma$ -aminobutyric acid-containing neurons. *J Pharm Exp Ther* **276**, 482-489.
- Yip GMS, Chen Z-W, Edge CJ, Smith CH, Dickinson R, Hohenester E, Townsend RR, Fuchs K, Sieghart W, Evers AS & Franks NP. (2013). A propofol binding site on mammalian GABAA receptors identified by photolabeling. *Nature Chem Biol* **9**, 715-720.

- Young GT, Zwart R, Walker AS, Sher E & Millar NS. (2008). Potentiation of  $\alpha 7$  nicotinic acetylcholine receptors via an allosteric transmembrane site. *Proc Natl Acad Sci USA* **105**, 14686-14691.
- Zhong W, Gallivan JP, Zhang Y, Li L, Lester HA & Dougherty DA. (1998). From *ad initio* quantum mechanics to molecular neurobiology: a cation- $\pi$  binding site in the nicotinic receptor. *Proc Natl Acad Sci USA* **95**, 12088-12093.
- Zhu CZ, Chin CL, Rustay NR, Zhong C, Mikusa J, Chandran P, Salyers A, Gomez E, Simler G, Lewis LG, Gauvin D, Baker S, Pai M, Tovcimak A, Brown J, Komater V, Fox GB, Decker MW, Jacobson PB, Gopalakrishnan M, Lee CH & Honore P. (2011). Potentiation of analgesic efficacy but not side effects: co-administration of an  $\alpha 4\beta 2$  neuronal nicotinic acetylcholine receptor agonist and its positive allosteric modulator in experimental models of pain in rats. *Biochem Pharmacol* **82**, 967-976.
- Ziebell MR, Nirthanan S, Husain SS, Miller KW & Cohen JB. (2004). Identification of binding sites in the nicotinic acetylcholine receptor for [3H]azietomidate, a photoactivatable general anesthetic. *J Biol Chem* **279**, 17640-17649.
- Zoli M, Léna C, Picciotto MR & Changeux JP. (1998). Identification of four classes of brain nicotinic receptors using  $\beta 2$  mutant mice. *J Neurosci* **18**, 4461-4472.
- Zwart R, De Filippi G, Broad LM, McPhie GI, Pearson KH, Baldwinson T & Sher E. (2002). 5-Hydroxyindole potentiates human  $\alpha 7$  nicotinic receptor-mediated responses and enhances acetylcholine-induced glutamate release in cerebellar slices. *Neuropharmacol* **43**, 374-384.
- Zwart R, Strotton M, Ching J, Astles PC & Sher E. (2014). Unique pharmacology of heteromeric  $\alpha 7\beta 2$  nicotinic acetylcholine receptors expressed in *Xenopus laevis* oocytes. *Eur J Pharmacol* **726**, 77-86.
- Zwart R & Vijverberg HP. (1997). Potentiation and inhibition of neuronal nicotinic receptors by atropine: competitive and noncompetitive effects. *Mol Pharmacol* **52**, 886-895.
- Zwart R & Vijverberg HPM. (1998). Four pharmacologically distinct subtypes of  $\alpha 4\beta 2$  nicotinic acetylcholine receptor expressed in *Xenopus laevis* oocytes. *Mol Pharmacol* **54**, 1124-1131.